8-2019

Epigenetic Reprogramming, Apoptosis, and Developmental Competence in Cloned Embryos

Laura A. Moley
Utah State University

EPIGENETIC REPROGRAMMING, APOPTOSIS, AND DEVELOPMENTAL COMPETENCE IN CLONED EMBRYOS

by

Laura A. Moley

A dissertation submitted in partial fulfillment
of the requirements for the degree

of

DOCTOR OF PHILOSOPHY

in

Animal, Dairy, and Veterinary Sciences

Approved:

_____	_____
S. Clay Isom, Ph.D. Major Professor	Abby D. Benninghoff, Ph.D. Committee Member
_____	_____
John Stevens, Ph.D. Committee Member	Trista Strauch, Ph.D. Committee Member
_____	_____
Aaron Thomas, Ph.D. Committee Member	Richard S. Inouye, Ph.D. Vice Provost for Graduate Studies

UTAH STATE UNIVERSITY
Logan, Utah

2019

ABSTRACT

Epigenetic Reprogramming, Apoptosis, and Developmental

Competence in Cloned Embryos

by

Laura A. Moley, Doctor of Philosophy

Utah State University, 2019

Major Professor: Dr. S. Clay Isom
Department: Animal, Dairy, and Veterinary Sciences

Cloning through somatic cell nuclear transfer (SCNT) remains highly inefficient twenty years after the first demonstration of the technology. The technology could be more routinely utilized to enhance animal agriculture production by increasing efficiency and decreasing cost through the selection of embryos that are most likely to succeed following transfer. We proposed the use of a non-toxic, non-invasive caspase activity reporter, SR-FLICA, to quantitatively assess embryo competency prior to transfer. We hypothesized that following SCNT, a majority of embryos undergo altered epigenetic reprogramming compared to *in vivo* embryos, resulting in aberrant gene expression and incidentally increased levels of apoptosis. Conversely, a fraction of the embryos undergo proper genome reprogramming, resulting in correct gene expression and low levels of apoptosis. Using porcine embryos, the non-toxic nature of SR-FLICA was validated on oocytes and embryos. No correlation between relative level of apoptosis and cell number was found in blastocysts. DNA methylation and gene expression patterns were analyzed through reduced-representation bisulfite sequencing and RNA-seq to provide global

patterns in high and low apoptosis SCNT blastocysts. No differences in global DNA methylation patterns were found between the high apoptosis SCNT, low apoptosis SCNT, and in vivo produced embryos. Comparing high apoptosis and low apoptosis porcine SCNT blastocyst identified 4,346 100 bp tiles that were differentially methylated and 413 genes that were differentially expressed. Hierarchical clustering of differentially methylated tiles separated the high apoptosis from low apoptosis SCNT samples. However, hierarchical clustering of differentially expressed genes did not separate samples based on apoptosis. Gene ontology analysis identified no significantly enriched terms or KEGG pathways from genes with a differentially methylated tile near the transcription start site or from differentially expressed genes. Embryo competency was evaluated using day 7 bovine SCNT blastocysts that were transferred into females for evaluation of pregnancy establishment. While SR-FLICA did not hinder pregnancy rates, apoptosis score was not an indicative measure for pregnancy establishment. Together, these data support a stochastic nature of epigenetic reprogramming following SCNT and reinforce the necessity to identify embryos most likely to be successful due to proper epigenetic reprogramming in order to increase SCNT efficiency.

(265 pages)

PUBLIC ABSTRACT

Epigenetic Reprogramming, Apoptosis, and Developmental
Competence in Cloned Embryos
Laura A. Moley

Cloning through somatic cell nuclear transfer (SCNT) remains highly inefficient twenty years after the first demonstration of the technology with the birth of Dolly. By increasing efficiency by selecting the embryos early in development that are most likely to succeed following transfer into a surrogate mother, the technology could be more routinely utilized to enhance animal agriculture production. SCNT is believed to be highly inefficient as a result of incorrect DNA methylation and gene expression that are accumulated because of the SCNT technique. We proposed the use of a non-toxic, non-invasive detector of cell death, to quantitatively assess embryo competency prior to embryo transfer. We believed we could use SR-FLICA to identify the embryos with low levels of cell death as a result of proper DNA methylation and gene expression. By analyzing the whole embryo, differences in gene expression and DNA methylation were identified in embryos with high and low levels of cell death. However, the level of cell death did not prove to be a reliable indicator of embryo quality in predicting pregnancy outcome. This data supports the commonly held hypothesis that DNA methylation and gene expression after SCNT have random defects as a result of the random nature of resetting the DNA for embryo development. More research is required to identify the embryos which will prove to be successful following SCNT and embryo transfer.

ACKNOWLEDGMENTS

This project could not have happened without financial support from the United States Department of Agriculture and the Agriculture and Food Research Initiative Competitive Grant no. 2013-67015-20964 from the USDA National Institute of Food and Agriculture. Additional funding from the Animal, Dairy, and Veterinary Science department and the department of Research and Graduate Studies at Utah State University was critical for the success of the project.

I am indebted to Dr. Clay Isom for the patience, guidance, and training provided over my time at Utah State University. No one could ask for a better mentor through their graduate career. He has shown me, through example, what a good scientist should be. Additionally, advice, support, and direction from my graduate student committee greatly aided my research and writing. Thank you to Dr. Abby Benninghoff, Dr. Aaron Thomas, Dr. John Stevens, and Dr. Trista Strauch for your time and talents throughout my graduate career.

This project would not have been possible without the help of numerous others. I am beyond grateful to all those who kept this project going along the way. The support I received from the Isom lab made all the difference, including help from Harry Zhao, Sameer, Alhojaily, Farnaz Malekjahani, Sierra Heywood, Connor Waldron, and Samantha Krieger. Dr. Rakesh Kaundal and Rousselene Larson provided bioinformatic analysis that was far beyond my capacity to conquer. Dr. Qinggang Meng and Dr. Ying Liu expertly performed micromanipulations to create cloned embryos. The White lab group, specifically Misha Regouski and Jake Keim, performed bovine cloning and organized embryo transfers after many failed attempts of porcine embryo transfers. The veterinary group of Utah State University, including Dr. Rust Stott, Dr. Lexi Sweat, and Sarah Behunin, performed the

embryo transfers. Finally, a huge thank you to the farm crew who took care of the animals, day in and day out.

Lastly, I could have never achieved all of this without the love and support of my family and friends. Words cannot express the gratitude I feel towards my parents, who prioritized and were the driving force behind my education from day one. This achievement is just as much yours as it is mine. I am so incredibly lucky to have met my fiancée along this journey. He was always there to celebrate the experiments that worked, but much more often hear the frustrations of those that did not. Steve- I truly could not have done this without you. Finally, to the many friends- Sydney, Amanda, Cara, Sam, Nikole, Laura, and many more- who been there every step of the way, I am eternally thankful.

Laura A. Moley

CONTENTS

LIST OF TABLES

LIST OF FIGURES

CHAPTER 1

REVIEW OF LITERATURE

While assisted reproductive technologies have become more common in agriculture and human medicine over the years, they could benefit from increased efficiency. A need for increased efficiency is especially true for somatic cell nuclear transfer (SCNT), which remains highly inefficient two decades after first being reported with the birth of Dolly. The poor efficiency of SCNT has limited its use in agricultural production. Scientists believe that the poor efficiency of SCNT is the result of abnormal nuclear reprogramming. Following normal fertilization, the epigenetic marks on the DNA of both the sperm and egg are erased and reprogrammed for proper embryo development to occur. Epigenetic reprogramming is altered following SCNT as SCNT embryos have been shown to have altered DNA methylation and gene expression profiles, which is believed to increase apoptosis in SCNT embryos. Apoptosis is cell-directed, programmed cell death that is critical for proper development of the embryo and fetus. Apoptosis could be a useful, non-invasive biomarker to determine which embryos have undergone proper genome reprogramming before embryo transfer as a tool to increase the overall efficiency of somatic cell nuclear transfer.

Assisted Reproductive Technologies

Assisted reproductive technologies are commonly utilized in animal agriculture and human medicine. Techniques, including artificial insemination (AI) and *in vitro* fertilization (IVF), have the potential to quickly advance the genetic merit of a herd in animal agriculture. In artificial insemination, semen is collected from a male. Through

the addition of extenders, the sperm cells are preserved and a single ejaculate can be extended for the insemination of many females. With AI, an elite male can pass his genetics to many more offspring than he could naturally sire. For instance, a boar could typically mate 4 sows each week. However, 10-20 sows can be bred from a single ejaculate using AI [1]. The use of AI in cattle has allowed genetic progress to increase up to 50% compared to natural mating [2]. AI also provides additional benefits such as reducing the risk of injury or disease spread during mating and eliminates the need to house a male for breeding purposes. For this reason, over 85% of all Holstein births are the result of AI according to the Holstein Association USA [2]. By comparison, in 2009, only 7.6% of beef operations utilized AI as a reproductive tool [3]. Similar to the dairy industry, most sows at operations over 500 pigs are bred through AI [1].

While AI provides a way to enhance the passage of male genetics to the next generation, IVF has provided a mechanism for an elite female to pass her genetics on to multiple offspring in a year. Using ovum pick up (OPU), oocytes can be collected from a live female whose ovaries have been hormonally stimulated for increased follicular growth. Following maturation, the oocytes are combined with sperm for *in vitro* fertilization to occur. Following fertilization, a single cell zygote is formed, containing both the maternal and paternal DNA. The zygote begins cleavage divisions, where a single cell divides into two cells without growing in size so the cells get progressively smaller. The single cell zygote cleaves into first a two-cell embryo, then four-cell, eight-cell and finally sixteen-cell embryo. At this point, the cells begin to compact to form a morula. At the morula stage, the first physiologic separation of cell type occurs, where the outer cells of the morula form tight junctions and begin to pump salts inside the

morula. Water follows the salt forming a fluid filled cavity, called the blastocoel, which now makes the embryo a blastocyst. Following embryo development, two-cell embryos or blastocysts are transferred into surrogate females. In 2011, over 450,000 IVF embryos were transferred into beef cows [3]. Additionally, a female could be superovulated using hormonal treatments and embryos can be flushed and transferred into surrogate females. Over 700,000 embryos were flushed and transferred in beef cows in 2011 [3]. Both AI and IVF can also utilize sex-sorted semen, which is when the X- and Y- bearing sperm cells are sorted based on slight differences in total DNA. Sex-sorted sperm results in a 95% gender bias but is also costly and results in decreased conception rates compared to conventional sperm [2].

Assisted reproductive technologies are commonly used to treat fertility issues in humans as well. In developed countries, studies estimated that 1-3% of all births are the result of assisted reproductive technologies [4]. In addition to IVF, intracytoplasmic sperm injection (ICSI) is commonly used to circumvent the need for sperm cells to successfully bind to and penetrate the oocyte, which is beneficial when fertility is decreased due to abnormalities in the sperm. In ICSI, a single sperm cell is injected into the oocyte and fertilization follows. ICSI is a common procedure in human fertility treatment and represented 63% of fertilization procedures in 2005 [5].

While assisted reproductive technologies have the potential to be extremely beneficial to both agriculture and human medicine, their efficiencies remain low compared to natural fertilization. In cattle for example, only 40-50% of immature oocytes collected from slaughtered animals, where the ovaries have not been stimulated, develop to the blastocyst stage following oocyte maturation, fertilization, and culture [6].

The number of embryos that successfully cleave into two-cells and then continue to progress to the blastocyst stage tends to decrease with each developmental stage. In bovine IVF embryos, about 80% cleave into two-cell embryos, while only 30% developed to blastocysts [7, 8]. Pregnancy rates of 45% or higher following transfer of bovine IVF embryos have been reported [9]. However, even lower rates have been reported in bovine blastocysts with rates closer to 30% [8]. Abortion and fetal loss are more common with IVF pregnancies compared to *in vivo* produced pregnancies [9]. Pregnancy rates at day 76 of gestation were reported as high as 50.5% following embryo transfer of a fresh IVF embryo, but only 45.6% calved [10]. Porcine IVF results in lower blastocyst rates of 15-30% in most cases [11-14]. About 25% of transferred blastocysts resulted in the birth of piglets [14]. In human IVF, blastocyst rates are between 30-40% [15, 16] and birth rates following blastocyst transfers between 30-50% [16]. Decreased developmental potential of *in vitro* produced embryos in multiple species points to clear differences between *in vivo* and *in vitro* produced embryos.

The differences between *in vivo* (IVV) and *in vitro* produced (IVP) embryos has been investigated in depth. These differences include changes in cell number, morphology, gene expression, and epigenetic marks. *In vivo* produced blastocysts are known to have increased cell numbers, including inner cell mass cell number and trophoblast cell number, compared to *in vitro* produced blastocysts [17]. Increased cell numbers are correlated with increased embryo quality [18]. A microscopic analysis of IVV and IVP bovine embryos showed only slight structural differences, but it was noted that there was a developmental delay in the IVF embryos [19]. IVV and IVP embryos are known to show differences in gene expression [20]. A microarray study comparing

gene expression of *in vivo* and *in vitro* produced four-cell and blastocyst stage embryo discovered 1409 and 1696 differentially expressed genes between the *in vivo* and *in vitro* produced four-cell embryos and blastocysts, respectively [21]. Even the difference in site of fertilization, *in vivo* or *in vitro*, followed by embryo culture resulted in differences in gene expression in embryos [22]. Previous research found that epigenetic dysregulation occurs in IVP embryos, resulting in the altered gene expression patterns. A change in gene expression almost becomes cyclical in nature. Previous studies have shown that *in vitro* culture decreases the expression of genes that control the epigenetic remodeling of chromatin which would increase the methylation and acetylation of chromatin resulting in an overall decrease in gene transcription [23]. Gene repression does not occur in parthenogenetic embryos, supporting the hypothesis that the paternal chromosome reorganization is the potential source for aberrant reprogramming leading to altered gene expression in IVP embryos [23]. *In vitro* cultured embryos have also shown increases in DNA methylation, another epigenetic modification, specifically at CpG islands [24]. Epigenetic regulation of embryo development is covered in depth below.

With *in vitro* fertilization and culture having known negative impacts on embryo development, selecting the "best" embryo for transfer becomes even more important. Studies have focused on determining non-invasive indicators of embryo quality. For instance, it is known that embryos that cleave into two-cells earlier are more likely to develop into blastocysts [25]. Current methods rely on a visual assessment of embryo quality. In bovine blastocysts, the embryos are ranked as good, regular, or poor [26]. In humans, blastocysts are graded on expansion and hatching status, development of inner cell mass, and trophectoderm quality [27]. High quality blastocysts showed increased

pregnancy rates and chance of twins compared to low quality blastocysts [27]. Morphological assessment of embryos is rather subjective, so more quantitative methods have been explored, such as the integrity of blastomere membranes, analysis of embryo metabolism, measurement of cellular respiration, and electron-microscopy analysis (reviewed in [26] However, these techniques can either damage or kill the embryo or are cost prohibitive. So, most embryo quality is performed through visual assessment.

Somatic Cell Nuclear Transfer

Somatic cell nuclear transfer (SCNT) was first reported with the birth of Dolly the sheep, a clone produced using a mammary cell as the somatic donor [28]. While SCNT is now viewed as an advanced assisted reproductive technology with many applications, it was first used as a technology to understand basic biology. Before the birth of Dolly, it was believed that somatic cells were too specialized to revert back to a totipotent state that would be required for proper embryonic and fetal development [29]. SCNT provided a way to investigate if cellular differentiation was a reversible genetic modification, which was proven with the reprogramming of the somatic cell to form an entire lamb from a mammary cell [28]. Before the successful birth of Dolly, embryonic stem cells had been used for cloning, but these cells are not differentiated [28]. Since the birth of Dolly, many species have been cloned using this technology including the mouse, cattle, goat, pig, mouflon, domestic cat, rabbit, rat, horse, mule, African wildcat, dog, wolf, ferret, red deer, buffalo, camel, and coyote [30].

In 2001, a voluntary moratorium went into effect keeping milk and meat products from clones out of the food market until the Food and Drug Administration could

perform a risk assessment of the technology. An Animal Cloning Risk Assessment by the Food and Drug Administration later found that there is no increased risk in consuming milk or meat from healthy clones or their offspring compared to sexually-derived animals [31]. The report additionally stated that products from clones and their offspring are indistinguishable from those of sexually-derived animals [31]. However, the FDA does note that it is unlikely for food products of clones to enter the market as these animals would most likely serve as genetically superior breeders. At this time, the FDA does not plan to require labeling of products from clones as there is not increased risk from consuming these products. While there are no concerns to humans from animal cloning, there are animal welfare concerns associated with the technique. SCNT has increased health risks to both the surrogate female and the cloned offspring. While there is an increased frequency of health risks, they are not different risks than what could occur with other assisted reproductive techniques and artificial insemination [31]. An explanation of the common risks associated with SCNT is discussed below.

Currently, SCNT has a variety of applications, including the duplication of animals with superior genetics or infertile or deceased animals, research or biomedical models including transgenic animal production, threatened or endangered species cloning, and commercial cloning. The replication of animals provides producers with insurance on those genes and a way to increase the number of offspring with those genes. For example, animals with high genetic merit for traits such as milk production or carcass traits can be insured though the possibility of cloning following an untimely death. Cloning could also be used to increase the total number of animals that have the high genetic merit so those genes are then used in more breedings ensuring the genes are

present in a larger percentage of offspring than what would have occurred naturally or though other assisted reproductive technologies. SCNT has also been shown to be an extremely valuable research tool. For example, the aberrant epigenetic reprogramming that occurs following SCNT has provided a mechanism to study the normal reprogramming that occurs in early embryos following fertilization [32]. SCNT has also provided a more efficient and precise mechanism for gene transfer compared to microinjection of a zygote [32]. SCNT allows for site-directed genetic edits to a somatic cell, which can then be selected for, before use as the somatic donor. Related to the production of transgenic animals is the production of transgenic animals for biomedical applications. The transgene could allow a cloned animal to produce a product, such as a protein or drug, which it would not naturally make in order to harvest these products on a large-scale. SCNT has also been used on a limited scale for the production of threatened or endangered species. Utilizing interspecies SCNT, a donor oocyte and surrogate female of a closely related species can be used in the cloning process to produce an offspring very similar to the threatened or endangered species. Finally, SCNT has taken a commercial aspect where clients can pay to have their pet cloned. Several companies offer pet cloning services for dogs, cats, and horses. However, until SCNT becomes a more efficient process, prices are likely to remain high for cloning services.

Somatic cell nuclear transfer utilizes a technical procedure to remove the genomic DNA of an oocyte and replace it with that of a somatic cell. In SCNT, a mature oocyte is enucleated through the removal of the first polar body and the cytoplasm directly beneath the polar body which contains the nucleus. Enucleation removes the genomic DNA of the oocyte. Next, a somatic cell from the donor animal being cloned is inserted under the

zona pellucida of the oocyte in contact with the cell membrane of the oocyte. An electric pulse stimulates the oocyte and somatic donor to fuse. Oocyte activation is stimulated though electrical or chemical protocols following fusion to simulate a fertilization event of the oocyte. Following activation, embryo development begins. The embryo is then transferred into a surrogate female for gestation.

There are many factors of the SCNT protocol that can affect efficiency. Oocyte quality is important as the oocyte must survive manipulations of enucleation and placement of the donor cell as well as fusion and activation. The oocyte is then responsible for reprogramming the donor cell nucleus, which will be covered in depth later. High oocyte quality results in increased blastocyst development rate following SCNT in human embryos [33]. In general, the more differentiated the donor cell type becomes, the less efficient SCNT becomes. For example, a blastomere of a two cell embryo produces more live offspring per embryo transferred following SCNT compared to a mature neuron, which has not been successfully used for SCNT [34]. Donor cell cycle coordination is another critical aspect to ensure correct chromosome numbers. Most commonly, a donor cell in the G0/G1 phase of the cell cycle is used to ensure that the cell is not actively replicating DNA [34]. Cell cycle coordination can be achieved through serum starvation or confluent culture [35].

SCNT efficiency remains extremely low with the success rate averaging between 1-5% depending on species [34, 36]. SCNT embryo production is compromised compared to IVF blastocyst development rates [37, 38]. In the first reported successful sheep cloning with the birth of Dolly, 277 fused couplets using mammary epithelium as donor cells resulted in the birth of one live lamb, a success rate of 0.36% [28]. However,

a 3.4% success rate was reported based on the number of morula or blastocysts transferred [28]. Low success rates have been linked to poor embryo transfer, pregnancy rates, and pregnancy loss [12, 39, 40]. In bovine SCNT pregnancies, a 75% loss has been reported by the end of gestation [40]. Porcine SCNT is limited by low blastocyst rates, typically ranging from 10-20% [12, 41]. Because high embryo death during the pre-implantation development period would increase recipient cost, cloned embryos are often transferred at the blastocyst stage. Therefore, being able to select blastocyst with an increased chance of developing into healthy offspring is an important goal for SCNT research [36]. Even when a cloned offspring does survive to birth, health concerns are typically present that have been linked to un-successful epigenetic reprogramming [29]. Bovine SCNT pregnancies are often associated with hydrops and increased fetal and placental weight, increasing the risk of death due to dystocia during parturition [9]. Porcine SCNT offspring tend to be undersized with decreased birthweight compared to offspring from natural mating [42].

Understanding the low success rates of SCNT has been complex, with many aspects of the procedure and resulting embryo development analyzed. Oocyte quality can affect the success of live births following SCNT. In mice, oocytes that were naturally ovulated and used in SCNT resulted in live pups while oocytes that were collected following superovulation did not result in any live offspring following SCNT [43]. Scientists believe that apoptosis plays a role in SCNT embryo development [12]. Porcine SCNT embryos had decreased cleavage and blastocyst rates compared to IVF embryos. SCNT embryos had increased apoptosis compared to IVF embryos. However, apoptosis

rates in SCNT and IVF blastocysts were similar, indicating that apoptosis could be limiting blastocyst development in SCNT embryos [12].

During the enucleation and placement of the somatic cell, micromanipulations of the oocyte can result in damage and effect downstream development. However, it appears that micromanipulation is not the root of SCNT failure as ICSI embryos (undergoing similar micromanipulations) develop at a higher rate [44], pointing to gene regulation being the root of the problem. SCNT embryos may be predisposed to altered gene expression of proteins responsible for establishing and maintaining donor cell epigenetic marks [36]. The resulting wide-spread gene mis-regulation alters many functions of the developing embryo, including oxidative phosphorylation, membrane transport, and mRNA transport and procession [36]. While transcript levels are known to differ between SCNT and IVP embryos, multiple small changes in transcript abundance were detected between individual bovine SCNT embryos, indicating a potential stochastic nature of gene expression in SCNT embryos [45].

Gene expression differences could be the result of altered DNA methylation. SCNT embryos show increased DNA methylation compared to IVF embryos leading to the theory that DNMT1, the enzyme responsible for maintaining DNA methylation, introduced through the donor cell, maintains DNA methylation when the DNA should be cleared of methylation marks [46]. The theory is supported as the expression of DNMT1 protein is misregulated in cloned embryos [47]. By down-regulating DNMT1 through the introduction of siRNA in bovine fibroblast cells used in SCNT, the resulting embryos had DNA methylation levels between the low methylation of the IVF embryos and the high methylation levels of the SCNT embryos. However, this technique did not increase

blastocyst development rates [46]. In addition, SCNT embryos show problems with bi-allelic expression of imprinted genes due to changes in DNA methylation of imprinted genes [42, 48].

Aberrant DNA methylation and gene expression results from altered epigenetic reprogramming following SCNT. Following fusion of the somatic cell with the oocyte, the somatic nucleus must stop expression of its gene products. The nucleus begins to express gene products of developmental-specific genes following the directions provided by the oocyte cytoplasm as the donor-specific marks are erased [29]. The donor nucleus is disassembled in response to high levels of maturation promoting factor (MPF) found in the cytoplasm of the MII-stage oocyte [29]. The reprogramming efficiency of the donor nucleus hinders the overall efficiency of SCNT, as evident by the fact that using an undifferentiated cell, a zygote, significantly increases the number of live births following SCNT in mice [43]. In order to increase the efficiency of nuclear reprogramming following SCNT, drugs have been used to alter the epigenetic mechanisms of the embryo. Treatment of a histone deacetylase inhibitor, Oxamflatin, increased blastocyst development rates in bovine embryos [49]. Oxamflatin treated embryos had increased H3K9 and H3K18 acetylation at the 2-cell, 4-cell, and 8-cell stage, changed gene expression, and decreased incidence of apoptosis [49]. 5-aza-2'-deoxyctytidine (5-aza), a methylation inhibitor, and trichostatin (TSA), a histone deacetylase inhibitor, have been used in combined treatment on donor cells and early bovine SCNT embryos to increase blastocyst development, alter gene expression, and decrease DNA methylation [50].

Epigenetics

Epigenetic marks are heritable controls of gene expression that do not change DNA, but rather control how the DNA is expressed in the cell. Epigenetic changes include histone modifications and DNA methylation; each will be discussed in depth below. Following fertilization, epigenetic reprogramming occurs to turn on gene expression of developmentally important genes. After SCNT, this epigenetic reprogramming must occur with the additional complexity of removing the somatic cell epigenetic marks before adding the marks for embryonic development. Artificial culture conditions and SCNT are known to produce embryos with altered epigenetic marks [51, 52].

In order to condense DNA in the cell, DNA is packaged into chromatin which contains 147 bp of DNA wrapped around a histone octamer [53]. The histone octamer is composed of two of each histone protein, H2A and H2B, H3 and H4 [53, 54]. Each histone protein contains an N- and C- terminal tail, which can undergo post-translational modifications that can alter chromatin structure, in turn changing gene expression. The most common post-translational histone modifications include acetylation, phosphorylation, methylation, and ubiquitylation [53]. Other less-common modifications include sumoylation, ADP-ribosylation, proline isomerization, citrullination, butyrylation, propionylation, and glycosylation [54]. The type and location of the histone modification will determine if it will activate or repress gene expression. Typically, lysine methylation on the tail of H3 and H4, trimethylation of H3 lysine 4, trimethylation of H3 lysine 79, ubiquitylation of H3B, and trimethylation of H3 lysine 36 are associated with active gene expression [53]. Trimethylation of H3 lysine 27, ubiquitylation of H2A

on lysine 119, and trimethylation of H3 lysine 9 are typical marks of gene repression [53]. Histone modifications can occur in combination resulting in inactive, bimodal, and active chromatin states [54]. Bimodal states include a combination of active and repressive marks in the promoter region of a gene, allowing for rapid change in gene expression [54]. *In vitro* culture has been shown to change histone marks and alter gene expression of the *Axin* ^{Fu} gene in mice [51]. SCNT embryos show regions where epigenetic reprogramming is repressed due to increased levels of H3 lysine 9 trimethylation, a repressive histone mark [55]. Additionally, histone methylation is altered in porcine SCNT early embryos in a developmentally stage-specific manner when compared to the IVF embryos [56].

DNA methylation is another epigenetic mechanism that results in gene silencing. In mammalian DNA, a methyl group can be added to the 5 position of cytosine in a CpG dinucleotide, creating a 5mC nucleotide. However, DNA methylation does rarely occur outside of a CpG dinucleotide [57]. About three-quarters of genes in the mammalian genome have a high CpG content in their promoter regions [52]. CpG dinucleotides are concentrated in areas called CpG islands, which are typically located in the promoter region of genes [54]. Unmethylated CpG islands allow gene transcription to occur while methylated CpG islands silence gene transcription [57]. Most CpG sites that are not contained within CpG islands are highly methylated [57]. DNA methylation plays a critical role during cell differentiation during development, X-chromosome inactivation, and maintenance of imprinted genes [57]. Enzymes responsible for DNA methylation include DNM1, DNMT3a, and DNMT3b. DNMT1 is responsible for maintaining DNA methylation while DNMT3a and DNMT3b are responsible for *de novo* methylation [58].

DNMT1 restores methylation to symmetrical CpG nucleotides in a semi-conservative manner following DNA replication [59]. DNA can be de-methylated through passive DNA replication or actively through the TET enzymes [57].

DNA methylation is directly responsible for imprinted genes. While mammalian cells are diploid, containing two copies of every gene, certain imprinted genes are exclusively expressed from either the paternal or maternal copy of the gene. DNA methylation of the imprinted control region (ICR) of either the maternal or paternal copy of a gene ensures expression from only the unmethylated copy of the gene. These methylation marks are maintained through mitotic cell divisions and through epigenetic reprogramming following fertilization, which is discussed in depth in below [60]. Only during primordial germ cell development are imprints wiped clean in order for new imprints to be set prior to gamete development. Imprinted genes are known to play a role in the growth of the embryo, placenta, and neonate [60]. Imprinted genes occur in clusters in the genome [61]. Paternally expressed imprinted genes include growth promoters such as *Igf2, Peg1, and Peg3* [60]. Maternally expressed imprinted genes include growth inhibitors such as *Igf2r, Gnas, Cdkn1c, H19 and Grb10* [60]. Alterations in the epigenetics of imprinted genes in humans are associated with clinical syndromes and connected to tumorigenesis [61]. Beckwith-Wiedemann syndrome (BWS) is an over-growth syndrome in humans that results from a loss of imprinting [61]. Assisted reproductive technologies, including SCNT, are known to alter imprinted gene methylation and gene expression. Embryo culture and transfer affects imprinting in extraembryonic tissues in mice resulting in biallelic expression of several imprinted genes during midgestation [61]. Cloned, aborted piglets and placentas showed hyper

methylation of the imprinted gene *Pre1* and demethylation of *H19* compared to non-aborted cloned piglets and placentas [62]. Additionally, 18 imprinted genes showed altered gene expression in aborted cloned pregnancies compared to controls [62] indicating that changes in methylation of imprinted regions could have an effect on gene expression and lead to ultimate failure of SCNT pregnancies.

Epigenetic reprogramming occurs at two times, primordial germ cell development and following fertilization. During primordial germ cell development, DNA methylation is removed and imprinted marks are re-set in the developing germ cells. Following fertilization, the maternal and paternal genomes must undergo epigenetic reprogramming to set up for proper embryo development. At this point, imprinted methylation marks are maintained [59]. After the sperm has penetrated into the oocyte, the sperm must go through many alterations including nuclear envelope breakdown, protamines which have been used to condense the DNA must be replaced with histones for chromatin decondensation, and the male pronucleus must form [59]. Additionally, the maternal and paternal DNA is highly methylated at the time of fertilization and must be demethylated before new marks can be set for embryo development. The paternal DNA is demethylated rapidly though active demethylation by action of the TET enzymes [57]. Demethylation of the maternal DNA occurs more slowly through the exclusion of DNMT1 from the nucleus, preventing the maintenance of methylation marks over cell divisions. Following demethylation of both the maternal and paternal genomes, *de novo* methylation occurs. Cells that go on to form the inner cell mass are highly methylated [59]. For the maternal to zygotic transition (MZT) to occur, it is critical that epigenetic reprogramming occurs correctly and at the appropriate time.

During the maternal to zygotic transition (MZT), the embryo stops relying on stored RNA molecules from the oocyte and begins to transcribe its own DNA. The MZT occurs at a species-specific time-point. In the mouse the MZT occurs at the two-cell stage and in porcine and human it occurs at the four to eight-cell stage and in bovine and ovine it occurs at the eight- to sixteen-cell stage [63]. The three main functions of the MZT are to first destroy all oocyte-specific RNA transcripts. Next, the MZT replaces common RNA transcripts involved in cellular function from the oocyte with new transcripts from the embryo. Finally, the MZT produces transcripts that are specific to embryo development. The change from demethylation following fertilization to re-methylation is associated with the major start of transcriptional activity of the embryo [52]. The MZT is delayed in cloned embryos, occurring at the eight-cell stage in porcine SCNT embryos compared to the normal four-cell stage [64]. Without proper gene expression starting during the MZT, the embryo will halt in development.

During SCNT, the differentiated somatic cell is inserted into an oocyte, which must first de-differentiate the cell by removing epigenetic marks before beginning embryo-specific gene expression, a process that involves complex epigenetic alterations [59]. To achieve embryo development following somatic cell nuclear transfer, the genome of the somatic cell must first be silenced and epigenetic marks of differentiation on the somatic cell must be completely erased. The oocyte must be properly activated to start embryo development and embryonic genes must be turned on. All of these steps involve complex epigenetic changes within the cell [59]. Typical nuclear reprogramming that occurs after fertilization is known to be altered in SCNT embryos. DNA methylation patterns separating the ICM from the trophectoderm are obscured by overall increases in

DNA methylation [59]. Previous studies have been demonstrated that the somatic cell is generally de-methylated following SCNT, however not completely de-methylated which could be driving the low efficiency of SCNT [52]. When analyzing five pluripotency genes in bovine cloned embryos, SCNT embryos showed weak reprogramming capabilities of four of the five genes analyzed [7]. *Oct4* had correct reprogramming while *Nanog* was hypomethylated and *Rex1*, *Fgf4*, and *Sox2* were hypermethylated [7]. Alternatively, in cloned mouse embryos, the *Oct4* promoter was gradually de-methylated during early embryo development but remained elevated compared to normal development [65]. Embryos with delayed development showed higher levels of *Oct4* methylation compared to SCNT embryos that showed normal development [65]. Problems with reprogramming of SCNT embryos could be a result of altered gene expression of enzymes responsible for epigenetic regulation. Bovine cloned embryos showed increased expression of *HDAC* genes and decreased expression of *DNMT3A* compared to IVF embryos [66]. Understanding the changes in epigenetic reprogramming following SCNT provides opportunity to increase the efficiency of the technique.

Epigenetic reprogramming of the donor cell in SCNT is critical to ensure proper gene expression in SCNT embryos. Data suggest that most genes are properly reprogrammed following SCNT as 95% of genes show similar transcript abundance between SCNT and IVF embryos [36]. Misexpressed genes seem to be random as no distinct set of genes has been found to be consistently misexpressed across studies and the gene expression changes that have been reported are on average a two-fold change with less than 3% showing more than a four-fold change [36]. These observations strengthen the hypothesis that epigenetic reprogramming following SCNT occurs in a

random nature leading to random differences in gene expression. A wide range of gene expression patterns in individual bovine SCNT embryos indicated that some blastocysts contain gene expression patterns much closer to *in vitro* produced controls than others [67]. However, *in vivo* produced embryos had decreased variability in gene expression compared to SCNT and *in vitro* produced counterparts [67]. A tool to predict SCNT embryos with epigenetic marks and gene expression patterns close to "normal" could provide a way to select blastocysts most likely to succeed following embryo transfer.

Apoptosis

Apoptosis, or programmed cell death, is the natural response to destroy compromised cells during development and disease states. Apoptosis is characterized by morphological changes in the cell resulting from the activation of enzymes called caspases, ending in eventual DNA degradation. Specific stimuli trigger apoptosis, resulting in a series of morphological events including cell shrinkage, appearance of membrane-bound apoptotic bodies, and phagocytosis by nearby cells [68]. The initiation phase of apoptosis begins when pro-apoptotic stimuli trigger the machinery involved in apoptosis [68]. In the effector phase, the apoptosis machinery becomes fully activated and results in apoptotic changes in the nucleus. Finally, in the degradation phase, the morphological changes of the cell become evident [68]. Apoptosis typically affects single cells rather than large groupings of cells.

As previously mentioned, apoptotic cells undergo characteristic morphological changes. The cell shrinks and the nucleus condenses and eventually breaks up. The cytoplasm condenses and any microvilli that were present disappear [69]. The cell

detaches from surrounding tissue at this point. Apoptotic bodies are formed containing organelles, cytoplasm, and fragments of the nucleus. The apoptotic bodies are released and phagocytosed and degraded by nearby cells. The fragmented cell is then phagocytosed by neighboring cells. Phagocytosis prevents an inflammatory response because the apoptotic cells do not release their cellular contents, they are quickly taken up by surrounding cells, and the engulfing cells do not produce anti-inflammatory cytokines [70].

In addition to morphological changes, specific biochemical changes are also associated with apoptosis, including protein cleavage, protein cross-linking, DNA degradation, and membrane markers for phagocytic recognition [70]. Protein cross-linking is carried out by the expression and activation of transglutaminase. DNA breakdown results from the activation endogenous DNase enzymes, including DFF40 and CAD [68]. The DNA is degraded into 180-200 base pairs fragments which creates a characteristic ladder when run on an agarose gel with ethidium bromide and exposed to ultraviolet light. Apoptotic cells are quickly phagocytized by neighboring cells due to the external expression of phosphatidylserine on the cell membrane. Combined, morphological changes and biochemical changes of apoptotic cells can be used for the detection of apoptosis.

In contrast to apoptosis is necrosis, which effects a large number of cells at once. Necrosis is a toxic process where the cell falls victim to damage resulting in an energy-independent form of death. Necrosis in uncontrolled and passive while apoptosis is controlled and energy-dependent [70]. Necrosis results from “interference with the energy supply of the cell or direct damage to cell membranes” [70]. Direct damage of

cells resulting in necrosis can include extreme environmental insults including hypoxia, heat shock, and exposure to environmental toxins [71]. Ultimately, necrosis results in cell swelling, cytoplasmic vacuoles and blebs, damaged mitochondria, ruptured organelle membranes, and eventual disruption of the cell membrane [70]. Necrosis lacks the budding of apoptotic bodies and the chromatin is irregularly clumped [68]. It is worth noting that apoptosis and necrosis, while the most commonly discussed forms of cell death, are not the only forms. Other, less studied forms of cell death include necroptosis, autophagic cell death, pyroptosis and caspase-independent cell death [72].

Apoptosis is carried out by a group of enzymes called caspases. Caspases are always present in the form of inactivated proenzymes. Cleavage at specific internal aspartate residues activates the enzymes [68]. Caspases can be classified as non-apoptotic, initiators, or effectors [73]. Non-apoptotic caspases include caspase-1, -4, -5, and -11. Initiator caspases include caspase-2, -8, -9, and -10. Initiator caspases are activated by "induced proximity" though the interaction of adaptor proteins and the prodomains to promote caspase dimerization [74]. Effector caspases include caspase-3, -6, and -7. Effector caspases form homodimers in their inactive forms. Once cleaved by initiator caspases, effector caspases act on specific cellular substrates in order to dismantle the cell [74]. Two major pathways exist to activate the initiator caspases to start the apoptosis cascade. One pathway, the extrinsic pathway, starts with the ligation of the death receptors, including Fas and TNF receptors. The other intrinsic or mitochondrial pathway releases cytochrome C and the apoptosis inducing factor (AIF) to activate initiator caspases.

The extrinsic pathway of apoptosis is activated when death receptors are activated by their respective ligands. The death receptors are members of the tumor necrosis factor (TNF) receptor superfamily and contain a cytoplasmic "death domain" containing about 80 amino acids [70]. The "death domain" transmits the signal from the cell membrane to an intracellular signaling pathway. Characterized death receptors include FasR, TNFR1, DR3, DR4, and DR5 and their respective ligands are FasL, TNF-α, Apo3L, Apo2L, and Apo2L [70]. When the ligand binds to its receptor, cytoplasmic adaptor proteins are recruited that contain death domains. For instance, when Fas ligand binds to the Fas receptor, the adapter protein FADD is recruited. Likewise, when the TNF ligand binds to the TNF receptor, the adapter protein TRADD is bound and recruits FADD and RIP [70]. These recruited adaptor proteins then promote the dimerization and activation of initiator caspases by binding their prodomains, forming structures called DISCs [74]. FADD dimerizes its death domain with procaspase-8, forming a death-induced signaling complex (DISC) resulting in the auto-catalytic activation of procaspase-8 and -10, which then cleave and activate the effector caspases [75]. In certain cells, activation of caspase-8 results in the activation of the intrinsic pathway of apoptosis through the cleavage of BID, a pro-apoptotic protein of the intrinsic pathway that then translocates to the mitochondria [75]. The execution phase of apoptosis is triggered with the activation of caspase-8 [70].

The intrinsic signaling pathway of apoptosis does not involve activation of receptors, but rather intracellular signals that act directly within the cell. The stimuli for the intrinsic pathway can work either in a positive or negative way. Negative signals lead to the failure to suppress apoptosis when signals such as growth factors, hormones, and

cytokines are absent [70]. Positive signals stimulate apoptosis in response to a stimulus such as radiation, toxins, hypoxia hyperthermia, viral infections, or free radicals being present [70]. These stimuli cause changes to the inner mitochondrial membrane and the opening of the mitochondrial permeability transition pore, loss of membrane potential and release of pro-apoptotic proteins into the cytosol [70]. Two groups of proteins are released. The first containing cytochrome *c*, Smac/DIABLO, and protease HtrA2/Omi. The second containing AIF, endonuclease G, and CAD are released when the cell has committed to die. Cytochrome *c* binds to and activates Apaf-1 and procaspase-9, which forms a structure called an "apoptosome." The apoptosome contains 7 molecules of Apaf-1 and 2 molecules of caspase-9 [74]. Caspase-9 then cleaves and activates effector caspases, such as caspase-3. Smac/DIABLO and HtrA2/Omi inhibit inhibitors of apoptosis proteins (IAP) action to promote apoptosis. After release from the mitochondria, AIF moves to the nucleus and causes DNA degradation into 50-300 kb fragments. Endonuclease G also moves to the nucleus and also has a role in cleavage of chromatin and DNA fragmentation. CAD is cleaved by caspase-3 in the nucleus and also aids in DNA fragmentation. The intrinsic pathway of apoptosis is controlled by the Bcl-2 protein family. The Bcl-2 family consists of anti- and pro-apoptotic members and BH3-only proteins. Anti-apoptotic proteins include Bcl-2, Bcl-x, Bcl-XL, Bcl-XS, Bcl-w and BAG. Pro-apoptotic proteins include Bcl-10, Bax Bak, Bid, Bad, Bim, Bik, and Blk. Apoptotic stimuli activate the BH3-only proteins, or initiators, which inhibit the anti-apoptosis members allowing for the activation of the pro-apoptosis members, BAX and BAK that disrupt the mitochondrial membrane allowing for release of cytochrome c [76].

Detecting apoptosis can be a relative challenge due to the fast time course of apoptosis. Previous reports have suggested that clearance times of apoptotic cells can be less than an hour depending on cell type and type of insult [77]. Even with this challenge, several techniques have commonly been used to detect apoptosis, including morphology, DNA fragmentation, TUNEL, and active caspases. Using morphology, the classic features of apoptosis can be visualized by electron microscopy or light microscopy using nucleic acid-binding dyes [77]. Microscopy looks for the classic morphologic signs of apoptosis including nuclear condensation, cell shrinkage, cytoplasmic blebs, and cell detachment. However, because cells are so rapidly phagocytized by neighboring cells, the most common sign of apoptosis is the appearance of apoptotic bodies inside other cells [77]. The advantage of morphological detection of apoptosis is the reliability and inexpensive nature of the method. However, the quantitative measurement lacks objectivity and reproducibility and the method is less sensitive and prone to errors [78]. DNA fragmentation assays detect the characteristic DNA fragmentation associated with apoptosis. Agarose electrophoresis reveals the distinct DNA ladder of 180-200 bp fragments. DNA fragmentation assays can identify apoptosis from necrosis as the DNA ladder is specific to apoptosis while necrosis would show a smear of DNA on agarose electrophoresis. Single cell gel electrophoresis is used to visualize DNA damage of individual cells and is known as the comet assay [78]. Using the comet method, apoptotic cells appear as comet-like structures while viable cells have large heads and only a small tail [78]. Terminal deoxynucleotidyl transferase dUTP nick end labeling, or TUNEL, is used to identify cells undergoing DNA fragmentation using enzymes that add labeled nucleotide to the DNA ends [77]. TUNEL

labels both double and single-stranded DNA breaks [78]. More recently, immunohistochemical methods have become more common as antibodies have been marketed for apoptosis research. Antibodies designed against caspases must be specific to activated caspases rather than pro-caspases, as pro-caspases are common in cells. Staining of caspases would also allow for the identification of the early stages of apoptosis rather than relying on the end stages such as nuclear condensation and can therefore identify a different population of cells that are beginning the apoptosis pathways [77]. Most recently, fluorescent tagging of activated caspases has been developed. SR-FLICA (Immunohistochemistry Technologies, Bloomington, MN, USA) uses SR-VAD-FMK reagent that covalently binds to active caspases for fluorescent detection. Additionally, this method is non-invasive and non-toxic, allowing for the analysis of live cells.

Apoptosis in embryos follows the morphologic characteristics observed in other cells. Dying cells in blastocysts of many species including mouse, cow, baboon, rhesus monkey and human showed nuclear condensation, nuclear and cytoplasmic fragmentation, and loss of the nuclear membrane [79]. Dying cells of the blastocyst are then engulfed by healthy neighboring cells. In pre-compaction human embryos, phagocytosis was not observed suggesting that apoptotic cells are not taken up by neighboring cells until the blastocyst stage [79]. In human embryos, it is not uncommon to find excluded cells between the developing embryo and the zona pellucida at compaction and blastocyst formation [80]. TUNEL staining confirmed that cells of the mouse blastocyst are undergoing apoptosis [79]. Even in *in vivo* produced embryos, over 80% of blastocysts had one or more dead cells [79]. In human *in vitro* produced

blastocysts, 75% had one or more dead cells on day 6 [80]. While some embryos had a significant incidence of apoptosis of greater than 15%, most had less than 10 apoptotic cells [80]. Cell death occurred equally in the trophectoderm and the cells of the inner cell mass and the incidence of cell death was correlated with embryo quality [80]. Apoptosis in blastocysts can be the result of gamete quality, suboptimal culture conditions, lack of survival factors, chromosomal and nuclear abnormalities, and elimination of cells that are no longer required.

Apoptosis in embryos can result from suboptimal culture conditions. While cell death has been observed in *in vivo* produced embryos, the *in vitro* environment also has an effect on cell death. Brison and Schultz showed that mouse embryos cultured *in vitro* had increased levels of apoptosis compared to *in vivo* embryos and the amount of cell death was higher in embryos cultured individually compared to those cultured in groups [79]. Various studies have also shown that the composition of culture media is important for apoptosis [79]. Even outside of the culture environment, the uterine environment during early development could have an effect on cell death in the developing embryos. Alterations such as heat stress could change the uterine environment. Heat stress in the first 22 hours of development induced by increasing the temperature of *in vitro* culture increased apoptosis in both IVF and parthenogenetic porcine embryos [13]. Culture systems are constantly evolving to try and optimize embryo growth for increased developmental success.

Embryonic apoptosis can also result from a lack of growth or survival factors. During *in vitro* culture, embryos are lacking paracrine factors produced by the maternal reproductive tract. Embryos express growth factor receptors and secrete numerous

growth factor ligands [79]. Supplementing culture media with growth factors, including epidermal growth factor, transforming growth factor-α, and transforming growth factor-β1 have been shown to improve embryo development *in vitro* [79]. Mouse embryos had an increased incidence of apoptosis when cultured individually. However, the incidence of apoptosis in the ICM was decreased when the embryos were cultured with transforming growth factor-α. If embryos do not have a high enough concentration of the embryo-derived factors that act in an autocrine action, the embryos will have an increased incidence of apoptosis [81].

Apoptosis has been detected in embryos from numerous species, including pigs [12], rabbits [82], mouse [83], cattle [39], and humans [84]. Embryos produced *in vivo* show low levels of apoptosis, indicating that it is a normal part of embryonic development [83]. Early in development, embryos are unable to undergo apoptosis as TUNEL detection found apoptotic cells in the morula and blastocyst stage bovine embryos, but not in zygotes or cleavage stage embryos [71]. In these bovine embryos, apoptosis became apparent in the 8-16 cell stage of development, coinciding with the MZT [71]. Bovine SCNT embryos show earlier and increased levels of apoptosis compared to IVF controls [39]. Additionally, apoptosis increased in bovine SCNT embryos as development continued [85]. One possibility is that the P53-induced pathway of apoptosis is activated during reprogramming in SCNT embryos leading to the increased incidence of apoptosis as this pathway is activated during induced pluripotent stem cell reprogramming [86]. Treating donor cells with an apoptosis inhibitor improved development following SCNT [85] Mouse blastocysts with fragmentation had increased DNA strand breaks that were detected with TUNEL staining, indicating an increase in

apoptosis in fragmented embryos [87]. Together indicating that apoptosis could be a novel predictor of embryo quality.

Significance of project

This project aims to use a non-toxic, non-invasive biomarker for active caspase activity to differentiate the good from bad blastocysts following SCNT. The primary goal of the project is to understand the relationship between apoptosis and nuclear reprogramming as it relates to embryo competence following SCNT. We hypothesize that following SCNT, a majority of embryos undergo aberrant genome reprogramming, resulting in altered DNA methylation and gene expression, increased incidence of apoptosis as a result of the activation of the P53 pathway, and eventual embryo failure following transfer. On the other hand, a small subset of the embryos undergo proper genome reprogramming, correct DNA methylation and gene expression, low levels of apoptosis, and eventual success of a live offspring following transfer. Analyzing individual SCNT embryos with high and low levels of apoptosis for DNA methylation patterns and gene expression profiles will provide evidence for differences in reprogramming that have occurred following SCNT in each individual embryo. Additionally, transfer of high and low incidence of apoptosis SCNT embryos will indicate differences in developmental potential of the embryos.

By using a non-toxic and non-invasive stain to detect active caspases, embryos will be analyzed for apoptosis without sacrificing the embryo, which has tremendous benefits compared to the classical approaches for detecting apoptosis, such as TUNEL, that require the fixing of the embryo before analysis rendering the embryo useless for

future use. This staining system allows for analysis of live embryos that can then be transferred following fluorescent microscopy analysis. Allowing for the first time, a non-invasive stain to analyze apoptosis in embryos.

The staining of embryos for level of apoptosis as another marker of embryo viability could be a valuable assessment not only for SCNT embryos, but also IVF and ISCI embryos. Identification of competent embryos is especially valuable in species where a very limited number of embryos can be transferred to each recipient, such as horses and cattle. Staining of active caspases could provide an additional biometric to determine the most appropriate embryo to transfer to obtain a pregnancy. In the future, this tool could even become a critical assessment in human infertility clinics, where multiple embryos are produced and only a limited number can be transferred into the patient. Increasing understanding of which embryos are most viable could drastically change the success of assisted reproductive technologies.

As evident by low success rates of assisted reproductive technologies, especially cloning through SCNT, there is vast room for improvement of the technologies in agriculturally important species. Increasing the efficacy of SCNT would allow the technology to be utilized for not only scientific research, but also by producers as a way to propagate superior genetics and an insurance policy on genetically superior individuals. However, until the technology becomes more efficient, the cost of the technology remains too high for most producers to utilize. Therefore, many different approaches are being studied at this time to optimize the technology, typically aiming at enhancing the reprogramming following SCNT for increased embryo development. By

being able to select the embryos that will be most successful following transfer, fewer recipient females are required, decreasing the cost of a large recipient herd.

In addition to the practical aspect of improving SCNT for production of cloned offspring, a greater understanding of the epigenetic reprogramming associated with SCNT increases the understanding of the epigenetic reprogramming of early embryo development. Uncertainty still exists if epigenetic reprogramming occurs in a directed manner or in a random fashion following SCNT. DNA methylation and gene expression analysis of individual blastocysts in this project will allow for greater understanding of the differences in reprogramming occurring in each individual embryo, compared to a pool of embryos that is typically used.

The key goals of this project are to determine if key developmental genes are differentially expressed in individual SCNT embryos with high and low levels of apoptosis, identify differences in DNA methylation patterns in individual embryos with high and low levels of apoptosis, and validate the use of a non-invasive apoptosis bioassay as a tool to improve the assessment of developmental competence in SCNT embryos. The study will yield a wealth of new knowledge concerning the apoptosis and developmental potential of SCNT embryos.

References

1. Knox RV. Impact of swine reproductive technologies on pig and global food production. Adv Exp Med Biol 2014; 752:131-160.
2. Stevenson JS. Impact of reproductive technologies on dairy food production in the dairy industry. Adv Exp Med Biol 2014; 752:115-129.

3. Dahlen C, Larson J, Lamb GC. Impacts of reproductive technologies on beef production in the United States. Adv Exp Med Biol 2014; 752:97-114.

4. Maher ER. Imprinting and assisted reproductive technology. Hum Mol Genet 2005; 14 Spec No 1:R133-138.

5. Zegers-Hochschild F, Mansour R, Ishihara O, Adamson GD, de Mouzon J, Nygren KG, Sullivan EA. International Committee for Monitoring Assisted Reproductive Technology: world report on assisted reproductive technology, 2005. Fertil Steril 2014; 101:366-378.

6. Lonergan P, Rizos D, Gutierrez-Adan A, Fair T, Boland MP. Effect of culture environment on embryo quality and gene expression - experience from animal studies. Reprod Biomed Online 2003; 7:657-663.

7. Lan J, Hua S, Zhang H, Song Y, Liu J, Zhang Y. Methylation patterns in 5' terminal regions of pluripotency-related genes in bovine in vitro fertilized and cloned embryos. J Genet Genomics 2010; 37:297-304.

8. Tesfaye D, Ponsuksili S, Wimmers K, Gilles M, Schellander K. A comparative expression analysis of gene transcripts in post-fertilization developmental stages of bovine embryos produced in vitro or in vivo. Reprod Domest Anim 2004; 39:396-404.

9. Farin PW, Piedrahita JA, Farin CE. Errors in development of fetuses and placentas from in vitro-produced bovine embryos. Theriogenology 2006; 65:178-191.

10. Bonilla L, Block J, Denicol AC, Hansen PJ. Consequences of transfer of an in vitro-produced embryo for the dam and resultant calf. J Dairy Sci 2014; 97:229-239.

11. Abeydeera LR, Wang WH, Cantley TC, Prather RS, Day BN. Presence of beta-mercaptoethanol can increase the glutathione content of pig oocytes matured in vitro and the rate of blastocyst development after in vitro fertilization. Theriogenology 1998; 50:747-756.

12. Hao Y, Lai L, Mao J, Im GS, Bonk A, Prather RS. Apoptosis and in vitro development of preimplantation porcine embryos derived in vitro or by nuclear transfer. Biol Reprod 2003; 69:501-507.

13. Isom SC, Prather RS, Rucker EB, 3rd. Heat stress-induced apoptosis in porcine in vitro fertilized and parthenogenetic preimplantation-stage embryos. Mol Reprod Dev 2007; 74:574-581.

14. Yoshioka K, Suzuki C, Itoh S, Kikuchi K, Iwamura S, Rodriguez-Martinez H. Production of piglets derived from in vitro-produced blastocysts fertilized and cultured in chemically defined media: effects of theophylline, adenosine, and cysteine during in vitro fertilization. Biol Reprod 2003; 69:2092-2099.

15. Dal Canto M, Coticchio G, Mignini Renzini M, De Ponti E, Novara PV, Brambillasca F, Comi R, Fadini R. Cleavage kinetics analysis of human embryos predicts development to blastocyst and implantation. Reprod Biomed Online 2012; 25:474-480.

16. Wirleitner B, Vanderzwalmen P, Stecher A, Zech MH, Zintz M, Zech NH. Individual demands of human embryos on IVF culture medium: influence on

blastocyst development and pregnancy outcome. Reprod Biomed Online 2010; 21:776-782.

17. Bauer BK, Isom SC, Spate LD, Whitworth KM, Spollen WG, Blake SM, Springer GK, Murphy CN, Prather RS. Transcriptional profiling by deep sequencing identifies differences in mRNA transcript abundance in in vivo-derived versus in vitro-cultured porcine blastocyst stage embryos. Biol Reprod 2010; 83:791-798.

18. Matsuura K, Hayashi N, Takiue C, Hirata R, Habara T, Naruse K. Blastocyst quality scoring based on morphologic grading correlates with cell number. Fertil Steril 2010; 94:1135-1137.

19. Plante L, King WA. Light and electron microscopic analysis of bovine embryos derived by in vitro and in vivo fertilization. J Assist Reprod Genet 1994; 11:515-529.

20. Smith SL, Everts RE, Sung LY, Du F, Page RL, Henderson B, Rodriguez-Zas SL, Nedambale TL, Renard JP, Lewin HA, Yang X, Tian XC. Gene expression profiling of single bovine embryos uncovers significant effects of in vitro maturation, fertilization and culture. Mol Reprod Dev 2009; 76:38-47.

21. Whitworth KM, Agca C, Kim JG, Patel RV, Springer GK, Bivens NJ, Forrester LJ, Mathialagan N, Green JA, Prather RS. Transcriptional profiling of pig embryogenesis by using a 15-K member unigene set specific for pig reproductive tissues and embryos. Biol Reprod 2005; 72:1437-1451.

22. Giritharan G, Talbi S, Donjacour A, Di Sebastiano F, Dobson AT, Rinaudo PF. Effect of in vitro fertilization on gene expression and development of mouse preimplantation embryos. Reproduction 2007; 134:63-72.

23. Kafer GR, Kaye PL, Pantaleon M, Moser RJ, Lehnert SA. In vitro manipulation of mammalian preimplantation embryos can alter transcript abundance of histone variants and associated factors. Cell Reprogram 2011; 13:391-401.

24. Wright K, Brown L, Brown G, Casson P, Brown S. Microarray assessment of methylation in individual mouse blastocyst stage embryos shows that in vitro culture may have widespread genomic effects. Hum Reprod 2011; 26:2576-2585.

25. Isom SC, Li RF, Whitworth KM, Prather RS. Timing of first embryonic cleavage is a positive indicator of the in vitro developmental potential of porcine embryos derived from in vitro fertilization, somatic cell nuclear transfer and parthenogenesis. Mol Reprod Dev 2012; 79:197-207.

26. Rocha JC, Passalia F, Matos FD, Maserati MP, Jr., Alves MF, Almeida TG, Cardoso BL, Basso AC, Nogueira MF. Methods for assessing the quality of mammalian embryos: How far we are from the gold standard? JBRA Assist Reprod 2016; 20:150-158.

27. Gardner DK, Lane M, Stevens J, Schlenker T, Schoolcraft WB. Blastocyst score affects implantation and pregnancy outcome: towards a single blastocyst transfer. Fertil Steril 2000; 73:1155-1158.

28. Wilmut I, Schnieke AE, McWhir J, Kind AJ, Campbell KH. Viable offspring derived from fetal and adult mammalian cells. Nature 1997; 385:810-813.

29. Armstrong L, Lako M, Dean W, Stojkovic M. Epigenetic modification is central to genome reprogramming in somatic cell nuclear transfer. Stem Cells 2006; 24:805-814.

30. Burgstaller JP, Brem G. Aging of Cloned Animals: A Mini-Review. Gerontology 2016.

31. Center for Veterinary Medicine USFaDA, and Department of Health and Human Services. Animal Cloning: A Risk Assessment. In. Rockville, MD; 2008.

32. Niemann H, Lucas-Hahn A. Somatic cell nuclear transfer cloning: practical applications and current legislation. Reprod Domest Anim 2012; 47 Suppl 5:2-10.

33. Yu Y, Mai Q, Chen X, Wang L, Gao L, Zhou C, Zhou Q. Assessment of the developmental competence of human somatic cell nuclear transfer embryos by oocyte morphology classification. Hum Reprod 2009; 24:649-657.

34. Oback B, Wells DN. Donor cell differentiation, reprogramming, and cloning efficiency: elusive or illusive correlation? Mol Reprod Dev 2007; 74:646-654.

35. Miyamoto K, Hoshino Y, Minami N, Yamada M, Imai H. Effects of synchronization of donor cell cycle on embryonic development and DNA synthesis in porcine nuclear transfer embryos. J Reprod Dev 2007; 53:237-246.

36. Oback B. Climbing Mount Efficiency--small steps, not giant leaps towards higher cloning success in farm animals. Reprod Domest Anim 2008; 43 Suppl 2:407-416.

37. Jeong YW, Hossein MS, Bhandari DP, Kim YW, Kim JH, Park SW, Lee E, Park SM, Jeong YI, Lee JY, Kim S, Hwang WS. Effects of insulin-transferrin-selenium in defined and porcine follicular fluid supplemented IVM media on porcine IVF and SCNT embryo production. Anim Reprod Sci 2008; 106:13-24.

38. Pandey A, Singh N, Gupta SC, Rana JS, Gupta N. Relative expression of cell growth regulatory genes insulin-like growth factors (IGF-1 and IGF-2) and their

receptors (IGF-1R and IGF-2R) in somatic cell nuclear transferred (SCNT) and in vitro fertilized (IVF) pre-implantation buffalo embryos. Cell Biol Int 2009; 33:555-564.

39. Fahrudin M, Otoi T, Karja NW, Mori M, Murakami M, Suzuki T. Analysis of DNA fragmentation in bovine somatic nuclear transfer embryos using TUNEL. Reproduction 2002; 124:813-819.

40. Bloise E, Feuer SK, Rinaudo PF. Comparative intrauterine development and placental function of ART concepti: implications for human reproductive medicine and animal breeding. Hum Reprod Update 2014; 20:822-839.

41. Ju S, Rui R, Lu Q, Lin P, Guo H. Analysis of apoptosis and methyltransferase mRNA expression in porcine cloned embryos cultured in vitro. J Assist Reprod Genet 2010; 27:49-59.

42. Han DW, Im YB, Do JT, Gupta MK, Uhm SJ, Kim JH, Scholer HR, Lee HT. Methylation status of putative differentially methylated regions of porcine IGF2 and H19. Mol Reprod Dev 2008; 75:777-784.

43. Hiiragi T, Solter D. Reprogramming is essential in nuclear transfer. Mol Reprod Dev 2005; 70:417-421.

44. Boiani M, Gentile L, Gambles VV, Cavaleri F, Redi CA, Scholer HR. Variable reprogramming of the pluripotent stem cell marker Oct4 in mouse clones: distinct developmental potentials in different culture environments. Stem Cells 2005; 23:1089-1104.

45. Somers J, Smith C, Donnison M, Wells DN, Henderson H, McLeay L, Pfeffer PL. Gene expression profiling of individual bovine nuclear transfer blastocysts. Reproduction 2006; 131:1073-1084.

46. Giraldo AM, Lynn JW, Purpera MN, Vaught TD, Ayares DL, Godke RA, Bondioli KR. Inhibition of DNA methyltransferase 1 expression in bovine fibroblast cells used for nuclear transfer. Reprod Fertil Dev 2009; 21:785-795.

47. Chung YG, Ratnam S, Chaillet JR, Latham KE. Abnormal regulation of DNA methyltransferase expression in cloned mouse embryos. Biol Reprod 2003; 69:146-153.

48. Suzuki J, Jr., Therrien J, Filion F, Lefebvre R, Goff AK, Smith LC. In vitro culture and somatic cell nuclear transfer affect imprinting of SNRPN gene in pre- and post-implantation stages of development in cattle. BMC Dev Biol 2009; 9:9.

49. Su J, Wang Y, Li Y, Li R, Li Q, Wu Y, Quan F, Liu J, Guo Z, Zhang Y. Oxamflatin significantly improves nuclear reprogramming, blastocyst quality, and in vitro development of bovine SCNT embryos. PLoS One 2011; 6:e23805.

50. Wang Y, Su J, Wang L, Xu W, Quan F, Liu J, Zhang Y. The effects of 5-aza-2'-deoxycytidine and trichostatin A on gene expression and DNA methylation status in cloned bovine blastocysts. Cell Reprogram 2011; 13:297-306.

51. Fernandez-Gonzalez R, Ramirez MA, Pericuesta E, Calle A, Gutierrez-Adan A. Histone modifications at the blastocyst Axin1(Fu) locus mark the heritability of in vitro culture-induced epigenetic alterations in mice. Biol Reprod 2010; 83:720-727.

52. Niemann H, Carnwath JW, Herrmann D, Wieczorek G, Lemme E, Lucas-Hahn A, Olek S. DNA methylation patterns reflect epigenetic reprogramming in bovine embryos. Cell Reprogram 2010; 12:33-42.

53. Zhang T, Cooper S, Brockdorff N. The interplay of histone modifications - writers that read. EMBO Rep 2015; 16:1467-1481.

54. Inbar-Feigenberg M, Choufani S, Butcher DT, Roifman M, Weksberg R. Basic concepts of epigenetics. Fertil Steril 2013; 99:607-615.

55. Matoba S, Liu Y, Lu F, Iwabuchi KA, Shen L, Inoue A, Zhang Y. Embryonic development following somatic cell nuclear transfer impeded by persisting histone methylation. Cell 2014; 159:884-895.

56. Cao Z, Li Y, Chen Z, Wang H, Zhang M, Zhou N, Wu R, Ling Y, Fang F, Li N, Zhang Y. Genome-Wide Dynamic Profiling of Histone Methylation during Nuclear Transfer-Mediated Porcine Somatic Cell Reprogramming. PLoS One 2015; 10:e0144897.

57. Meng H, Cao Y, Qin J, Song X, Zhang Q, Shi Y, Cao L. DNA methylation, its mediators and genome integrity. Int J Biol Sci 2015; 11:604-617.

58. Anifandis G, Messini CI, Dafopoulos K, Messinis IE. Genes and Conditions Controlling Mammalian Pre- and Post-implantation Embryo Development. Curr Genomics 2015; 16:32-46.

59. Dean W, Santos F, Reik W. Epigenetic reprogramming in early mammalian development and following somatic nuclear transfer. Semin Cell Dev Biol 2003; 14:93-100.

60. Barlow DP, Bartolomei MS. Genomic imprinting in mammals. Cold Spring Harb Perspect Biol 2014; 6.

61. Rivera RM, Stein P, Weaver JR, Mager J, Schultz RM, Bartolomei MS. Manipulations of mouse embryos prior to implantation result in aberrant expression of imprinted genes on day 9.5 of development. Hum Mol Genet 2008; 17:1-14.

62. Zhang X, Wang D, Han Y, Duan F, Lv Q, Li Z. Altered imprinted gene expression and methylation patterns in mid-gestation aborted cloned porcine fetuses and placentas. J Assist Reprod Genet 2014; 31:1511-1517.

63. Schultz RM. The molecular foundations of the maternal to zygotic transition in the preimplantation embryo. Hum Reprod Update 2002; 8:323-331.

64. Cao S, Han J, Wu J, Li Q, Liu S, Zhang W, Pei Y, Ruan X, Liu Z, Wang X, Lim B, Li N. Specific gene-regulation networks during the pre-implantation development of the pig embryo as revealed by deep sequencing. BMC Genomics 2014; 15:4.

65. Yamazaki Y, Fujita TC, Low EW, Alarcon VB, Yanagimachi R, Marikawa Y. Gradual DNA demethylation of the Oct4 promoter in cloned mouse embryos. Mol Reprod Dev 2006; 73:180-188.

66. Beyhan Z, Forsberg EJ, Eilertsen KJ, Kent-First M, First NL. Gene expression in bovine nuclear transfer embryos in relation to donor cell efficiency in producing live offspring. Mol Reprod Dev 2007; 74:18-27.

67. Smith C, Berg D, Beaumont S, Standley NT, Wells DN, Pfeffer PL. Simultaneous gene quantitation of multiple genes in individual bovine nuclear transfer blastocysts. Reproduction 2007; 133:231-242.

68. Saraste A, Pulkki K. Morphologic and biochemical hallmarks of apoptosis. Cardiovasc Res 2000; 45:528-537.

69. Wyllie AH, Kerr JF, Currie AR. Cell death: the significance of apoptosis. Int Rev Cytol 1980; 68:251-306.

70. Elmore S. Apoptosis: a review of programmed cell death. Toxicol Pathol 2007; 35:495-516.

71. Matwee C, Betts DH, King WA. Apoptosis in the early bovine embryo. Zygote 2000; 8:57-68.

72. Tait SW, Ichim G, Green DR. Die another way--non-apoptotic mechanisms of cell death. J Cell Sci 2014; 127:2135-2144.

73. Kidd VJ, Lahti JM, Teitz T. Proteolytic regulation of apoptosis. Semin Cell Dev Biol 2000; 11:191-201.

74. Parrish AB, Freel CD, Kornbluth S. Cellular Mechanisms Controlling Caspase Activation and Function. Cold Spring Harb Perspect Biol 2013; 5.

75. Wu H, Medeiros LJ, Young KH. Apoptosis signaling and BCL-2 pathways provide opportunities for novel targeted therapeutic strategies in hematologic malignances. Blood Rev 2018; 32:8-28.

76. Czabotar PE, Lessene G, Strasser A, Adams JM. Control of apoptosis by the BCL-2 protein family: implications for physiology and therapy. Nat Rev Mol Cell Biol 2014; 15:49-63.

77. Save V, Hall PA, Coates PJ. Detecting and quantifying apoptosis in tissue sections. Methods Mol Biol 2004; 282:67-84.

78. Archana M, Yogesh TL, Kumaraswamy KL. Various methods available for detection of apoptotic cells--a review. Indian J Cancer 2013; 50:274-283.

79. Hardy K. Cell death in the mammalian blastocyst. Mol Hum Reprod 1997; 3:919-925.

80. Hardy K. Apoptosis in the human embryo. Rev Reprod 1999; 4:125-134.

81. O'Neill C. Autocrine mediators are required to act on the embryo by the 2-cell stage to promote normal development and survival of mouse preimplantation embryos in vitro. Biol Reprod 1998; 58:1303-1309.

82. Liu SZ, Yao LJ, Jiang MX, Lei ZL, Zhang LS, Zhang YL, Sun QY, Zheng YL, Song XF, Chen DY. Apoptosis in rabbit embryos produced by fertilization or nuclear transfer with fibroblasts and cumulus cells. Reproduction 2005; 130:359-366.

83. El-Shershaby AM, Hinchliffe JR. Cell redundancy in the zona-intact preimplantation mouse blastocyst: a light and electron microscope study of dead cells and their fate. J Embryol Exp Morphol 1974; 31:643-654.

84. Hardy K, Handyside AH, Winston RM. The human blastocyst: cell number, death and allocation during late preimplantation development in vitro. Development 1989; 107:597-604.

85. Park ES, Hwang WS, Jang G, Cho JK, Kang SK, Lee BC, Han JY, Lim JM. Incidence of apoptosis in clone embryos and improved development by the

treatment of donor somatic cells with putative apoptosis inhibitors. Mol Reprod Dev 2004; 68:65-71.

86. Kim E, Hyun SH. Apoptosis in Porcine Pluripotent Cells: From ICM to iPSCs. Int J Mol Sci 2016; 17.

87. Exley GE, Tang C, McElhinny AS, Warner CM. Expression of caspase and BCL-2 apoptotic family members in mouse preimplantation embryos. Biol Reprod 1999; 61:231-239.

CHAPTER II

CHARACTERIZING PORCINE SOMATIC CELL NUCLEAR TRANSFER BLASTOCYSTS WITH HIGH AND LOW INCIDENCE OF APOPTOSIS

Abstract

Cloning through somatic cell nuclear transfer (SCNT) remains highly inefficient twenty years after the first demonstration of the technology with the birth of Dolly. Increasing the efficiency of the technology would allow its utilization in the animal agriculture industry. Identifying the embryos most likely to succeed following embryo transfer is one way to increase the efficiency of the technology. Current methods to do this include culturing embryos to the blastocyst stage and then morphologically assessing the embryos, which is qualitative and inconsistent. We propose the use of a non-toxic, non-invasive caspase activity reporter, SR-FLICA, to quantitatively assess embryo competency prior to transfer. In this study, SR-FLICA staining to detect apoptotic cells was validated through comparison to TUNEL, a more traditionally used apoptosis detection method. The non-toxic nature of SR-FLICA was tested on oocytes and development compared to a control group found no difference in development rates. High and low apoptosis embryos were characterized on day 3 and 6 of development. No correlation between relative level of apoptosis and cell number was found and high and low apoptosis embryos on day 3 of development had no statistical difference in blastocyst rates on day 5, 6, or 7 of development. And finally gene expression of 65 genes in high and low apoptosis SCNT blastocysts was analyzed compared to *in vivo* produced

blastocysts. High and low apoptosis blastocysts showed no significant difference in gene expression. Taken together, SR-FLICA could provide a novel biomarker for embryo competency. However, it is still unclear how relative apoptosis level will affect development following embryo transfer.

Introduction

Assisted reproductive technologies such as *in vitro* fertilization (IVF) and somatic cell nuclear transfer (SCNT) remain inefficient and overall efficiency could be increased through improving the technologies. SCNT, in particular, remains highly inefficient with success rates between 1-5% depending on the species [34]. The low efficiency of SCNT has limited its use in the animal agriculture industry as the cost of the technology remains high and improving SCNT efficiency would allow for its application in the animal agriculture industry. Many factors influence SCNT efficiency, including oocyte quality [43], micromanipulations [44], and nuclear reprogramming [36]. Altered nuclear reprogramming following SCNT has been shown to lead to altered gene expression leading to changed functions of the developing embryo, including oxidative phosphorylation, membrane transport, and mRNA transport and processing [36].

Nuclear reprogramming occurs following the fusion of the donor, somatic cell with the oocyte. In order for normal embryo development to occur, DNA methylation must be reset for proper gene expression to occur. First, the donor cell DNA must be erased of donor-specific marks so that developmental-specific genes can be turned on and properly expressed [29]. This reprogramming involves complicated epigenetic changes

in the donor cell nucleus [59]. Following normal fertilization of an oocyte, the DNA methylation of the maternal and paternal genome is erased before new, embryonic specific DNA methylation patterns are established [59]. Previous studies have shown that the somatic cell is generally de-methylated following SCNT, however the donor cell is not completely de-methylated [52]. The result of this altered methylation status is misexpressed genes, where up to 5% of genes have altered transcript abundance between SCNT and IVF embryos [36]. However, a wide range of gene expression patterns have been demonstrated in bovine SCNT blastocysts, indicating that some embryos may have gene expression patterns which more closely resemble that of an *in vivo* produced embryo [67].

Often as a means to reduce the cost of failed pregnancies in surrogate animals, SCNT embryos are allowed to develop to the blastocyst stage before transfer, making it clear which embryos have undergone successful development to that point. However, once embryos reach the blastocyst stage, it is not clear which blastocysts will go on to have successful development following transfer into a surrogate. Current assessment of blastocyst before transfer involves a morphological evaluation which is subjective and qualitative [26]. More quantitative assessments of embryo quality, such as measurement of cellular respiration or analysis of embryo metabolism, can be detrimental to the developing embryo or are cost prohibitive [26]. Therefore, developing the use of a biomarker to quantify the health and overall quality of a blastocyst could provide the necessary tool needed to increase the efficiency of reproductive technologies, including SCNT. With this in mind, we propose the use of SR-FLICA (Immunochemistry

Technologies, Bloomington, MN), a non-toxic, non-invasive caspase activity reporter with a fluorescent tag to quantify the level of apoptosis to better evaluate embryo quality.

SR-FLICA covalently binds to active caspases, which are proteins involved in the final stages of apoptosis and are responsible for activating the proteases and nucleases that carryout apoptosis in the cell [73]. Caspases are always present in cells in their inactive pro-enzyme form [68]. Cleavage of the caspase activates its enzymatic activity following the intrinsic or extrinsic pathway of apoptosis [70]. The intrinsic pathway of apoptosis is also referred to as the mitochondrial pathway and releases cytochrome C and the apoptosis inducing factor to activate initiator caspases [70]. The extrinsic pathway of apoptosis begins with the ligation of death receptors as a result of an external stimulus activating initiator caspases [70]. Initiator caspases in turn activate effector caspases which act on specific cellular substrates to dismantle the cell [74]. While embryos have been shown to contain cells undergoing apoptosis [79], this is the first reported use of SR-FLICA to analyze active caspase activity in mammalian embryos.

Methods that have been previously used to analyze apoptosis in embryos, including TUNEL analysis, have the disadvantage of requiring the embryo to be fixed or destroyed prior to analysis so that subsequent transfer of the embryo into a surrogate is not possible. Traditional methods to detect apoptosis include morphological assessment, DNA fragmentation, or TUNEL. While morphological assessment is an inexpensive method to detect apoptosis through visual assessment using microscopy, it lacks objectivity and reproducibility and is prone to errors, which could be enhanced in fragmented embryos as visual indications of apoptosis, including nuclear condensation,

cell shrinkage, cytoplasmic blebs, and cell detachment, could be difficult to assess in fragmented embryos. Cells undergoing apoptosis show a distinctive DNA fragmentation ladder. However, to visualize this ladder, the cell must be destroyed so the DNA can be run using agarose electrophoresis, which is not compatible with selecting embryos most likely to succeed following transfer. Finally, TUNEL (terminal deoxynucleotidyl transferase dUTP nick end labeling) is used to identify cells undergoing DNA fragmentation by using enzymes that add a labeled nucleotide to the ends of DNA to identify DNA breaks. While effective and commonly reported as a tool to identify individual cells undergoing apoptosis, TUNEL requires the cells to be fixed and permeabilized before the staining can be performed, making it impossible for further development following staining. By using SR-FLICA, we have developed a protocol to analyze apoptosis levels in live embryos that can be analyzed for future developmental potential.

Our main hypothesis is that, following SCNT, most embryos undergo erroneous epigenetic reprogramming resulting in aberrant gene expression. As a result, these embryos will have an increased incidence of apoptosis and eventual failure following transfer. However, a subset of embryos following SCNT undergo proper epigenetic reprogramming leading to appropriate gene expression. These embryos will have a low level of apoptosis and successful development following transfer. The specific objectives of this study were carried out in four experiments. The first experiment was to compare SR-FLICA staining to the commonly reported TUNEL staining in porcine fetal fibroblast cells and blastocysts. The second experiment was to verify the non-toxic nature of SR-FLICA during embryo development by treating embryos on day 3 of development. The

third experiment was to evaluate embryo development by means of the number of cells and blastocyst development rate in embryos with a high and low level of apoptosis. Finally, the fourth experiment was designed to understand gene expression patterns in blastocysts showing high and low levels of apoptosis.

Materials and Methods

All chemicals and reagents were purchased from Sigma-Aldrich (St. Louis, MO) unless otherwise noted. All procedures performed with animals were in agreement with principles of animal welfare as approved by the veterinary staff and Institutional Animal Care and Use Committee at Utah State University (IACUC protocol #2636).

Oocyte collection and in vitro maturation

Cumulus oocyte complexes for SCNT were purchased from Desoto Biosciences (Seymore, TN). Cumulus oocyte complexes for parthenogenetic (PA) embryo production were aspirated from 3-6 mm antral follicles of ovaries collected from a local abattoir using 18 gauge needles. Oocyte maturation, manipulation, activation, and embryo culture were performed as described previously [88]. Briefly, oocytes with multiple layers of cumulus cells were collected, washed in maturation media, and allowed to mature for 40-44 hours at 39°C and 6.2% CO_2. Increased CO_2 concentrations (compared to the commonly reported 5.0%) were used to account for the higher elevation of Utah State University. Maturation media was composed of a base of m199 with Earl's

Balanced Salts and L-Glutamine (Fisher Scientific; Waltham, MA) supplemented with 0.1% PVA, 0.05 mM D-glucose, 0.91 mM sodium pyruvate, and 0.02 mg/ml gentamicin (Caisson Labs; Smithfield, UT). Additionally, 0.57 mM cysteine (Thermo Fisher Scientific; New Jersey, USA), 0.5 µg/mL of follicle stimulating hormone (Sioux Biochemical, Sioux Center, IA), 0.5 µg/mL of luteinizing hormone (Sioux Biochemical), 10 ng/mL epidermal growth factor, and 10% (v:v) porcine follicular fluid were added fresh each time.

Donor Cell Preparation

Porcine fetal fibroblasts (PFF) cells served as donor cells for nuclear transfer. The PFF cells had been isolated and frozen previously. For SCNT, the PFF cells were expanded and frozen for subsequent cloning using the same cell line at passage six. PFF culture media was prepared using DMEM (Fisher Scientific) as the base supplemented with 15% fetal bovine serum, 25 µg/ml basic human fibroblast growth factor, and 40 mg/ml gentamicin. PFF cells were seeded in a 4-well dish one week prior to SCNT and allowed to become confluent for several days for cell synchronization before cloning. To prepare for donor cell injection, medium was removed from the well, rinsed with PBS, and trypsin was added for 3 minutes. The cells were then collected by centrifugation at 400 x g for 5 minutes. Trypsin was removed and the cells were resuspended in manipulation media.

SCNT and Parthenogenetic Activation

Following oocyte maturation, oocytes were denuded of cumulus cells in medium containing 100 mg Hyaluronidase, 6 g mannitol, 5 mL PVA-TL-Hepes stock, and 95 mL double distilled water. Oocytes were placed in the hyaluronidase media at 39 °C for 5 minutes then pipetted 40 times to remove the cumulus cells. Oocytes were washed through manipulation medium containing a base of m199 supplemented with 5.95 mM sodium bicarbonate, 3.14 mM HEPES, 30 mM NaCl, 0.3% BSA, and 0.04 mg/ml gentamicin. Oocytes with an extruded polar body were selected for SCNT or parthenogenetic activation.

Oocytes undergoing SCNT were enucleated in drops of enucleation media under light mineral oil. Enucleation took place using a beveled glass pipette to aspirate the first polar body and the metaphase II plate by removing a small amount of the cytoplasm adjacent to the polar body. Following enucleation, the donor cell was injected into the perivitelline space. Donor cell injection was performed by placing the donor cells into the droplet with the enucleated oocytes. A single donor cell was picked up with the glass pipette and inserted through the same slit in the zona pellucida that was created during enucleation. Donor cells were fused with oocytes at the same time of oocyte activation in activation media composed of 0.3 M mannitol, 1.0 mM $CaCl_2$, 0.1 mM $MgCl_2$, and 0.5 mM HEPES (pH 7.0-7.4). Fusion and activation occurred with two direct current pulses of 1.2 kV/cm^2 for 30 µsec. Fusion of the donor cell was checked after 30 minutes.

Parthenogenetic (PA) embryos were produced in the same manner. In activation media, oocytes were exposed to two direct current pulses of 1.2 kV/cm^2 for 30 µsec.

Embryos were cultured at 39°C and 6.2% CO_2 in PZM3 media up to day 7 of development. PZM3 media [89] was composed of 108 mM NaCl, 10 mM KCl, 0.35 mM KH_2PO_4, 0.4 mM $MgSO_4$, 25.07 mM $NaHCO_3$, 0.2 mM sodium pyruvate, 2 mM calcium lactate, 1 mM L-Glutamine, 5 mM hypotaurine, 2% (v/v) BME amino acids (Fisher Scientific), 1% (v/v), MEM amino acids (Fischer Scientific), 0.005% (w/v) gentamicin, and 0.3% (w/v) FA-free BSA. The pH was adjusted to 7.3-7.4.

SR-FLICA and Hoechst 33342 Staining

SR-FLICA was resuspended as recommended by the manufacturer. Briefly, 50 µL DMSO was added to one vial SR-FLICA. Embryos were stained in 500 µL PZM3 culture media with 2 µL reconstituted SR-FLICA for 2 hours in the incubator. Embryos were moved to a fresh 500 µL PZM3 and placed back in the incubator for 30 minutes. Next, embryos were stained to visualize nuclei in order to count number of cells. Embryos were stained in 1 µg/ml of Hoechst 33342 for 10 minutes in the incubator. Embryos were then washed in PZM3 and transferred to individual 10 µL PZM3 droplets under mineral oil for fluorescent microscopy.

Microscopy and Image Analysis

Individual embryos were imaged at the 10X objective using the Zeiss Axio Observer.Z1 (Carl Zeiss Microscopy; Thornwood, NY). Fluorescent images of SR-FLICA (excitation 550-580 nm, emission 590-600 nm) and Hoechst 33342 (excitation

350 nm, emission 461 nm) stained embryos were captured with an Axiocam HRc (Carl Zeiss Microscopy) creating a black and white image and color was artificially added using Zen software (Carl Zeiss Microscopy; v. 2.0). SR-FLICA was assigned a red color and Hoechst 33342 a blue color. Both SR-FLICA and Hoechst 33342 images had a 1 second exposure time and light excitation intensity remained constant between embryos for accurate comparisons of incidence of apoptosis. SR-FLICA was analyzed using Adobe Photoshop (v. 2017.1.1.20174025) to determine the average red pixel intensity within the space of the zona pellucida of the embryo. In blastocysts that were hatching, both the space inside the zona pellucida and the hatching extrusion was included in the analysis. Average red pixel intensity for each embryo was ranked, and the top and bottom 20% were considered high and low apoptosis, respectively. For cell counts, embryos were transferred onto a glass slide and the number of nuclei were counted to ensure accurate cell counts.

Experiment 1

Experiment 1 aimed to validate SR-FLICA staining with the more commonly used method of TUNEL staining. Apoptosis was induced in PFF cells (P6) and PA blastocysts using staurosporine treatments. For PFF cell analysis, cells were treated with 0 µM, 0.08 µM, 0.4 µM, and 2 µM staurosporine in PFF cell media for 3 hours in the incubator. The PFF cell media was changed and the cells were treated with FLICA for 1 hour in the incubator. The media was again changed and the cells were allowed to rest for 30 minutes in the incubator. The cells were then treated with 1mg/ml Hoechst 33342

for 10 minutes in the incubator. The cell culture media was again removed and the cells were rinsed with PBS. The cells were fixed in formalin for 1 hour at room temperature. The cells were again rinsed with PBS then incubated with a permeabilization solution for 2 minutes on ice, as per TUNEL manufacturer directions (In Situ Cell Death Kit-Fluorescein). The cells were washed with PBS twice. 95 µL of TUNEL reaction mixture was then added to each well and allowed to incubate at 39°C for one hour. The cells were again washed with PBS twice then covered in 500 µL PBS for imaging. Exposure times for TUNEL, SR-FLICA, and DAPI were 3.31 seconds, 7.85 seconds, and 2.49 seconds, respectively. Three different regions of the well were imaged for analysis and results were averaged. Staining of the 4 staurosporine treatments was replicated 3 times (n = 3). The number of cells in each photo was counted from the Hoechst 33342 staining as well as the number of apoptosis positive cells in both the TUNEL and SR-FLICA staining to determine a percentage of cells that were apoptosis positive. Correlation between percent of cells positive for SR-FLICA staining and TUNEL staining was calculated using GraphPad Prism (version 7.04; GraphPad Software, Inc; La Jolla, CA).

Experiment 2

The aim of experiment 2 was to confirm the non-toxic nature of SR-FLICA during embryo development. Oocytes were treated with SR-FLICA (n = 4, total 237 oocytes) or remained un-treated to serve as a control group (n = 4, total 237 oocytes). Oocytes were then parthenogenetically activated and cleavage rates at 24 hours and blastocyst development at day 5, 6, and 7 were recorded. Student's t-tests at each

developmental stage were conducted using Graphpad Prism to determine if treated and control groups developed differently. P-values were corrected for multiple comparisons using the Holm-Sidak method with an alpha value of 0.05.

Experiment 3

The aim of experiment 3 was to characterize the development of high and low apoptosis embryos. SCNT embryos were stained with SR-FLICA and Hoechst 33342 on day 3 of development. SR-FLICA exposure time was 1 second and Hoechst 33342 was used for counting of nuclei once embryos were mounted onto slides. Day 3 SCNT embryos (n = 3, total 156 embryos) were fixed following SR-FLICA imaging and cell numbers were counted to determine if there was a correlation between incidence of apoptosis and cell number on day 3 of development. Additionally, embryos were classified as high (n = 31) or low (n = 31) incidence of apoptosis and average cell number was compared between groups using a student t-test for statistical analysis. Both correlation analysis and t-test were performed using GraphPad Prism. In four separate replicates, day 3 embryos that had cleaved by 24 hours (732 embryos) were stained with SR-FLICA, sorted by incidence of apoptosis (high and low, 156 and 150 embryos respectively), and allowed to continue development to day 7. Blastocyst rates were recorded for the high and low incidence of apoptosis groups. On day 7, all embryos, whether they had reached the blastocyst stage or not, were stained with Hoechst 33342 and cell numbers were recorded. Average cell number for embryos with high and low

levels of apoptosis on day 3 were recorded on day 7. A student t-test was used for statistical analysis using GraphPad Prism.

Additionally, cell number was analyzed using blastocysts (3 replicates, total n = 132) with apoptosis analyzed on day 7 of development. PA embryos were allowed to develop to day 7, then blastocysts were collected and stained with SR-FLICA and Hoechst 33342. Apoptosis level was determined for each blastocyst as well as total cell number. The correlation between apoptosis and cell number was examined as well as a student t-test comparing cell number of the high and low apoptosis blastocyst using GraphPad Prism.

Experiment 4

The goal of experiment 4 was to understand gene expression patterns in high and low incidence of apoptosis day 6 SCNT blastocysts. Following three cloning sessions, embryos developed to day 6. Blastocysts were stained with SR-FLICA and Hoechst 33342 and the top and bottom 20% of average red pixel intensity were classified as high (n = 13) and low (n = 13) apoptosis blastocysts. Additionally, *in vivo* produced blastocysts were collected 5 days after natural mating of the sow (2 sows, total n = 11 blastocysts collected). Blastocysts were stored at -80°C until RNA extraction could be performed. RNA extraction and cDNA conversion was performed on individual blastocysts as reported previously in individual oocytes [90]. Briefly, RNA was isolated using the ZR-DUET DNA/RNA MiniPrep (Zymo Research; Irvine, CA) following manufacturer instructions except the final elution was performed using 20 µL

DNase/RNase-free water. RNA was converted to cDNA using GoScript Reverse Transcriptase System (Promega; Madison, WI) again with minor modifications to the manufacturer's protocol. 8 µL of RNA was combined with 1 µL of oligo primers and 1 µL of random primers and water was then left out of the reverse transcription reaction mix; otherwise the reaction was performed as per the manufacturer's recommended protocol.

Gene expression analysis was performed through qPCR using the Fluidigm (South San Francisco, CA) 96.96 TaqMan Assay. The Fluidigm platform follows standard PCR chemistry in nanoliter-scale reactions to evaluate 96 genes for each of 96 samples using the 96.96 Dynamic Array integrated fluidic circuit (IFC) chip. Gene categories evaluated include apoptosis (*AIFM1, APAF1, ATM, BAD, BAX, BACL2, BCLX, BID, CASP3, CASP9, CDKN1A, HSP70, P53,* and *XIAP*) , epigenetic regulation (*ASH2L, DMAP1, DNMT1, DNMT3A, DNMT3B, EHMT2, EZH2, HAT1, HDAC1, HDAC2, HDAC3, KAT2A, KDM3A, KDM4C, KDM5B, MECP2, SIRT1,* and *SUV39H1*), imprinted genes (*ASCL2, DIRAS3, GNAS, GRB10, HAND1, IGF2, IGF2R, IMPACT, MEG3, NECD, NNAT, PEG3, PEG10, RTL1, SNRPN,* and *UBE3A*), maternal effect (*BMP15, DAZL, DDX4, FIGLA, GDF9, MOS, NLRP5, ZAR1, ZP2,* and *ZP3*), pluripotency (*CMYC, ID1, ID3, KLF4, LIN28, NANOG, POU5F1, SOX2,* and *ZIC1*), trophoblast differentiation and function (*CDX2, CYP17A1, DLX3, ELF5, ESRRB, ETS2, HSD17B1, KRT8, SFN, TACSTD2, TEAD4,* and *VIM*), and housekeeping (*ACTB, EIF4A1, GAPDH, HSP90, RPS5, SF3A1, TAF11,* and *YWHAZ*). Fluidigm Corporation's DeltaGene assay design service designed custom primers based on NCBI's reference

sequence for pigs. Gene names and PCR primer sequence for each gene symbol can be found on Supplementary Table 2-2 and 2-3, respectively.

To perform quantitative PCR gene expression analysis using the Biomark system, Fludigm's protocol (PN 68000130) was followed. Specific target amplification was performed to each sample before qPCR by created a 200 nM primer mix by pooling 1 µL of each combined forward and reverse primer set (20 µM each). The specific target amplification is performed by combining 1.25 µL of the pooled primer mix, 2.5 µL of TaqMan PreAmp Master Mix (Applied Biosystems; Foster City, CA) and 1.25 µL of cDNA. The polymerase is activated at 95°C for 10 minutes and then the reaction is amplified for 14 cycles of 95°C for 15 seconds then 60°C for 4 minutes. The reaction is then treated with Endonuclease I (ExoI; New England Biolabs; Ipswich, MA) to remove any primers that were not integrated in the specific target amplification. The ExoI treatment added 1.4 µL of water, 0.2 µL of ExoI reaction buffer, and 0.4 µL ExoI enzyme to each specific target amplification reaction. The reactions were incubated at 37°C for 30 minutes to allow for complete digestion of the non-integrated primers. Then, reactions were inactivated at 80°C for 15 minutes. Following ExoI treatment, each reaction was diluted 5-fold to a total volume of 25 µL. Reactions were stored at -20°C until further gene expression analysis was performed.

Next, individual sample and primer solutions were prepared for qPCR. Two microliters of the diluted specific target amplification were combined with 2.5 µL of 2X TaqMan Gene Expression Master Mix (Applied Biosystems), 0.25 µL of 20x DNA binding dye sample loading reagent (Fluidigm), and 0.25 µL of 20X EvaGreen DNA

Binding Dye (Biotium; Hayward, CA). Primer mixes were made by combining 2.25 µL each primer (20 µM) with 2.5 µL of 2x Assay loading reagent (Fluidigm) and 0.25 µL water. The IFC chip was primed prior to loading samples and primers using the Prime Script (136X) of the HX IFC controller. Once priming was complete, 5 µL of each primer mix and 5 µL of each sample mix were pipetted into their correct inlets on the chip. The chip was again inserted into the IFC controller and the samples and primers were loaded into the chip using the Load Mix Script (136X) so that the samples and primers were moved into the reaction chambers. After the chip was loaded, the chip was placed in the BioMark thermal cycler for quantitative PCR where cycles consisted of 5 minutes of enzyme activation at 95°C, followed by 35 cycles of 95°C for 15 seconds then 60°C for 60 seconds for denaturation and extension, and finished with a 3 minute final extension cycle at 60°C. Following PCR amplification, a melt curve analysis was performed to assess the quality of each product. Each sample was run in duplicate on the chip and the chip run was duplicated yielding 4 reactions of each sample and primer. Downstream analysis averaged ΔΔCT values for statistical analysis.

Analysis of qPCR data was performed using the Fluidigm Real-Time PCR Analysis Software (v 4.3.1). Delta-delta CT values were calculated using a positive control sample containing cDNA from day7 PA blastocysts, MII oocytes, and cumulus cells as reference and multiple housekeeping genes. While 96 different primers were run on the Fluidigm chip, primers were removed from analysis if they yielded a signal in more than 40% of the negative control samples, failed to work in more than 60% of the IVV sample reactions, or failed to work in at least 3 high and 3 low SCNT samples. These criteria removed 31 genes from further analysis. Sixty-five genes were analyzed

for difference in expression between high and low apoptosis embryos and *in vivo* (IVV) samples. Statistical analysis was performed in SAS by fitting a generalized linear mixed model (proc glimmix) to analyze ΔΔCT values for each group type. Sample type (high apoptosis, low apoptosis, or *in vivo*) and collection day were class variables. Additionally, collection day was considered a random variable. Four estimates were performed. The first compared high apoptosis to low apoptosis samples. The second compared high apoptosis and IVV samples. The third compared low apoptosis and IVV samples. And the final compared cloned (including high and low apoptosis samples) to IVV samples. Because not all reactions worked properly, the number of samples analyzed in each group for each gene has been provided in Supplementary Table 2-1. All p-values were corrected for false discovery rate (FDR) as described by Benjamini and Hochberg [91]. Fold change values were calculated from ΔΔCT values and normalized to the average IVV fold change. Log2 fold change values were then graphed.

Hierarchical clustering was analyzed through an unsupervised hierarchical clustering created through the ClustVis program [92]. Raw ΔΔCT values, before normalization to the IVV samples, for each sample and gene analyzed were uploaded into the program. Clustering analysis was performed using the correlation metric with average linkage clustering. Additionally, ClustVis was used to perform PCA using raw ΔΔCT values. For both analyses, no scaling was performed on rows and SVD with imputation was used.

Results

Experiment 1

Induction of apoptosis through staurosporine treatment of PFF cells resulted in a statistically significant correlation (Figure 2-1a) between the percentages of SR-FLICA and TUNEL positive cells ($R^2 = 0.69$, $P = 0.00079$). The relationship is visible in the percent of SR-FLICA and TUNEL positive cells when graphed by concentration of staurosporine treatment (Figure 2-1b). With no staurosporine treatment (0 µM), 1.29% (± 0.2) of cells were TUNEL positive while 7.30% (± 2.15) of cells were SR-FLICA positive. These values increase with a 0.08 µM staurosporine treatment to 3.92% (± 1.08) of cells being TUNEL positive and 16.36% (± 3.8) of cells being SR-FLICA positive. At a staurosporine treatment level of 0.4 µM, 39.42% (± 9.8) of cells were positive for TUNEL and 46.14% (± 7.0) for SR-FLICA. Finally, after a 2 µM staurosporine treatment, 36.56% (± 5.7) of cells were positive for TUNEL while 41.85% (± 5.7) were positive for SR-FLICA. These results indicate a dose response from 0-0.4 µM of staurosporine.

Experiment 2

Oocytes stained with SR-FLICA developed at the same rates compared to those not stained (Figure 2-2 and Table 2-1). At 24 hours of development, 81.42% (± 3.3) of oocytes that had been treated with SR-FLICA had cleaved compared to 82.23% (± 4.8) of control oocytes. On day 5 of development, 5.3% (± 0.6) of oocytes treated with SR-FLICA had developed into blastocysts compared to 6.23% (± 2.5) of the control oocytes.

The following day on day 6 of development, 15.30% (± 3.3) of the SR-FLICA stained oocytes had developed to blastocysts compared to 12.2% (± 2.4) of the control oocytes. By day 7, 17.73% (± 4.4) of SR-FLICA stained oocytes had developed into blastocysts compared to 16.40% (± 3.9) of oocytes not exposed to the stain. No statistical differences were identified at any of the 4 stages of development ($P \geq 0.95$).

Experiment 3

Embryos stained with SR-FLICA on day 3 of development (Figure 2-3) showed no significant correlation between SR-FLICA score that indicates the relative level of apoptosis and number of cells ($R^2 = 0.01$, $P = 0.2$). On day 3 of development, SR-FLICA scores appear to be normally distributed with a skew towards high SR-FLICA values (Supplemental Figure 2-1a). Day 3 embryos that were sorted into high and low incidence of apoptosis groups had a statistically different relative level of apoptosis ($P < 0.0001$) with the average high apoptosis SR-FLICA score of 54.93 (± 2.7) and the average low apoptosis SR-FLICA score of 33.76 (± 0.3) (Supplemental Figure 2-1b).

When day 3 embryos were sorted into high and low apoptosis groups and then followed for development (Figure 2-4, Table 2-2), no significant differences in blastocyst rates occurred on day 5 ($P = 0.49$), day 6 ($P = 0.99$), or day 7 ($P = 0.49$). On day 5, 7.73% (± 2.1) of the embryos sorted into the high apoptosis group on day 3 of development had reached the blastocyst stage while 13.74% (± 3.8) of the embryos considered low apoptosis on day 3 had reached the blastocyst stage. On day 6 of development, 22.48% (± 1.7) of the high apoptosis embryos were blastocysts while

22.53% (± 4.8) of the low apoptosis embryo had reached the blastocyst stage. On day 7 of development, 21.68% (± 1.3) of the high apoptosis embryos had reached the blastocyst stage of development and 27.9% (± 4.4) of the low apoptosis embryos had reached this stage.

After tracking development of day 3 sorted embryos through day 7 of development, cell numbers were counted for all embryos in the high and low apoptosis groups (Figure 2-5), whether they had reached the blastocyst stage or not. The average number of cells in day 7 embryos was 7.70 ± 0.6 for high apoptosis embryos and 8.13 ± 0.7 for low apoptosis embryos with no statistical difference between the two groups ($P = 0.63$). Cell numbers per embryo were low because a majority of the embryos stalled in development and failed to reach the blastocyst stage of development.

When embryos were not stained until the blastocyst stage on day 6 of development, again no statistically significant correlation was found between the relative level of apoptosis and cell number per blastocysts ($R^2 = 0.003$, $P = 0.53$; Figure 2-6a). Sorting these blastocysts into high and low incidence of apoptosis showed no significant difference in cell numbers ($P = 0.18$) with high apoptosis blastocysts containing an average of 34.22 ± 2.6 cells and low apoptosis embryos containing an average of 39.54 ±3.0 cells (Figure 2-6b). For reference, *in vivo* produced porcine blastocysts typically contain more than 50 cells per embryo [93, 94]. Again there was a significant statistical difference in SR-FLICA scores for the high compared to low apoptosis blastocyst ($P < 0.0001$, Supplemental Figure 2-2b). SR-FLICA staining of day 6 embryos again showed

SR-FLICA scores with a close to normal distribution but skewed towards high SR-FLICA scores (Supplemental Figure 2-2a).

Experiment 4

Comparing gene expression of high to low apoptosis SCNT blastocysts found no genes with significantly different gene expression (Table 2-3). High apoptosis SCNT blastocyst and *in vivo* blastocysts had 5 genes with significantly different levels of expression (*AIFM1*, P = 0.05; *BAX*, P = 0.004, *CDKN1A*, P = 0.007, *GNAS*, P = 0.047, and *GRB10*, P = 0.004). Interestingly, 3 of these genes have a function in apoptosis while 2 are imprinted genes. Low apoptosis SCNT blastocysts and *in vivo* blastocysts had 5 genes with significantly different expression levels (*ATM*, P = 0.02; *BAX*, P = 0.004; *CDKN1A*, P = 0.005; *GRB10*, P = 0.004; and *IGF2*, P = 0.02). Again, it is noteworthy that 3 of these genes have a functional classification of apoptosis and 2 of imprinted genes. Finally, comparing SCNT blastocysts (combining the high and low apoptosis blastocysts) to *in vivo* produced blastocysts, 6 genes are statistically different in gene expression level (*ATM*, P = 0.02; *BAX*, P = 0.002, *CDKN1A*, P = 0.002, *GNAS*, P = 0.04, *GRB10*, 0.002, and *CMYC*, P = 0.04).

In the apoptosis gene functional class, statistically different expression was found in *AIFM1* [high vs IVV (FDR P = 0.047)], *ATM* [low vs. IVV (FDR P = 0.02) and SCNT vs. IVV (FDR P = 0.02)], *BAX* [high vs. IVV (FDR P = 0.003), low vs. IVV (FDR P = 0.003) and SCNT vs. IVV (FDR P = 0.002)], and *CDKN1A* [high vs. IVV (FDR P = 0.007), low vs. IVV (FDR P = 0.005), and SCNT vs. IVV (FDR P = 0.002)] (Figure 2-7).

Genes involved in epigenetic regulation had no statistical differences in any of the comparisons. However, three comparisons trended towards significance [DNMT1A low vs. IVV (FDR P = 0.07), DNMT1A SCNT vs. IVV (FDR P = 0.09), and KDM4C SCNT vs. IVV (FDR P = 0.09)] (Figure 2-8). In the imprinted gene category, statistically different expression was found in *GNAS* [high vs. IVV (FDR P = 0.047) and SCNT vs. IVV (FDR P = 0.042)], *GRB10* [high vs. IVV (FDR P = 0.004), low vs. IVV (FDR P = 0.004), and SCNT vs. IVV (FDR P = 0.002)], and *IGF2* [low vs. IVV (FDR P = 0.012)]. (Figure 2-9). No maternal effect genes showed significantly different expression levels in any of the comparisons (Figure 2-10). In the pluripotency genes, one statistically different comparison was identified and three trended towards significance [CMYC SCNT vs. IVV (FDR P = 0.04), CMYC low vs. IVV (FDR P = 0.06), LIN28 low vs. IVV (FDR P = 0.08), and LIN28 SCNT vs. IVV (FDR P = .052)]. (Figure 2-11). In trophoblast differentiation and function genes, no significantly differentially expressed genes were identified (Figure 2-12). Housekeeping genes showed relatively consistent gene expression as intended and no significant differences in expression were identified in any of the analyses (Figure 2-13).

Unsupervised hierarchical clustering of gene expression data using ΔΔCT values indicated that the *in vivo* blastocysts generally clustered separately from the SCNT blastocysts (Figure 2-14). IVV samples additionally clustered separately based on the sow they were collected from (IVV 1-6 were collected from sow 1 while IVV 7-11 were collected from sow 2) which was expected as there were clear morphological differences in the embryos from each collection. However, there was no clear separation of the high and low apoptosis SCNT blastocysts.

PCA found that PC1 accounted for 36.1% of the variation while PC2 accounted for 10.8% of variation (Figure 2-15). SCNT blastocysts separated away from the IVV samples. But again there was no clear separation of the high and low apoptosis blastocysts as the prediction ellipses were nearly identical.

Discussion

While SR-FLICA has been used to detect active caspase activity in other cell lines, this is the first report of its use in fetal fibroblasts and developing embryos. The potential to evaluate apoptosis in live, developing embryos could prove to be a vital non-invasive biomarker for embryo competence following transfer. However, before this technology can be used to identify healthy embryos, it had to first be validated to accurately mark embryos undergoing apoptosis and prove to be non-toxic during the sensitive period accompanying early embryo development. SR-FLICA staining of porcine fetal fibroblast (PFF) cells showed a significant correlation with the more traditionally used TUNEL staining. By inducing cells to undergo apoptosis through staurosporine treatment, a dose response was seen in both SR-FLICA and TUNEL staining from 0 µM to 0.4 µM of staurosporine treatment. The percent of cells positive for SR-FLICA and TUNEL staining following 2 µM staurosporine treatment was equal to or even a little less than the percent of positive cells after 0.4 µM staurosporine treatment. The decrease in percent of apoptotic cells could be an effect of the highest dose of staurosporine inducing apoptosis earlier than the lower doses, the cells completing apoptosis, and being sloughed off before the staining procedure was

performed. These results validate the use of SR-FLICA to identify cells undergoing apoptosis.

In order for SR-FLICA to be a relevant biomarker of embryo competency, it must be compatible with early embryo development. Oocytes treated with SR-FLICA developed at equivalent rates at cleavage and the blastocyst stage compared to oocytes that were not treated. The lack of hindrance on development is one early indication that the staining process is non-toxic at these early stages of development. However, until embryo transfers are performed following SR-FLICA staining, it is impossible to know the long-term effects of the treatment during this critical window of development. Additionally, it is unknown if the specific timing of staining will have an effect different from treatment at the oocyte stage and what stage will provide the best time point to use apoptosis as a biomarker for future development.

Previous studies have noted that apoptosis detected by TUNEL staining is not apparent in zygote and cleavage stage embryos and does not appear until around the time of the maternal-to-zygotic transition [71]. With the maternal-to-zygotic transition occurring at the 4-8 cell stage in porcine embryos, we performed staining on day 3 of development, as this process should be beginning. At day 3 of development, there was no correlation between the relative level of apoptosis and number of cells in the embryo. Additionally, sorting these embryos into high and low incidence of apoptosis groups showed no difference in blastocyst rates on day 5, 6, and 7 of development. On day 7 of development, embryos from high and low incidence of apoptosis groups had no significant difference in total number of cells per embryo. Together, these results

indicate that sorting SCNT embryos on day 3 of development based on incidence of apoptosis does not isolate the embryos most likely to develop into blastocysts or develop more cells by day 7, an indication of embryo quality.

Therefore, we turned our attention from day 3 embryos to day 6 blastocysts, a stage commonly transferred into surrogate females. By waiting until day 6 of development, the embryos have proved some level of developmental competence by reaching the blastocyst stage. Day 6 PA blastocysts showed no correlation between relative level of apoptosis and cell number. In addition, high apoptosis blastocysts and low apoptosis blastocysts had no significant difference in cell number which is related to embryo quality. To better understand embryo competence based on relative incidence of apoptosis, gene expression analysis of individual blastocysts was performed.

Quantitative PCR was used to analyze relative gene expression of high and low apoptosis day 6 SCNT blastocysts relative to *in vivo* produced blastocysts. Seven functional gene classes were analyzed including apoptosis genes, epigenetic regulation genes, imprinted genes, maternal effect genes, pluripotency genes, trophoblast differentiation and function genes, and housekeeping genes. Fold change values were normalized to *in vivo* produced blastocysts and average log2 fold change values were graphed for each group. Notably, no genes were differentially expressed between the high and low apoptosis groups. One possibility is that we did not select the correct genes for analysis, and as a result missed finding gene expression differences that are present between the high and low apoptosis blastocysts. It is also possible that changes in gene expression in high quality embryos are not consistent, and thus, not discernable by the

statistical methods used in this study for data analyses. Further studies using RNA-seq would provide a more complete picture of the gene expression differences between high and low apoptosis embryos.

SCNT compared to *in vivo* produced embryos are expected to show more gene expression differences as it has already been reported in numerous studies that cloned embryos show altered gene expression patterns compared to *in vivo* produced embryos [21, 64, 95]. In this case, 6 of 65 genes were significantly differentially expressed in SCNT embryos compared to *in vivo* embryos, including *ATM*, *BAX*, *CDKN1A*, *GNAS*, *GRB10*, and *CMYC*. Interestingly, half of these genes are related to apoptosis, two are imprinted genes, and one is related to pluripotency. All three apoptosis genes, *ATM*, *BAX*, and *CDKN1A*, have increased expression in SCNT blastocysts compared to *in vivo* blastocysts. *GNAS* and *GRB10*, both imprinted genes, also show increased expression levels in SCNT embryos compared to the *in vivo* blastocysts. Finally, *CMYC*, a pluripotency gene, had decreased expression in SCNT blastocysts compared to the *in vivo* reference samples. Together, these altered gene expression patterns of SCNT blastocysts compared to *in vivo* blastocysts indicate the possibility of less competent embryos due to increased apoptosis gene expression, increased imprinted gene expression, and decreased pluripotency gene expression.

Unsupervised hierarchical clustering analysis also indicated no clear difference between high and low apoptosis SCNT blastocysts. Rather than sorting by incidence of apoptosis, high and low apoptosis blastocysts were muddled together while *in vivo* blastocysts sorted on their own. There were two clear groups of *in vivo* produced

blastocysts that sorted based on the collection day, indicating that there could have been a slight difference in developmental timing between each collection. Similar clustering patterns were also evident in principal component analysis.

In conclusion, these data indicate that SR-FLICA could be a useful biomarker of apoptosis during embryo development. Initial data supports the non-toxic nature of SR-FLICA, even during early embryo development. Induction of apoptosis in PFF cells validates that SR-FLICA identifies apoptosis similarly to the more traditionally used TUNEL method, without the need to sacrifice the cells prior to staining. These *in vitro* experiments did not find a difference in high and low apoptosis embryos in terms of cell numbers, developmental potential, or gene expression patterns. But it is still unknown how high and low apoptosis embryos would develop *in vivo* following embryo transfer. Future studies focusing on global gene expression patterns and epigenetic reprogramming as indicated by DNA methylation will provide a more complete explanation of the differences between high and low apoptosis embryos. Additional studies following high and low apoptosis embryos after transfer will provide insight into the developmental potential of these embryos at both establishing and maintaining pregnancy following SCNT in an attempt to increase overall efficiency by selecting the embryos most likely to succeed.

References

1. Oback B, Wells DN. Donor cell differentiation, reprogramming, and cloning efficiency: elusive or illusive correlation? Mol Reprod Dev 2007; 74:646-654.

2. Hiiragi T, Solter D. Reprogramming is essential in nuclear transfer. Mol Reprod Dev 2005; 70:417-421.

3. Boiani M, Gentile L, Gambles VV, Cavaleri F, Redi CA, Scholer HR. Variable reprogramming of the pluripotent stem cell marker Oct4 in mouse clones: distinct developmental potentials in different culture environments. Stem Cells 2005; 23:1089-1104.

4. Oback B. Climbing Mount Efficiency--small steps, not giant leaps towards higher cloning success in farm animals. Reprod Domest Anim 2008; 43 Suppl 2:407-416.

5. Armstrong L, Lako M, Dean W, Stojkovic M. Epigenetic modification is central to genome reprogramming in somatic cell nuclear transfer. Stem Cells 2006; 24:805-814.

6. Dean W, Santos F, Reik W. Epigenetic reprogramming in early mammalian development and following somatic nuclear transfer. Semin Cell Dev Biol 2003; 14:93-100.

7. Niemann H, Carnwath JW, Herrmann D, Wieczorek G, Lemme E, Lucas-Hahn A, Olek S. DNA methylation patterns reflect epigenetic reprogramming in bovine embryos. Cell Reprogram 2010; 12:33-42.

8. Smith C, Berg D, Beaumont S, Standley NT, Wells DN, Pfeffer PL. Simultaneous gene quantitation of multiple genes in individual bovine nuclear transfer blastocysts. Reproduction 2007; 133:231-242.

9. Rocha JC, Passalia F, Matos FD, Maserati MP, Jr., Alves MF, Almeida TG, Cardoso BL, Basso AC, Nogueira MF. Methods for assessing the quality of

mammalian embryos: How far we are from the gold standard? JBRA Assist Reprod 2016; 20:150-158.

10. Kidd VJ, Lahti JM, Teitz T. Proteolytic regulation of apoptosis. Semin Cell Dev Biol 2000; 11:191-201.
11. Saraste A, Pulkki K. Morphologic and biochemical hallmarks of apoptosis. Cardiovasc Res 2000; 45:528-537.
12. Elmore S. Apoptosis: a review of programmed cell death. Toxicol Pathol 2007; 35:495-516.
13. Parrish AB, Freel CD, Kornbluth S. Cellular Mechanisms Controlling Caspase Activation and Function. Cold Spring Harb Perspect Biol 2013; 5.
14. Hardy K. Cell death in the mammalian blastocyst. Mol Hum Reprod 1997; 3:919-925.
15. Lai L, Prather RS. Production of cloned pigs by using somatic cells as donors. Cloning Stem Cells 2003; 5:233-241.
16. Yoshioka K, Suzuki C, Tanaka A, Anas IM, Iwamura S. Birth of piglets derived from porcine zygotes cultured in a chemically defined medium. Biol Reprod 2002; 66:112-119.
17. Cox L, Vanderwall DK, Parkinson KC, Sweat A, Isom SC. Expression profiles of select genes in cumulus-oocyte complexes from young and aged mares. Reprod Fertil Dev 2015; 27:914-924.
18. Benjamini Y, Hochberg Y. Controlling the False Discovery Rate: A Practical and Powerful Approach to Multiple Testing. Journal of the Royal Statistical Society. Series B (Methodological) 1995; 57:289-300.

19. Metsalu T, Vilo J. ClustVis: a web tool for visualizing clustering of multivariate data using Principal Component Analysis and heatmap. Nucleic Acids Res 2015; 43:W566-570.

20. Day BN, Macháty Z, Prather RS. Development of Early Porcine Embryos In Vitro and In Vivo1. Biology of Reproduction 1998; 59:451-455.

21. Pomar FJR, Teerds KJ, Kidson A, Colenbrander B, Tharasanit T, Aguilar B, Roelen BAJ. Differences in the incidence of apoptosis between in vivo and in vitro produced blastocysts of farm animal species: a comparative study. Theriogenology 2005; 63:2254-2268.

22. Matwee C, Betts DH, King WA. Apoptosis in the early bovine embryo. Zygote 2000; 8:57-68.

23. Whitworth KM, Agca C, Kim JG, Patel RV, Springer GK, Bivens NJ, Forrester LJ, Mathialagan N, Green JA, Prather RS. Transcriptional profiling of pig embryogenesis by using a 15-K member unigene set specific for pig reproductive tissues and embryos. Biol Reprod 2005; 72:1437-1451.

24. Cao S, Han J, Wu J, Li Q, Liu S, Zhang W, Pei Y, Ruan X, Liu Z, Wang X, Lim B, Li N. Specific gene-regulation networks during the pre-implantation development of the pig embryo as revealed by deep sequencing. BMC Genomics 2014; 15:4.

25. Prather RS, Redel BK, Whitworth KM, Zhao MT. Genomic profiling to improve embryogenesis in the pig. Anim Reprod Sci 2014; 149:39-45.

Tables

Table 2-1. Parthenogenetic development rates of oocytes treated with SR-FLICA compared to controls.

Treatment Group	No. of Oocytes	Cleaved[1], n (%)	D5[2], n (%)	D6[2], n (%)	D7[2], n (%)
SR-FLICA	237	190 (80.2%)	12 (5.1%)	35 (14.8%)	41 (17.3%)
Control	227	180 (79.3%)	16 (7.0%)	29 (12.8%)	40 (17.6%)

[1] Cleaved within 24 hours
[2] Blastocyst development rates on day 5, 6, and 7

Table 2-2. Blastocyst development rates from SCNT embryos sorted on day 3 of development.

Level of Apoptosis	No. of Embryos	D5[1], n (%)	D6[1], n (%)	D7[1], n (%)
High	153	13 (8.5%)	34 (22.2%)	33 (21.6%)
Low	153	22 (14.4%)	37 (24.2%)	43 (28.1%)

[1] Blastocyst development rates on day 5, 6, and 7

Table 2-3. FDR-corrected P-values following differential gene expression analysis[1].

Category and gene	High vs. Low	High vs. IVV	Low vs. IVV	SCNT vs. IVV
Apoptosis				
AIFM1	0.6926	0.0469*	0.2038	*0.0529*[#]
APAF1	0.9936	0.1302	0.1689	*0.0931*[#]
ATM	0.9511	0.1013	0.0189*	0.0185*
BAD	0.9511	0.7499	0.7965	0.7369
BAX	0.9511	0.0036*	0.0036*	0.0024*
BCLX	0.9511	0.2182	0.2879	0.2101
BID	0.6926	0.4728	0.9365	0.6894
CDKN1A	0.9936	0.0071*	0.0047*	0.0024*
HSP70	0.9511	0.4583	0.6673	0.5454
P53	0.9936	0.9259	0.8832	0.8888
XIAP	0.9936	0.3933	0.3296	0.2999
Epigenetic Regulation				
ASH2L	0.7745	0.2904	0.1529	0.1840
DMAP1	0.9936	0.2182	0.1809	0.1199
DNMT1A	0.6926	0.3379	0.0737[#]	0.0931[#]
DNMT3A	0.6869	0.6253	0.8326	0.8616
EHMT2	0.6869	0.2904	0.8703	0.5975
EZH2	0.6926	0.1302	0.4214	0.2093
HAT1	0.5148	0.1302	0.7553	0.2619
HDAC1	0.9936	0.6253	0.4775	0.4952
HDAC2	0.3962	0.6253	0.2879	0.7049
HDAC3	0.9931	0.5782	0.3296	0.3600
KAT2A	0.9936	0.6253	0.6371	0.5975
KDM3A	0.9936	0.3379	0.2997	0.2907
KDM4C	0.9936	0.2182	0.1529	0.0931[#]
MECP2	0.9511	0.4583	0.8437	0.5995
SIRT1	0.3745	0.8949	0.4160	0.6099
SUV39H1	0.9511	0.1302	0.2538	0.1480

Category and gene	High vs. Low	High vs. IVV	Low vs. IVV	SCNT vs. IVV
Imprinted Genes				
GNAS	0.9511	0.0469*	0.0813#	0.0416*
GRB10	0.6919	0.0036*	0.0036*	0.0024*
IGF2	0.2734	0.2375	0.0189*	0.0529#
IGF2R	0.9936	0.6002	0.5697	0.5829
IMPACT	0.9511	0.9259	0.6911	0.8615
NECT	0.9936	0.2182	0.1809	0.1840
NNAT	0.9511	0.1013	0.2879	0.0931#
RTL1	0.9511	0.3930	0.2997	0.3209
SNRPN	0.6926	0.8525	0.2734	0.4370
UBE3A	0.7452	0.6177	0.9365	0.7621
Maternal Effect				
BMP15	0.9931	0.2375	0.2879	0.2168
GDF9	0.9936	0.2375	0.2157	0.2101
MOS	0.9511	0.2375	0.2019	0.2093
ZP2	0.9931	0.2599	0.2157	0.2101
ZP3	0.6926	0.8949	0.3515	0.5959
Pluripotency				
CMYC	0.9936	0.1013	0.0619#	0.0416*
ID1	0.6926	0.8525	0.3296	0.5975
ID3	0.9931	0.4280	0.3296	0.3600
KLF4	0.9936	0.7558	0.6766	0.6886
LIN28	0.9936	0.1013	0.0838#	0.0515#
NANOG	0.9936	0.2904	0.2997	0.2168
POU5F1	0.9936	0.3379	0.3195	0.3104
SOX2	0.8887	0.4467	0.2879	0.3250
Trophoblast Differentiation and Function				
DLX3	0.9936	0.5782	0.487	0.5309
ESRRB	0.9936	0.5782	0.6673	0.5975
ETS2	0.7452	0.1750	0.5448	0.2168
KRT8	0.9511	0.3379	0.1598	0.1840
SFN	0.9936	0.6745	0.6673	0.6292
TACSTD2	0.6926	0.3379	0.2019	0.2168
TEAD4	0.9936	0.6414	0.6371	0.5995
VIM	0.7452	0.9259	0.3988	0.6099

Category and gene	High vs. Low	High vs. IVV	Low vs. IVV	SCNT vs. IVV
Housekeeping				
ACTB	0.3745	0.2874	0.6911	0.4370
EIF4a1	0.9931	0.1509	0.0983[#]	0.0931[#]
HSP90	0.9936	0.1013	0.0882[#]	0.0529[#]
RPS5	0.9936	0.3379	0.2808	0.2446
SF3A1	0.9511	0.7558	0.7553	0.9936
TAF11	0.2734	0.6273	0.0882*	0.2101
YWHAZ	0.9511	0.8404	0.5448	0.6292

[1] General linear mixed model analysis of gene expression comparing high apoptosis vs. low apoptosis samples, high apoptosis vs. IVV samples, low apoptosis vs. IVV samples, and SCNT vs. IVV samples where the high and low apoptosis samples are both compared to IVV samples. False discovery rate (FDR) P-values are reported. P-values deemed as significant (< 0.05) are indicated by *. P-values deemed as trending towards significant (< 0.1) are indicated by [#].

Figures

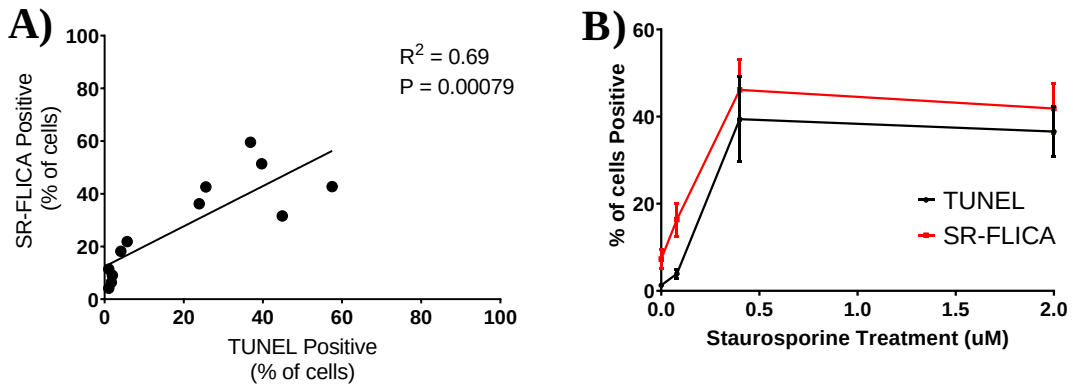

Figure 2-1. Relationship between percent of PFF cells SR-FLICA positive and TUNEL positive. Panel A shows the correlation between percent of cells that are SR-FLICA and TUNEL positive, indicating a close relationship between the two stains to detect apoptosis with an R^2 of 0.69 and a p-value of 0.0008. The three replicates of each staurosporine treatment (0 µM, 0.08 µM, 0.4 µM, and 2 µM) are represented on the graph with a linear regression line. Panel B indicates the average percent of cells from the 3 replicates that SR-FLICA or TUNEL positive at each staurosporine concentration (0 µM, 0.08 µM, 0.4 µM, and 2 µM) with error bars representing the standard error of the mean.

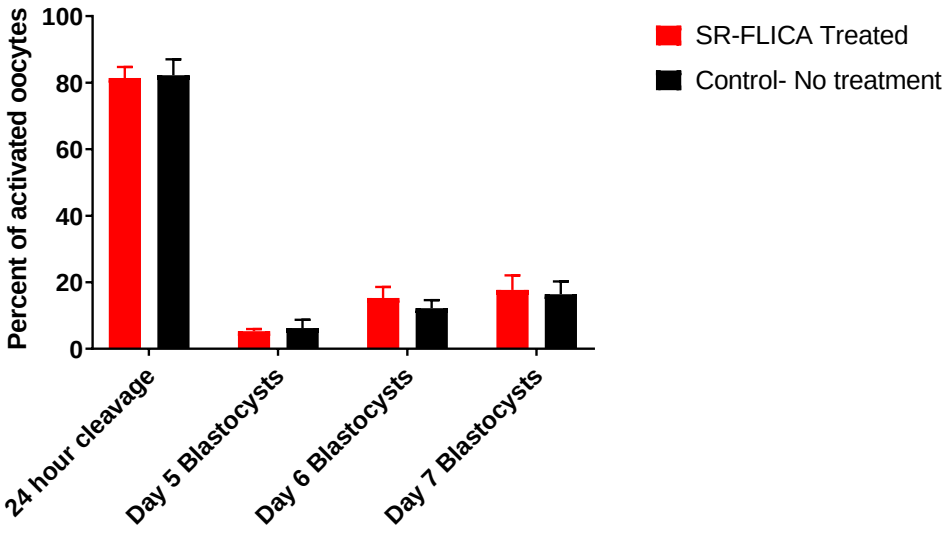

Figure 2-2. Embryo development from parthenogenetic activation following SR-FLICA treatment of oocytes compared to controls. SR-FLICA treated oocytes (n = 4, total 237 oocytes) compared to oocytes that had received no treatment (n = 4, total 227 oocytes). No significant difference was found at any of the developmental stages (24 hour cleavage, adjusted P = 0.99; Day 5 blastocysts, adjusted P = 0.99; Day 6 blastocysts, adjusted P = 0.95; Day 7 blastocysts, adjusted P = 0.99). Error bars indicate the standard error of the mean.

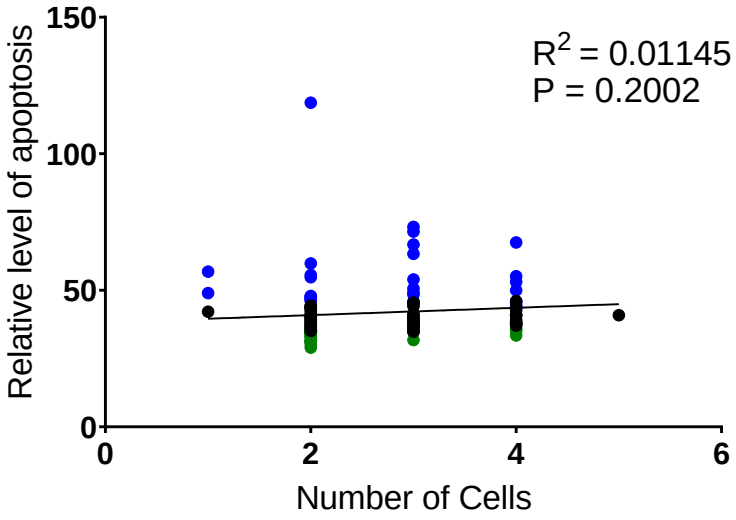

Figure 2-3. The correlation between SR-FLICA score and the number of cells in day 3 SCNT embryos (n = 156). There is no clear correlation between number of cells and level of apoptosis (r^2 = 0.01, P = 0.2). Blue indicates embryos in the top 20% of SR-FLICA scores and are considered high apoptosis. Green indicates embryos in the bottom 20% of SR-FLICA scores and are considered low apoptosis. Black is the remaining 60% of embryos.

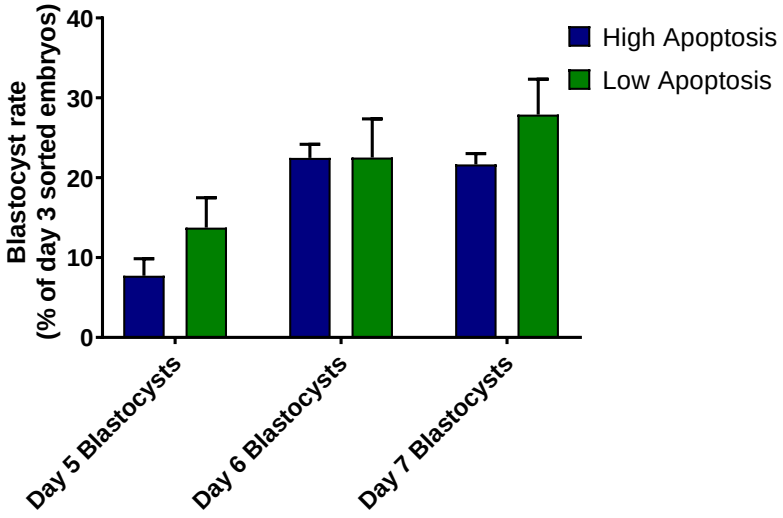

Figure 2-4. SCNT blastocyst development following SR-FLICA sorting on day 3 of development. Average blastocyst development rate (4 replicates) on day 5, 6, and 7 following SR-FLICA staining and embryo sorting on day 3 of development with error bars indicating the standard error. High apoptosis (n = 153) represents the embryos in the top 20% of SR-FLICA scores and low apoptosis (n = 153) represents the embryos in the bottom 20% of SR-FLICA scores. No significant differences in development were found on any day of development (day 5 blastocysts, adjusted P = 0.49; day 6 blastocysts, adjusted P = 0.99; day 7 blastocysts, adjusted P = 0.49).

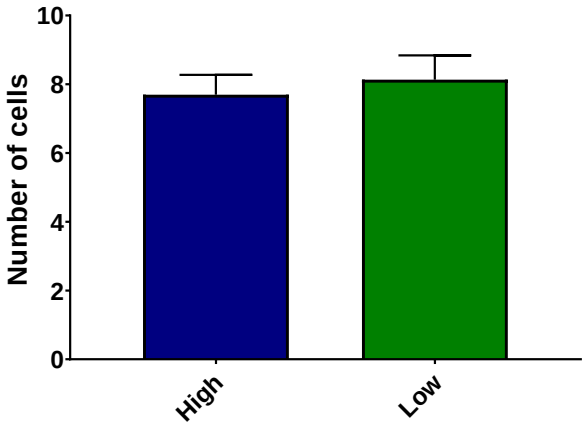

Figure 2-5. Average number of cells in day 7 embryos sorted by apoptosis levels on day 3. Average number of cells of high (4 replicates, total n = 151) and low (4 replicates, total n = 150) apoptosis day 7 SCNT embryos sorted on day 3 of development with standard error bars. All embryos had cells counted, regardless of their developmental stage on day 7. There was no significant difference between high and low apoptosis embryos (P = 0.63).

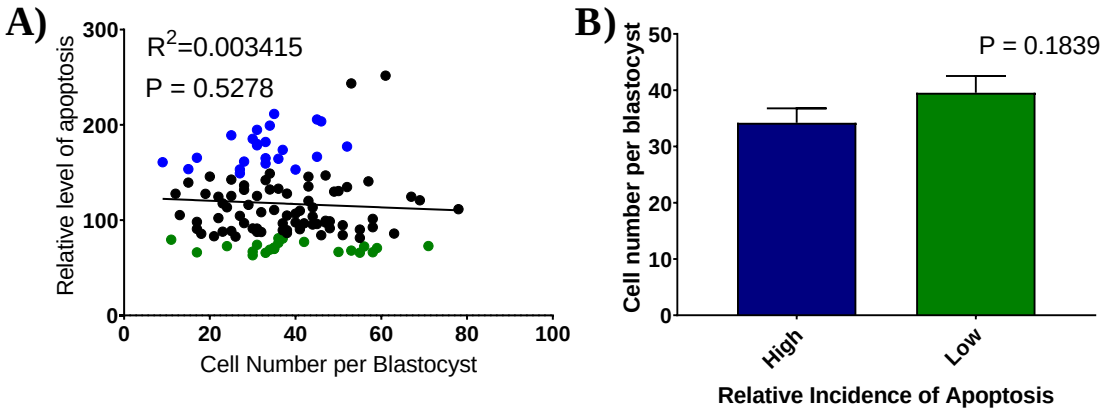

Figure 2-6. Connection between cell number and incidence of apoptosis. Panel A shows the relationship between cell number and the incidence of apoptosis in day 6 PA blastocysts (3 replicates, total n = 132). No correlation was found between the number of cells and relative level of apoptosis (r^2 = 0.003, P = 0.5). Blue and green indicate the top and bottom 20% of incidence of apoptosis, respectively. Panel B depicts the average number of cells per day 6 PA blastocyst in high (3 replicates, total n = 23) and low (3 replicates, total n = 24) incidence of apoptosis blastocysts. Error bars represent the standard error. No significant difference in the number of cells per embryo in high compared to low apoptosis blastocysts (P = 0.18).

\

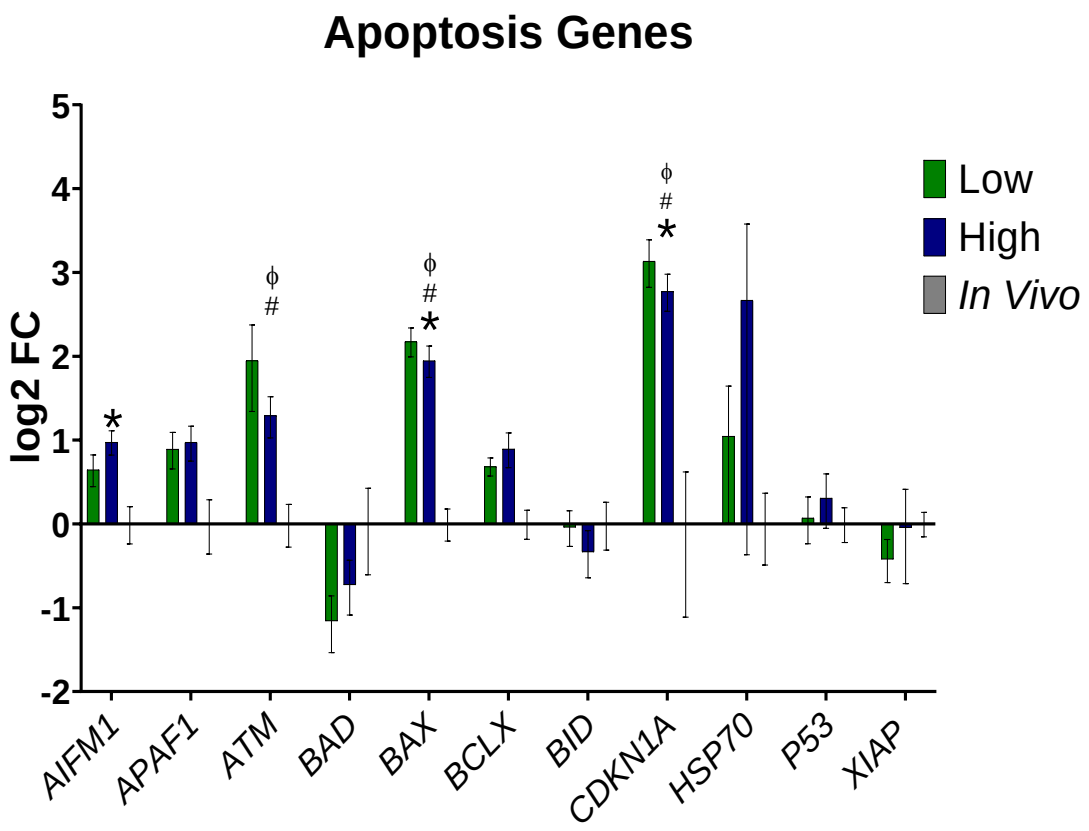

Figure 2-7. Gene expression of apoptosis genes. Log2 fold change comparing gene expression of apoptosis genes between *in vivo* produced blastocysts and SCNT blastocysts with high and low levels of apoptosis with standard error bars. Fold change values have been normalized to the *in vivo* blastocysts. Data represents 3 replicate cloning sessions (high n=13; low n=13) and 2 replicate *in vivo* blastocyst collections (n=11). However, not every qPCR reaction worked, so number of samples analyzed per group for each gene can be found in Supplemental Table 1. A generalized linear mixed model was fit to the data and analysis compared gene expression of high vs. low, high vs. IVV, low vs. IVV, and SCNT vs. IVV.

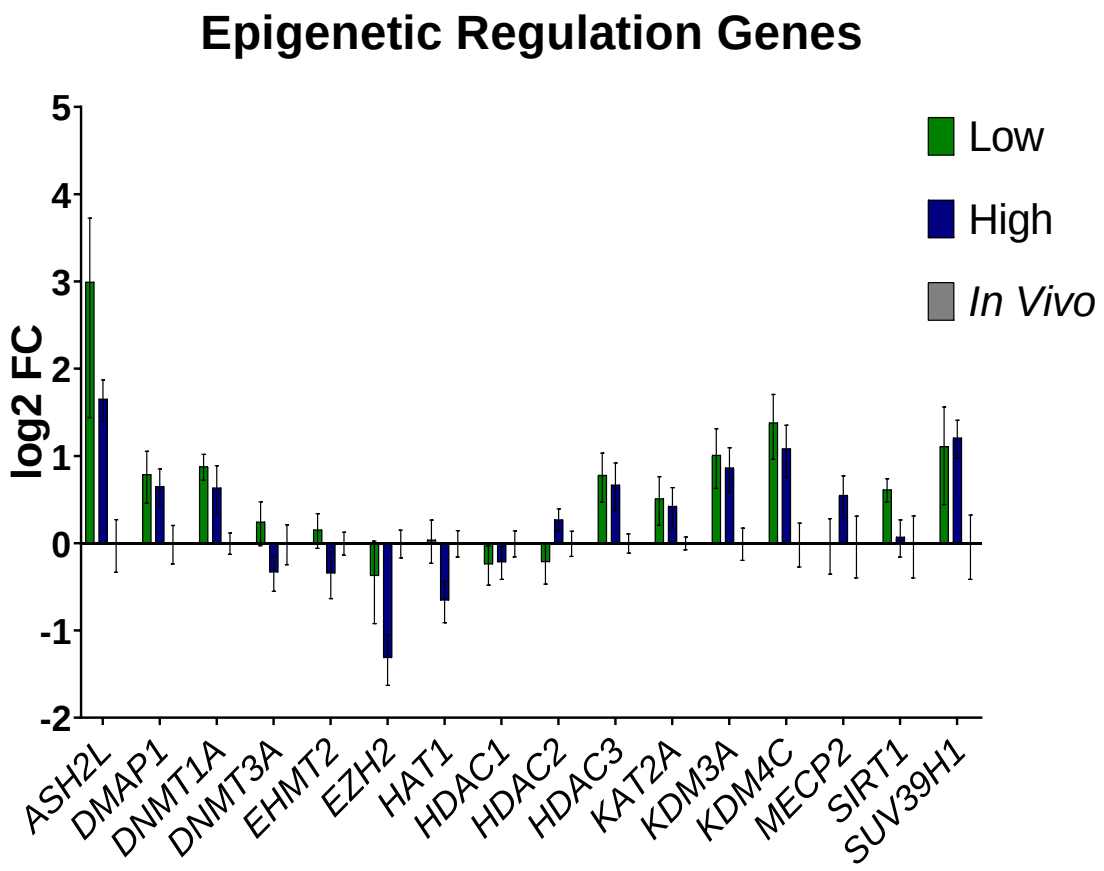

Figure 2-8. Gene expression of epigenetic regulation genes. Log2 fold change comparing gene expression of epigenetic regulation genes between *in vivo* produced blastocysts and SCNT blastocysts with high and low levels of apoptosis with standard error bars. Fold change values have been normalized to the *in vivo* blastocysts. Data represents 3 replicate cloning sessions (high n=13; low n=13) and 2 replicate *in vivo* blastocyst collections (n=11). However, not every qPCR reaction worked, so number of samples analyzed per group for each gene can be found in Supplemental Table 1. A generalized linear mixed model was fit to the data and analysis compared gene expression of high vs. low, high vs. IVV, low vs. IVV, and SCNT vs. IVV. No statistical differences were found in any of the comparisons.

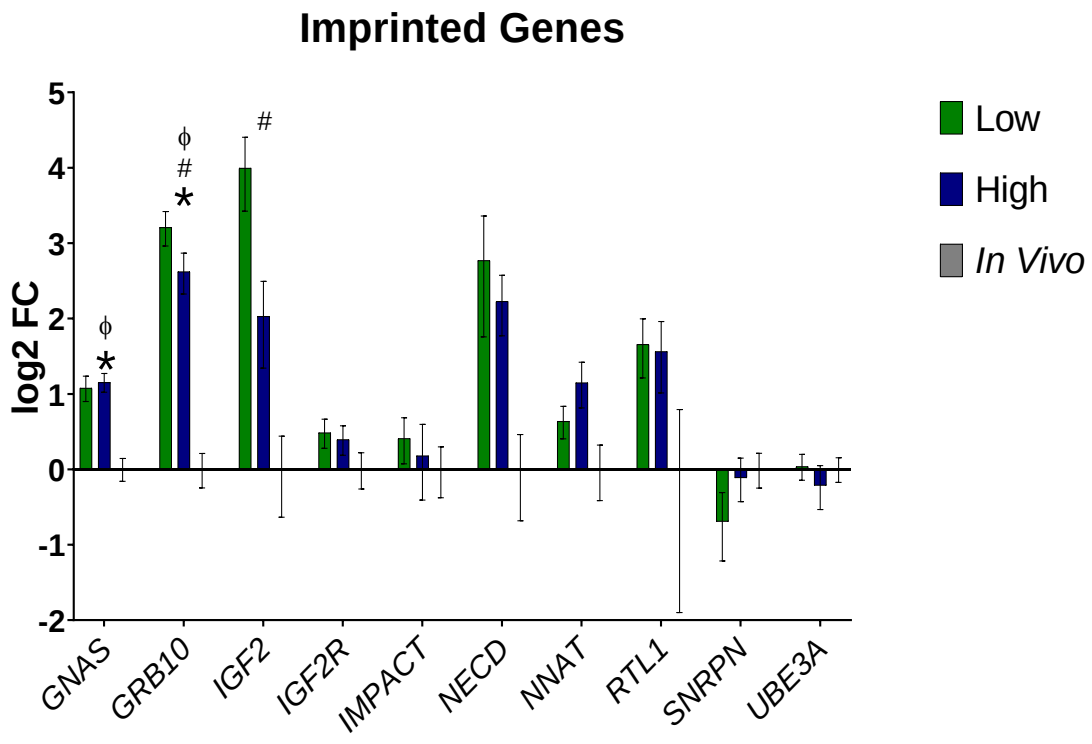

Signficant Difference in gene expression:* High v. IVV, # Low v. IVV, ϕ SCNT v. IVV

Figure 2-9. Gene expression of imprinted genes. Log2 fold change comparing gene expression of imprinted genes between *in vivo* produced blastocysts and SCNT blastocysts with high and low levels of apoptosis with standard error bars. Fold change values have been normalized to the *in vivo* blastocysts. Data represents 3 replicate cloning sessions (high n=13; low n=13) and 2 replicate *in vivo* blastocyst collections (n=11). However, not every qPCR reaction worked, so number of samples analyzed per group for each gene can be found in Supplemental Table 1. A generalized linear mixed model was fit to the data and analysis compared gene expression of high vs. low, high vs. IVV, low vs. IVV, and SCNT vs. IVV.

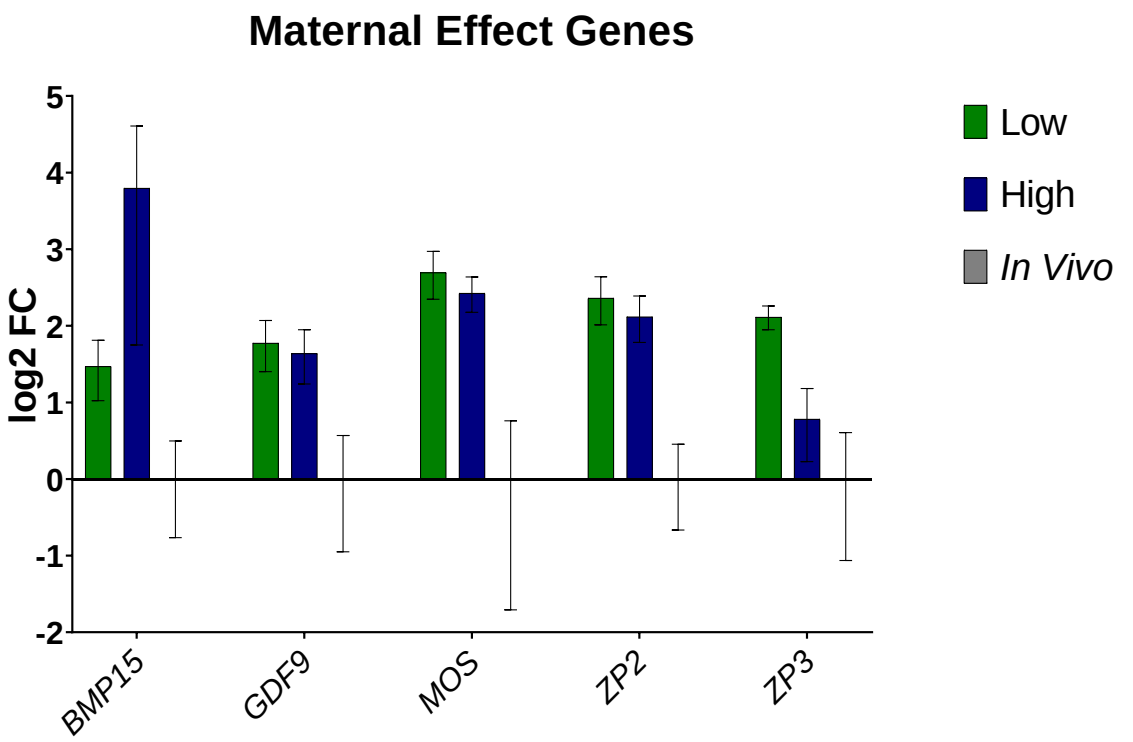

Figure 2-10. Gene expression of maternal effect genes. Log2 fold change comparing gene expression of maternal effect genes between *in vivo* produced blastocysts and SCNT blastocysts with high and low levels of apoptosis with standard error bars. Fold change values have been normalized to the *in vivo* blastocysts. Data represents 3 replicate cloning sessions (high n=13; low n=13) and 2 replicate *in vivo* blastocyst collections (n=11). However, not every qPCR reaction worked, so number of samples analyzed per group for each gene can be found in Supplemental Table 1. A generalized linear mixed model was fit to the data and analysis compared gene expression of high vs. low, high vs. IVV, low vs. IVV, and SCNT vs. IVV. No statistically significant differences were determined between any of the comparisons.

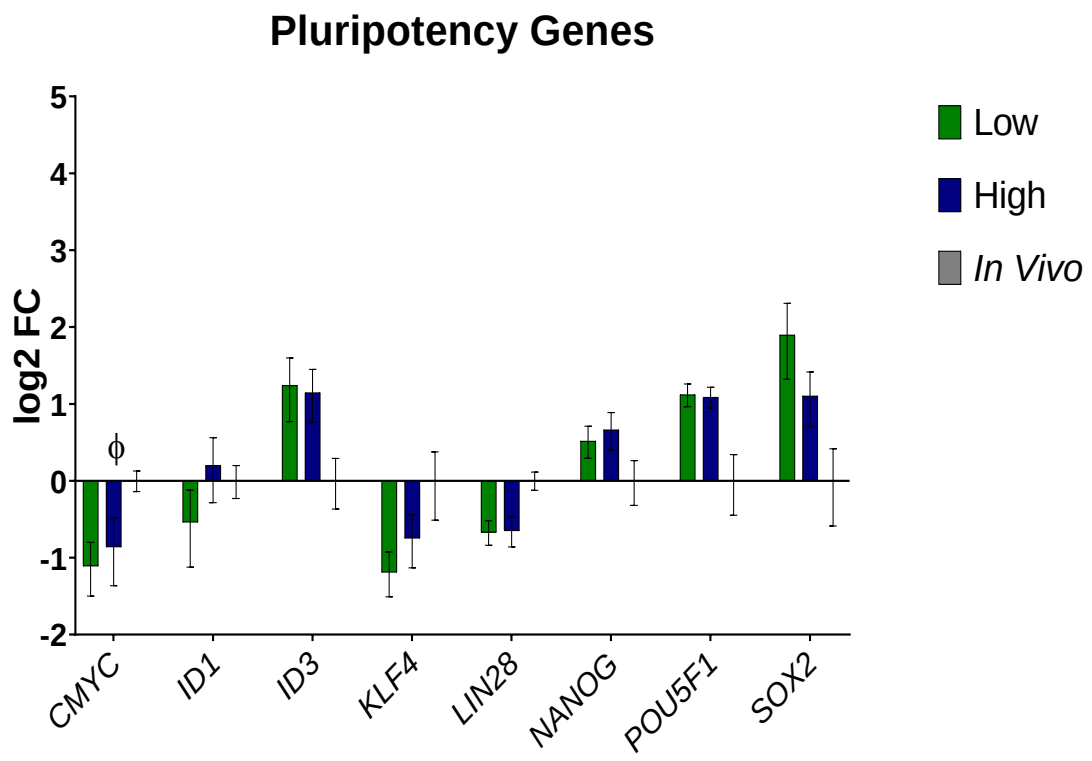

Figure 2-11. Gene expression of pluripotency genes. Log2 fold change comparing gene expression of pluripotency genes between *in vivo* produced blastocysts and SCNT blastocysts with high and low levels of apoptosis with standard error bars. Fold change values have been normalized to the *in vivo* blastocysts. Data represents 3 replicate cloning sessions (high n=13; low n=13) and 2 replicate *in vivo* blastocyst collections (n=11). However, not every qPCR reaction worked, so number of samples analyzed per group for each gene can be found in Supplemental Table 1. A generalized linear mixed model was fit to the data and analysis compared gene expression of high vs. low, high vs. IVV, low vs. IVV, and SCNT vs. IVV.

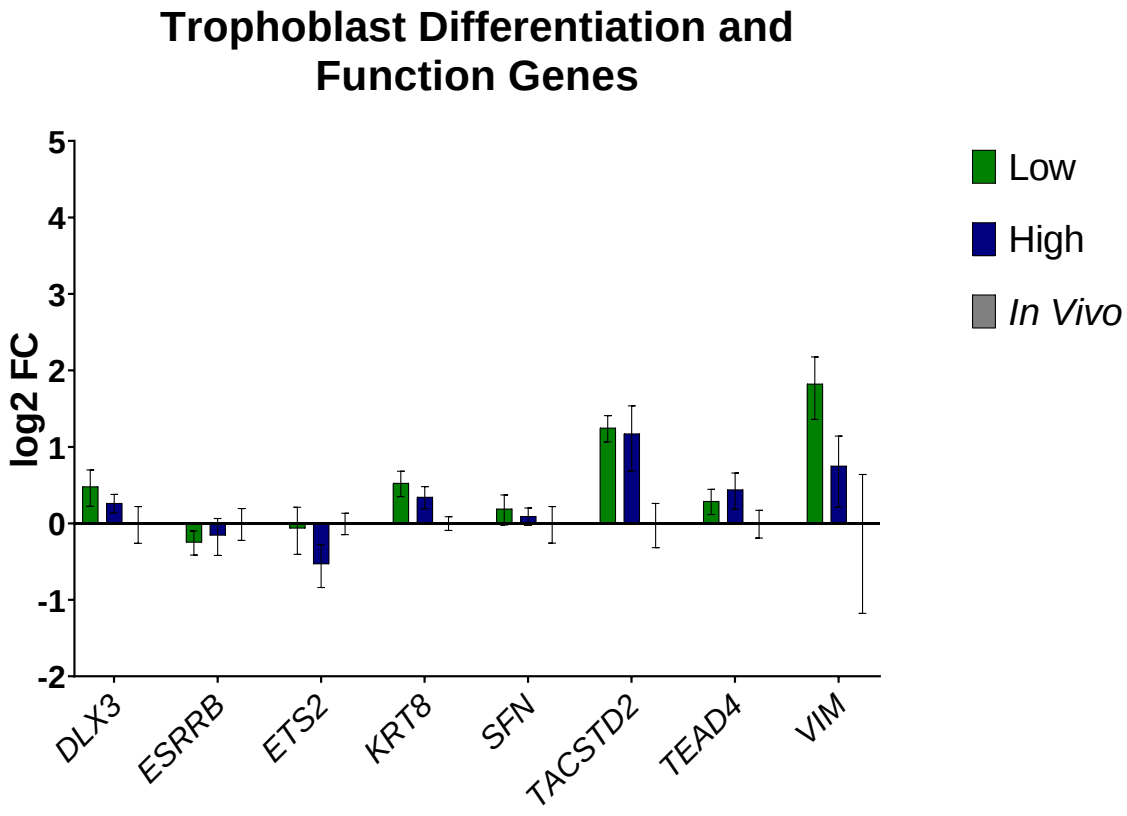

Figure 2-12. Gene expression of trophoblast differentiation and function genes. Log2 fold change comparing gene expression of trophoblast differentiation and function genes between *in vivo* produced blastocysts and SCNT blastocysts with high and low levels of apoptosis with standard error bars. Fold change values have been normalized to the *in vivo* blastocysts. Data represents 3 replicate cloning sessions (high n=13; low n=13) and 2 replicate *in vivo* blastocyst collections (n=11). However, not every qPCR reaction worked, so number of samples analyzed per group for each gene can be found in Supplemental Table 1. A generalized linear mixed model was fit to the data and analysis compared gene expression of high vs. low, high vs. IVV, low vs. IVV, and SCNT vs. IVV. No statistically significant differences were determined between any of the comparisons.

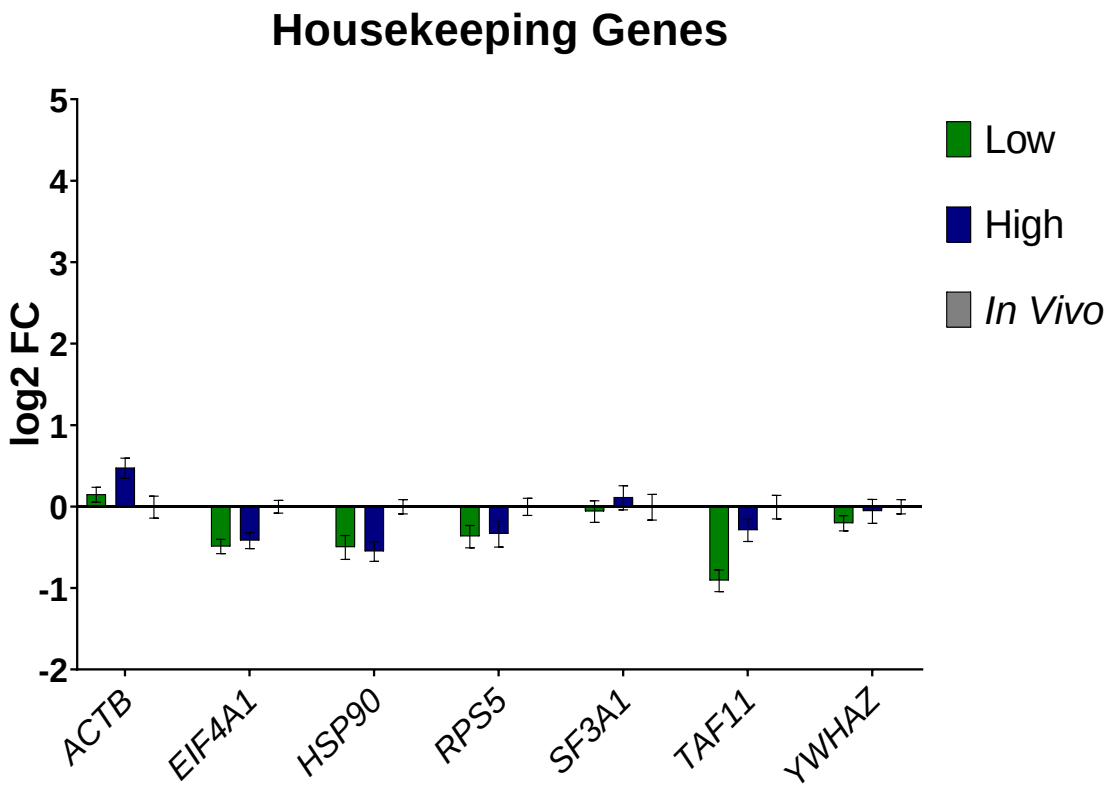

Figure 2-13. Gene expression of housekeeping genes. Log2 fold change comparing gene expression of housekeeping genes between *in vivo* produced blastocysts and SCNT blastocysts with high and low levels of apoptosis with standard error bars. Fold change values have been normalized to the *in vivo* blastocysts. Data represents 3 replicate cloning sessions (high n=13; low n=13) and 2 replicate *in vivo* blastocyst collections (n=11). However, not every qPCR reaction worked, so number of samples analyzed per group for each gene can be found in Supplemental Table 1. A generalized linear mixed model was fit to the data and analysis compared gene expression of high vs. low, high vs. IVV, low vs. IVV, and SCNT vs. IVV. No statistically significant differences were determined between any of the comparisons.

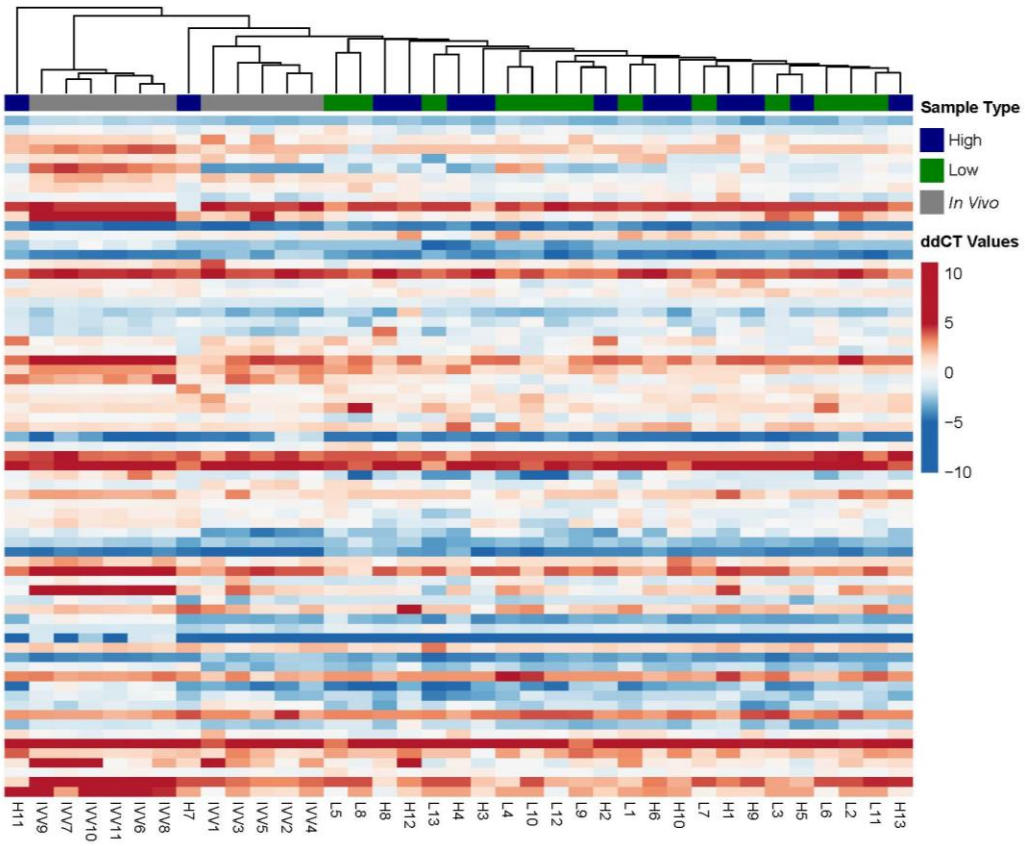

Figure 2-14. Unsupervised hierarchical clustering. An unsupervised hierarchical clustering analysis of gene expression data using ΔΔCT values. Hierarchical clustering produced using correlation metric with average linkage clustering using the Clustvis program. Blue and red indicates ΔΔCT values. On the sample tree, green indicates a low apoptosis sample, navy a high apoptosis sample, and grey an *in vivo* samples.

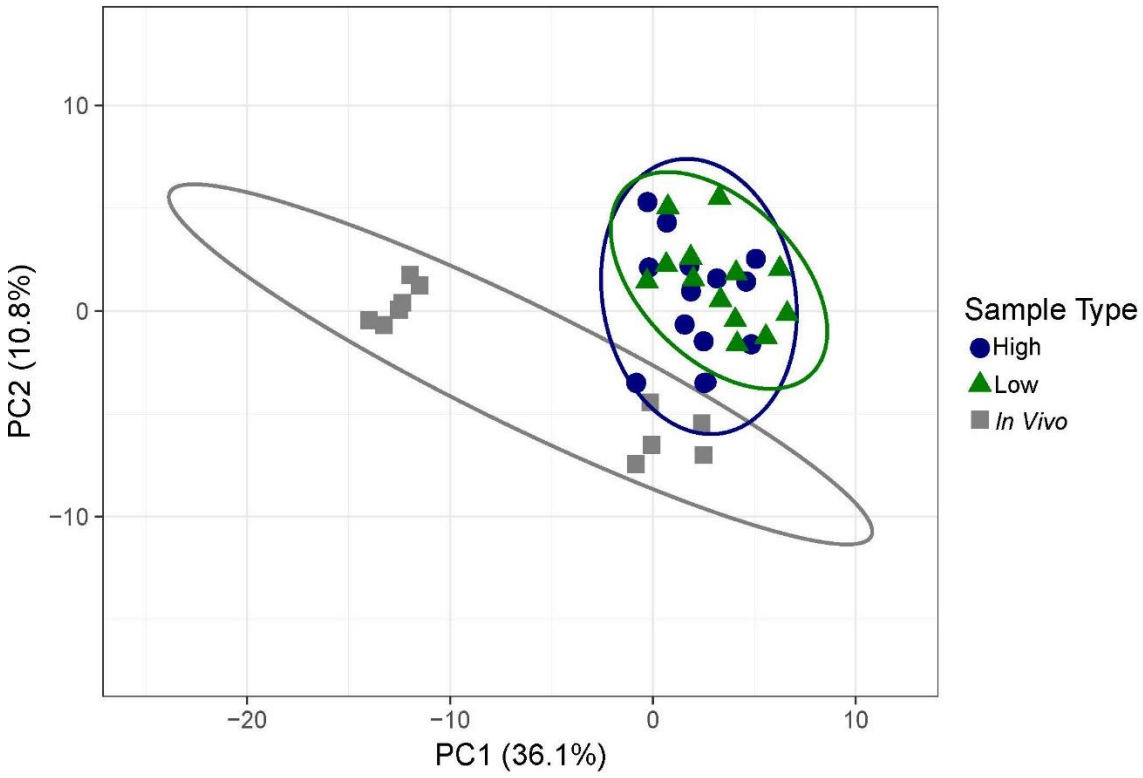

Figure 2-15. Principal component analysis of gene expression. A PCA of gene expression data using ΔΔCT values. No scaling was applied to rows. SVD with imputation is used to calculate principal components. X and Y axis show PC1 and 2 that explain 36.1% and 10.8% of the total variance, respectively. Prediction ellipses are such that with 95% confidence, a new observation from the same group should fall within the ellipse. Blue circles indicate high apoptosis samples. Green triangles indicate low apoptosis samples. Grey squares indicate *in vivo* samples. N = 37 data points.

Supplemental Tables and Figures

Supplementary Table 2-1. The number of samples analyzed per group for each gene analyzed in qPCR analysis.

Category and Gene	Low	High	*In Vivo*
Apoptosis			
APAF1	13	13	11
AIFM1	11	13	11
ATM	13	13	11
BAD	13	12	11
BAX	13	13	11
BCLX	13	13	11
BID	10	13	11
CDKN1A	13	13	9
HSP70	8	7	10
P53	12	11	11
XIAP	11	9	11
Epigenetic Regulation			
ASH2L	3	3	10
DMAP1	11	12	11
DNMT1A	11	10	11
DNMT3A	11	13	11
EHMT2	12	11	11
EZH2	7	9	11
HAT1	13	12	11
HDAC1	11	12	11
HDAC2	13	13	11
HDAC3	13	13	11
KAT2A	12	11	11
KDM3A	12	13	11
KDM4C	10	12	11
MECP2	4	10	11
SIRT1	13	13	11
SUV39H1	8	12	11
Imprinted Genes			
GNAS	13	13	11
GRB10	12	13	10
IGF2	12	9	9
IGF2R	13	13	11
IMPACT	9	7	11
NECT	11	10	11
NNAT	3	5	10
RTL1	5	6	6
SNRPN	7	6	11
UBE3A	13	12	11

Category and Gene	Low	High	*In Vivo*
Maternal Effect			
BMP15	4	7	5
GDF9	10	7	10
MOS	9	8	8
ZP2	6	12	10
ZP3	4	10	8
CMYC	9	8	11
ID1	4	5	11
ID3	9	7	8
KLF4	12	13	11
LIN28	13	13	11
NANOG	12	10	11
POU5F1	13	13	11
SOX2	12	12	11
Trophoblast Differentiation and Function			
DLX3	12	12	11
ESRRB	13	13	11
ETS2	11	13	11
KRT8	13	13	11
SFN	13	13	11
TACSTD2	13	13	11
TEAD4	13	13	11
VIM	5	3	7
Housekeeping			
ACTB	13	13	11
EIF4a1	13	13	11
HSP90	13	13	11
RPS5	13	13	11
SF3A1	13	13	11
TAF11	10	13	11
YWHAZ	13	13	11

Supplemental Table 2-2. Gene symbols of genes analyzed in qPCR with functional classification and gene name.

Category and Gene Symbol	Gene Name
Apoptosis	
AIFM1	Apoptosis Inducing Factor Mitochondria Associated 1
APAF1	Apoptotic Peptidase Activating Factor 1
ATM	ATM Serine/Threonine Kinase
BAD	BCL2 Associated Agonist of Cell Death
BAX	BCL2 Associated X. Apoptosis Regulator
BCL2	BCL2 Apoptosis Regulator
BCLX	BCL2 like 1
BID	BH3 Interacting Domain Death Agonist
CASP3	Caspase 3
CASP9	Caspase 9
CDKN1A	Cyclin Dependent Kinase Inhibitor 1A
HSP70	Heat Shock Protein 70
XIAP	X-Linked Inhibitor of Apoptosis
Epigenetic Regulation	
ASH2L	ASH2 Like, Histone Lysine Methyltransferase Complex Subunit
DMAP1	DNA Methyltransferase 1 Associated Protein 1
DNMT1	DNA Methyltransferase 1
DNMT3A	DNA Methyltransferase 3A
DNMT3B	DNA Methyltransferase 3B
EHMT2	Euchromatic Histone Lysine Methyltransferase 2
EZH2	Enhancer of Zeste 2 Polycomb Repressive Complex 2 Subunit
HAT1	Histone Acetyltransferase 1
HDAC1	Histone Deacetylase 1
HDAC2	Histone Deacetylase 2
HDAC3	Histone Deacetylase 3
KAT2A	Lysine Acetyltransferase 2A
KDM3A	Lysine Demethylase 3A
KDM4C	Lysine Demethylase 4C
KDM5B	Lysine Demethylase 5B
MECP2	Methyl-CpG Binding Protein 2
SIRT1	Sirtuin 1
SUV39H1	Suppressor of Variegation 3-9 Homolog 1
Imprinted Genes	
ASCL2	Achaete-Scute Family BHLH Transcription Factor 2
DIRAS3	DIRAS Family GTPase 3
GNAS	GNAS Complex Locus
GRB10	Growth Factor Receptor Bound Protein 10
HAND1	Heart and Neural Crest Derivatives Expressed 1

Category and Gene Symbol	Gene Name
IGF2	Insulin Like Growth Factor 2
IGF2R	Insulin Like Growth Factor 2 Receptor
IMPACT	Impact RWD Domain Protein
MEG3	Maternally Expressed 3
NECD	Notch Receptor Extracellular Domain
NNAT	Nauronatin
PEG3	Paternally Expressed 3
PEG10	Paternally Expressed 10
RTL1	Retrotransposon Gag Like 1
SNRPN	Small Nuclear Ribonucleoprotein Polypeptide N
UBE3A	Ubiquitin Protein Ligase E3A
Maternal Effect	
BMP15	Bone Morphogenetic Protein 15
DAZL	Deleted in Azoospermia Like
DDX4	DEAD-Box Helicase 4
FIGLA	Folliculogenesis Specific BHLH Transcription Factor
GDF9	Growth Differentiation Factor 9
MOS	MOS Proto-Oncogene, Serine/Threonine Kinase
NLRP5	NLR Family Pyrin Domain Containing 5
ZAR1	Zygote Arrest 1
ZP2	Zona Pellucida Glycoprotein 2
ZP3	Zone Pellucida Glycoprotein 3
Pluripotency	
CMYC	Cellular-myelocytomatosis proto-oncoprotein
ID1	Inhibitor of DNA Binding 1
ID3	Inhibitor of DNA Binding 3
KLF4	Kruppel Like Factor 4
LIN28	Lin-28 Homolog A
NANOG	Nanog Homeobox
POU5F1	POU Class 5 Homeobox 1
SOX2	SRY-Box 2
ZIC1	Zic Family Member 1
Trophoblast Differentiation and Function	
CDX2	Caudal Type Homeobox 2
CYP17A1	Cytochrome P450 Family 17 Subfamily A Member 1
DLX3	Distal-Less Homeobox 3
ELF5	E74 Like ETS Transcription Factor 5
ESRRB	Estrogen Related Receptor Beta
ETS2	ETS Proto-Oncogene 2, Transcription Factor
HSD17B1	Hydroxysteroid 17-Beta Dehydrogenase 1
KRT8	Keratin 8
SFN	Stratifin

Category and Gene Symbol	Gene Name
TACSTD2	Tumor Associated Calcium Signal Transducer 2
TEAD4	TEA Domain Transcription Factor 4
VIM	Vimentin
Housekeeping	
ACTB	Actin Beta
EIF4A1	Eukaryotic translation Initiation Factor 4A1
GAPDH	Glyceraldehyde-3-Phospahete Dehydrogenase
HSP90	Heat Shock Protein 90
RPS5	Ribosomal Protein S5
SF3A1	Splicing Factor 3a Subunit 1
TAF11	TATA-Box Protein Associated Factor 11
YWHAZ	Tyrosine 3-Monooxygenase/Tryptophan 5-Monooxygenase Activation Protein Zeta

Supplemental Table 2-3. Gene symbol of genes analyzed with qPCR with accession number used to design forward and reverse primers and respective primer sequences.

Gene Symbol	Accession Number	Primer Sequences
ACTB	XM_003124280.2	For:CCTGAACCCCAAAGCCAAC Rev:TACATGGCTGGGGTGTTGAA
AIFM1	NM_001297632.N	For:CATGGGAAAGATCCTCCCTGAA Rev:TAGCATTGGGCAGCACCTTA
APAF1	XM_003481742.3	For:TGCCAGAACAAGCTCACAGTA Rev:GCGGTTGGGAAAATCACGTAA
ASCL2	NM_001122991.1	For:TTTCCGGCCATCTCACTGTA Rev:TCCTTCGGCGGATACTTGAA
ASH2L	NM_001243568.	For:TTTCCGGCCATCTCACTGTA Rev:TCCTTCGGCGGATACTTGAA
ATM	NM_001123080	For:TTAAGAGCTTGGGCTCTGGAA Rev:TGGTACAGCGAGATCACAC
BAD	XM_003122573.3	For:GCTCCGGAGGATGAGTGAC Rev:CTTCGGGCGAGGAAGTCC
BAX	XM_003127290.3	For:GCGCTTTTCTACTTTGCCAGTA Rev:GCCGATCTCGAAGGAAGTCC
BCL2	XM_003121700.4	For:GCCCTGTGGATGACTGAGTAC Rev:GGCCCATACAGCTCCACAAA
BCLX	NM_214285.1	For:AGCGTAGACAAGGAGATGCA Rev:TTCAGGTAAGTGGCCATCCA
BID	NM_001030535.N	For:TGCAGCTACTTCATGGAGGAC Rev:CTGGCAATGTCCCGAATGAC
BMP15	NM_001005155.	For:GGCCATTGGTTAATGGAGCAA Rev:GCTACCCGGTTTGGTCTCA
CASP3	NM_214131.1	For:TCAGAGGGGACTGCTGTAGAA Rev:CGTCTCAATCCCACAGTCCAA
CASP9	XM_003127618.3	For:ACTGTGAGGACCTGCTGAC Rev:ACAGCCAGGAATCTGCTTGTA
CDKN1A	XM_001929558.3	For:ACCTCCCAGGGCAGGAAA Rev:CGGCGTTTGGAGTGGTAGAA
CDX2	NM_001278769.N	For:CGCTACATCACCATTCGGAGAA Rev:TTCGCTCTGCGGTTCTGAAA
CMYC	NM_001005154.1	For:CGAACCCTTGGCTCTCCA Rev:GCTGCCTCTTTTCCACAGAAA

Gene Symbol	Accession Number	Primer Sequences
CYP17A1	NM_214428.1	For:GGACACAGATGTCGTCGTCAA Rev:AAGCGCTCAGGCATGAACA
DAZL	XM_003358321.2	For:TTACATGCAGCCTCCAACCA Rev:CCTGAACTGGTGAACTTGGGTA
DDX4	NM_001291682.N	For:AGGAGGAGAAAGTGGTGACA Rev:AAGATGGAGTCCTCATCCTCA
DIRAS3	NM_001044598.N	For:CGAATTTGCCGCGAGGTT Rev:GACAGGTGCACAGGTTCTCT
DLX3	XM_003131590.4	For:TACCGGCAATACGGAGCCTA Rev:CTTCAGCTTCCGGCTCTTCC
DMAP1	NM_001243640.	For:GACGGAGCCATGTTCTTCCA Rev:ACCTGCACCGTCTTGTTGAA
DNMT1	NM_001032355.	For:AAAGGCGCTCATAGGCTTCA Rev:ACGCTGAACAGTGGTGCAT
DNMT3A	NM_001097437.	For:ATGACCTCTCCATCGTCAACC Rev:CAGGAGGCGGTAGAACTCA
DNMT3B	NM_001162404.1	For:AGCTGTACCCTGCCATTCC Rev:AAGTACCCTGTTGCGATTCCA
EHMT2	NM_001101823.	For:CGCATTGCCTTCTTCAGTTCA Rev:CAGAAGCGGTCACCATAGTCA
EIF4A1	NM_001100196	For:AGGATCATGTCTGCGAGTCA Rev:CCTTCGGGCTCCATCC
ELF5	NM_001243711.1	For:AGTGGCATCAAAAGCCAAGAC Rev:GCAGGTCTCGTACAAATTCCC
ESRRB	XM_001928051.6	For:CCTGCAAGGCCTTCTTCAA Rev:TCCGTTTGGTGATCTCACAC
ETS2	XM_013991815.1	For:TGCCAACAGGCTTGGATTCA Rev:TTGCTGCATGGGGTCAACA
EZH2	NM_001244309.	For:GCTGCACACTGCAGAAAGATAC Rev:GTCGCAGGGCTGATAGTTGTA
FIGLA	XM_005662486.2	For:TCACCAGAGGGCGAAGTCTA Rev:TGATGCAGTTTCACTTCTGGGAA
GAPDH	NM_001206359.1	For:AGTGGACATTGTCGCCATCA Rev:CGTGGGTGGAATCATACTGGAA
GDF9	NM_001001909.	For:AACACTGTCCGGCTCTTCAC Rev:TCAACAGCAGTAACACGAT

Gene Symbol	Accession Number	Primer Sequences
GNAS	NM_214312.2	For:AAGGCAGAGGAGAAGAAGCA Rev:GATGGGTCCCCTCTTGGAA
GRB10	NM_001134965.1	For:AAGCACGCGGATGAATATCCTA Rev:AGTGCTGCGTCCTGTGAA
HAND1	NM_001014428.1	For:GCGAGAGCAAGCGGAAAA Rev:CCTGTGCGCCCTTTAATCC
HAT1	XM_003483674.3	For:GTCTGGTGGCCATGGAGAA Rev:TCTCGAAAGCCTCTACATGTCA
HDAC1	XM_013999116.1	For:CTCCATCCGCCCAGATAACA Rev:AACACCGGACAGTCCTCAC
HDAC2	XM_001925318.5	For:TCTGCGTTCAATAAGGCCAGATA Rev:GACTGGACAATCCTCTCCAACA
HDAC3	NM_001243827.	For:ATCGATTGGGCTGCTTCAAC Rev:GAGGGATGTTGAAGCTCTTG
HSD17B1	NM_001128472.1	For:TCGGGTCGCATATTGGTGAC Rev:AAACTTGCTGGCGCAGTAAAC
HSP70	NM_001123127.N	For:GCCGGCTGAGCAAGGAA Rev:CTCTGGGCCTCATCCTCAAC
HSP90	NM_213973.1	For:GCACGCCAACAGGATCTAC Rev:GTGGGGTCGTCCTCATCAA
ID1	NM_001244700.N	For:ACCCTCAACGGCGAAATCA Rev:ATCGTCCGCTGGAACACA
ID3	NM_001243602.N	For:ACGGCCCGCATCTTCC Rev:GCCAGGTCAGTGGCAGAA
IGF2	NM_213883.2	For:CAGCCCACAGCGATTCCAA Rev:GAGGCCAAGGCCAAGAAGAC
IGF2R	NM_001244473.	For:TGTGGTGGTGGCAAGAGAATA Rev:CAGCACTGGAGCACTCTCTA
IMPACT	XM_005665327.2	For:AGTGCCACCCACAACATCTA Rev:TGTTTCCCCATCATCCTCACA
KAT2A	XM_003131405.4	For:TGTCCAAAGTGCTACCAGGAA Rev:TTGCACGGCTTCTTCATCAC
KDM3A	XM_003124935.5	For:TGCCTGCAAGATCCCAACAA Rev:TGCACTCCTGACACCATCAC
KDM4C	XM_013988752.1	For:GTGAAAAGCCAGGAGAAGCA Rev:ATCCAGCTGCATCCTGCTA
KDM5B	XM_005668019.2	For:GAGAACCGGGACCTCCA Rev:TTGTGGATGAAGGCGAAGG
KLF4	NM_001031782.1	For:GGGAAGGGAGAAGACACTG Rev:TCTTTGCTTCATGTGGGAGA

Gene Symbol	Accession Number	Primer Sequences
KRT8	NM_001159615.1	For:AAGCGTACCGACATGGAGAA Rev:TCCAGCTCGACCTTGTTCA
LIN28	NM_001123133.1	For:TTCGGCTTCCTGTCCATGAC Rev:GCCCTCCATGTGCAGCTTA
MECP2	XM_003135493.4	For:GGACCCGAAAGCTTAAGCAA Rev:CGAAGTACGCAATCAACTCCA
MEG3	NR_021488.N	For:CCACGCGAGAACCTCCCTA Rev:CGTAGGCTGGTGGGATCCA
MOS	NM_001113219	For:GGCTTCGGCTCGGTATACAA Rev:GTTCTTGGTGCATCTGCTCA
NANOG	NM_001129971.1	For:CTTGGAAACTGCTGGGGAAA Rev:CCATGATTTGCTGCTGGGTA
NECD	NM_001123144.1	For:ATGTGGTACGTGCTGGTCAA Rev:CACTTCTTGTAACTGCCGATGAC
NLRP5	NM_001163407.1	For:CAATGGGACCATCGCGAAC Rev:ACCCCGTGTGGACTGGATA
NNAT	NM_001122990.1	For:TTTCGAAATCCTCCAGGGACAC Rev:CCAGCTTCTGCAGGGAGTAC
PEG10	NM_001109944.	For:AGTCCTCGCGTGGTGAGTA Rev:CCCAGGTGTAGCTTCACTCC
PEG3	XM_013995362.1	For:AGGGAGCACAAACACAGAGAC Rev:CCCATGTCCTGGTACGACAC
POU5F1	NM_001129971.1	For:AGAAGAGGATCACCCTGGGATA Rev:ATGGTCGTTTGGCTGAACAC
RPS5	XM_003128133.3	For:CACCGACGATGTGCAGATTA Rev:GGGCAGGTACTTGGCATAC
RTL1	NM_001134358.N	For:CGGACGAGCAGAAGAGTCC Rev:CAGAGAGATGAGCGACCTCAC
SF3A1	XM_003483452.3	For:AGCAGGGAAACAGAAGCTACA Rev:GCACCATTGGCCATGTTGTA
SFN	NM_001044564.N	For:GGTGCGAGAATATCGGGAGAA Rev:GTGTTCAGCAAGCCAAGCA
SIRT1	NM_001145750.	For:TGTCAGAGTTACCACCCACAC Rev:ACTGAAGAAGCTGGTGGTG
SNRPN	NM_001243699.N	For:GGCACCTTTAAGGCTTTTGACA Rev:CCCAAAACCCGCTTTTCTTCA
SOX2	NM_001123197.1	For:CCTGCAGTACAACTCCATGAC Rev:TGCGAGTAGGACATGCTGTA
SUV39H1	XM_013992210.1	For:TTCTTGGAATCAGCTCCAGGAC Rev:CGCACAGGTACTCGACTTCA
TACSTD2	XM_003127967.3	For:AGCCTGTTTCAGCTGTTTCC Rev:AAGAAGGGCAAGCTGAAGAAC

Gene Symbol	Accession Number	Primer Sequences
TAF11	NM_001184894.1	For:AGAGAAGAAGCAGAAAGTGGATGAA Rev:GGTTCAGCTGCTCCTCAGAA
TEAD4	NM_001142666.1	For:TGTTGGAGTTCTCTGCCTTCC Rev:GGCCGATGTGCACAAACAA
UBE3A	NM_001243181.	For:ACTTTTCGTGACTTGGGAGAC Rev:CTTCCACACTTCCTTCATAC
VIM	XM_005668106.2	For:CCTACAGGAAGCTGCTGGAA Rev:CCCTCAGGTTCAGGGAAGAAAA
XIAP	NM_001097436	For:GAGTGCTCAGAAAGACAATGCA Rev:CCTCAGCTGTTCTTCAGCAC
YWHAZ	NM_001315726.N	For:AACAGCAGATGGCTCGAGAA Rev:GTGAAGCATTGGGGATCAAGAAC
ZAR1	NM_001129956.	For:CCCTTATCGCGTGGAGGATA Rev:TCCACGTGGCGAAGTTTTAC
ZIC1	XM_003358599.2	For:CCCCAGTTCATTGCGCAAAC Rev:GGAGGCGTGGAGGACTCATA
ZP2	NM_213848.1	For:TGTTGTCAGATGGCTCTTCAC Rev:CTGCTGAAGCAACCATAGCA
ZP3	NM_213893.1	For:CACCGTAATGGTGGAGTGTCA Rev:CCTGATGAGCTTCCCGGTAC

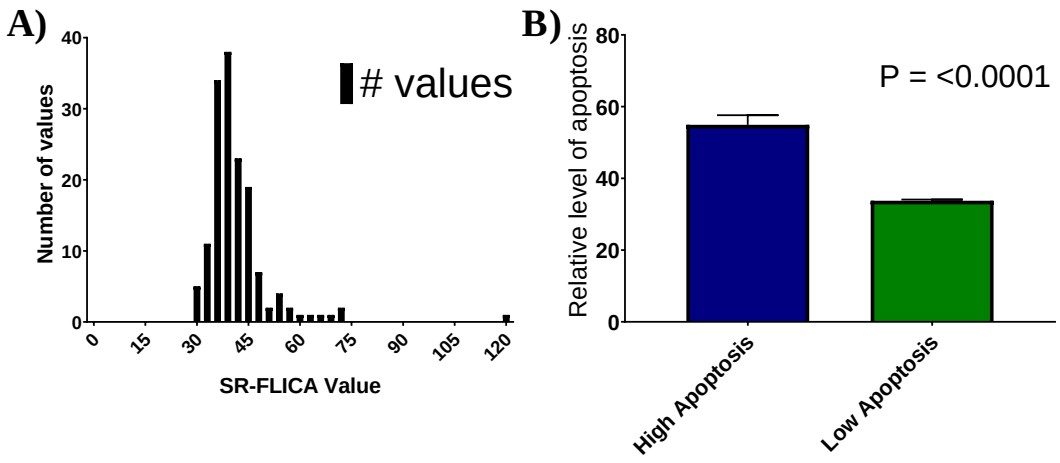

Supplemental Figure 2-1. SR-FLICA score histogram and values for groups sorted day 3 of development. Panel A is a histogram of distribution of SR-FLICA scores from day 3 SCNT stained embryos (n = 156) that were subsequently fixed for cell count analysis. The top and bottom 20% of each replicate were classified as high (n = 30) and low (n = 30) incidence of apoptosis. Panel B then shows the average SR-FLICA score for each group with error bars representing the standard error of the mean. A student's t-test indicated a significant difference (P = <0.0001) in SR-FLICA value between the high and low apoptosis groups.

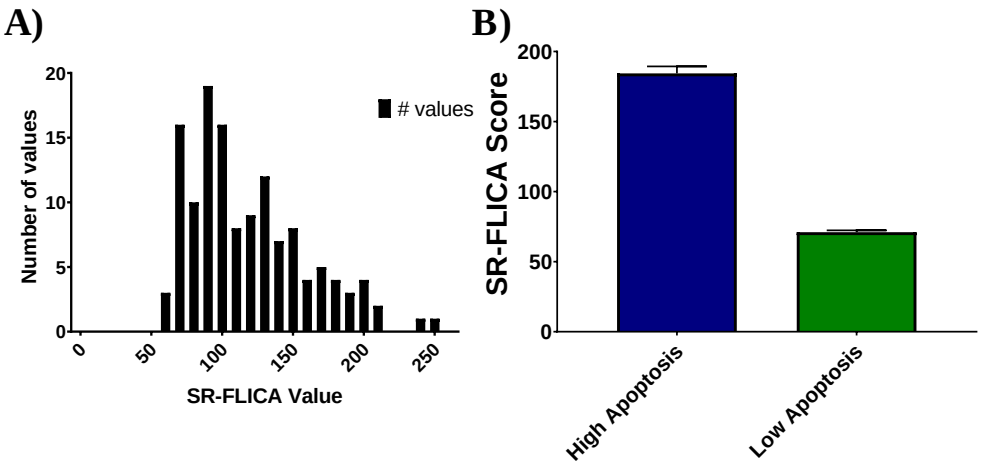

Supplemental Figure 2-2. SR-FLICA score histogram and values for groups sorted day 6 of development. Panel A depicts a histogram of distribution of SR-FLICA scores from day 6 PA blastocysts (n = 132). The top and bottom 20% of each replicate were classified as high (n = 26) and low (n = 26) incidence of apoptosis. Panel B shows the average SR-FLICA score of these high and low apoptosis embryos with standard error bars. The average SR-FLICA score is significantly different between high and low apoptosis embryos (P = <0.0001).

CHAPTER III

GENE EXPRESSION AND DNA METHYLATION PATTERNS OF HIGH AND LOW APOPTOSIS PORCINE SOMATIC CELL NUCLEAR TRANSFER BLASTOCYTS

Abstract

Somatic cell nuclear transfer (SCNT) is extremely costly due to the inefficient nature of the technology, limiting its use in animal agriculture. Increasing efficiency and decreasing cost by being able to select the embryos early in development that are most likely to succeed following transfer, would allow the technology to be more routinely utilized to enhance animal agriculture production. We hypothesize that following SCNT, a majority of embryos undergo faulty epigenetic reprogramming, resulting in aberrant gene expression and incidentally increased levels of apoptosis. Conversely, a fraction of the embryos undergo proper genome reprogramming, resulting in correct gene expression and low levels of apoptosis. In this study, DNA methylation and gene expression patterns are analyzed in individual blastocyst-stage embryos through reduced-representation bisulfite sequencing and RNA-seq to provide global patterns in high and low apoptosis SCNT blastocysts. *In vivo* produced (IVV) blastocysts were collected and included as controls. No differences in global DNA methylation patterns were found between the three groups: high apoptosis SCNT (HA), low apoptosis SCNT (LA), and IVV. Comparing high apoptosis and low apoptosis SCNT blastocysts identified 4,346 100 bp tiles that were differentially methylated and 413 genes that were differentially

expressed. Hierarchical clustering of tiles which were found to be differentially methylated in at least one of the three analyses (HA v LA, HA v IVV, or LA v IVV) did not clearly separate samples by sample type. Additionally, hierarchical clustering of differentially expressed genes, again where the genes were found to be differentially expressed in at least one of three analyses, did not separate the high apoptosis from low apoptosis samples. Gene ontology analysis identified no significantly enriched terms or KEGG pathways from the list of genes with differentially methylated promoters, or from the list of differentially expressed genes themselves. Together, these data support a stochastic nature of epigenetic reprogramming following SCNT and reinforce the necessity to identify embryos most likely to be successful due to proper epigenetic reprogramming in order to increase SCNT efficiency.

Introduction

Nuclear reprogramming is the erasure and subsequent reestablishment of epigenetic marks on DNA that occurs following fertilization of an oocyte. The nucleus begins to express gene products of developmental-specific genes following the directions provided by the oocyte cytoplasm as the donor-specific marks are erased [29]. The DNA of both the sperm and egg are highly methylated, and these marks must be removed and reset, with the exception of imprinted marks [59], before embryo development can properly occur. The paternal genome undergoes an active demethylation though enzymatic removal of methylation marks that occurs rapidly following fertilization [57]. On the other hand, demethylation of the maternal genome occurs passively through the

exclusion of DNMT1, the methyltransferase responsible for maintaining DNA methylation, from the nucleus [57] through the first several embryonic mitoses of early development. After both the maternal and paternal genomes are demethylated, *de novo* methylation occurs. A critical part of development is for epigenetic reprogramming at the time of fertilization to occur correctly and in a timely manner so proper embryo development can take place, including the maternal to zygotic transition when the embryo begins transcribing its own RNA and stops relying on maternal stores of RNA.

During SCNT, nuclear reprogramming is known to occur erroneously and is believed to be the cause of the low success rates associated with SCNT [7, 52, 59]. A differentiated somatic cell is utilized as the karyoplast donor in somatic cell nuclear transfer The epigenetic marks of the donor cell DNA must be removed so that embryo development begins [59]. The somatic specific genes must be completely silenced and embryonic genes need to start being expressed in order for proper development of SCNT embryos to occur. The reprogramming efficiency of the donor nucleus hinders the overall efficiency of SCNT, as evident by the fact that using an undifferentiated cell, a zygote, significantly increases the number of live births following SCNT in mice [43]. SCNT embryos show overall increases in DNA methylation levels compared to *in vitro* produced embryos [52], obscuring the typical methylation patterns observed in the trophectoderm and inner cell mass cells [59]. Due to the overall increase in DNA methylation compared to IVF embryos, it was hypothesized that DNMT1, the enzyme responsible for maintaining DNA methylation, introduced through the donor cell, maintains DNA methylation when the DNA should be cleared of methylation marks [46]. However, experimental data suggest that the donor cell goes through the de-methylation

process following SCNT, however not all genes are properly de-methylated [52]. These altered epigenetic marks are then responsible for altered gene expression observed in SCNT embryos.

Most genes are properly reprogrammed and expressed following SCNT, as 95% of genes show similar expression patterns between SCNT and *in vitro* fertilized (IVF) embryos [36]. However, this leaves 5% of genes that are misexpressed, which could have deleterious consequences on a developing embryo and fetus. A noteworthy observation is that misexpressed genes seem to be random, with no distinct set of genes being consistently misexpressed across studies [36]. Additionally, most misexpressed genes are mildly changed in expression level, with less than 3% of genes showing more than a four-fold change in gene expression [36]. Previous studies have reported that in bovine SCNT embryos, some individual embryos contain gene expression patterns much closer to *in vitro* produced controls than other SCNT embryos [67] indicating that some embryos could be more competent as they are more similar to *in vitro* produced embryos. In addition, *in vivo* produced embryos had less variability in gene expression compared to SCNT and IVF embryos [67]. Together, these observations have contributed to the hypothesis that epigenetic reprogramming after SCNT happens in a random nature, leading to random differences in gene expression.

Altered DNA methylation and gene expression patterns have been shown to result in increased cell death through apoptosis [96]. Fibroblasts deficient in *Dnmt1*, which resulted in widespread DNA demethylation, showed a prevalent apoptotic phenotype mediated through p53 [96]. p53-dependent apoptosis has also been shown to result from

dysregulation of gene expression in cancer cell culture systems [97]. Studies have also indicated that disruption of the epigenetic makeup by treatment of various pharmacological methods results in apoptosis in somatic cell culture models [98, 99]. Therefore, we propose that the stochastic defects in genome reprogramming which result from the process of SCNT directly relate to the incidence of apoptosis within each individual embryo.

In order to improve the overall efficiency of SCNT, we propose the use of a non-toxic, non-invasive caspase activity reporter, SR-FLICA (Immunochemistry Technologies, Bloomington, MN), to detect the relative incidence of apoptosis in SCNT blastocysts as an indicator of the blastocyst(s) most likely to succeed following embryo transfer. We hypothesize that following SCNT, a majority of embryos will undergo aberrant epigenetic reprogramming, resulting in altered gene expression which in turn leads to an increase in apoptosis. Conversely, a portion of embryos will undergo proper epigenetic reprogramming, leading to appropriate gene expression and low levels of apoptosis.

The objective of this study is to characterize DNA methylation and gene expression patterns in day 6, porcine SCNT blastocysts exhibiting high and low incidence of apoptosis. Using a whole genome approach to characterize patterns of both DNA methylation and mRNA expression of individual blastocysts, we hope to piece together a thorough picture of the individual blastocyst following SCNT to identify the characteristics of a blastocyst that would be most successful following embryo transfer. We propose the use of a modified single-cell reduced representation bisulfite sequencing

(RRBS) protocol [100] and RNA-sequencing utilizing DNA and mRNA collected from the same individual blastocyst. RRBS is a high-throughput technique to analyze genome-wide methylation [101]. The RRBS procedure provides a cost-effective alternative to deep sequencing the entire genome. In experiments using mouse and human samples where approximately 10% of the genome was sequenced using RRBS, it was shown that a large proportion of the CpG-rich sites were able to be evaluated, including more than 70% of gene promoters and more than 80% of CpG Islands [100]. However, traditional RRBS protocols require nanogram quantities of DNA, which are not available in individual blastocysts. Therefore, modification of a single-cell RRBS protocol [100] is required for the analysis of such small amounts of DNA.

Materials and Methods

All chemicals and reagents were purchased from Sigma-Aldrich (St. Louis, MO) unless otherwise noted. All procedures performed with animals were in agreement with principles of animal welfare as approved by the veterinary staff and Institutional Animal Care and Use Committee at Utah State University (IACUC protocol #2636).

Oocyte source and in vitro maturation

Cumulus oocyte complexes for SCNT were purchased from Desoto Biosciences (Seymore, TN). Oocyte maturation, manipulation, activation, and embryo culture were performed as described previously [88]. Briefly, oocytes with multiple layers of cumulus cells were collected by Desoto Biosciences, washed in maturation media, and allowed to mature for 40-44 hours at 39°C and 5.0% CO_2. During the 40-44 hour maturation period,

cumulus oocyte complexes were shipped to Utah State University in a portable incubator maintaining the temperature of 39°C. Upon arrival, increased CO_2 concentrations (compared to the commonly reported 5.0%) were used to account for the higher elevation of Utah State University. Maturation media was provided by Desoto Biosciences.

Donor Cell Preparation

Porcine fetal fibroblasts (PFF) cells served as donor cells for nuclear transfer. The PFF cells had been isolated and frozen previously. For SCNT, the PFF cells were expanded and frozen for subsequent cloning using the same cell line at passage six. PFF culture medium was prepared using Dulbecco's Modified Eagle's Medium (DMEM, Fisher Scientific) as the base supplemented with 15% fetal bovine serum (FBS, Atlanta Biologicals, Flowery Branch, GA), 25 µg/ml fibroblast growth factor (FGF2), and 40 mg/ml gentamicin. PFF cells were seeded in a 4-well dish one week prior to SCNT and allowed to become confluent for several days for cell synchronization before cloning. To prepare for donor cell injection, medium was removed from the well, fibroblast cells were rinsed with PBS, and 0.25% trypsin-EDTA (Fisher Scientific) was added for 3 minutes. The cells were then transferred into a 1.5 mL tube and 1 mL of PFF culture medium was added to inactivate the trypsin. Cells were isolated by centrifugation at 400 x g for 5 minutes. Trypsin was removed and the cells were resuspended in manipulation medium consisting of 3.14 mM TL-Hepes, 40 µg/mL gentamicin, 30 mM NaCL and 0.3% BSA diluted in M199 with Earl's Balanced Salts and L-Glutamine

SCNT

Following oocyte maturation, oocytes were denuded of cumulus cells in medium that consisted of 100 mg Hyaluronidase, 6 g mannitol, 5 mL PVA-TL-Hepes stock [88], and 95 mL double distilled water. Oocytes were placed in the hyaluronidase media at 39 °C for 5 minutes then pipetted 40 times to remove the cumulus cells. Oocytes were washed through manipulation medium containing a base of m199 supplemented with 5.95 mM sodium bicarbonate, 3.14 mM HEPES, 30 mM NaCl, 0.3% BSA, and 0.04 mg/ml gentamicin. Oocytes with an extruded polar body were selected for SCNT.

Oocytes undergoing SCNT were enucleated in drops of enucleation media [88] under light mineral oil. Enucleation took place using a beveled glass pipette to aspirate the first polar body and the metaphase II plate by removing a small amount of the cytoplasm adjacent to the polar body. Following enucleation, the donor cell was injected into the perivitelline space. Donor cell injection was performed by placing the donor cells into the droplet with the enucleated oocytes. A single donor cell was picked up with the glass pipette and inserted through the same slit in the zona pellucida that was created during enucleation. Donor cells were fused with oocytes at the same time of oocyte activation in activation media composed of 0.3 M mannitol, 1.0 mM $CaCl_2$, 0.1 mM $MgCl_2$, and 0.5 mM HEPES (pH 7.0-7.4). Fusion and activation occurred with 2 direct current pulses of 1.2 kV/cm^2 for 30 µsec. Fusion of the donor cell was checked after 30 minutes.

Embryos were cultured at 39°C and 6.2% CO_2 in PZM3 medium [89] up to day 7 of development. PZM3 media was composed of 108 mM NaCl, 10 mM KCl, 0.35 mM

KH_2PO_4, 0.4 mM $MgSO_4$, 25.07 mM $NaHCO_3$, 0.2 mM sodium pyruvate, 2 mM calcium lactate, 1 mM L-Glutamine, 5 mM hypotaurine, 2% (v/v) Basal Medium Eagle (BME) amino acids (Fisher Scientific), 1% (v/v), Minimum Essential Medium (MEM) amino acids (Fischer Scientific), 0.005% (w/v) gentamicin, and 0.3% (w/v) Fatty-acid-free BSA. The pH was adjusted to 7.3-7.4. SCNT blastocysts were collected from 3 replicate SCNT sessions with a minimum of 15 blastocysts for subsequent staining.

SR-FLICA Staining

SR-FLICA (Immunochemistry Technologies) was resuspended as recommended by the manufacturer. Briefly, 50 µL DMSO was added to one vial SR-FLICA. Embryos were stained in 500 µL PZM3 culture media with 2 µL reconstituted SR-FLICA for 2 hours in the incubator. Embryos were moved to a fresh 500 µL PZM3 and placed back in the incubator for 30 minutes. Embryos were then washed in PZM3 and transferred to individual 10 µL PZM3 droplets under mineral oil for fluorescent microscopy.

Microscopy and Image Analysis

Individual embryos were imaged at the 10X objective using the Zeiss Axio Obserer.Z1 (Carl Zeiss Microscopy; Thornwood, NY). Fluorescent images of SR-FLICA (excitation 550-580 nm, emission 590-600 nm) stained embryos were captured with an Axiocam HRc (Carl Zeiss Microscopy) creating a black and white image and a red color was artificially added using Zen software (Carl Zeiss Microscopy; v. 2.0). Images had a

1 second exposure time and light excitation intensity between embryos for accurate comparisons of incidence of apoptosis. SR-FLICA excitation in each image was analyzed using Adobe Photoshop (v. 2017.1.1.20174025) to determine the average pixel intensity within the space of the zona pellucida of the embryo. In blastocysts that were hatching, both the space inside the zona pellucida and the hatching extrusion was included in the analysis. Average pixel intensity for each embryo was ranked, and the top and bottom 20% were considered high (n = 13) and low (n = 13) apoptosis, respectively. Using microdroplets to minimize the amount of medium remaining, individual blastocysts were stored at -80°C until DNA and mRNA were isolated.

In Vivo Embryo Collection

In vivo produced blastocysts were collected 5 days after natural breeding of the sow (2 sows, total n = 11 blastocysts collected). Blastocysts were collected by flushing the isolated uterus with TL-Hepes [88]. Blastocysts were isolated and washed in TL-Hepes. Again using microdroplets to minimize the amount of medium remaining, individual blastocysts were then stored at -80°C until DNA and mRNA were isolated.

DNA and RNA Isolation

DNA and total RNA were isolated from previously frozen individual blastocysts using the ZR-DUET DNA/RNA MiniPrep kit (Zymo Research; Irvine, CA) following manufacturer instructions except for two minor changes. Rather than 400 µL of

DNA/RNA Lysis buffer being used as recommended, 200 µL was used instead. Additionally, the final RNA elution was performed using 20 µL DNase/RNase-free water from a single elution. Collected DNA and RNA were stored at -80°C until library preparation was performed.

RRBS Library Preparation and Sequencing

Reduced representation bisulfite sequencing libraries were prepared using the single-cell RRBS protocol developed by Guo et al. [100] with some modification. The 50 µL of eluted DNA was air dried to 5 µL to concentrate the DNA. Samples were then digested with MspI using 9 U MspI (Thermo Fisher Scientific; New Jersey, USA), 1X Tango Buffer (Thermo Fisher Scientific), and 2280 fg unmethylated λ-DNA (dam^-, dcm^-; Thermo Fischer Scientific). Nuclease-free water was added to bring the total reaction volume to 18 µL. Tubes were mixed well by vortexing and centrifuged. The reaction was then incubated at 37°C for 3 hours, then 80°C for 20 minutes to inactivate the MspI enzyme. The tubes were placed on ice. The samples then underwent the end-repair/dA-tailing reaction. Five U of Klenow fragment (exo^-; Thermo Fischer Scientific), 1X Tango buffer, 40 µM dATP (New England Biolabs; Ipswich, MA), 4 µM dCTP (New England Biolabs), and 4 µM dGTP (New England Biolabs) were added to each reaction bringing the total reaction volume to 20 µL. The reactions were then incubated at 37°C for 40 min and then 75°C for 15 minutes to inactivate the Klenow enzyme.

Next, the adapter ligation step was performed. Reactions were mixed with 30 Weiss U T4 DNA ligase (Thermo Fischer Scientific), 1X Tango buffer, 1mM ATP

(Thermo Fischer Scientific), and 1 µL of 1:20 diluted adapter (NEXTflex Bisulfite-Seq Barcodes; Bioo Scientific; Austin, TX, adapter sequence: 5'-AATGATACGGCGACCACCGAGATCTACACTCTTTCCCTACACGACGCTCTTCCGATCTGATCGGAAGAGCACACGTCTGAACTCCAGTCACXXXXXXATCTCGTATGCCGTCTTCTGCTTG-3' where XXXX indicates the Index sequence for each sample which can be found in Supplemental Table 3-1). Nuclease-free water was added to bring the entire reaction volume to 25 µL. Reactions were incubated at 16°C for 30 minutes then at 4°C overnight. The enzyme was heat-inactivated at 65°C for 20 minutes. All 25 µL of the reaction were used to perform the bisulfite treatment using the MethylCode bisulfite conversion kit (Thermo Fischer Scientific) following manufacturer's directions. Ten ng of tRNA was added to the supplied DNA binding buffer to serve a protective carrier. DNA was eluted in 30 µL of elution buffer that had been pre-heated to 50°C.

Reactions then underwent the first-round of PCR enrichment. To the DNA, 5 µL of 10X PCR Pfu Cx buffer (Agilent Technologies; Santa Clara, CA), 1 U Pfu Turbo Cx hotstart DNA polymerase (Agilent Technologies), 200 µM each dNTP mix (Takara Bio; Mountain View, CA), 300 nM each of QP1 and QP2 primer (QP1 5'-AATGATACGGCGACCACCGA-3'; QP2 5'-CAAGCAGAAGACGGCATACGA-3'), and 2.5 µL of 20X Evagreen (Biotium; Hayward, CA) were added. Nuclease-free water was used to bring the total volume of the reaction to 50 µL. PCR cycling conditions were as follows: 95°C for 2 min, 15-25 cycles of 95°C for 20 seconds, 65°C for 30 seconds, 72°C for 1 minute, 72°C for 5 minutes, followed by a 4°C hold. The number of amplification cycles ranged between 15 to 25 cycles because reactions were tracked using real-time PCR, and reactions were removed after 5 cycles of exponential increase. PCR

reactions were purified twice via a 1:1-fold (sample volume to bead volume) Agencourt AMPure XP beads (Beckman Coulter; Atlanta, GA). A second-round of PCR enrichment was performed using 25 µL of 2X Phusion HF PCR master mix (New England Biolabs), 2.5 µL of 20X Evagreen, 500 nM each of QP1 and QP2 primers bringing the total reaction volume to 50 µL. PCR cycling conditions were as follows: 95°C for 2 min, 7 cycles of 95°C for 20 seconds, 65°C for 30 seconds, 72°C for 1 minute, 72°C for 5 minutes, followed by a 4°C hold. Reactions were purified once using 1:1-fold (sample volume to bead volume) Agencourt AMPure XP beads and eluted in 20 µL of nuclease-free water. The samples were then purified once using 1:1.3-fold (sample volume to bead volume) Agencourt AMPure XP beads to remove primer-dimers present in the samples. DNA was eluted in 20 µL of nuclease-free water. Samples were analyzed for fragment size and the absence of primer-dimers to ensure successful sequencing using the TapeStation (Agilent Genomics; Santa Clara, CA) and sequenced on the NextSeq (Illumina; San Diego, CA) using high output 150 bp single-end reads.

RRBS library analysis

At first, we performed quality check on the raw reads with FastQC (https://www.bioinformatics. babraham.ac.uk/projects/fastqc/) for all the 41 samples. Further read quality control was performed using Trim Galore (http://www.bioinformatics.babraham.ac.uk/projects/trim_galore/) to remove the standard 13 bp adapters (5'-AGATCGGAAGAGC-3'). Low-quality base calls were trimmed off the 3' end of the reads before adapter removal. Trim Galore also removed biased

methylation positions in the RRBS sequence. The trimmed reads were then aligned using Bismark [102] against the bisulfite converted pig genome (*Sus scrofa 11.1*). Context dependent (CpG/CHG/CHH) methylation was extracted using Bismark's methylation_extractor from the mapped reads and methylation analysis was performed using MethylKit [103], an R package for DNA methylation analysis and annotation of high-throughput bisulfite sequencing. MethylKit analysis included basic statistics such as the coverage and percent methylation, sample correlation, sample clustering, PCA analysis, differential methylation at an individual base and region level (100bp), and visualization of methylation events including bar plots of hyper- and hypomethylation per chromosome, and annotation of differentially methylation regions. Analysis was only performed on regions with at least 10X coverage in a minimum of 6 samples per group. DNA methylation level considered was the average of the 100bp tiles. Differential methylation was determined between two groups if there was greater than 25% difference in methylation with an FDR less than 0.05, all calculated and determined by MethylKit. Differential methylation was performed on two groups at a time creating 3 different comparisons: High Apoptosis (n = 13) vs Low Apoptosis (n = 12), High Apoptosis (n = 13) vs IVV (n = 11), and Low Apoptosis (n = 12) vs IVV (n = 11). To analyze the conversion rate of the bisulfite reaction, unmethylated λDNA was added to each sample. Each trimmed sample was then aligned to the λ genome and conversion rate was calculated.

RNA-Seq Library Preparation and Sequencing

RNA sequencing libraries were prepared using the Ovation SoLo RNA-Seq

System (NuGen Technologies; San Carlos, CA) following the manufacturer's protocol for total RNA Input. 10 µL of RNA was mixed with 1 µL DNase Buffer, 2.6 µL first strand primer mix, 1.7 µL DTT solution, 0.7 µL nuclease-free water, and 2 µL HL-dsDNase. The reaction was then heated to 37°C for 10 minutes followed by 65°C for 5 minutes. The first strand cDNA synthesis was then performed by adding the 1 µL first strand buffer mix and 1 µL first strand enzyme mix to the reaction followed by heating to 25°C for 5 minutes, 40°C for 30 minutes, and 70°C for 10 minutes. The reaction next underwent cDNA processing by addition of 0.5 µL cDNA processing enzyme I and 0.5 µL cDNA processing enzyme II. Reactions were heated to 37°C for 30 minutes. Two µL of cDNA processing reagent were added and the reactions were heated to 90°C for 20 minutes. Next, 2 µL of cDNA processing reagent II were added. One µL cDNA processing reagent III and 1 µL cDNA processing enzyme III were added and reactions were heated to 37°C for 30 minutes followed by 70°C for 10 minutes. Seven µL cDNA processing reagent IV and 1 µL cDNA processing enzyme IV were added and reactions were heated to 37°C for 30 minutes then 75°C for 20 minutes. Second strand synthesis was performed by adding 3.5 µL second strand buffer mix, 3.5 µL second strand primer mix, and 1 µL second strand enzyme mix. Reactions were then heated to 25°C for 15 minutes, 37°C for 15 minutes, and 70°C for 10 minutes. End repair was conducted by adding 1 µL of end repair enzyme mix I and 1 µL end repair enzyme mix II to each reaction followed by heating to 25°C for 30 minutes then 70°C for 10 minutes. Reactions were stored at -20°C overnight.

Adapter ligation was performed by adding 3.25 µL of the barcoded adapter mix to each sample. Additionally, 13 µL of ligation buffer mix, 2 µL of ligation enzyme mix,

and 1.75 µL of nuclease-free water were added to each sample reaction. Reactions were heated to 25°C for 30 minutes then 70°C for 10 minutes. Adapter ligation purification was performed using Agencourt beads and DNA resuspension buffer mix as follows. 35 µL of nuclease-free water was added to each sample to bring the total volume to 100 µL. The beads were resuspended by mixing and 100 µL of beads were added to each sample. The sample-bead mixture was incubated at room temperature for 10 minutes then transferred to a magnet and allowed to sit for 5 minutes to clear the beads. The binding buffer was removed and discarded. The tubes were washed with 200 µL of 70% ethanol and allowed to stand for 30 seconds. The ethanol was removed and the samples were washed one more time. The beads were allowed to air dry for 10 minutes and the sample was resuspended in 30 µL of DNA resuspension buffer mix. The beads were again collected by a magnet for 3 minutes and the eluate was removed and placed in a clean PCR tube.

Library amplification was optimized for qPCR following the recommended protocol provided in the SoLo RNA-seq system. Three µL of DNA resuspension buffer mix was added to each sample. Then, 2 µL amplification buffer mix, 1.9 µL amplification primer mix I, 0.1 µL amplification enzyme mix, 0.5 µL EvaGreen, and 2.5 µL nuclease-free water was mixed with 3 µL of sample in a fresh set of tubes. qPCR was performed using the following cycling parameters: 70°C for 10 minutes, 35 cycles of 94°C for 30 seconds, 60°C for 30 seconds and 72°C for 1 minute, and then finally 72°C for 5 minutes. The suggested cycle number for subsequent amplifications was determined from the exponential phase of amplification to be approximately 19 cycles.

Libraries were then amplified for the first time by mixing 10 µL amplification buffer mix, 9.5 µL amplification primer mix I, 2 µL EvaGreen, and 0.5 µL of amplification enzyme mix to 30 µL of each sample. Samples were amplified using qPCR to track each sample and the sample was removed after 4 cycles in the exponential phase of amplification. Cycling parameters were the same used for library amplification optimization. Libraries were then purified using Agencourt beads by adding 40 µL of beads to the library amplification reaction product. Purification was performed as previously explained. The sample was eluted in 50 µL DNA resuspension buffer and bead purification was performed again. Finally, the sample was eluted in 25 µL DNA resuspension buffer.

Libraries were quantified using the Qubit dsDNA HS Assay (Thermo Fischer Scientific). The concentration of DNA for each sample came back lower than expected, so the library amplification I was repeated prior to InDA-C treatment to increase DNA in each sample. Samples were amplified until 4 cycles of amplification occurred and then removed from the thermocycler. The repeated amplification was effective at increasing concentration to an acceptable level.

InDA-C treatment was conducted by aliquoting 10 ng of each library into a new tube with nuclease-free water for a total volume of 8.5 µL. Five µL amplification buffer mix, 10 µL InDa-C primer mix, 0.5 µL InDA-C enzyme mix, and 1 µL amplification enzyme mix was added to each sample and samples were heated to 37°C for 10 minutes, 95°C for 2 minutes, 50°C for 1 minute, and 65°C for 10 minutes. Five µL amplification buffer mix, 2.5 µL adaptor cleavage enzyme mix, and 17.5 µL nuclease-free water was

added to each sample and the reaction was heated to 55°C for 30 minutes followed by 95°C for 5 minutes.

Libraries were then amplified for a second time by mixing 10 µL amplification buffer mix, 39.5 µL amplification primer mix II, and 0.5 µL amplification enzyme mix to each sample. Amplification used the following thermocycling conditions: 95°C for 2 minutes, 2 cycles of 95°C for 30 seconds and 60°C for 90 seconds, 6 cycles of 95°C for 30 seconds and 65°C for 90 seconds, then 65°C for 5 minutes. Libraries were purified twice with a 1:1 mixture of Agencourt beads and final libraries were eluted in 25 µL of DNA resuspension buffer mix.

Libraries were sequenced on the Illumina NextSeq using single-end 75 bp reads.

RNA library analysis

RNA-seq libraries were aligned to the pig genome (*Sus scrofa 11.1*) using the Star-aligner. Only reads that aligned uniquely to the genome were used in down-stream analysis. Differential gene expression was determined if a gene had a fold-change greater than 1.5 and false discovery rate less than 0.05 using EdgeR.

Two samples (one low apoptosis and one IVV) were determined to be outliers based on principal component biplot analysis so were removed from the analysis. Additionally, many genes had very low read counts, so additional restrictions were added to the genes that were analyzed. Genes were only analyzed if they had observed counts of 10 or more in at least 20% of all samples and a coefficient of variation between 0.7 and 5.5. The range for the coefficient of variation was determined empirically based on the distribution of the variation. The range kept the genes from the mode to the max to

focus on the genes with more variation and drop those with very little variation, those less than the mode. Of the original 25,880 genes included in the sequencing reads that had aligned to the genome, 7,915 were kept in the analysis.

A generalized linear mixed model accounting for collection day and sample type using the lme4 package [104] was fit to the data to determine differential expression. The glmer.nb function for negative binomial distribution of read count data was used. The data was normalized using the log of the total read counts within each sample. The model did not converge for 1 of the 7,915 genes tested.

Gene Ontology Analysis

Gene ontology analysis of genes that were differentially methylated and differentially expressed between groups was analyzed using DAVID EASE (version 6.8; [105, 106]). Official gene symbols were uploaded to form a gene list. The list was submitted and the annotations were used for all species. *Sus scrofa* was used as the background. Gene ontology analysis of biological process, cellular component, and molecular function was analyzed in addition to KEGG pathways. Terms or pathways considered significantly enriched had a false discovery rate corrected p-value less than 0.05.

Results

RRBS sequencing

RRBS libraries were sequenced producing between 5.09 and 39.39 million reads (Table 3-1). The high apoptosis blastocysts (HA), low apoptosis blastocysts (LA), and *in vivo* (IVV) produced blastocysts averaged 28.31 ± 3.92 million, 24.21 ± 6.62 million, and 27.41 ± 5.92 million total reads, respectively (Table 3-1). Of these raw reads, 5.35 ± 1.96 million, 4.57 ± 1.84 million, and 8.63 ± 3.89 million reads aligned to the bisulfite converted genome in the HA, LA, and IVV samples, representing an average percent alignment of 18.4% ± 5.5, 18.9% ± 6.0, and 30.5% ± 11.7, respectively (Table 3-1). Together, this provided 69.52 million, 54.88 million, and 93.9 million aligned reads for the HA, LAs, and IVV samples, respectively (Table 3-1). While these mapping efficiencies may seem low, they are appropriate according to previously published RRBS protocols [100].

During RRBS library preparation, unmethylated lambda-DNA was added to each sample to serve as a control for bisulfite conversion efficiency. Because every cytosine of the lambda-DNA is unmethylated, they should all be turned to uracil in the conversion process, and then sequenced as thymine. The conversion efficiency ranged from 96.4% to 98.6% (Table 3-2). The HA, LA, and IVV samples had a conversion efficiency of 97.9% ± 0.4, 97.9% ± 0.5, and 97.9% ± 0.7, respectively (Table 3-2).

Differential methylation was determined on 100 base pair, consecutive tile fragments throughout sequenced regions. Due to limitations in the MethylKit program, only two groups could be compared at a time, resulting in three different pairwise

analyses: HA vs LA, HA vs IVV, and LA vs IVV. A tile was considered to be differentially methylated if the difference in methylation was greater than 25% and FDR corrected p-value less than 0.05. Between the three analyses, a total of 224,786 unique tiles were analyzed. In each analysis, approximately 32.9%, 44.9%, 8.8%, and 11.6% of tiles were located within intergenic regions, introns, exons, and promoters, respectively (Figure 3-1A). A majority (90%) of differentially methylated tiles were found in intergenic regions of the genome (Figure 3-1B). Approximately 6% of the tiles were located in introns and 2% located in exons (Figure 3-1B). Only 1% of the differentially methylated tiles were located in promoter regions of the genome (Figure 3-1B).

Global methylation patterns

Global methylation patterns were analyzed by evaluating average percent methylation across all tiles analyzed. HA blastocysts (n=13) had an average tile methylation of 17.25% ± 3.5 (Figure 3-2). LA blastocyst (n=12) had an average tile methylation of 16.47% ± 2.4 (Figure 3-2). Finally, average tile methylation of IVV blastocysts (n=11) was 15.0% ± 5.7 (Figure 3.2). A one-way ANOVA showed no statistical difference in variance of percent methylation of tiles ($P = 0.4$).

Global methylation patterns were also evaluated by depicting the percent of tiles methylated at varying levels of methylation from 0-20%, 20-40%, 40-60%, 60-80%, and 80-100% methylated (Figure 3-3). Each sample was plotted separately to visually show the unique nature of each sample. A majority of tiles in each sample had low levels of methylation, between 0-20% and a very small fraction of tiles were highly methylated

(80-100%) (Figure 3-3). The individual breakdown of the fraction of tiles that were methylated at each level was unique for each sample, even within HA, LA, and IVV groups. LA samples visually had the least amount of variability, while IVV had the most (Figure 3-3).

Tile Methylation Patterns

Differential methylation of tiles was determined in the HA vs LA, HA vs IVV, and LA vs IVV samples if tiles were greater than 25% differentially methylated with an FDR corrected p-value less than 0.05. In the HA (n = 13) vs LA (n = 12) comparison, 1627 tiles were hypomethylated, meaning lower methylation levels in the HA compared to the LA, while 2719 tiles were hypermethylated, meaning higher methylation levels in the HA compared to the LA (Figure 3-4). In the HA vs IVV (n = 11) comparison, 649 tiles were hypomethylated while 8494 tiles were hypermethylated (Figure 3-4). Finally, in the LA vs IVV analysis, 451 tiles were hypomethylated while 3764 were hypermethylated (Figure 3-4).

When all three of the analyses were brought together, overlap of differentially methylated tiles was present. The HA vs LA analysis, HA vs IVV analysis, and LA vs IVV analysis contained 2,222, 6,663, and 2,745 tiles, respectively, that were uniquely differentially methylated (Figure 3-5). The HA vs LA and HA vs IVV analyses shared 1,337 differentially methylated tiles (Figure 3-5). The HA vs LA and LA vs IVV analyses shared 590 differentially methylated tiles (Figure 3-5). The HA vs IVV and LA

vs IVV analyses had 659 differentially methylated tiles in common (Figure 3-5). And finally, 15 tiles were differentially methylated in all three analyses.

Principal component analyses (PCA) of a random subset of all tiles analyzed and only those differentially methylated provided insight to overall trends in methylation patterns (Figure 3-6). Due to limitations in the ClustVis program, only a 2 MB file can be analyzed in the PCA analysis. Fig. 3-6A shows the PCA of a random subset of all tiles analyzed. Principal component (PC) 1 and PC 2 explain 11.6% and 6.2% of the variance, respectively (Figure 3-6A). Interestingly, when all tiles are considered, the samples are all centered and overlap. The LA samples are the most tightly clustered, but both the HA and IVV samples sit on top of this cluster (Figure 3-6A). When only differentially methylated tiles are analyzed, PC1 and PC2 explain 16.1% and 6.1% of the variance, respectively (Figure 3-6B). Again it is interesting that the HA, LA, and IVV samples overlap on a central point (Figure 3-6B). But unlike the co-localized nature of the PCA when all tiles were included, the differentially methylated tiles within each group radiate away from each other from the centralized overlapping area (Figure 3-6B).

Hierarchical clustering of 1197 tiles (again a random subset was used because ClustVis only allows for clustering up to 1200 rows) of all tiles analyzed, shows very little clustering by sample type (Figure 3-7). Additionally, a heat map of the percent methylation for each sample indicates no clear pattern by sample type. Rather, noticeable differences in patterning of the heat map are at an individual blastocyst level (Figure 3-7). Conversely, when only a random subset of 1200 differentially methylated tiles are included in the hierarchical clustering and heat map analysis, samples do generally

separate by type, but still no distinct clusters are evident (Figure 3-8). And while not overly distinct, some heat map patterns can be identified by group rather than only by sample, as before (Figure 3-8).

RRBS Gene Ontology Analysis

Differentially methylated tiles were associated with the nearest transcription start site, which ranged from 9,565,509 base pairs downstream to 19,920,929 base pairs upstream. On average, the tiles were 15,974 base pairs upstream of the transcription start site. A histogram shows the number of tiles found within 500,000 base pairs up or downstream of the transcription start site (Supplemental Figure 3-1). The genes of the nearest transcription start site for the differentially methylated tiles were used for gene ontology analysis.

When all genes associated with differentially methylated tiles were used in gene ontology analyses, many gene ontology terms were found to be significantly enriched. In the HA vs LA analysis, the top ten biological process gene ontology terms found to be enriched (Table 3-3) include cellular response to chemical stimulus (FDR = $5.3x10^{-11}$), positive regulation of response to stimulus (FDR = $8.4x10^{-11}$), programmed cell death (FDR = $2.3x10^{-10}$), developmental process involved in reproduction (FDR = $2.6x10^{-10}$), cell death (FDR = $2.7x10^{-10}$), regulation of apoptotic process (FDR = $2.8x10^{-10}$), single organism reproductive process (FDR = $2.9x10^{-10}$), reproduction (FDR = $3.0x10^{-10}$), regulation of cell death (FDR = $3.2x10^{-10}$), and regulation of programmed cell death (FDR = $3.2x10^{-10}$). However, when limited to genes only with a differentially methylated

tile within 5,000 base pairs up or downstream of the TSS, no biological process gene ontology terms were significantly enriched in the high vs low analysis (Table 3-4).

Similar findings are true in the HA vs IVV and LA vs IVV analysis for biological process gene ontology terms. In the HA vs IVV analysis with all genes included (Table 3-3), the top ten gene ontology terms that were found to be significantly enriched included cellular response to chemical stimulus (FDR = $6.1x10^{-17}$), positive regulation of metabolic process (FDR = $1.8x10^{-15}$), oxidation-reduction process (FDR = $2.4x10^{-14}$), response to organic substance (FDR = $2.7x10^{-14}$), regulation of molecular function (FDR = $2.7x10^{-14}$), positive regulation of response to stimulus (FDR = $2.8x10^{-14}$), positive regulation of cellular metabolic process (FDR = $2.1x10^{-13}$), positive regulation of cell communication (FDR = $2.3x10^{-13}$), cellular response to organic substance (FDR = $2.7x10^{-13}$), and positive regulation of signaling (FDR = $3.7x10^{-13}$). In the LA vs IVV analysis, the top ten gene ontology terms (Table 3-3) that were found to be significantly enriched included cellular response to chemical stimulus (FDR = $4.9x10^{-12}$), cellular response to organic substance (FDR = $9.3x10^{-10}$), response to organic substance (FDR = $2.2x10^{-9}$), positive regulation of metabolic process (FDR = $2.8x10^{-9}$), positive regulation of response to stimulus (FDR = $6.6x10^{-9}$), positive regulation of biosynthetic process (FDR = $1.0x10^{-8}$), cellular response to endogenous stimulus (FDR = $1.1x10^{-8}$), positive regulation of signal transduction (FDR = $1.4x10^{-8}$), reproductive structure development (FDR = $1.4x10^{-8}$), and positive regulation of cell communication (FDR = $1.5x10^{-8}$). Again, when gene ontology analysis is limited to the genes with a differentially methylated tile within 5,000 bp up or downstream of the TSS, no terms were significantly enriched for biological processes in the HA vs IVV or LA vs IVV analyses (Table 3-4).

Similar patterns hold true for gene ontology analysis for terms associated with cellular components. When including all genes, regardless of distance from the differentially methylated tile to the TSS, many terms were found to be significantly enriched. In the HA vs LA analysis, the top ten significantly enriched cellular component terms (Table 3-5) included extracellular region (FDR = $4.2x10^{-5}$), cytosol (FDR = $2.3x10^{-4}$), membrane-bounded vesicle (FDR = $4.7x10^{-4}$), membrane region (FDR = $1.9x10^{-3}$), extracellular region part (FDR = $2.0x10^{-3}$), membrane microdomain (FDR = $2.0x10^{-3}$), membrane raft (FDR = $2.0x10^{-3}$), troponin complex (FDR = $5.2x10^{-3}$), pigment granule (FDR = $1.2x10^{-2}$), and melanosome (FDR = $1.2x10^{-2}$). The top ten significantly enriched cellular component terms (Table 3-5) for the high vs IVV analysis included extracellular region (FDR = $6.7x10^{-10}$), membrane-bounded vesicle (FDR = $2.7x10^{-8}$), extracellular region part (FDR = $4.2x10^{-8}$), extracellular exosome (FDR = $2.2x10^{-6}$), extracellular organelle (FDR = $2.5x10^{-6}$), extracellular vesicle (FDR = $2.9x10^{-6}$), cytosol (FDR = $2.9x10^{-5}$), endoplasmic reticulum part (FDR = $1.6x10^{-3}$), plasma membrane region (FDR = $3.1x10^{-3}$), and lipid particle (FDR = $4.2x10^{-3}$). Many terms were also identified as significantly enriched in the LA vs IVV cellular component gene ontology analysis (Table 3-5). The top ten included extracellular region (FDR = $2.0x10^{-6}$), membrane-bounded vesicle (FDR = $1.6x10^{-5}$), extracellular region part (FDR = $9.4x10^{-5}$), extracellular organelle (FDR = $2.3x10^{-4}$), extracellular exosome (FDR = $2.5x10^{-4}$), extracellular vesicle (FDR = $2.7x10^{-4}$), cytosol (FDR = $2.7x10^{-3}$), extracellular space (FDR = $2.8x10^{-2}$), mitochondrion (FDR = $3.2x10^{-2}$), and cell projection cytoplasm (FDR = $3.4x10^{-2}$). Again, when limited to the genes with a differentially methylated tile within

5,000 bp of the TSS, no cellular component gene ontology terms were significantly enriched in any of the analyses (Table 3-6).

In the HA vs LA gene ontology analysis for terms associated with molecular function (Table 3-7) identified from all genes with an associated differentially methylated tile, the significantly enriched terms included receptor binding (FDR = $7.1x10^{-4}$), protein dimerization activity (FDR = $1.9x10^{-3}$), hormone activity (FDR = $6.8x10^{-3}$), identical protein binding (FDR = $8.8x10^{-3}$), glycoprotein binding (FDR = $9.0x10^{-3}$), growth factor activity (FDR = $2.6x10^{-2}$), and sulfur compound binding (FDR = $4.0x10^{-2}$). The top ten molecular function gene ontology terms (Table 3-7) significantly enriched in the HA vs IVV analysis for all genes with an associated differentially methylated tile included hormone activity (FDR = $4.0x10^{-8}$), receptor binding (FDR = $5.7x10^{-6}$), protein dimerization activity (FDR = $2.1x10^{-5}$), identical protein binding (FDR = $3.3x10^{-4}$), glycoprotein binding (FDR = $1.1x10^{-3}$), growth factor activity (FDR = $2.3x10^{-3}$), cofactor binding (FDR = $2.6x10^{-3}$), coenzyme binding (FDR = $2.9x10^{-3}$), G-protein coupled peptide receptor activity (FDR = $4.4x10^{-3}$), and peptide receptor activity (FDR = $6.0x10^{-3}$). Only three molecular function gene ontology terms were significantly enriched in the LA vs IVV analysis of all genes associated with differentially methylated tiles (Table 3-7). These terms included receptor binding (FDR = $1.2x10^{-2}$), hormone activity (FDR = $1.4x10^{-2}$), and growth factor binding (FDR = $2.2x10^{-2}$). Again, when gene ontology analysis is limited only to the genes with a significantly differentially methylated tile within 5,000 bp, no significant molecular function terms are enriched in the analysis (Table 3-8).

Similar to the gene ontology analyses, significantly enriched KEGG pathways were also identified in all genes and those genes with a differentially methylated tile within 5,000 bp of the TSS. Again, all genes resulted in a large number of enriched KEGG pathways (Table 3-9) while those with a TSS within 5,000 bp of a differentially methylated tile had no enriched pathways (Table 3-10). The top ten significantly enriched KEGG pathways in the HA vs LA analysis (Table 3-9) included TGF-beta signaling pathway (FDR = $8.1x10^{-4}$), insulin signaling pathway (FDR = $1.1x10^{-3}$), inflammatory bowel disease (FDR = $1.4x10^{-3}$), Jak-STAT signaling pathway (FDR = $1.9x10^{-3}$), metabolic pathways (FDR = $2.2x10^{-3}$), FoxO signaling pathway (FDR = $2.3x10^{-3}$), HIF-1 signaling pathway (FDR = $2.7x10^{-3}$), Leishmaniasis (FDR = $3.1x10^{-3}$), carbon metabolism (FDR = $3.2x10^{-3}$) and hepatitis C (FDR = $3.3x10^{-3}$). In the HA vs IVV analysis, the top ten significantly enriched KEGG pathways (Table 3-9) included TGF-beta signaling pathway (FDR = $8.6x10^{-6}$), hepatitis C (FDR = $1.4x10^{-5}$), prolactin signaling pathway (FDR = $1.5x10^{-5}$), FoxO signaling pathway (FDR = $3.0x10^{-5}$), AMPK signaling pathway (FDR = $1.1x10^{-4}$), insulin signaling pathway (FDR = $2.6x10^{-4}$), Chagas disease (American trypanosomiasis) (FDR = $4.1x10^{-4}$), PPAR signaling pathway (FDR = $4.3x10^{-4)}$, signaling pathways regulating pluripotency of stem cells (FDR = $4.8x10^{-4}$), and hippo signaling pathway (FDR = $5.1x10^{-4}$). The top ten significantly enriched KEGG pathways in LA vs IVV analysis (Table 3-9) included pertussis (FDR = $9.8x10^{-4}$), tuberculosis (FDR = $1.3x10^{-3}$), hepatitis C (FDR = $1.5x10^{-3}$), TGF-beta signaling pathway (FDR = $1.8x10^{-3}$), Hippo signaling pathway (FDR = $2.1x10^{-3}$), metabolic pathways (FDR = $5.1x10^{-3}$), osteoclast differentiation (FDR = $1.1x10^{-2}$), insulin signaling

pathway (FDR = $1.5x10^{-2}$), PPAR signaling pathway (FDR = $1.6x10^{-2}$), and Chagas disease (American trypanosomiasis) (FDR = $1.9x10^{-2}$).

RNA sequencing

RNA-seq libraries were sequenced to an average of 6.33 ± 1.25 million, 7.09 ± 0.66 million, and 11.16 ± 4.5 million reads for the HA, LA, and IVV group, respectively (Table 3-11). Of these total reads, 4.56 ± 1.01 million (71.6% ± 4.3), 4.77 ± 0.85 million (66.7% ± 8.8), and 9.31 ± 4.43 (80.2% ± 10.2) million reads aligned on averaged in the HA, LA and IVV group, respectively (Table 3-11). Sequencing resulted in a total of 59.25 million, 59.53 million, and 93.04 million aligned reads analyzed for the HA, LA, and IVV groups, respectively (Table 3-11).

Differentially Expressed Genes

Genes were considered to be differentially expressed between sample types if they had a fold change greater than 1.5 and FDR corrected p-value less than 0.05. For easier comparison to the RRBS data, analyses were again performed with two groups at a time, resulting in three separate analyses of HA (n = 13) vs LA (n = 12), HA vs IVV (n = 10), and LA vs IVV. In the HA vs LA analysis, 18 genes had increased expression in the high apoptosis group compared to the low apoptosis, while 395 genes had decreased expression in the high group compared to the low apoptosis group (Figure 3-9). In the HA vs IVV analysis, 709 genes had increased expression while 885 had decreased

expression (Figure 3-9). Lastly, in the LA vs IVV analysis, 1,761 genes had increased expression while 777 had decreased expression (Figure 3-9).

Some of the genes determined to be differentially expressed in each analysis were also found to be differentially expressed in one or both of the other analyses. In the HA vs LA analysis, 128 genes were uniquely differentially expressed (Figure 3-10). The HA vs IVV analysis and the LA vs IVV analysis contained 219 and 1,022 uniquely differentially expressed genes, respectively (Figure 3-10). The HA vs LA and HA vs IVV analyses had 34 genes commonly differentially expressed while the HA vs LA and LA vs IVV analyses had 175 commonly differentially expressed genes (Figure 3-10). The HA vs IVV and LA vs IVV analyses had 1,265 genes commonly differentially expressed (Figure 3-10). All three analyses found 76 common differentially expressed genes. (Figure 3-10).

PCA was performed on a random subset of all genes analyzed as well as on only differentially expressed genes (Figure 3-11). PCA of all genes indicated that PC 1 and PC2 explained 51.1% and 25.5% of the variation, respectively (Figure 3-11A). In this analysis, each sample type overlaps. In the PCA of only differentially expressed genes, PC1 and PC2 explain 62.5% and 24.3% of the variation, respectively (Figure 3-11B). In this analysis, the high apoptosis and IVV samples overlap, while the low apoptosis samples show a slightly different patter but still overlap with the high apoptosis and IVV samples (Figure 3-11B).

Hierarchical clustering and a heat map analysis was performed on a random subset of all genes analyzed (Figure 3-12). In the hierarchical clustering analysis, all of

the IVV samples cluster together, with the HA and LA sample scattered without clustering (Figure 3-12). When only differentially expressed genes are analyzed, all of the IVV samples cluster separately from the cloned samples in the hierarchical clustering analysis (Figure 3-13). The cloned samples, while not as scattered as when all genes were included, still do not separate into HA and LA groups (Figure 3-13).

RNA-Seq Gene Ontology Analysis

Gene ontology analysis was performed on genes that were differentially expressed in each analysis. In the HA vs LA and HA vs IVV analyses, gene ontology analysis found no biological process terms that were significantly enriched (Table 3-12). The LA vs IVV analysis resulted in 9 biological process terms that were significantly enriched (Table 3-12), including biological adhesion (FDR = 0.003), cell adhesion (FDR = 0.0069), taxis (FDR = 0.019), chemotaxis (FDR = 0.02), response to external stimulus (FDR = 0.021), ion transport (FDR = 0.023), regulation of cell proliferation (FDR = 0.024), positive regulation of immune system process (FDR = 0.028), and regulation of response to stress (FDR = 0.038).

Gene ontology analysis of cellular component (Table 3-13) terms identified 3 significantly enriched terms from the HA vs LA analysis including intrinsic component of plasma membrane (FDR = 0.009), integral component of plasma membrane (FDR = 0.0099), and extracellular space (FDR = 0.02). In the HA vs IVV analysis, no significantly enriched terms were identified from the cellular component gene ontology analysis (Table 3-13). And six cellular component gene ontology terms (Table 3-13)

were significantly enriched in the LA vs IVV analysis including extracellular region (FDR = 0.000055), intrinsic component of plasma membrane (FDR = 0.0033), extracellular space (FDR = 0.0037), integral component of plasma membrane (FDR = 0.0038), extracellular region part (FDR = 0.0083), and extracellular matrix (FDR = 0.02).

Gene ontology analysis of molecular function terms resulted in no significantly enriched terms in the HA vs LA and HA vs IVV analyses (Table 3-14). The top ten significantly enriched molecular function gene ontology terms (Table 3-14) in the LA vs IVV analysis included cation transmembrane transporter activity (FDR = 0.022), secondary active transmembrane transporter activity (FDR = 0.034), ligand-gated ion channel activity (FDR = 0.037), ligand-gated channel activity (FDR = 0.037), calcium ion binding (FDR = 0.039), active transmembrane transporter activity (FDR = 0.04), channel activity (FDR = 0.041), passive transmembrane transporter activity (FDR = 0.041), peptidase regulator activity (FDR = 0.046), and peptidase inhibitor activity (FDR = 0.048).

Gene ontology analysis also analyzed for KEGG pathways that were significantly enriched in each analysis (Table 3-15). No KEGG pathways were identified as significantly enriched in the HA vs LA and HA vs IVV analyses (Table 3-15). Only one KEGG pathway was significantly enriched in the LA vs IVV analysis (Table 3-15): neuroactive ligand-receptor interaction (FDR = 0.0037).

Combined differential methylation and gene expression

To piece together DNA methylation and RNA expression data, genes from each analysis were identified that had a differentially methylated tile within 5,000 bp and were differentially expressed. In the HA vs LA analysis, 4 genes met this criteria: *ADGRF1, CCND2, SPATA17,* and *TMEM86B* (Table 3-16). The difference in percent methylation and gene expression fold change can be found in Table 3-16. In the HA vs IVV analysis, 12 genes met this criteria: *ACTC1, AUTS2, GIP, LPL, MYOZ1, TDRKH, TMEM126A, TRA2B, TSSK2,* NSSSCG00000015664, ENSSSCG00000032383, and ENSSSCG00000013387. (Table 3-17). In the LA vs IVV analysis, 8 genes matched the criteria: *C2, COL5A2, LGALS2, MYOZ1, PRXL2B, RSAD2, TNNT3,* and *TSSK2*.

Using these genes, which were found to be differentially expressed and with a differentially methylated tile within 5,000 bp in at least one comparison, correlation between RPKM values and tile percent methylation was calculated (Figure 3-14). Of the 22 genes, 5 genes showed significant correlation between RPKM value and percent methylation and 3 genes trended towards significance: *ACTC1* ($p = 0.002$), *AUTS2* ($p = 0.04$), *GIP* ($p = 0.04$), *TDRKH* ($p = 0.02$), and ENSSSCG00000032383 ($p = 0.03$) were significantly correlated while *ADGRF1* ($p = 0.08$), *MYOZ1* ($p = 0.07$), and *TRA2B* ($p = 0.06$) trended towards significance. However, contrary to expectation, *ACTC1, MYOZ1, TDRKH,* and ENSSSCG00000032383 all showed a positive correlation between RPKM value and percent methylation. Additionally, r^2 values were overall low.

Discussion

For the first time, both DNA methylation and gene expression from individual blastocysts with high and low incidence of apoptosis were compared to *in vivo* produced blastocysts. This study provided deeper insight into the epigenetic reprograming of individual embryos following SCNT. Additionally, a large number of biological replicates were included which provided a deeper understanding of the stochastic DNA methylation and gene expression patterns in each individual embryo. The global perspective used in this study yielded vast amounts of data.

While the high apoptosis SCNT and low apoptosis SCNT blastocysts were selected to tease apart differences between them, they are extremely similar as they are cloned porcine blastocysts. In order to reach the blastocyst stage of development, the embryos had to overcome nuclear reprogramming, the maternal to zygotic transition, embryonic genome activation, and multiple rounds of mitosis. Many cloned embryos stall development and fail to reach the blastocyst stage due to altered gene expression and epigenetic reprogramming [107]. Therefore by isolating and analyzing only blastocysts, these embryos have shown a level of competence to have successfully continued development. Because of this milestone, it was expected that differences in DNA methylation and gene expression would be limited when comparing the high apoptosis to low apoptosis SCNT embryos. However, any differences that were identified could be incredibly important to be able to identify the most competent of cloned blastocysts.

Rather than a targeted approach, RRBS provides a global perspective of DNA methylation patterns while maximizing returns by sequencing areas of the genome that

are rich in CpG content. However, this broadens the scope of the analyzed genome to areas outside of the traditionally analyzed CpG islands located in promoter regions of genes of interest. From our sequencing efforts, we did successfully enrich for promoter regions. Nearly 12% of all tiles analyzed fell within a promoter regions, which is significantly enriched when less than 1% of the genome comprises promoter regions. However, only 1% of the differentially methylated regions were located in the promotor regions of genes and 90-92% occurred in intergenic regions of the genome. This is rather interesting as it appears that the cloned embryos are more successful at conserving methylation patterns of the promoter regions which would be critical for the development and success of the embryo. However, limited differential methylation of promoters makes it very difficult to find cause and effect relationships between DNA methylation and RNA expression as DNA methylation of gene promoters are the traditional drivers of gene expression. Due to the connection between DNA methylation driving gene expression patterns, there is a desire to make direct links between DNA methylation level and gene expression patterns. However, because we did not use a targeted approach, it is difficult to identify any direct correlations between DNA methylation level and gene expression patterns. Additionally, differential methylation was determined on a 100 bp tile rather than overall methylation levels of promoter regions. Rather, a majority of the analysis occurred on a genome wide as well as 100 bp tile scale, rather than a gene promoter scale.

Global DNA methylation patterns showed similar overall methylation levels to previously reported RRBS studies of *in vivo* blastocysts in cattle [108] but provided no statistically significant differences in percent methylation across all tiles analyzed

between high apoptosis (HA) SCNT blastocysts, low apoptosis (LA) SCNT blastocysts and *in vivo* produced (IVV) blastocyst. Previous studies have reported differential demethylation of the inner cell mass and trophectoderm in cloned bovine blastocysts [109], and assuming that porcine SCNT blastocyst show similar differences in methylation patterns it could be possible that global dysregulation of DNA methylation is being obscured by analyzing the whole embryo. Unexpectedly, the IVV samples had the largest amount of variation between samples at global percent methylation, which is also apparent when looking at the fraction of tiles that contained various levels of methylation. This inconsistency could be the result of developmental variation noted in the IVV blastocysts where one collection was clearly more developed from the second collection. From visual assessment, the high apoptosis samples had more variability in methylation patterns based on fraction of tiles methylated at varying methylation levels compared to the low apoptosis samples, which were fairly consistent from sample to sample. Increased variation in the high apoptosis global methylation profiles could indicate more variable and inappropriate DNA reprogramming following SCNT and indicate the embryos were less competent.

Analyzing DNA methylation patterns at a 100 base pair tile resolution, more tiles were hypermethylated than hypomethylated in all three of the analyses; high apoptosis vs low apoptosis, high apoptosis vs IVV, and low apoptosis vs IVV. Previous research supports these findings as cloned embryos have been shown to generally de-methylate but do not do so completely, thereby increased methylation levels in cloned embryos would be expected and would explain why more regions were hypermethylated [52]. Comparing the high apoptosis samples to the low apoptosis samples, the percent of tiles

that were hypomethylated and hypermethylated was closer to equal, however more tiles were still hypermethylated indicating no distinct pattern of reprogramming but rather some level of failure to both de-methylate and re-methylate certain regions adding evidence to the hypothesis of random reprogramming following SCNT as no distinct methylation pattern emerged in the cloned embryos. The trend from more regions of hypermethylation across analyses supports the global methylation findings that suggested slightly higher levels of methylation in the cloned samples compared to the IVV samples, although these differences were not significant. The high apoptosis vs IVV analysis found the most tiles to be differentially methylated greater than 25 percent, perhaps indicating a greater difference in overall methylation patterns comparing the high apoptosis embryos to the IVV embryos while the low apoptosis embryos may be more similar to the IVV embryos. This similarity of the low apoptosis and IVV samples is supported by the Venn diagram breakdown of differentially methylated tiles where more than double the number of tiles were uniquely differentially methylated in the HA v IVV analysis compared to the LA v IVV and HA v LA analyses. Only 15 of the tiles were found to be differentially methylated in all 3 analyses indicating distinct methylation patterns between the groups and again supporting a random nature of reprogramming. DNA methylation at a 100 bp tile level indicates that low apoptosis blastocysts are more similar to IVV blastocysts and could therefore be more successful than the high apoptosis blastocysts.

PCA of methylation tells a different story. PCA on a global scale where all tiles were included shows similarities between all 3 groups as the samples overlap on a central point, indicating similar overall methylation patterns which would be expected as all the

embryos have successfully reached the blastocyst stage of development which would require some level of competence. In the PCA analysis representing all tiles, the three sample types all overlap on one central location. The overall similarity in global methylation is supported by the non-descript heat map of percent methylation of all tiles where very little variance in percent methylation is seen between samples. This is supported by the PCA of only differentially methylated tiles that still have an overlapping section of all three groups. While these three groups then radiate out and away from each other, which is expected as these tiles have previously been identified as different, the three still group together indicating some similarity in methylation, even in the tiles that are different. The heat map of differentially methylated tiles also shows small changes in methylation level across samples. This data continues to support the concept that methylation had to be "normal" at some level in order to reach the blastocyst stage of development.

When differentially methylated tiles were associated with the nearest transcription start site for gene ontology analysis, a remarkably large number of biological process, cellular component, and molecular function gene ontology terms were found to be significantly enriched in each analysis. In the high vs low apoptosis analysis, the top ten enriched biological process terms included terms associated with apoptosis, reproduction, and response to stimulus. Just as interesting, the high apoptosis vs IVV analysis provided terms related to metabolic process, cell communication, and response to stimulus while the low apoptosis vs IVV analysis provided terms associated with response to stimulus, cell communication, and the metabolic process. Gene ontology terms found to be significantly enriched in the high vs low apoptosis for the molecular function analysis

included terms such as receptor binding, growth factor activity, hormone activity, and protein dimerization. Similar terms were identified in the high apoptosis vs IVV and low apoptosis vs IVV analysis. All of these pathways were interesting as they are integral components of successful embryo development and could provide direction of future studies to identify specific gene promoters of importance for embryo competency.

When analyzing KEGG pathways that were significantly enriched in the high apoptosis vs low apoptosis embryos, the most significantly enriched pathway was the TGF-beta signaling pathway, an important signaling cascade in embryo development (reviewed in [110]. Interestingly, terms associated with immune response, such as inflammatory bowel disease, Hepatitis C, and Tuberculosis were found in all three analyses. The fact that genes associated with immune response altered in cloned blastocysts with high and low apoptosis compared to IVV blastocysts adds to the need to better understand the immune response to cloned embryos, as it has been previously reported that cloned pregnancies are lost as a result of immune-mediated rejection of the fetus [111].

While these gene ontology findings provided exciting terms of significance, it is crucial to note that the average distance of the differentially methylated tiles to the transcription start site was nearly 16,000 base pairs away which brings into question the biological significance of the findings. While scientific understanding of DNA methylation regulation of gene expression continues to grow, traditional thinking is that DNA methylation of promoter regions of genes regulates gene expression and most promoters will be located 2,000-3,000 base pairs upstream of the transcription start site.

Therefore, in an effort to limit the analysis to tiles that are more likely to be relevant to gene expression control, differentially methylated tiles were limited to those within 5,000 base pairs of the transcription start site. With the new restricted list of genes for gene ontology analysis, no gene ontology terms or KEGG pathways were found to be enriched, indicating a random nature of DNA reprogramming in cloned embryos as no pattern of reprogramming at sites near transcription start sites which could be directly responsible for gene expression was evident. Although, it is also possible that by restricting the gene list, the number of genes analyzed was significantly reduced and the power to call terms significantly enriched was lost, which is why no terms were determined to be significantly enriched in these analyses. The limiting of the gene list in combination with an overall randomness of nuclear reprogramming in cloned embryos would make identifying altered pathways extremely difficult with a large number of samples.

Nuclear reprogramming abnormalities are also present through gene expression in the high apoptosis, low apoptosis, and IVV blastocysts, where gene expression changes varied depending on the analysis, unlike the methylation data where across all three analyses more tiles were hypermethylated. In the high vs low apoptosis analysis, significantly more genes had decreased expression compared to increased expression which does not fit with the methylation data where more genes were hypermethylated compared to hypomethylated. While not anticipated, this data is not alarming due to the many controls of gene expression outside of DNA methylation alone, including histone methylation, chromatin structure, and RNA interference [112]. Another interesting observation is that the low apoptosis vs IVV gene expression analysis yielded the most

genes that were significantly differentially expressed while the high apoptosis vs IVV comparison resulted in the most differentially methylated tiles.

When analyzing the overlap of the genes that were found to be differentially expressed in each comparison, only 128 genes were uniquely differentially expressed in the high vs low apoptosis SCNT samples. As expected, most of the differential gene expression was associated with differences in gene expression patterns between cloned embryos and IVV embryos which was expected as numerous reports have found large numbers of gene expression abnormalities when comparing cloned embryos to IVF or IVV [36]. The conclusion that IVV embryos share a gene expression profile which is different from cloned embryos is evident in the hierarchical clustering where the IVV samples cluster separately from cloned samples when all genes and only differentially expressed genes are analyzed, yet the high apoptosis and low apoptosis samples scatter together as a cloned group rather than separating based on incidence of apoptosis. The hierarchical clustering was performed on genes that were found to be differentially expressed in at least one analysis, so a majority of the genes included in the analysis were not found to be differentially expressed in the high vs low analysis which explains why the high and low groups are not separating form each other. Taken together, the two hierarchical clustering analyses of gene expression indicate that the high and low apoptosis samples share gene expression profiles and cannot be separated on gene expression alone.

Gene ontology analysis of differentially expressed genes found only significantly enriched gene ontology terms for cellular component terms from the high and low

apoptosis analysis. Even then, only three terms were significantly enriched, two of which involved the plasma membrane. Oddly, the high apoptosis vs IVV differentially expressed genes resulted in no gene ontology terms or KEGG pathways that were significantly enriched while the low apoptosis vs IVV differentially expressed genes resulted in numerous significantly enriched terms and pathways in each gene ontology category. The low apoptosis vs IVV analysis did result in nearly five times the number of uniquely differentially expressed genes that did not appear in the other two analyses, which could simply be providing the statistical power in gene ontology analysis to drive such different results compared to the high apoptosis vs IVV gene ontology analysis. While other studies have reported gene ontology differences in cloned and IVF blastocysts [113], a review of misexpressed genes in cloned embryos failed to identify consistently misexpressed genes supporting the hypothesis of the random nature of epigenetic reprogramming following SCNT [36]. As a result of using a small number of samples and a large degree of variation among the samples, there could be an increased probability of false positives. However, by increasing the sample size in our study, we reduced the probability of false positives by having an increased representation of the variation present in cloned embryos. Because most RNA-seq studies use a relatively small number of samples, typically three to four, it could be that by analyzing so many samples in our study the random epigenetic reprogramming was observed within one study and obscured any gene ontology results that could have been present in a subset of the samples.

In an attempt to blend together the DNA methylation data with the gene expression data, genes from each analysis were identified that were differentially

expressed with a fold change of at least 1.5 and had a differentially methylated tile at least 25% differentially methylated within 5,000 base pairs of the gene transcription start site. These criteria identified a total of 22 total genes from the three analyses. Correlation of RPKM values and percent tile methylation was determined for each gene and 5 genes had a statistically significant correlation while 3 genes trended on significance. Because increased levels of methylation decrease gene expression levels, a negative correlation is expected between percent methylation and RPKM values. In half of the significantly correlated genes, a positive correlation was present. Previous studies have found a complicated association between DNA methylation and gene expression depending on the genomic context of the methylation and gene expression levels [114], where findings outside the traditional concept of increased methylation results in decreased gene expression where found. For instance, genes that had high levels of gene expression resulted in a negative correlation between gene expression levels and DNA methylation [114]. Additionally, cancer cells have shown instances where CpG islands were aberrantly hypermethylated and the corresponding gene did not show decreased expression levels, as would be expected [115]. Even in the genes with the appropriate negative correlation, low r^2 values indicate that there was not a strong fit for the linear regression. Taken together these findings are not surprising as a majority of these genes had a single 100 bp tile that was differentially methylated within 5,000 base pairs up or downstream of the transcription start site. A typical gene promoter would be larger than 100 base pairs. So at best, this one tile would be significantly differentially methylated tile and fall within the promoter region, but the rest of the promoter region was not found to be differentially methylated, so gene expression patterns would most likely not be

completely explained by a singular tile. To better understand the link between DNA methylation and gene expression patterns in these embryos, a different approach that focused on the promoter region rather than a genome wide approach could be pursued.

The hypothesis of this study centered on the concept that certain SCNT embryos undergo proper genome reprogramming, resulting in proper gene expression patterns, leading to low levels of apoptosis. Apoptosis could then serve as a useful biomarker of embryo competency early in development in order to increase the efficiency of the technology by being able to select the most successful embryos and minimizing cost of maintaining excessive recipient animals that either will not get pregnant or would lose the pregnancy. However, based on the presented findings, there were relatively few differences in the high apoptosis SCNT blastocysts compared to the low apoptosis SCNT blastocysts in terms of DNA methylation and gene expression profiles. While there were regions that were identified to be significantly differentially methylated as well as genes which were differentially expressed in the high apoptosis compared to low apoptosis samples, no clear patterns emerged. In the methylation data, the low apoptosis samples were less variable than the high apoptosis samples in the PCA, yet the opposite is true of the gene expression data. In the methylation data, hierarchical clustering of differentially methylated tiles separated the high apoptosis from the low apoptosis samples, but this is not true of the differentially expressed genes. So while there may be some more distinct patterns of methylation in the high and low apoptosis embryos, there does not appear to be a distinct pattern of gene expression between the groups. Finally, gene ontology analysis of both genes with a differentially methylated tile within 5,000 base pairs as well

as gene ontology analysis of differentially expressed genes resulted in no gene ontology terms or KEGG pathways that were enriched.

In conclusion, global methylation patterns were similar between the HA, LA, and IVV samples. This methylation pattern contradicts previously published reports that have shown vast differences in global and gene promoter DNA methylation [62, 109]. However, different techniques to detect methylation were used. While we did report difference in DNA methylation, the differences were not as abundant as expected indicating that more epigenetic regulatory mechanisms could be involved than DNA methylation alone. More differences were found in gene expression, especially when comparing the cloned blastocysts to the IVV blastocysts, but very few gene ontology pathways were identified as different in the comparisons [109]. Taken together, these data support the concept of stochastic epigenetic reprogramming following SCNT. Our results suggest that each embryo undergoes a unique reprogramming process, resulting in no clear patterns of DNA methylation and consequently no distinct patterns of RNA expression which is why so few differences between the high and low apoptosis embryos were discovered.

References

1. Armstrong L, Lako M, Dean W, Stojkovic M. Epigenetic modification is central to genome reprogramming in somatic cell nuclear transfer. Stem Cells 2006; 24:805-814.

2. Dean W, Santos F, Reik W. Epigenetic reprogramming in early mammalian development and following somatic nuclear transfer. Semin Cell Dev Biol 2003; 14:93-100.

3. Meng H, Cao Y, Qin J, Song X, Zhang Q, Shi Y, Cao L. DNA methylation, its mediators and genome integrity. Int J Biol Sci 2015; 11:604-617.

4. Niemann H, Carnwath JW, Herrmann D, Wieczorek G, Lemme E, Lucas-Hahn A, Olek S. DNA methylation patterns reflect epigenetic reprogramming in bovine embryos. Cell Reprogram 2010; 12:33-42.

5. Lan J, Hua S, Zhang H, Song Y, Liu J, Zhang Y. Methylation patterns in 5' terminal regions of pluripotency-related genes in bovine in vitro fertilized and cloned embryos. J Genet Genomics 2010; 37:297-304.

6. Hiiragi T, Solter D. Reprogramming is essential in nuclear transfer. Mol Reprod Dev 2005; 70:417-421.

7. Giraldo AM, Lynn JW, Purpera MN, Vaught TD, Ayares DL, Godke RA, Bondioli KR. Inhibition of DNA methyltransferase 1 expression in bovine fibroblast cells used for nuclear transfer. Reprod Fertil Dev 2009; 21:785-795.

8. Oback B. Climbing Mount Efficiency--small steps, not giant leaps towards higher cloning success in farm animals. Reprod Domest Anim 2008; 43 Suppl 2:407-416.

9. Smith C, Berg D, Beaumont S, Standley NT, Wells DN, Pfeffer PL. Simultaneous gene quantitation of multiple genes in individual bovine nuclear transfer blastocysts. Reproduction 2007; 133:231-242.

10. Jackson-Grusby L, Beard C, Possemato R, Tudor M, Fambrough D, Csankovszki G, Dausman J, Lee P, Wilson C, Lander E, Jaenisch R. Loss of genomic methylation causes p53-dependent apoptosis and epigenetic deregulation. Nat Genet 2001; 27:31-39.

11. Gartel AL. Transcriptional inhibitors, p53 and apoptosis. Biochim Biophys Acta 2008; 1786:83-86.

12. Radhakrishnan SK, Gartel AL. A novel transcriptional inhibitor induces apoptosis in tumor cells and exhibits antiangiogenic activity. Cancer Res 2006; 66:3264-3270.

13. Balasubramanyam K, Altaf M, Varier RA, Swaminathan V, Ravindran A, Sadhale PP, Kundu TK. Polyisoprenylated benzophenone, garcinol, a natural histone acetyltransferase inhibitor, represses chromatin transcription and alters global gene expression. J Biol Chem 2004; 279:33716-33726.

14. Guo H, Zhu P, Guo F, Li X, Wu X, Fan X, Wen L, Tang F. Profiling DNA methylome landscapes of mammalian cells with single-cell reduced-representation bisulfite sequencing. Nat Protoc 2015; 10:645-659.

15. Meissner A, Gnirke A, Bell GW, Ramsahoye B, Lander ES, Jaenisch R. Reduced representation bisulfite sequencing for comparative high-resolution DNA methylation analysis. Nucleic Acids Res 2005; 33:5868-5877.

16. Lai L, Prather RS. Production of cloned pigs by using somatic cells as donors. Cloning Stem Cells 2003; 5:233-241.

17. Yoshioka K, Suzuki C, Tanaka A, Anas IM, Iwamura S. Birth of piglets derived from porcine zygotes cultured in a chemically defined medium. Biol Reprod 2002; 66:112-119.

18. Krueger F, Andrews SR. Bismark: a flexible aligner and methylation caller for Bisulfite-Seq applications. Bioinformatics 2011; 27:1571-1572.

19. Akalin A, Kormaksson M, Li S, Garrett-Bakelman FE, Figueroa ME, Melnick A, Mason CE. methylKit: a comprehensive R package for the analysis of genome-wide DNA methylation profiles. Genome Biol 2012; 13:R87.

20. Bates D, Mächler M, Bolker B, Walker S. Fitting Linear Mixed-Effects Models Using lme4. 2015 2015; 67:48.

21. Huang da W, Sherman BT, Lempicki RA. Systematic and integrative analysis of large gene lists using DAVID bioinformatics resources. Nat Protoc 2009; 4:44-57.

22. Huang da W, Sherman BT, Lempicki RA. Bioinformatics enrichment tools: paths toward the comprehensive functional analysis of large gene lists. Nucleic Acids Res 2009; 37:1-13.

23. Liu W, Liu X, Wang C, Gao Y, Gao R, Kou X, Zhao Y, Li J, Wu Y, Xiu W, Wang S, Yin J, et al. Identification of key factors conquering developmental arrest of somatic cell cloned embryos by combining embryo biopsy and single-cell sequencing. Cell discovery 2016; 2:16010-16010.

24. Jiang Z, Lin J, Ouyang Z, Dong H, Zheng X, Chen J, Marjani SL, Duan J, Tian X. DNA methylomes of bovine gametes and in vivo produced preimplantation embryos. Biology of Reproduction 2018; 99:949-959.

25. Kang Y-K, Park JS, Koo D-B, Choi Y-H, Kim S-U, Lee K-K, Han Y-M. Limited demethylation leaves mosaic-type methylation states in cloned bovine pre-implantation embryos. The EMBO journal 2002; 21:1092-1100.

26. Wu MY, Hill CS. TGF-β Superfamily Signaling in Embryonic Development and Homeostasis. Developmental Cell 2009; 16:329-343.

27. Rutigliano HM, Thomas AJ, Wilhelm A, Sessions BR, Hicks BA, Schlafer DH, White KL, Davies CJ. Trophoblast Major Histocompatibility Complex Class I Expression Is Associated with Immune-Mediated Rejection of Bovine Fetuses Produced by Cloning. Biol Reprod 2016; 95:39.

28. Reik W. Stability and flexibility of epigenetic gene regulation in mammalian development. Nature 2007; 447:425.

29. Min B, Cho S, Park JS, Lee Y-G, Kim N, Kang Y-K. Transcriptomic Features of Bovine Blastocysts Derived by Somatic Cell Nuclear Transfer. G3 (Bethesda, Md.) 2015; 5:2527-2538.

30. Lim YC, Li J, Ni Y, Liang Q, Zhang J, Yeo GSH, Lyu J, Jin S, Ding C. A complex association between DNA methylation and gene expression in human placenta at first and third trimesters. PLoS One 2017; 12:e0181155.

31. Moarii M, Boeva V, Vert JP, Reyal F. Changes in correlation between promoter methylation and gene expression in cancer. BMC Genomics 2015; 16:873.

32. Zhang X, Wang D, Han Y, Duan F, Lv Q, Li Z. Altered imprinted gene expression and methylation patterns in mid-gestation aborted cloned porcine fetuses and placentas. J Assist Reprod Genet 2014; 31:1511-1517.

Tables

Table 3-1. RRBS sequencing data.

	Total Reads[1]	Number of Aligned Reads[1]	Percent Aligned
High			
1	29.34	5.22	17.8
2	28.48	5.36	18.8
3	27.96	4.39	15.7
4	31.34	6.44	20.5
5	34.12	8.64	25.3
6	26.24	7.29	27.8
7	28.59	4.64	16.2
8	19.66	1.77	9.0
9	21.88	2.35	10.8
10	29.57	3.85	13.0
11	32.31	7.15	22.1
12	29.67	6.12	20.6
13	28.90	6.30	21.8
Total	368.06	69.52	
Average	28.31	5.35	18.4
Standard Deviation	3.92	1.96	5.5
Low			
1	25.13	6.51	25.9
3	23.69	6.50	27.4
4	27.58	4.94	17.9
5	25.89	4.33	16.7
6	24.62	7.07	28.7
7	20.75	2.90	14.0
8	29.97	4.42	14.8
9	24.16	5.09	21.1
10	30.84	5.48	17.8
11	5.09	0.83	16.4
12	27.60	2.21	8.0
13	25.21	4.60	18.2
Total	290.53	54.88	
Average	24.21	4.57	18.9

	Total Reads[1]	Number of Aligned Reads[1]	Percent Aligned
Standard Deviation	6.62	1.84	6
In Vivo			
1	20.42	1.33	6.5
2	39.39	10.98	27.9
3	20.05	2.56	12.8
4	27.88	9.32	33.4
5	27.14	9.34	34.4
6	28.35	7.11	25.1
7	23.32	9.75	41.8
8	26.02	10.13	38.9
9	30.23	12.05	39.9
10	23.47	7.68	32.7
11	35.23	14.65	41.6
Total	301.50	94.90	
Average	27.41	8.63	30.5
Standard Deviation	5.92	3.89	11.7

[1] In millions of reads

Table 3-2. Bisulfite conversion efficiency determined by exogenous un-methylated lambda-DNA.

	Percent Conversion
High	
1	98.2
2	98.2
3	98.0
4	98.1
5	97.4
6	98.2
7	97.6
8	96.7
9	97.6
10	98.1
11	97.8
12	98.2
13	98.0
Average	97.9
Standard Deviation	0.4
Low	
Low 1	98.0
Low 3	97.2
Low 4	98.3
Low 5	98.1
Low 6	98.1
Low 7	98.2
Low 8	97.5
Low 9	98.1
Low 10	98.2
Low 11	97.7
Low 12	96.9
Low 13	98.5
Average	97.9
Standard Deviation	0.5
In Vivo	
IVV 1	97.3
IVV 2	97.7
IVV 3	96.4
IVV 4	98.4
IVV 5	98.1
IVV 6	96.9
IVV 7	98.4
IVV 8	98.4
IVV 9	98.6
IVV 10	97.8
IVV 11	98.5
Average	97.9
Standard Deviation	0.7

Table 3-3. The top ten biological process gene ontology terms from genes with associated differentially methylated tiles any distance from transcription start site in each analysis.

Term	Count[1]	FDR[2]
High vs. Low		
cellular response to chemical stimulus	221	5.3E-11*
positive regulation of response to stimulus	183	8.4E-11*
programmed cell death	166	2.3E-10*
developmental process involved in reproduction	90	2.6E-10*
cell death	173	2.7E-10*
regulation of apoptotic process	144	2.8E-10*
single organism reproductive process	125	2.9E-10*
reproduction	130	3.0E-10*
regulation of cell death	150	3.2E-10*
regulation of programmed cell death	144	3.2E-10*
High vs. IVV		
cellular response to chemical stimulus	294	6.1E-17*
positive regulation of metabolic process	342	1.8E-15*
oxidation-reduction process	109	2.4E-14*
response to organic substance	283	2.7E-14*
regulation of molecular function	267	2.7E-14*
positive regulation of response to stimulus	236	2.8E-14*
positive regulation of cellular metabolic process	316	2.1E-13*
positive regulation of cell communication	196	2.3E-13*
cellular response to organic substance	237	2.7E-13*
positive regulation of signaling	196	3.7E-13*
Low vs. IVV		
cellular response to chemical stimulus	219	4.9E-12*
cellular response to organic substance	178	9.3E-10*
response to organic substance	208	2.2E-09*
positive regulation of metabolic process	247	2.8E-09*
positive regulation of response to stimulus	171	6.6E-09*
positive regulation of biosynthetic process	154	1.0E-08*
cellular response to endogenous stimulus	109	1.1E-08*
positive regulation of signal transduction	135	1.4E-08*
reproductive structure development	61	1.4E-08*
positive regulation of cell communication	142	1.5E-08*

[1] Count indicates the number of genes represented in each gene ontology term.
[2] FDR-corrected p-values less than 0.05 were considered significant. FDR corrections performed using the Benjamini Hochberg method.

Table 3-4. The top ten biological process gene ontology terms from genes with associated differentially methylated tiles within 5,000 base pairs up or downstream of the transcription start site in each analysis

Term	Count[1]	FDR[2]
High vs. Low		
skeletal muscle contraction	2	9.2E-01
cytoplasmic pattern recognition receptor signaling pathway	2	9.2E-01
cellular response to cytokine stimulus	6	9.2E-01
immune response-regulating signaling pathway	4	9.3E-01
response to virus	5	9.3E-01
immune effector process	7	9.3E-01
response to biotic stimulus	8	9.3E-01
regulation of cell death	11	9.3E-01
homeostatic process	12	9.3E-01
response to oxygen-containing compound	9	9.3E-01
High vs. IVV		
positive regulation of cytokine production	11	1.1E-01
positive regulation of immune system process	16	1.2E-01
cytokine production	14	1.4E-01
regulation of immune response	14	1.5E-01
positive regulation of immune response	13	1.6E-01
lymphocyte mediated immunity	8	2.1E-01
immune effector process	16	2.1E-01
negative regulation of viral process	6	2.1E-01
adaptive immune response based on somatic recombination of immune receptors built from immunoglobulin superfamily domains	8	2.2E-01
cellular response to type I interferon	4	2.3E-01
Low vs. IVV		
monocarboxylic acid metabolic process	7	6.8E-01
single organism reproductive process	11	6.9E-01
oxidation-reduction process	8	6.9E-01
glycerolipid biosynthetic process	4	7.0E-01
multicellular organismal reproductive process	8	7.1E-01
T cell differentiation	5	7.1E-01
oxoacid metabolic process	9	7.1E-01
carboxylic acid metabolic process	9	7.2E-01
multicellular organism reproduction	8	7.2E-01
multi-organism reproductive process	9	7.2E-01

[1] Count indicates the number of genes represented in each gene ontology term.

[2] FDR-corrected p-values less than 0.05 were considered significant. FDR corrections performed using the Benjamini Hochberg method.

Table 3-5. The top ten cellular component gene ontology terms from genes with associated differentially methylated tiles any distance from transcription start site in each analysis

Term	Count[1]	FDR[2]
High vs. Low		
extracellular region	365	4.2E-05*
cytosol	149	2.3E-04*
membrane-bounded vesicle	277	4.7E-04*
membrane region	37	1.9E-03*
extracellular region part	316	2.0E-03*
membrane microdomain	32	2.0E-03*
membrane raft	32	2.0E-03*
troponin complex	7	5.2E-03*
pigment granule	15	1.2E-02*
melanosome	15	1.2E-02*
High vs. IVV		
extracellular region	495	6.7E-10*
membrane-bounded vesicle	380	2.7E-08*
extracellular region part	437	4.2E-08*
extracellular exosome	313	2.2E-06*
extracellular organelle	314	2.5E-06*
extracellular vesicle	314	2.9E-06*
cytosol	189	2.9E-05*
endoplasmic reticulum part	91	1.6E-03*
plasma membrane region	83	3.1E-03*
lipid particle	17	4.2E-03*
Low vs. IVV		
extracellular region	364	2.0E-06*
membrane-bounded vesicle	280	1.6E-05*
extracellular region part	318	9.4E-05*
extracellular organelle	232	2.3E-04*
extracellular exosome	231	2.5E-04*
extracellular vesicle	232	2.7E-04*
cytosol	138	2.7E-03*
extracellular space	123	2.8E-02*
mitochondrion	158	3.2E-02*
cell projection cytoplasm	10	3.4E-02*

[1] Count indicates the number of genes represented in each gene ontology term.
[2] FDR-corrected p-values less than 0.05 were considered significant. FDR corrections performed using the Benjamini Hochberg method.

Table 3-6. The top ten cellular component gene ontology terms from genes with associated differentially methylated tiles within 5,000 base pairs up or downstream of the transcription start site in each analysis.

Term	Count[1]	FDR[2]
High vs. Low		
extracellular region	29	7.0E-01
cytosol	11	9.3E-01
peroxisome	3	9.5E-01
microbody	3	9.5E-01
extracellular organelle	17	9.6E-01
membrane-bounded vesicle	21	9.8E-01
extracellular vesicle	17	9.8E-01
mitochondrion	13	9.9E-01
extracellular exosome	17	1.0E+00
High vs. IVV		
membrane-bounded vesicle	41	1.7E-01
extracellular organelle	34	1.8E-01
extracellular vesicle	34	2.3E-01
extracellular exosome	34	3.0E-01
extracellular region	46	4.3E-01
axon	7	4.7E-01
extracellular region part	41	4.9E-01
cytosol	20	5.2E-01
nuclear outer membrane-endoplasmic reticulum membrane network	10	7.3E-01
anchored component of membrane	3	7.4E-01
Low vs. IVV		
extracellular organelle	22	3.9E-01
acrosomal vesicle	4	4.4E-01
extracellular vesicle	22	4.4E-01
extracellular exosome	22	4.8E-01
membrane-bounded vesicle	26	5.2E-01
lipid particle	4	5.7E-01
extrinsic component of plasma membrane	4	5.7E-01
sperm part	4	6.1E-01
mitochondrial part	9	6.8E-01
extracellular region part	26	7.0E-01

[1] Count indicates the number of genes represented in each gene ontology term.
[2] FDR-corrected p-values less than 0.05 were considered significant. FDR corrections performed using the Benjamini Hochberg method.

Table 3-7. The top ten molecular function gene ontology terms from genes with associated differentially methylated tiles any distance from transcription start site in each analysis.

Term	Count[1]	FDR[2]
High vs. Low		
receptor binding	84	7.1E-04*
protein dimerization activity	28	1.9E-03*
hormone activity	21	6.8E-03*
identical protein binding	27	8.8E-03*
glycoprotein binding	18	9.0E-03*
growth factor activity	16	2.6E-02*
sulfur compound binding	27	4.0E-02*
cofactor binding	38	5.1E-02
cytokine receptor binding	32	7.4E-02
cytokine activity	30	1.0E-01
High vs. IVV		
hormone activity	33	4.0E-08*
receptor binding	108	5.7E-06*
protein dimerization activity	36	2.1E-05*
identical protein binding	35	3.3E-04*
glycoprotein binding	22	1.1E-03*
growth factor activity	20	2.3E-03*
cofactor binding	50	2.6E-03*
coenzyme binding	38	2.9E-03*
G-protein coupled peptide receptor activity	31	4.4E-03*
peptide receptor activity	31	6.0E-03*
Low vs. IVV		
receptor binding	74	1.2E-02*
hormone activity	20	1.4E-02*
growth factor binding	11	2.2E-02*
steroid binding	16	5.8E-02
cofactor binding	37	5.8E-02
protein dimerization activity	22	1.3E-01
G-protein coupled peptide receptor activity	22	1.5E-01
insulin-like growth factor binding	6	1.5E-01
transforming growth factor beta receptor, cytoplasmic mediator activity	5	1.5E-01
peptide receptor activity	22	1.7E-01

[1] Count indicates the number of genes represented in each gene ontology term.
[2] FDR-corrected p-values less than 0.05 were considered significant. FDR corrections performed using the Benjamini Hochberg method.

Table 3-8. The top ten molecular function gene ontology terms from genes with associated differentially methylated tiles within 5,000 base pairs up or downstream of the transcription start site in each analysis.

Term	Count[1]	FDR[2]
High vs. Low		
cysteine-type endopeptidase inhibitor activity	4	7.3E-01
peptidase inhibitor activity	4	9.1E-01
core promoter proximal region DNA binding	5	9.2E-01
transcriptional repressor activity, RNA polymerase II core promoter proximal region sequence-specific binding	3	9.4E-01
core promoter proximal region sequence-specific DNA binding	5	9.4E-01
insulin-like growth factor binding	2	9.4E-01
hormone activity	3	9.4E-01
endopeptidase regulator activity	4	9.5E-01
RNA polymerase II core promoter proximal region sequence-specific DNA binding	5	9.6E-01
endopeptidase inhibitor activity	4	9.8E-01
High vs. IVV		
insulin-like growth factor binding	3	5.7E-01
transcription factor activity, RNA polymerase II core promoter proximal region sequence-specific binding	8	5.8E-01
core promoter proximal region DNA binding	8	6.0E-01
core promoter proximal region sequence-specific DNA binding	8	6.3E-01
regulatory region nucleic acid binding	14	6.7E-01
regulatory region DNA binding	14	6.7E-01
cysteine-type endopeptidase inhibitor activity involved in apoptotic process	3	6.8E-01
sequence-specific double-stranded DNA binding	11	6.9E-01
RNA polymerase II transcription factor activity, sequence-specific DNA binding	11	6.9E-01
transcription regulatory region DNA binding	14	7.0E-01
Low vs. IVV		
ribonucleotide binding	19	1.5E-01
purine nucleotide binding	19	1.6E-01
purine ribonucleotide binding	19	1.7E-01
nucleoside phosphate binding	22	1.8E-01
nucleotide binding	22	1.8E-01
nucleoside binding	19	1.8E-01
ribonucleoside binding	19	2.1E-01
purine ribonucleoside binding	19	2.5E-01
purine nucleoside binding	19	2.5E-01
ATP binding	15	2.9E-01

[1] Count indicates the number of genes represented in each gene ontology term.
[2] FDR-corrected p-values less than 0.05 were considered significant. FDR corrections performed using the Benjamini Hochberg method.

Table 3-9. The top KEGG pathway terms from genes with associated differentially methylated tiles any distance from transcription start site in each analysis.

Term	Count[1]	FDR[2]
High vs. Low		
TGF-beta signaling pathway	24	8.1E-04*
Insulin signaling pathway	33	1.1E-03*
Inflammatory bowel disease (IBD)	21	1.4E-03*
Jak-STAT signaling pathway	33	1.9E-03*
Metabolic pathways	170	2.2E-03*
FoxO signaling pathway	32	2.3E-03*
HIF-1 signaling pathway	26	2.7E-03*
Leishmaniasis	19	3.1E-03*
Carbon metabolism	26	3.2E-03*
Hepatitis C	30	3.3E-03*
High vs. IVV		
TGF-beta signaling pathway	32	8.6E-06*
Hepatitis C	43	1.4E-05*
Prolactin signaling pathway	28	1.5E-05*
FoxO signaling pathway	43	3.0E-05*
AMPK signaling pathway	38	1.1E-04*
Insulin signaling pathway	40	2.6E-04*
Chagas disease (American trypanosomiasis)	34	4.1E-04*
PPAR signaling pathway	25	4.3E-04*
Signaling pathways regulating pluripotency of stem cells	39	4.8E-04*
Hippo signaling pathway	40	5.1E-04*
Low vs. IVV		
Pertussis	23	9.8E-04*
Tuberculosis	39	1.3E-03*
Hepatitis C	31	1.5E-03*
TGF-beta signaling pathway	22	1.8E-03*
Hippo signaling pathway	32	2.1E-03*
Metabolic pathways	161	5.1E-03*
Osteoclast differentiation	29	1.1E-02*
Insulin signaling pathway	28	1.5E-02*
PPAR signaling pathway	18	1.6E-02*
Chagas disease (American trypanosomiasis)	24	1.9E-02*

[1] Count indicates the number of genes represented in each gene ontology term.
[2] FDR-corrected p-values less than 0.05 were considered significant. FDR corrections performed using the Benjamini Hochberg method.

Table 3-10. The KEGG pathways identified from genes with associated differentially methylated tiles within 5,000 base pairs up or downstream of the transcription start site in each analysis.

Term	Count[1]	FDR[2]
High vs. Low		
cAMP signaling pathway	6	5.9E-01
Hepatitis B	5	6.5E-01
RIG-I-like receptor signaling pathway	4	8.3E-01
Amphetamine addiction	3	9.4E-01
HTLV-I infection	5	9.5E-01
High vs. IVV		
Hepatitis C	7	7.9E-01
RIG-I-like receptor signaling pathway	4	9.2E-01
AMPK signaling pathway	5	9.2E-01
Alzheimer's disease	6	9.3E-01
Prolactin signaling pathway	4	9.5E-01
Hepatitis B	6	9.8E-01
Regulation of autophagy	3	9.9E-01
Low vs. IVV		
Osteoclast differentiation	4	9.3E-01
Endocytosis	5	9.4E-01
Insulin signaling pathway	4	9.7E-01
Neurotrophin signaling pathway	4	9.8E-01
Alzheimer's disease	5	1.0E+00

[1] Count indicates the number of genes represented in each gene ontology term.
[2] FDR-corrected p-values less than 0.05 were considered significant. FDR corrections performed using the Benjamini Hochberg method.

Table 3-11. RNA sequencing data.

	Total Reads[1]	Number of Aligned Reads[1]	Percent Aligned
High			
1	2.67	1.68	62.9
2	5.54	4.24	76.6
3	6.84	5.08	74.3
4	7.13	5.05	70.8
5	7.55	5.74	76.0
6	6.64	4.99	75.2
7	6.15	4.19	68.2
8	6.87	4.90	71.4
9	6.10	3.98	65.3
10	6.49	4.41	67.9
11	5.97	4.38	73.5
12	7.50	5.49	73.2
13	6.80	5.12	75.2
Total	82.25	59.25	
Average	6.33	4.56	71.6
Standard Deviation	1.25	1.01	4.3
Low			
1	6.63	4.88	73.6
3	7.53	5.36	69.8
4	7.18	4.82	64.8
5	7.20	4.74	65.8
6	8.17	5.73	70.1
7	6.45	4.07	63.1
8	7.48	4.50	60.1
9	7.05	5.33	75.6
10	7.93	5.28	66.6
11	6.33	4.21	66.5
12	7.50	5.49	73.2
13	6.80	5.12	75.2
Total	86.25	59.53	
Average	7.09	4.77	66.7
Standard Deviation	0.66	0.85	8.8
In Vivo			
1	5.66	3.57	63.1
2	6.65	5.11	76.9
3	5.27	3.24	61.5
4	6.97	5.54	79.6
5	14.63	12.27	83.8
6	17.32	15.24	88.0
7	13.24	11.63	87.9
8	12.94	11.23	86.8
9	14.38	12.72	88.5
11	14.57	12.49	85.8
Total	111.63	93.04	
Average	11.16	9.31	80.2
Standard Deviation	4.50	4.43	10.2

[1] In millions.

Table 3-12. The top ten biological process gene ontology terms from genes differentially expressed in each analysis.

Term	Count[1]	FDR[2]
High vs. Low		
biological adhesion	21	2.0E-01
positive regulation of response to stimulus	26	2.2E-01
cell adhesion	21	2.3E-01
circulatory system development	18	2.5E-01
cardiovascular system development	18	2.5E-01
vasculature development	13	2.8E-01
regulation of angiogenesis	7	5.4E-01
cell-substrate adhesion	8	5.8E-01
positive regulation of signal transduction	19	6.1E-01
regulation of vasculature development	7	6.6E-01
High vs. IVV		
negative regulation of response to external stimulus	17	1.7E-01
regulation of response to stress	45	1.9E-01
regulation of response to external stimulus	33	2.2E-01
negative regulation of reproductive process	9	2.4E-01
negative regulation of defense response	12	2.7E-01
negative regulation of inflammatory response	10	3.5E-01
regulation of defense response	24	5.2E-01
multi-organism reproductive process	29	5.2E-01
epithelial cell proliferation	17	5.2E-01
wound healing	17	5.2E-01
Low vs. IVV		
biological adhesion	93	3.0E-03*
cell adhesion	90	6.9E-03*
taxis	46	1.9E-02*
chemotaxis	46	2.0E-02*
response to external stimulus	121	2.1E-02*
ion transport	77	2.3E-02*
regulation of cell proliferation	90	2.4E-02*
positive regulation of immune system process	56	2.8E-02*
regulation of response to stress	75	3.8E-02*
regulation of programmed cell death	84	5.4E-02

[1] Count indicates the number of genes represented in each gene ontology term.

[2] FDR-corrected p-values less than 0.05 were considered significant. FDR corrections performed using the Benjamini Hochberg method.

Table 3-13. The top ten cellular component gene ontology terms from genes differentially expressed in each analysis.

Term	Count[1]	FDR[2]
High vs. Low		
intrinsic component of plasma membrane	25	9.0E-03*
integral component of plasma membrane	25	9.9E-03*
extracellular space	23	2.0E-02*
extracellular region part	42	1.0E-01
extracellular matrix	10	1.8E-01
extracellular region	44	2.3E-01
cell surface	11	4.9E-01
collagen trimer	4	5.0E-01
membrane region	6	6.2E-01
external side of plasma membrane	5	8.2E-01
High vs. IVV		
extracellular region	135	1.9E-01
extracellular region part	116	7.0E-01
extracellular matrix	20	8.2E-01
proteinaceous extracellular matrix	15	8.6E-01
extracellular space	47	8.8E-01
lytic vacuole	17	9.4E-01
neuron projection terminus	4	9.4E-01
lipid particle	5	9.5E-01
nuclear speck	7	9.5E-01
extracellular organelle	78	9.5E-01
Low vs. IVV		
extracellular region	259	5.5E-05*
intrinsic component of plasma membrane	102	3.3E-03*
extracellular space	96	3.7E-03*
integral component of plasma membrane	98	3.8E-03*
extracellular region part	219	8.3E-03*
extracellular matrix	38	2.0E-02*
extracellular organelle	152	1.2E-01
cell surface	48	1.2E-01
lipid particle	10	1.3E-01
extracellular vesicle	152	1.3E-01

[1] Count indicates the number of genes represented in each gene ontology term.
[2] FDR-corrected p-values less than 0.05 were considered significant. FDR corrections performed using the Benjamini Hochberg method.

Table 3-14. The top ten molecular function gene ontology terms from genes differentially expressed.

Term	Count[1]	FDR[2]
High vs. Low		
potassium channel activity	5	5.3E-01
cation channel activity	8	5.5E-01
purinergic nucleotide receptor activity	3	5.5E-01
nucleotide receptor activity	3	5.5E-01
inorganic cation transmembrane transporter activity	10	5.6E-01
gated channel activity	8	5.7E-01
molecular transducer activity	29	5.7E-01
receptor activity	29	5.7E-01
receptor binding	12	6.0E-01
purinergic receptor activity	3	6.2E-01
High vs. IVV		
carboxylic ester hydrolase activity	9	5.9E-01
growth factor binding	5	5.9E-01
channel activity	21	6.0E-01
passive transmembrane transporter activity	21	6.0E-01
endopeptidase regulator activity	11	6.0E-01
integrin binding	5	6.1E-01
calcium-activated potassium channel activity	4	6.2E-01
protein complex binding	15	6.2E-01
metal ion transmembrane transporter activity	19	6.3E-01
peptidase inhibitor activity	11	6.3E-01
Low vs. IVV		
cation transmembrane transporter activity	53	2.2E-02*
secondary active transmembrane transporter activity	27	3.4E-02*
ligand-gated ion channel activity	18	3.7E-02*
ligand-gated channel activity	18	3.7E-02*
calcium ion binding	55	3.9E-02*
active transmembrane transporter activity	36	4.0E-02*
channel activity	41	4.1E-02*
passive transmembrane transporter activity	41	4.1E-02*
peptidase regulator activity	23	4.6E-02*
peptidase inhibitor activity	21	4.8E-02*

[1] Count indicates the number of genes represented in each gene ontology term.
[2] FDR-corrected p-values less than 0.05 were considered significant. FDR corrections performed using the Benjamini Hochberg method.

Table 3-15. The top ten KEGG pathway terms from genes differentially expressed in each analysis.

Term	Count[1]	FDR[2]
High vs. Low		
Cell adhesion molecules (CAMs)	6	6.0E-01
Hippo signaling pathway	6	7.9E-01
High vs. IVV		
Protein processing in endoplasmic reticulum	14	4.3E-01
Protein digestion and absorption	9	4.3E-01
MAPK signaling pathway	16	6.0E-01
Regulation of actin cytoskeleton	14	6.5E-01
PPAR signaling pathway	7	6.6E-01
Insulin resistance	9	7.2E-01
Lysosome	9	7.4E-01
Vasopressin-regulated water reabsorption	5	7.7E-01
Transcriptional misregulation in cancer	10	7.9E-01
PI3K-Akt signaling pathway	17	8.0E-01
Low vs. IVV		
Neuroactive ligand-receptor interaction	36	3.7E-03*
Type I diabetes mellitus	10	8.6E-02
Histidine metabolism	7	1.0E-01
Cell adhesion molecules (CAMs)	19	1.7E-01
Complement and coagulation cascades	12	2.0E-01
Cholinergic synapse	15	2.9E-01
Protein digestion and absorption	12	2.9E-01
PI3K-Akt signaling pathway	31	3.2E-01
Graft-versus-host disease	7	3.4E-01
PPAR signaling pathway	10	3.6E-01

[1] Count indicates the number of genes represented in each gene ontology term.
[2] FDR-corrected p-values less than 0.05 were considered significant. FDR corrections performed using the Benjamini Hochberg method.

Table 3-16. Genes with differentially expressed with a differentially methylated tile within 5,000 bp in the HA vs LA blastocysts.

Gene	Chr[1]	Start[1]	Methylation			Gene Expression	
			Dist to TSS[2]	Diff in Methyl[3]	FDR[3]	FC[4]	FDR[4]
ADGRF1 (ENSSSCG00000001726)	7	41842401	-4985	36.29	3.00E-21	0.01	1.40E-02
CCND2 (ENSSSCG00000038694)	5	66113001	1476	27.06	2.20E-08	0.03	3.10E-02
SPATA17 (ENSSSCG00000029778)	10	7797201	-218	-31.3	1.30E-15	0.03	3.00E-02
TMEM86B (ENSSSCG00000003302)	6	59428101	-2016	31.14	5.80E-05	0.03	2.90E-02

[1] Chr and start refers to the chromosome location of the tile that was differentially methylated.
[2] Distance to TSS is the distance to the gene's transcription start site, where a negative number is the number of bases before the transcription start site and a positive number is the number of bases after the transcription start site.
[3] Diff in Methyl is the difference in percent methylation of the tile comparing high to low apoptosis samples with the associated FDR corrected P-value.
[4] Fold change is the fold change gene expression level based on RPKM values comparing high to low samples with the FDR adjusted p-value.

Table 3-17. Genes with differentially expressed with a differentially methylated tile within 5,000 bp in the HA vs IVV blastocysts.

Gene	Chr[1]	Start[1]	Methylation			Gene Expression	
			Dist to TSS[2]	Diff in Methyl[3]	FDR[3]	FC[4]	FDR[4]
ACTC1 (ENSSSCG00000004803)	1	136276901	-4119	-31.00	2.3E-53	0.37	8.3E-08
AUTS2 (ENSSSCG00000007727)	3	13563601	-1739	26.30	7.7E-14	5.08	2.2E-02
GIP (ENSSSCG00000026330)	12	25162201	3971	26.86	1.2E-20	3.00	5.0E-03
LPL (ENSSSCG00000040631)	14	4106601	1789	26.31	4.4E-34	4.06	4.3E-02
MYOZ1 (ENSSSCG00000010304)	14	76455201	-2256	40.30	1.7E-39	3.79	1.9E-02
TDRKH (ENSSSCG00000027770)	4	97418501	2563	32.60	5.8E-116	4.45	3.5E-08
TMEM126A (ENSSSCG00000025187)	9	19572001	-4199	32.35	2.0E-104	0.47	2.1E-07
TRA2B (ENSSSCG00000030225)	13	123784401	-3651	27.55	1.8E-15	0.50	8.3E-13
TSSK2 (ENSSSCG00000010113)	14	50943901	886	33.38	6.6E-15	7.51	1.1E-02
			3086	44.24	2.0E-46		
			3186	29.86	2.1E-16		
(ENSSSCG00000015664)	9	67932501	-793	28.04	6.5E-36	3.86	6.9E-04
(ENSSSCG00000032383)	2	150558101	-3182	26.90	3.7E-19	4.24	8.4E-03
(ENSSSCG00000013387)	2	44250801	-1749	26.64	3.2E-12	4.68	1.0E-02

[1] Chr and start refers to the chromosome location of the tile that was differentially methylated.
[2] Distance to TSS is the distance to the gene's transcription start site, where a negative number is the number of bases before the transcription start site and a positive number is the number of bases after the transcription start site.
[3] Diff in Methyl is the difference in percent methylation of the tile comparing high to low apoptosis samples with the associated FDR corrected P-value.
[4] Fold change is the fold change gene expression level based on RPKM values comparing high to low samples with the FDR adjusted p-value.

Table 3-18. Genes with differentially expressed with a differentially methylated tile within 5,000 bp in the LA vs IVV blastocysts.

			Methylation			Gene Expression	
Gene	Chr[1]	Start[1]	Dist to TSS[2]	Diff in Methyl[3]	FDR[3]	FC[4]	FDR[4]
C2 (ENSSSCG00000001422)	7	24024901	4313	27.90	4.4E-08	2.73	9.5E-05
COL5A2 (ENSSSCG00000016035)	15	93758701	-12	-26.71	1.3E-09	3.64	2.5E-02
LGALS2 (ENSSSCG00000021728)	5	10234001	-3672	36.75	1.2E-20	17.01	1.4E-04
MYOZ1 (ENSSSCG00000010304)	14	76455201	-2256	35.54	1.2E-16	6.82	2.9E-04
PRXL2B (ENSSSCG00000026554)	6	64434101	1809	35.27	1.1E-10	7.04	4.0E-02
RSAD2 (ENSSSCG00000008648)	3	1.29E+08	3810	29.48	6.5E-16	2.06	1.3E-02
TNNT3 (ENSSSCG00000031903)	2	1306601	4295	25.54	4.9E-07	10.87	6.5E-04
TSSK2 (ENSSSCG00000010113)	14	50943901	886	25.22	3.1E-08	6.18	2.0E-02

[1] Chr and start refers to the chromosome location of the tile that was differentially methylated.
[2] Distance to TSS is the distance to the gene's transcription start site, where a negative number is the number of bases before the transcription start site and a positive number is the number of bases after the transcription start site.
[3] Diff in Methyl is the difference in percent methylation of the tile comparing high to low apoptosis samples with the associated FDR corrected P-value.
[4] Fold change is the fold change gene expression level based on RPKM values comparing high to low samples with the FDR adjusted p-value.

Figures

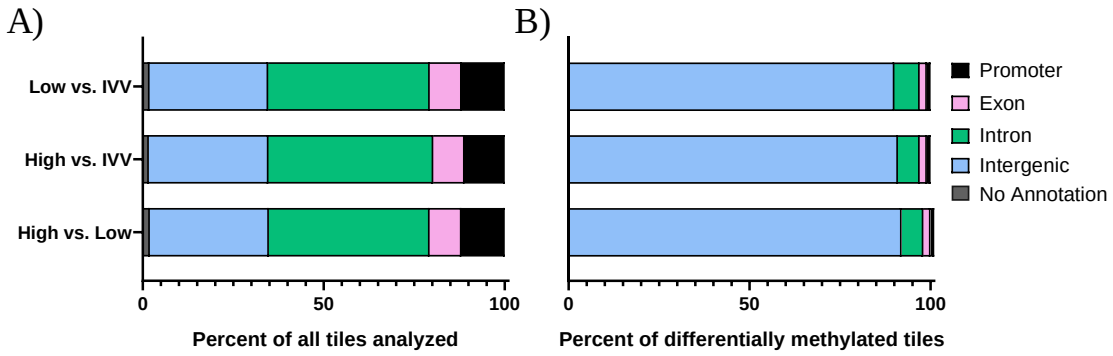

Figure 3-1. Annotation of tiles. Panel A indicates the percent of all tiles analyzed that fell within promoters (black), exons (pink), introns (green), intergenic regions (blue), and regions that were not annotated (grey). Panel B only includes the tiles that were differentially methylated.

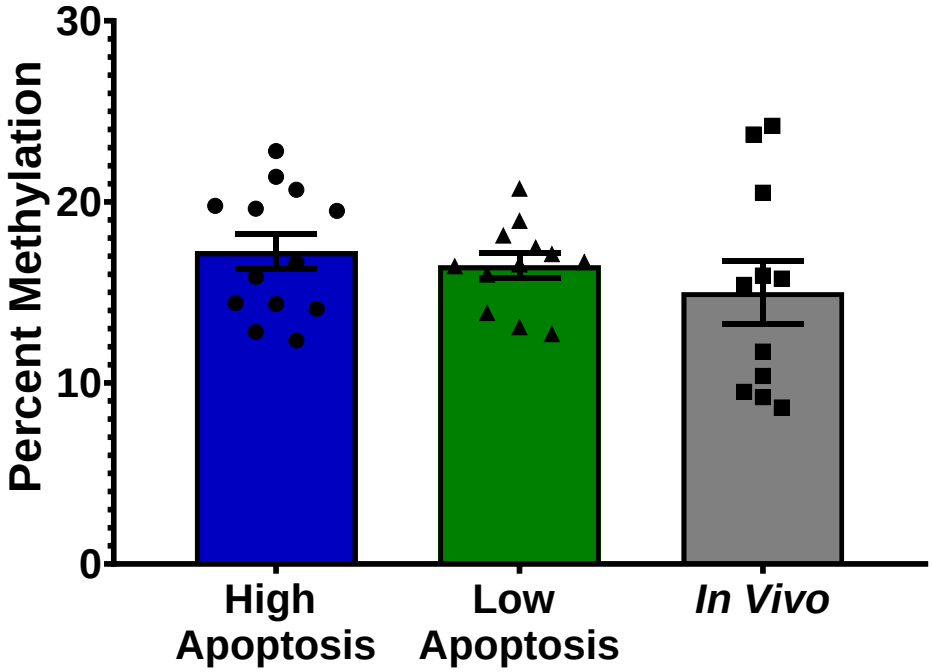

Figure 3-2. Global methylation patterns of average percent methylation of all tiles analyzed. Error bars represent the standard error of the mean.

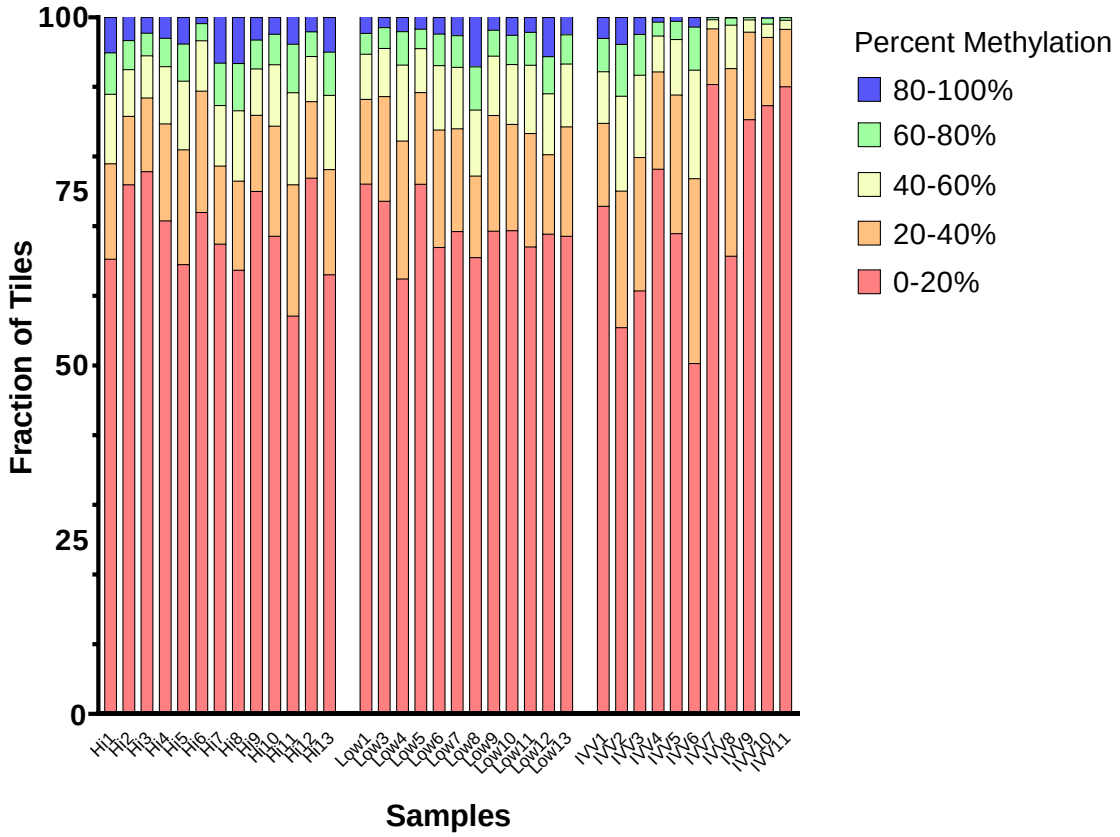

Figure 3-3. Fraction of tiles methylated at varying levels of methylation. The fraction of tiles in each sample that are methylated from 0-20% (red), 20-40% (orange), 40-60% (yellow), 60-80% (green), and 80-100% (blue). Samples are grouped by sample type; high, low, and IVV, respectively.

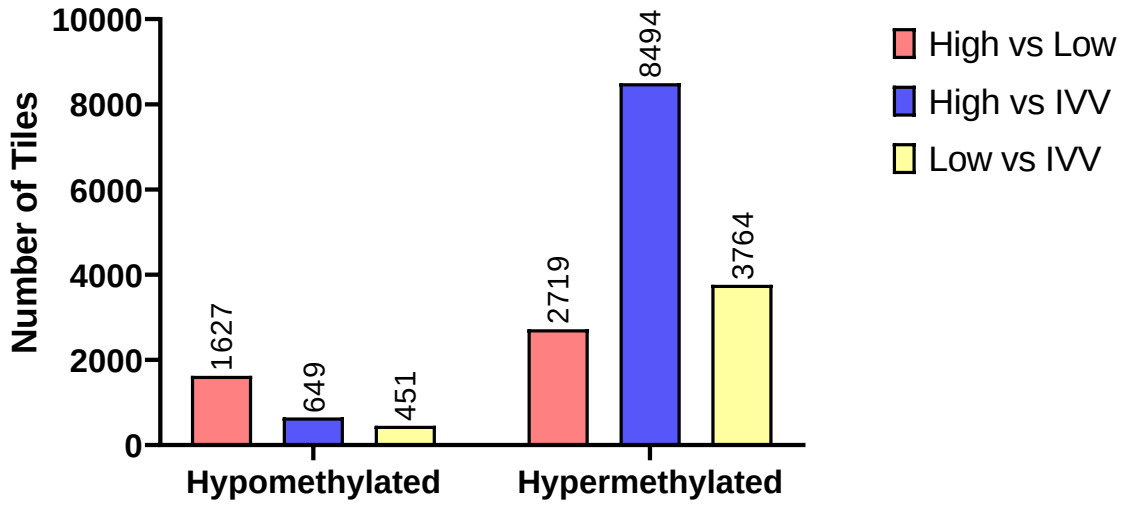

Figure 3-4. The number of differentially methylated tiles in each analysis. The number of tiles at least 25% differentially methylated in the high (n = 13) vs low (n = 12), high vs IVV (n = 11), and low vs IVV analyses shown in red, blue, and yellow, respectively. Hypomethylated tiles refer to tiles with lower methylation levels in the first group of the analysis compared to the second group. Conversely, hypermethylated tiles refers to tiles with higher levels of methylation in the first group of the analysis compared to the second group.

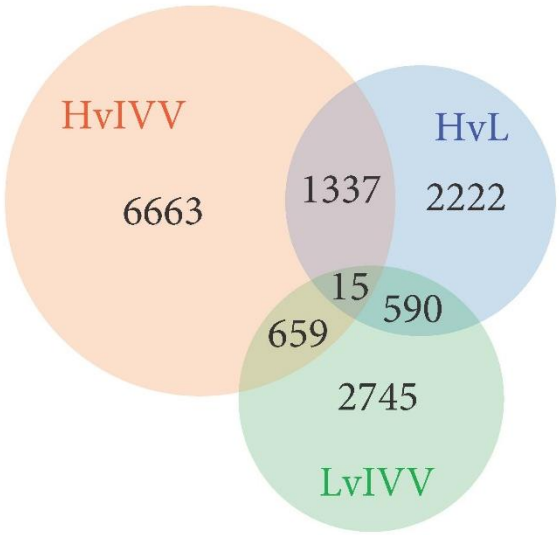

Figure 3-5. Venn diagram depicting similarities and differences in differentially methylated tiles from each analysis. Values in the uniquely blue, green, and orange segments indicate tiles that were uniquely differentially methylated in the high vs low, low vs IVV, and high vs IVV analysis, respectively. Overlapping segments represent the genes that were found to be differentially methylated in multiple analyses.

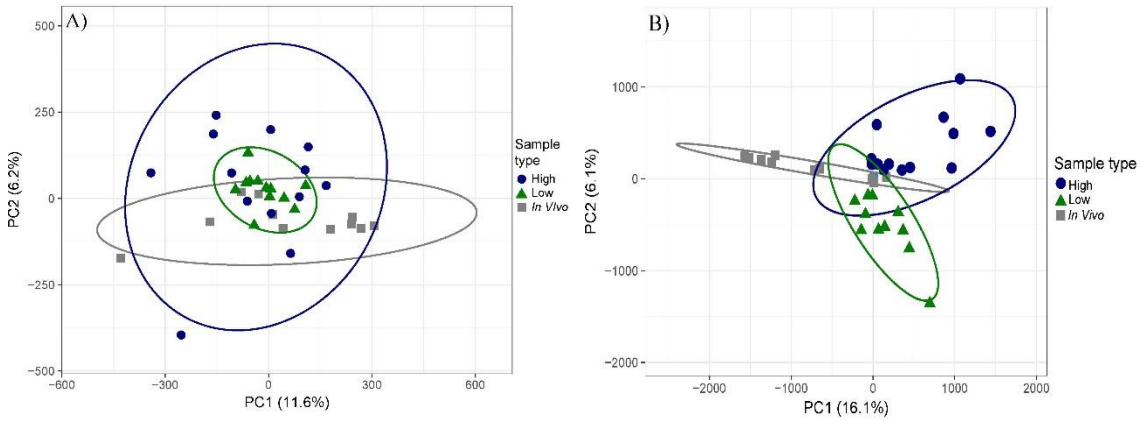

Figure 3-6. Principal component analyses of gene expression analysis. Panel A includes all tiles analyzed while panel B includes only differentially methylated tiles. High apoptosis, low apoptosis, and *in vivo* embryos are plotted in blue circles, green triangles, and grey squares, respectively. No unit variance scaling is applied to rows. SVD with imputation is used to calculate principal components. X and Y axis show principal component 1 and 2, respectively. Prediction ellipses are such that with a probability of 0.95, a new observation from the same group will fall inside the ellipse.

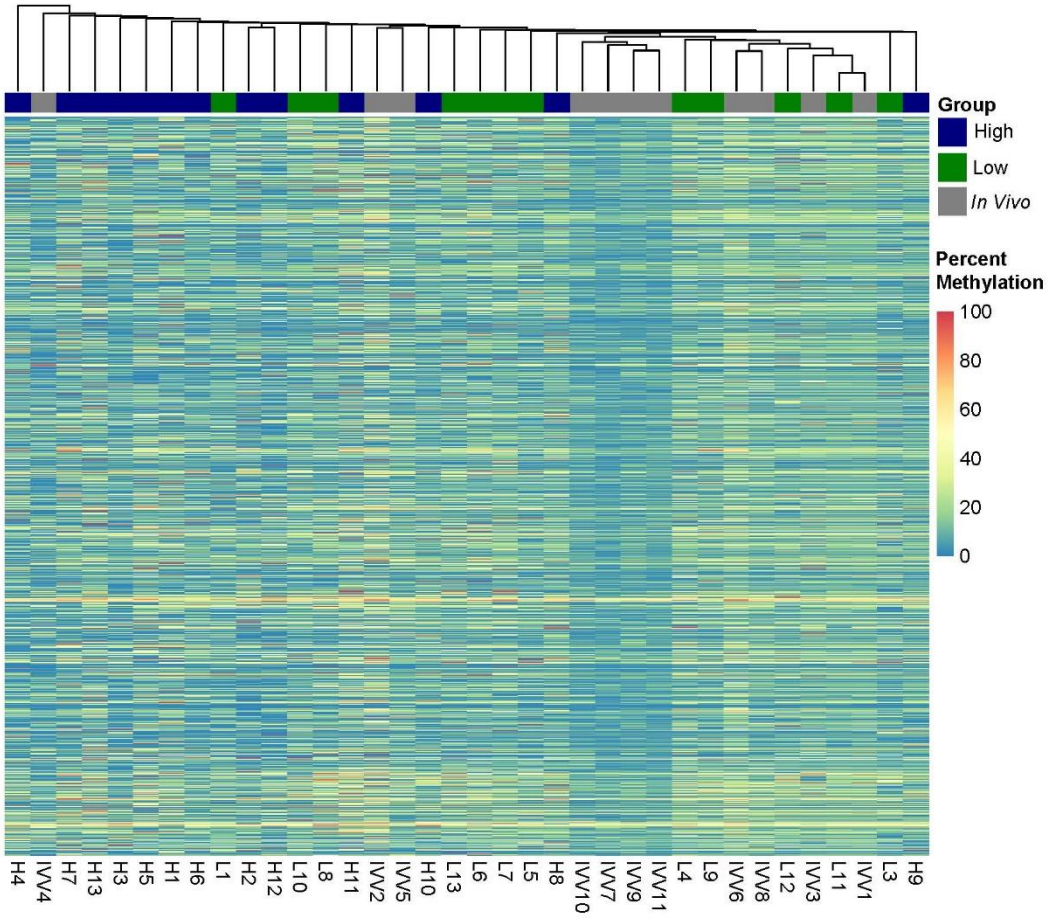

Figure 3-7. Heat map and clustering analysis of a representative sub-set of all tiles analyzed for DNA methylation patterns. Rows (1197 tiles) had no unit variance scaling applied. Columns (N = 36) are clustered using correlation distance and average linkage. High apoptosis are represented in hierarchical clustering by blue, low apoptosis by green, and *in vivo* by grey. Red, yellow, and blue in the heat map indicates percent methylation.

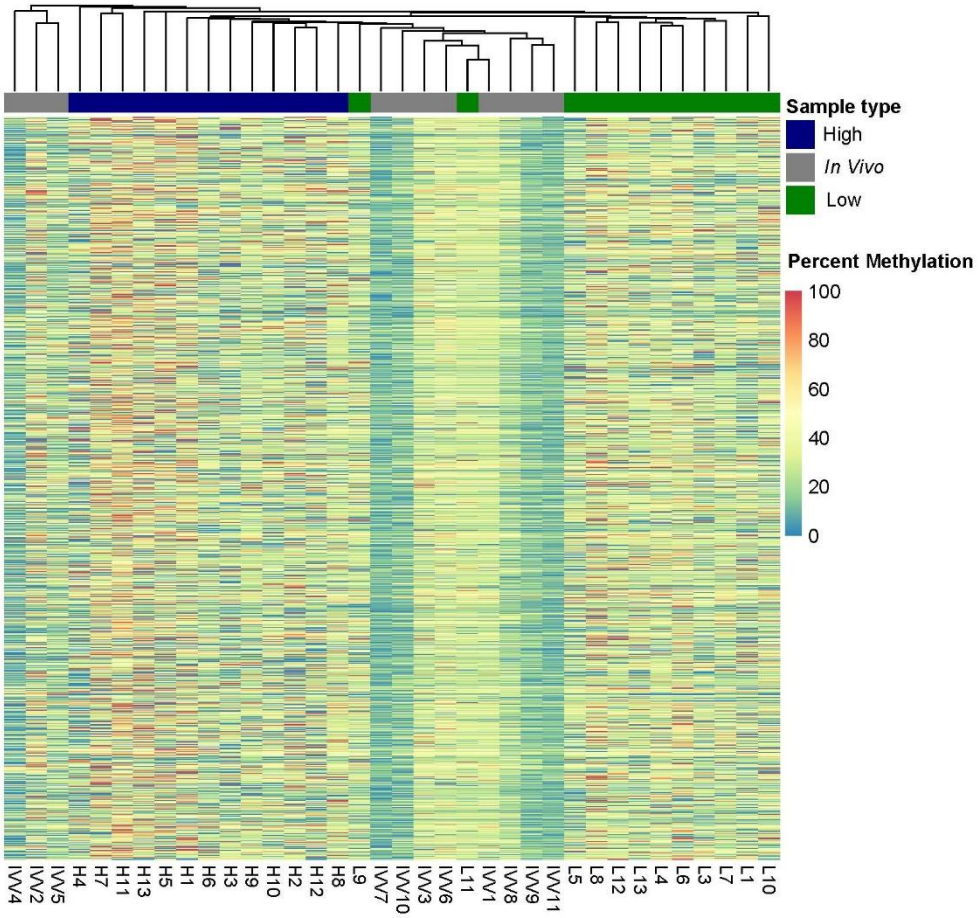

Figure 3-8. Heat map and clustering analysis of a representative sub-set of the differentially methylated tiles identified as differentially methylated in at least one of the analysis; high vs low, high vs IVV, or low vs IVV. Rows (1200 genes) had no unit variance scaling applied. Columns (N = 36) are clustered using correlation distance and average linkage. High apoptosis are represented in hierarchical clustering by blue, low apoptosis by green, and *in vivo* by grey. Red, yellow, and blue in the heat map indicates percent methylation value.

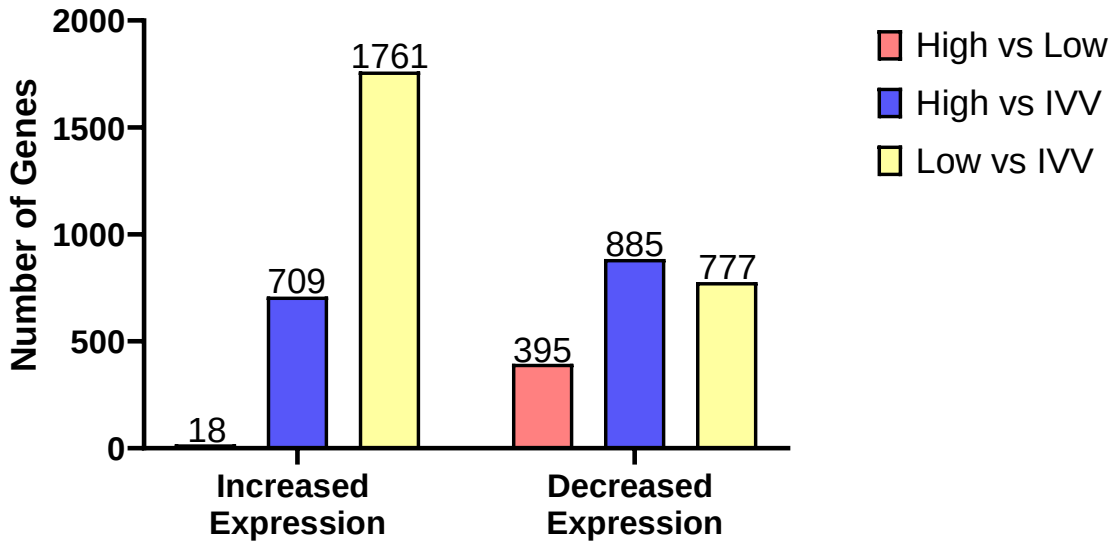

Figure 3-9. The number of differentially expressed genes in each analysis. The number of genes differentially expressed with a fold-change greater than 1.5 and FDR-corrected p-value less than 0.05 comparing high apoptosis (n = 13) to low apoptosis (n = 12) samples, high apoptosis to *in vivo* embryos (n = 10), and low apoptosis to *in vivo* embryos indicated by red, blue, and yellow bars, respectively. Genes with increased expression showed increased RPKM counts in the first sample type compared to the second sample type of the comparison, while genes with decreased counts showed decreased RPKM counts in the first sample type compared to the second sample type of the comparison.

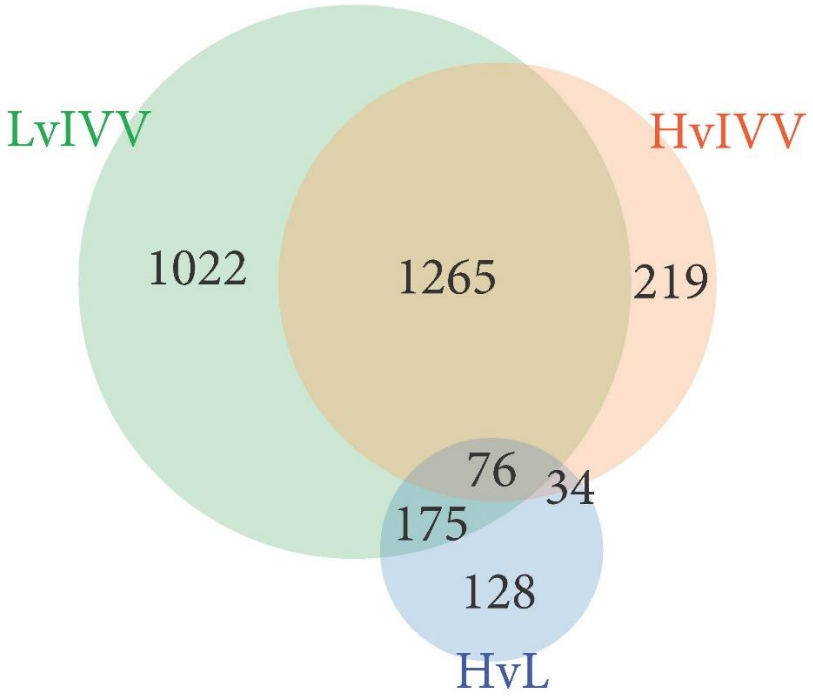

Figure 3-10. Venn diagram depicting similarities and differences in differentially expressed genes from each analysis. Values in the uniquely blue, green, and orange segments indicate genes that were uniquely differentially expressed in the high vs low, low vs IVV, and high vs IVV analysis, respectively. Overlapping segments represent the genes that were found to be differentially expressed in multiple analyses.

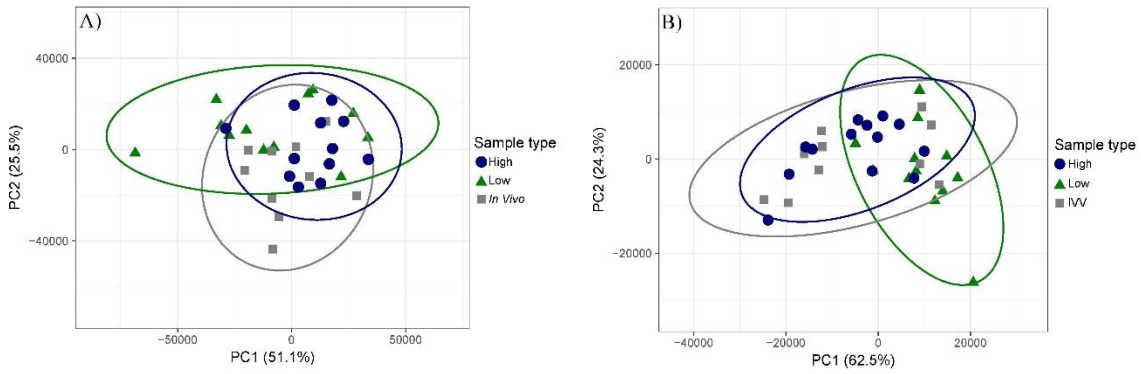

Figure 3-11. Principal component analyses of gene expression analysis. Panel A includes all genes analyzed while panel B includes only differentially expressed genes. High apoptosis, low apoptosis, and *in vivo* embryos are plotted in blue circles, green triangles, and grey squares, respectively. No unit variance scaling is applied to rows. SVD with imputation is used to calculate principal components. X and Y axis show principal component 1 and 2, respectively. Prediction ellipses are such that with a probability of 0.95, a new observation from the same group will fall inside the ellipse.

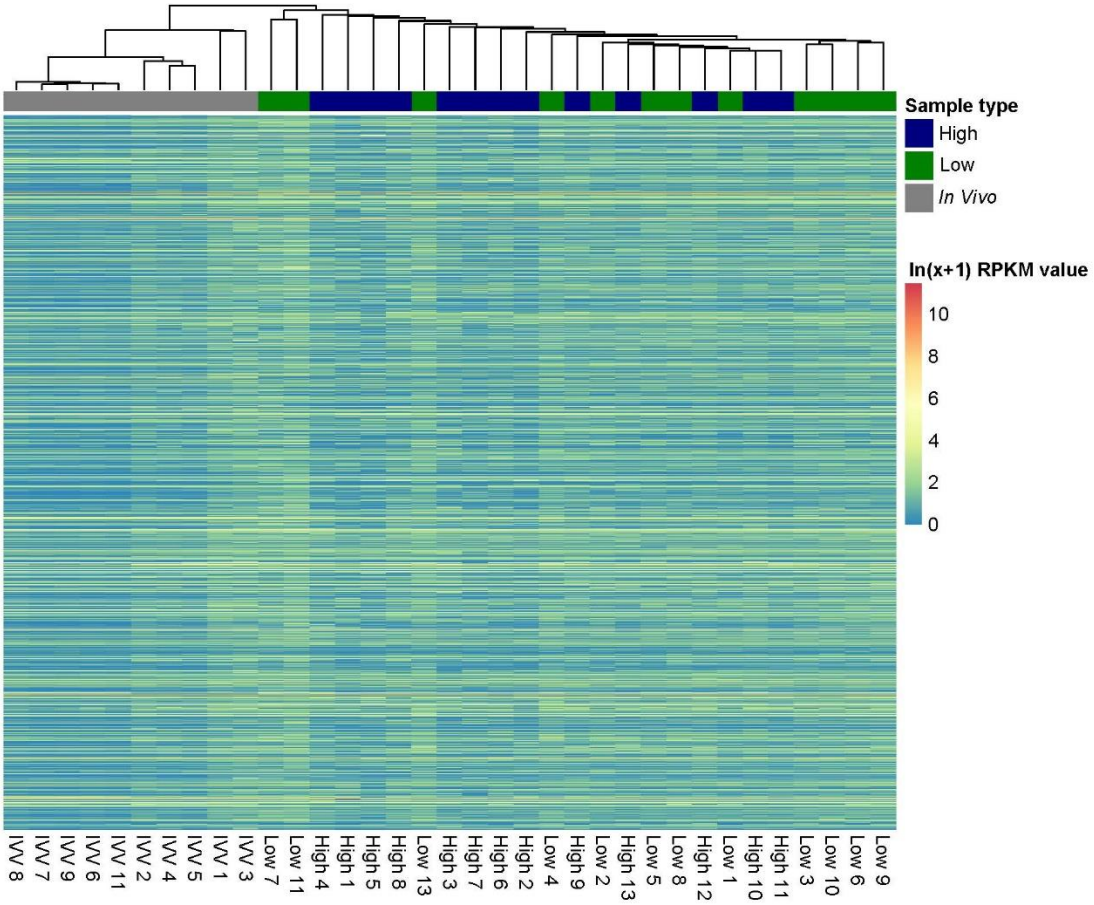

Figure 3-12. Heat map and clustering analysis of a representative sub-set of all genes analyzed for gene expression patterns. Rows (1192 genes) had unit variance scaling applied. Columns (N = 35) are clustered using correlation distance and average linkage. High apoptosis are represented in hierarchical clustering by blue, low apoptosis by green, and *in vivo* by grey. Red, yellow, blue in the heat map indicates ln(x+1) transformed RPKM value.

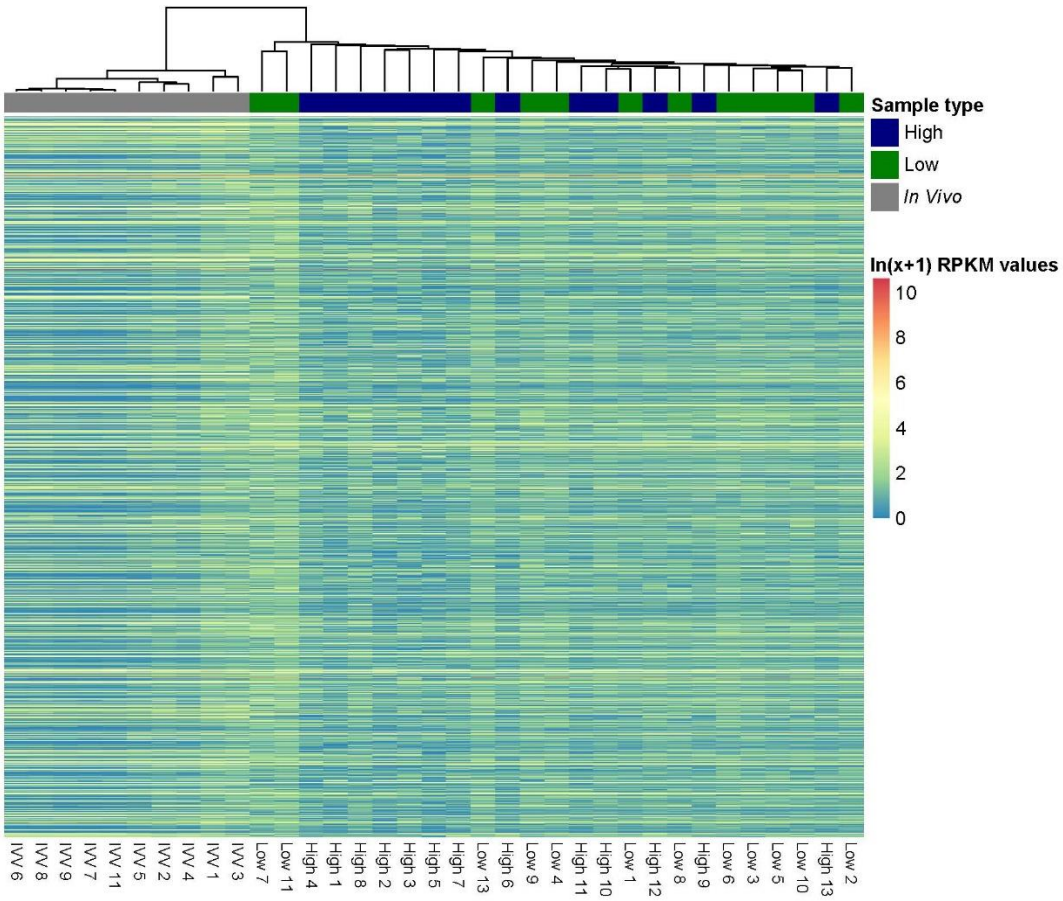

Figure 3-13. Heat map and clustering analysis of a representative sub-set of the differentially expressed genes identified as differentially expressed in at least one of the analysis; high vs low, high vs IVV, or low vs IVV. Rows (1198 genes) had no unit variance scaling applied. Columns (N = 35) are clustered using correlation distance and average linkage. High apoptosis are represented in hierarchical clustering by blue, low apoptosis by green, and *in vivo* by grey. Red, yellow, and blue in the heat map indicates ln(x+1) transformed RPKM value.

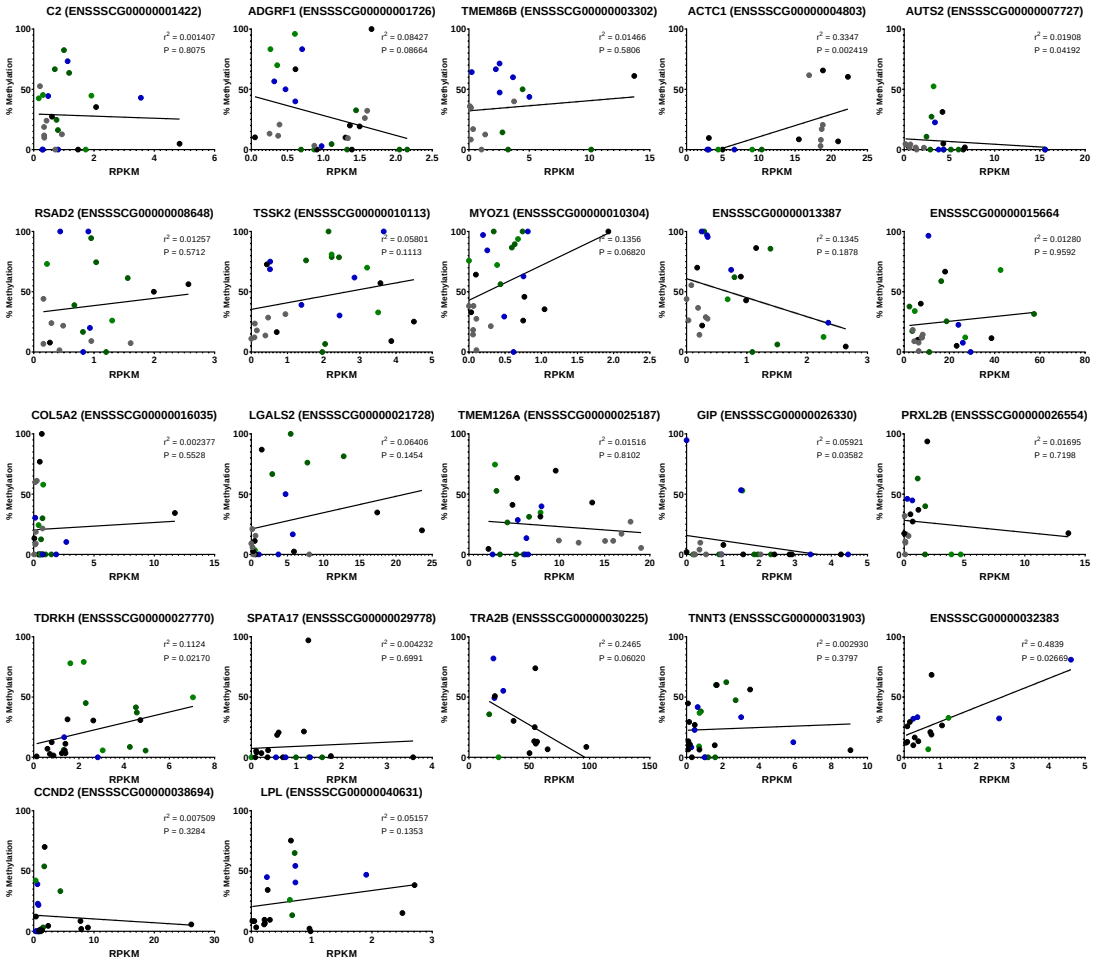

Figure 3-14. Correlation between RPKM values and percent methylation of genes found to be differentially expressed with at least one differentially methylated tile within 5,000 bp of the transcription start site in at least one of the comparisons: high vs low, high vs IVV, or low vs IVV. Blue dots are high apoptosis samples. Green dots are low apoptosis samples. And black dots are IVV samples. Linear regression lines are shown with goodness of fit indicated by r^2 value. Statistical correlation is indicated by p-values.

Supplemental Tables and Figures

Supplemental Table 3-1. RRBS library sample adapter number and index sequence.

Sample	Adapter	Index
L1	17	GTAGAG
L2	28	CAAAAG
L3	31	CACGAT
L4	34	CATGGC
L5	37	CGGAAT
L6	40	CTCAGA
L7	43	TACAGC
L8	17	GTAGAG
L9	28	CAAAAG
L10	31	CACGAT
L11	34	CATGGC
L12	37	CGGAAT
L13	40	CTCAGA
H1	24	GGTAGC
H2	29	CAACTA
H3	32	CACTCA
H4	35	CATTTT
H5	38	CTAGCT
H6	41	GCGCTA
H7	44	TATAAT
H8	24	GGTAGC
H9	29	CAACTA
H10	32	CACTCA
H11	35	CATTTT
H12	38	CTAGCT
H13	41	GCGCTA
IVV1	26	ATGAGC
IVV2	30	CACCGG
IVV3	33	CAGGCG
IVV4	36	CCAACA
IVV5	39	CTATAC
IVV6	42	TAATCG
IVV7	26	ATGAGC
IVV8	30	CACCGG
IVV9	33	CAGGCG
IVV10	36	CCAACA
IVV11	39	CTATAC

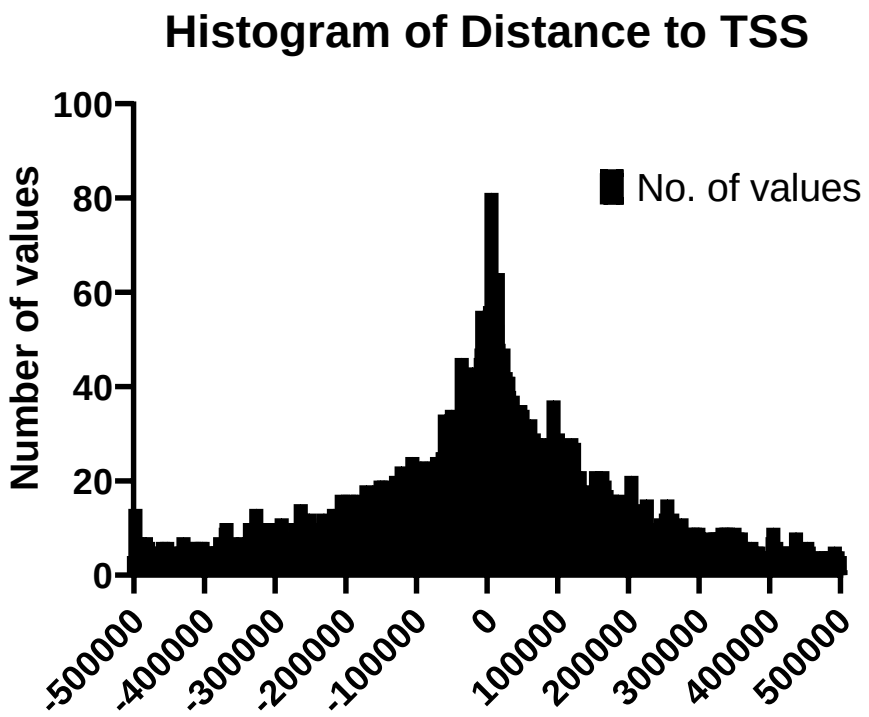

Supplemental Figure 3-1. Histogram of distance to transcription start site of tiles differentially methylated in each analysis. The farthest downstream tile was 9,565,509 base pairs from the TSS while the farthest upstream tile was 19,920,929 base pairs upstream. The average distance to the TSS was 15,974 base pairs.

CHAPTER IV

ACTIVE CASPASE ACTIVITY AS AN INDICATOR OF EMBRYO QUALITY IN BOVINE SCNT BLASTOCYSTS

Abstract

Somatic cell nuclear transfer (SCNT) remains highly inefficient and therefore expensive due to the number of embryos that must be transferred in order to achieve a live and surviving offspring. Increasing the efficiency of the technology by being able to select the embryos most likely to succeed following transfer would allow for the increased use of the technology in the animal agriculture industry. We hypothesize that incidence of apoptosis in blastocysts could serve as a useful biomarker of those embryos which will be most successful following transfer due to their proper epigenetic reprogramming resulting in appropriate gene expression and low levels of apoptosis. Conversely, the blastocysts likely to fail following embryo transfer will have increased incidence of apoptosis as a result of aberrant epigenetic reprogramming and gene expression. SR-FLICA, a non-toxic, non-invasive caspase activity reporter to measure the incidence of apoptosis could serve as the necessary biomarker to identify the most competent embryos. In this study, the correlation between cell number and incidence of apoptosis and gene expression patterns based on incidence of apoptosis were evaluated in day 7 bovine SCNT blastocysts. Additionally, day 7 blastocysts were transferred to recipient females for evaluation of pregnancy establishment and pregnancy associated glycoprotein (PAG) concentration as they relate to SR-FLICA staining intensity. A

significant correlation was identified between incidence of apoptosis and average cell number per blastocysts. Only one of twenty genes analyzed, *KLF4*, was differentially expressed in blastocysts with high versus low incidence of apoptosis. But no genes showed a correlation between FLICA score and $\log_2$ fold change gene expression. Finally, while SR-FLICA did not hinder pregnancy rates, apoptosis score was not an indicative measure for pregnancy establishment or PAG concentration on day 29 to 33 of gestation. In conclusion, SR-FLICA was not toxic to embryos, but neither did it provide an accurate prediction of embryo success following transfer when the entire embryo was analyzed for incidence of apoptosis.

Introduction

Somatic cell nuclear transfer (SCNT) is extremely inefficient at producing live and surviving offspring. While SCNT was first successful in mammals in 1997 with the birth of Dolly, the cloned sheep, the first successful use of the technology set the stage for inefficiency. In the creation of Dolly, only 29 of 247 embryos (11.7%) survived to the morula or blastocyst stage and these 29 surviving embryos were transferred to 13 total recipients with only 1 live birth, representing a 7.7% success rate when calculated as percent of live births per recipient (Wilmut *et al.* 1997). However, when considering the success on a per blastocyst basis, only one of 29 blastocysts resulted in a live birth, representing a success rate of 3.4% (Wilmut *et al.* 1997). Furthermore, when calculating the success rate as the number of live births to the total number of embryos cultured, an

even lower success rate is evident with only 0.4% of embryos developing into a living offspring (Wilmut *et al.* 1997).

Twenty years following the birth of Dolly, success rates have not increased, despite ongoing research in the field to improve the technology. In a more recent study of bovine SCNT, 303 embryos were started in culture of which only 229 (75.6%) began embryo development by cleaving into a 2-cell embryo (Wang *et al.* 2011). By day 7 of development, only 82 (27.1%) had developed into blastocyst stage embryos (Wang *et al.* 2011). Of these, 77 blastocysts were transferred individually and 30, 6, and 4 pregnancies remained at day 40, 90, and 240 of gestation, respectively (Wang *et al.* 2011). From there, 3 calves were born and only 2 survived to 60-days of age (Wang *et al.* 2011). A reported success rate of 2.6% represents the number of surviving offspring from the total number of transferred blastocysts; however, again factoring in the number of embryos that did not even make it to the blastocyst stage of development, the overall success rate is even lower where only 0.6% of the created embryos resulted in live and surviving offspring. This study also tested the use of treatment on both donor cells and early embryos with 0.01 µM 5-aza-2'-Deoxycytidine and 0.05 µM trichostatin A, chemicals that aid in the nuclear reprogramming of the donor cell by partial erasure of pre-existing epigenetic marks, and the percent of calves born was significantly increased from 3.9% to 20.7% (Wang *et al.* 2011). The percent of surviving calves was also increased from 2.6% to 13.4%, however the results were not significant (Wang *et al.* 2011). Even with these improvements though, the overall efficiency of the technology leaves plenty of room for improvement.

Taken together, these data indicate the continued need to increase SCNT efficiency in order to lower costs and make the technology a reality for production agriculture. Current research to increase the efficiency of SCNT focuses on improving the nuclear reprogramming of SCNT embryos during early development. Scientists understand that SCNT embryos undergo faulty epigenetic reprogramming (Giraldo *et al.* 2009), resulting in aberrant gene expression (Somers *et al.* 2006). Altered gene expression seems to be random in cloned embryos, with no distinct list of differentially expressed genes consistently identified between cloned and control embryos across studies, and most differences in gene expression appear to be smaller differences, with less than 3% of differentially expressed genes showing more than a four-fold change in gene expression compared to *in vitro* produced embryos (Oback 2008). Additionally, a wide range of gene expression patterns in SCNT embryos suggests that some individual SCNT embryos are more similar to *in vitro* produced embryos than other SCNT embryos (Smith *et al.* 2007). These findings indicate that within a pool of SCNT embryos, certain embryos may be predisposed to have a better chance of surviving to term and providing surviving offspring, and this phenomenon could be capitalized on to improve cloning efficiency if the high quality embryos could be identified somehow before embryo transfer.

Following embryo transfer, altered DNA methylation and gene expression continue in the fetuses that proceed through development and are often accompanied by characteristic abnormalities. Abnormalities of bovine SCNT pregnancies include abnormal placental development, fetal overgrowth or large offspring syndrome, enlarged umbilical cord, cardiac enlargement, fatty liver disease, and renal lesions [reviewed in

(Chavatte-Palmer *et al.* 2012)]. Associated with placental developmental abnormalities, bovine SCNT pregnancies are also associated with increased maternal circulating pregnancy associated glycoproteins (PAGs) concentrations on day 62 of gestation (Constant *et al.* 2011). PAGs are a family of proteins produced by binucleated giant cells of the placenta. PAGs serve as a pregnancy marker in cattle because they are exclusively produced in the placenta and are then transferred to the maternal circulation. Maternal circulating PAG concentration on day 31 of gestation indicates the probability of late embryonic loss, where cows likely to lose the pregnancy between day 31 and 59 of gestation had decreased circulating levels of PAGs (Pohler *et al.* 2016). If increased caspase activity on day 7 of development indicated increased abnormalities in the developing embryo, high caspase activity could be an early biomarker of future placental abnormalities and increased PAG concentrations. Conversely, a blastocyst with low caspase activity could serve as a biomarker of normal placental development and normal PAG concentration.

Most current methods to assess embryo quality rely on visual assessment of the embryos during development. One indicator of superior embryo quality is the time required to cleave from one cell into two cells where faster cleavage indicates embryos more likely to develop to the blastocyst stage of development (Isom *et al.* 2012). Current non-invasive methods to evaluate blastocyst quality rely on morphological assessment, which is known to be subjective (Rocha *et al.* 2016). A more quantitative method of morphological assessment is the number of cells in a blastocyst, as increased cell numbers are correlated with increased embryo quality (Matsuura *et al.* 2010). More invasive methods of analysis include analysis of the integrity of blastomere membranes,

analysis of embryo metabolism, measurement of cellular respiration, and electron-microscopy analysis- all of which can either damage or kill the embryo or are cost prohibitive (Rocha *et al.* 2016). Because there is no optimized embryo quality metric for selecting SCNT embryos, strategies are typically taken to simply enhance the probability of a live birth. These include performing a large number of transfers if only one blastocyst is transferred to each surrogate, such as in cattle where multiple offspring could be a complication during pregnancy and parturition, or by transferring a large number of blastocysts to each surrogate, such as in pigs where multiple pregnancies are not a problem in the litter bearing species. By developing a non-invasive assay to select the high quality blastocysts, the efficiency of SCNT could be improved by not wasting resources in order to hedge bets that a successful pregnancy will develop.

A novel indicator of embryo quality could be through the detection of apoptosis. Apoptosis has been detected in embryos of numerous species including pigs (Hao *et al.* 2003), cattle (Fahrudin *et al.* 2002), and humans (Hardy *et al.* 1989). Apoptosis appears to be a normal part of embryo development, as apoptosis has been detected in *in vivo* produced embryos (El-Shershaby and Hinchliffe 1974). Additionally, bovine SCNT embryos show earlier and increased levels of apoptosis compared to *in vitro* produced controls and the apoptosis continued as development continued in SCNT embryos (Park *et al.* 2004). We hypothesize that apoptosis can be detected non-invasively through staining to quantify active caspase molecules to identify the blastocysts most likely to develop to term. We believe that the blastocysts with low caspase activity will have undergone proper nuclear reprogramming leading to proper gene expression and low levels of apoptosis. Conversely, the blastocysts that have undergone altered nuclear

reprogramming resulting in aberrant gene expression will show increased levels of caspase activity and will fail following embryo transfer.

In this experiment, the ability of SR-FLICA (a non-toxic, non-invasive caspase activity reporter; Immunochemistry Technologies, Bloomington, MN) to successfully predict the day 7 bovine SCNT embryos which will establish pregnancies was validated. Additionally, the non-toxic nature of SR-FLICA on live embryos was confirmed through embryo transfers following staining and the resulting pregnancies. Pregnancy status will be diagnosed by ultrasound between day 29 and 33 of gestation. A blood sample was collected to analyze the connection between early apoptosis and circulating PAG concentrations. Embryo quality metrics was also evaluated by staining day 7 blastocysts with SR-FLICA then determining embryo cell number and gene expression patterns.

Materials and Methods

All chemicals and reagents were purchased from Sigma-Aldrich (St. Louis, MO) unless otherwise noted. All procedures performed with animals were in agreement with principles of animal welfare as approved by the veterinary staff and Institutional Animal Care and Use Committee at Utah State University (IACUC protocol #2303).

Oocyte Collection and Maturation

Bovine ovaries were collected from a local abattoir and transported to the laboratory in 0.9% saline solution. Oocytes were aspirated using a vacuum system from

follicles with a 3-8 mm diameter. Only oocytes with compact cumulus-oocyte complexes (COCs) were saved. Once isolated, COCs were cultured in TCM199 maturation medium with Earle's salts, L-glutamine, and sodium bicarbonate (Hyclone, Logan, Utah) supplemented with 10% fetal bovine serum (FBS), 0.05 mg/ml bovine follicle stimulating hormone (Sioux Biochemicals, Sioux city, IA), 5 mg/ml bovine luteinizing hormone (Sioux Biochemicals), 100 U/ml penicillin, and 100 mg/ml streptomycin at 39 °C with 5% CO_2 for 22 to 24 hr.

Somatic cell nuclear transfer embryo production

Primary somatic cell cultures were created using well-established procedures (Aston *et al.* 2009). From frozen stocks, thawed cells, passage 4-5, were grown to 80-100% confluence for use as nuclear donors. Eight hours prior to cloning, 20 µg/mL α-amanatin was added to donor cell culture. SCNT was performed as previously reported (Aston *et al.* 2009). Briefly, oocytes with a first polar body were isolated and used for SCNT. Fusion of the donor occurred first through electrical stimulation of one DC pulse of 2.2 kV/cm for 25 µS in mannitol fusion medium (Wells *et al.* 1999). After fusion, embryos were placed in SOFaa medium with 3% FBS for 1.5 hours to allow for activation. Next, chemical activation by treatment with 5 µM ionomycin for 5 minutes followed by a 4 hour treatment of 10 µg/ml cycloheximide. Following activation, embryos were cultured under mineral oil in 50 µL drops of SOFaa (Holm *et al.* 1999) with 3% FBS on a single layer of bovine cumulus cells. The embryos were cultured at 39˚C at 100% humidity with 5% CO2. Every other day beginning the day after

activation, 25 µL of the SOFaa medium was replaced with fresh medium. Embryos used in cell count and gene expression experiments used the same cell line throughout the experiment, unlike the transfer experiments which used multiple cell lines.

SR-FLICA and Hoechst 33342 Staining

SR-FLICA was resuspended as recommended by the manufacturer. Briefly, 50 µL DMSO was added to one vial SR-FLICA. Embryos were stained in 500 µL SOFaa culture media with 2 µL reconstituted SR-FLICA for 2 hours in the incubator. Embryos were moved to a fresh 500 µL SOFaa and placed back in the incubator for 30 minutes. Embryos used for cell count analysis were then stained with Hoechst 33342 to visualize nuclei in order to count number of cells, but all other embryos were only stained with SR-FLICA. Embryos were stained in 1 mg/ml of Hoechst 33342 for 10 minutes in the incubator. Embryos were then washed in SOFaa and transferred to individual 10 µL SOFaa droplets under mineral oil for fluorescent microscopy.

Microscopy and Image Analysis

Individual embryos were imaged at the 10X objective using the Zeiss Axio Observer.Z1 (Carl Zeiss Microscopy; Thornwood, NY). Fluorescent images of SR-FLICA (excitation 550-580 nm, emission 590-600 nm) stained embryos were captured with an axiocam HRc (Carl Zeiss Microscopy) creating a black and white image and color was artificially added using Zen software (Carl Zeiss Microscopy; v. 2.0) where

SR-FLICA was assigned a red color. SR-FLICA images had a 1 second exposure time and light excitation intensity remained constant between embryos for accurate comparisons of incidence of apoptosis. SR-FLICA staining intensity was analyzed using Adobe Photoshop (v. 2017.1.1.20174025) to determine the average pixel intensity within the space of the zona pellucida of the embryo. In blastocysts that were hatching, both the space inside the zona pellucida and the hatching extrusion was included in the analysis.

Cell Counts

Day 7 SCNT blastocysts were stained with SR-FLICA and Hoechst 33342. Embryos were analyzed for levels of apoptosis using SR-FLICA staining and subsequent analysis. Blastocysts were then mounted onto slides for counting of nuclei. In 3 replicates, day 7 SCNT embryos (n = 26) were fixed following SR-FLICA imaging and cell numbers were counted to determine if there was a correlation between incidence of apoptosis and cell number on day 7 of development. Additionally, embryos were classified as high (n = 7) or low (n = 6) incidence of apoptosis and average cell number was compared between groups using a student's t-test for statistical analysis. Both correlation analysis and t-test were performed using GraphPad Prism (version 8.0.1; GraphPad Software, Inc; La Jolla, CA).

Gene Expression Analysis

Following 4 cloning sessions, embryos developed to day 7. Blastocysts were stained with SR-FLICA and average red pixel intensity was calculated. Blastocysts were stored at -80°C until RNA extraction could be performed. RNA extraction and cDNA conversion was performed on individual blastocysts as reported previously in individual oocytes (Cox *et al.* 2015). Briefly, RNA was isolated using the Quick RNA Micro Prep kit (Zymo Research; Irvine, CA) following manufacturer instructions except the final elution was performed using 20 µL DNase/RNase-free water. RNA was converted to cDNA using the GoScript Reverse Transcriptase System (Promega; Madison, WI) again with minor modifications to the manufacturer's protocol. 8 µL of RNA was combined with 1 µL of oligo primers and 1 µL of random primers and water was then left out of the reverse transcription reaction mix; otherwise the reaction was performed as per the manufacturer's protocol.

Gene expression analysis was performed through qPCR using the Fluidigm (South San Francisco, CA) 96.96 Dynamic Array™ IFC for gene expression and 48.48 Dynamic Array™ IFC for gene expression. The 96.96 platform follows standard PCR chemistry in nanoliter-scale reactions to evaluate 96 genes for each of 96 samples using the 96.96 Dynamic Array integrated fluidic circuit (IFC) chip. Similarly, the 48.48 platform allows for the evaluation of 48 genes for each of 48 samples. Gene categories evaluated include apoptosis (*BAX, BID,* and *TP53*), epigenetic regulation (*ASH2L, DNMT3A, DNMT3B, HDAC1, HDAC2, HDAC3,* and *KDM3A*), imprinted genes (*GNAS, GRB10, IGF2R,* and *UBE3A*), pluripotency (*KLF4, LIN28, POU5F1,* and *SOX2*), trophoblast differentiation and function (*ETS2*), and housekeeping (*EIF4A1, GAPDH,*

HSP90, TAF11, and *YWHAZ*). A small number of apoptosis genes were selected as previous studies in bovine blastocysts found that genes related to apoptosis were not reliable markers of apoptosis as their expression levels did not change with the induction of apoptosis (Vandaele *et al.* 2008). Fluidigm Corporation's DeltaGene assay design service designed custom primers based on NCBI's reference sequence for cattle. Gene names and PCR primer sequence for each gene symbol can be found on Supplementary Table 4-5 and 4-6, respectively.

To perform quantitative PCR gene expression analysis using the Biomark system, Fludigm's protocol (PN 68000130) was followed. Specific target amplification was performed to each sample before qPCR by creating a 200 nM primer mix by pooling 1 µL of each combined forward and reverse primer set (20 µM each). The specific target amplification is performed by combining 1.25 µL of the pooled primer mix, 2.5 µL of TaqMan PreAmp Master Mix (Applied Biosystems; Foster City, CA) and 1.25 µL of cDNA. The polymerase is activated at 95°C for 10 minutes and then the reaction is amplified for 14 cycles of 95°C for 15 seconds then 60°C for 4 minutes. The reaction is then treated with Exonuclease I (ExoI; New England Biolabs; Ipswich, MA) to remove any primers that were not integrated in the specific target amplification. The ExoI treatment added 1.4 µL of water, 0.2 µL of ExoI reaction buffer, and 0.4 µL ExoI enzyme to each specific target amplification reaction. The reactions were incubated at 37°C for 30 minutes to allow for complete digestion of the non-integrated primers. Then, reactions were inactivated at 80°C for 15 minutes. Following ExoI treatment, each reaction was diluted 5-fold to a total volume of 25 µL. Reactions were stored at -20°C until further gene expression analysis was performed.

Next, individual sample and primer solutions were prepared for qPCR. Two microliters of the diluted specific target amplification were combined with 2.5 µL of 2X TaqMan Gene Expression Master Mix (Applied Biosystems), 0.25 µL of 20x DNA binding dye sample loading reagent (Fluidigm), and 0.25 µL of 20X EvaGreen DNA Binding Dye (Biotium; Hayward, CA). Samples were run in duplicate on one chip and individually on a second chip for technical replication. Primer mixes were made by combining 2.25 µL of each primer (20 µM) with 2.5 µL of 2x Assay loading reagent (Fluidigm) and 0.25 µL water. Primers were ran in duplicate for technical replication on both chips. The IFC chip was primed prior to loading samples and primers using the Prime Script (136X) of the HX IFC controller. Once priming was complete, 5 µL of each primer mix and 5 µL of each sample mix were pipetted into their correct inlets on the chip. The chip was again inserted into the IFC controller and the samples and primers were loaded into the chip using the Load Mix Script (136X) so that the samples and primers were moved into the reaction chambers. After the chip was loaded, the chip was placed in the BioMark thermal cycler for quantitative PCR where cycles consisted of 5 minutes of enzyme activation at 95°C, followed by 35 cycles of 95°C for 15 seconds then 60°C for 60 seconds for denaturation and extension, and finished with a three minute final extension cycle at 60°C. Following PCR amplification, a melt curve analysis was performed to assess the quality of each product. Each gene was run in duplicate on the chip yielding two reactions of each sample and primer.

Analysis of qPCR data was performed using the Fluidigm Real-Time PCR Analysis Software (v 4.3.1). Using a positive control sample as reference and a combined pool of all housekeeping genes as normalizer samples and assays, respectively,

ΔΔCT values were calculated. While 24 different primers were run on the Fluidigm chip, 4 primers (*BAX*, *DNMT3B*, *SOX2*, and *ETS2*) did not work in the positive control sample and were therefore not analyzed. Twenty genes were analyzed for correlation between apoptosis score and gene expression, as well as, difference in expression between high and low apoptosis embryos. Statistical analysis was performed in Graphpad Prism through correlation analysis and student's t-test to analyze log2 fold change values for each group type. Student's t-test was performed on the averaged log 2-fold change values from the six technical replicates. Samples where at least 3 of the 6 technical replicates did not work were not included in downstream analyses. Because not all reactions worked properly, the number of samples analyzed in the correlation analysis and for each group of the high vs low analysis has been provided in Supplementary Table 4-3 and 4-4, respectively. All p-values were corrected for false discovery rate (FDR) as described by Benjamini and Hochberg (Benjamini and Hochberg 1995).

Principal component analysis and hierarchical clustering was analyzed through an unsupervised hierarchical clustering created through the ClustVis program using ΔΔCT values from the 6 technical replicates (Metsalu and Vilo 2015). ΔΔCT values for each sample and gene analyzed were uploaded into the program. No unit variance scaling was applied to each gene and singular value decomposition with imputation was used to calculate principal components. Imputation was used for missing value estimations. Samples were clustered using correlation distance and average linkage.

Embryo Transfers

Embryo transfers were performed after 4 cloning sessions with a total of 98 transferred blastocysts. Because this study took advantage of a cloning system in place to produce cloned bulls for a client, multiple cell lines were used (n = 5). In addition, some embryos were created from donor cells treated with α-amanatin (n = 72) and some were not (n = 26) – this was a side experiment to analyze the effectiveness of the treatment to increase cloning success, results of which will not be discussed here. To ensure that the SR-FLICA was not having a negative impact on embryonic development, some embryos were stained and analyzed (n = 64) and some were left as controls (n = 34). All factors were included in statistical analysis, as discussed below. The cell line, α-amanatin treatment, SR-FLICA staining, apoptosis score, and pregnancy diagnosis for each transferred embryo can be found in Supplemental Table 4-8.

Cows were synchronized for embryo transfer. Nine days prior to SCNT, EAZI-BREED CIDRs (Zoetis Animal Health; Parsippany, NJ) were placed vaginally in the cows and remained in place for 7 days. Concurrent to CIDR placement, an injection of 25 mg Lutalyse® (Zoetis Animal Health) was administered IM. Seven days later, the CIDRs were removed and heat detection patches were placed on the tail head of the cattle. Two days after, on the day of SCNT, GnRH was administered through 100 mcg of Cystorelin® (Boehringer Ingelheim International Gmbh; Germany) IM and estrous behavior was detected by checking of the heat detection patch. Embryo transfers were performed a week later on day 7 of embryonic development.

On day 7 of development, a subset of blastocysts were stained with SR-FLICA and analyzed as described above. All blastocysts were then loaded individually into 0.25cc artificial insemination straws and transported to the farm in a portable incubator maintained at 39°C. Cows were administered an epidural by veterinarians to minimize rectal movement. Ovaries were palpated by a veterinarian to identify which ovary had a corpus luteum and check the size of the corpus luteum to ensure adequate tissue prevalence for proper progesterone levels. A pipette containing the blastocysts was then passed through the vagina and cervix; the blastocyst was deposited into the uterine horn on the same side as the corpus luteum.

Establishment of pregnancy was diagnosed by the same veterinarian on day 29 to 33 of gestation through ultrasound. At that time, a blood sample was collected in a vacutainer tube through venipuncture. The blood sample was allowed to clot at room temperature for at least 1 hour. Serum was isolated through centrifugation at 3,000 x g for 20 min at 4°C. Serum was collected and stored at -20°C until PAG concentration was measured.

Pregnancies from high and low apoptosis blastocysts (n = 11 each) were monitored throughout gestation and pregnancy survival was plotted. At the time of writing, one low apoptosis pregnancy is still viable approximately one month prior to calving.

PAG Analysis

PAG analysis was generously provided by the Pohler lab at Texas A&M University. PAG concentration was determined using previously reported methods (Pohler *et al.* 2016). Briefly, a commercially available test from Idexx Laboratories Inc. (Westbrook, ME) was used. In addition to the test samples, a standard curve, a sample from a known pregnant cow at day 60 of gestation, and a sample from a non-pregnant cow was included on the plate. Manufacturer protocol was followed.

Statistical Analysis of Embryo Transfer Data

For statistical analysis of embryo transfer, many factors were included in the analysis, although the primary factor of interest focused on SR-FLICA staining compared to controls and SR-FLICA scores. Random factors included cloning session, cell line, embryo transfer technician, α-amanatin treatment well (nested in cloning session), and SR-FLICA staining well (nested in α-amanatin treatment well). Fixed factors included whether donor cells received α-amanatin treatment and if the embryos were stained with SR-FLICA. A binary response model using PROC GLIMMIX in SAS was fit to analyze if SR-FLICA staining had an effect on pregnancy outcome. The same model was then used which also accounted for apoptosis score in an ANCOVA model to determine if SR-FLICA score was predictive of pregnancy outcome. To determine if SR-FLICA staining effected PAG concentration, a Gaussian response model was fit in SAS again using PROC GLIMMIX. Finally, a Gaussian model using PROC GLIMMIX in SAS with an

ANCOVA model to account for SR-FLICA score was used to determine if SR-FLICA score was predictive of PAG concentration.

Results

SR-FLICA Staining

While bovine SCNT blastocysts did show active caspase activity through SR-FLICA staining (Fig. 4-1), staining patterns were different than previously observed in porcine SCNT blastocysts (Supplemental Fig. 4-1). In the bovine blastocysts, even those embryos with high levels of apoptosis showed splotchy areas of red (Fig. 4-1, panel A and B), indicating active caspase activity. The bovine blastocysts that were classified as low apoptosis had such low levels of active caspase activity, that the fluorescent image appears to be empty as no red is evident (Fig. 4-1, panel C). In contrast, porcine high apoptosis blastocysts have been uniformly red throughout the entire embryo. Additionally, even the low apoptosis embryos show some level of active caspase activity.

Cell counts

Developmental rates from the three cloning sessions used in cell count analysis is found in Supplemental Table 4-1. On average from the three cloning sessions, blastocyst development was 21% of the cleaved embryos. In day 7 bovine SCNT blastocysts (3 replicates, total n = 26 blastocysts), Fig. 4-2 shows that there was a significant negative

correlation between SR-FLICA score and number of cells per blastocyst (P = 0.01). However, the fit of a linear regression line did not have a tight fit (r^2 = 0.25).

Embryos were sorted by incidence of apoptosis and the top and bottom 25% were considered high and low apoptosis, respectively. When the average number of cells in high (3 replicates, total n = 7) apoptosis and low (3 replicates, total n = 6) apoptosis blastocysts was compared with a Student's t-test (Fig. 4-3), the low apoptosis blastocysts had significantly more cells compared to high apoptosis embryos (P = 0.005) by 23.17 ± 6.5 cells. High apoptosis blastocysts had 25.17 ± 3.06 cells while low apoptosis blastocysts had 48.33 ± 5.76 cells. For reference, *in vivo* produced bovine blastocysts typically contain over 100 cells (Enright *et al.* 2000; Hosoe *et al.* 2017).

Gene expression analysis

Development rates from the four cloning sessions used in the gene expression analysis are located in Supplemental Table 4-2. On average, blastocyst development was 13.9% of cleaved embryos from the four replicates.

Twenty genes were analyzed for the correlation between SR-FLICA score and log2 fold change of gene expression. No genes showed significant correlation between incidence of apoptosis and gene expression levels (Fig. 4-4). Additionally, linear regression fit was extremely low, noted by the low r^2 values (Fig. 4-4). The number of samples included in the analysis and statistical summary can be found in Supplemental Table 4-3.

When the top and bottom 20% of incidence of apoptosis, high and low apoptosis, respectively, are compared by gene for gene expression levels, only 1 of twenty genes was found to be significantly differentially expressed (Fig. 4-5). *KLF4*, a pluripotency gene, had significantly increased expression in low apoptosis blastocysts compared to high apoptosis blastocysts (FDR corrected P = 0.03). The other 19 genes analyzed showed no difference in gene expression between high and low apoptosis blastocysts.

This similar pattern of gene expression in high and low apoptosis blastocysts is supported by principal component analysis (PCA, Fig. 4-6) and unsupervised hierarchical clustering (Fig. 4-7). PCA shows overlapping prediction ellipses for high apoptosis and low apoptosis blastocysts. Additionally, the middle apoptosis blastocysts representing the middle 60% of incidence of apoptosis overlap with the high and low apoptosis blastocysts. Similar findings are reported in the hierarchical clustering and heat map where samples do not segregate based on level of apoptosis and no distinct patterns emerge in the heat map based on level of apoptosis.

Embryo Transfers

Embryo development from cloning sessions used for embryo transfer can be found in Supplemental Table 4-7. On average, 23.3% of the cleaved embryos developed to the blastocyst stage. Statistical analyses accounting for the complicated experimental design were performed as described in the methods section. To address whether SR-FLICA staining affected pregnancy outcome, a binary response model was fit using PROC GLIMMIX in SAS. There was no evidence of significant staining effect on

pregnancy rate (P = 0.544). Pregnancy rate of SR-FLICA stained and unstained embryos is shown in Fig. 4-8. Additionally, the average SR-FLICA score of embryos which resulted in a not-pregnant (n = 27) and pregnant (n = 9) recipient is presented in Fig. 4-9. A student's t-test indicated no significant difference (P = 0.23) in average SR-FLICA score of embryos resulting in pregnant and not-pregnant recipients.

A second model was fit using a binary response model using PROC GLIMMIX in SAS, which also accounted for apoptosis score in an ANCOVA model to determine if SR-FLICA score was predictive of pregnancy outcome. This model found a negative but non-significant (P = 0.2143) effect of SR-FLICA score (effect estimate -0.01869) on the probability of pregnancy. High apoptosis blastocysts had a non-significant decrease in probability of pregnancy (Fig. 4-10) compared to low apoptosis embryos.

To verify that PAG concentration was predictive of pregnancy, a logistic regression model was fit. There was a clear significant relationship (P = 0.0001) indicating a clear relationship between PAG concentration and pregnancy.

To determine if SR-FLICA staining affected PAG concentration, a Gaussian response model using PROC GLIMMEX in SAS was fit to the study design. However, because so many transfers resulted in no pregnancy being established, the data had a zero-inflated mixture distribution because no PAG could be detected in most cases. No transformation could make these data normally distributed, so a two-part model was fitted. The first part of the model was a generalized linear mixed model to predict the probability of detecting any PAG level (but only for the observations where a protein level amount was reported, even if it was zero). None of the study design factors were

found to be significant predictors in this model. All random effects in the model had zero effect. The random effects were then dropped from the model. The remaining fixed effects (α-amanitin treatment and SR-FLICA staining) did not have significant effect on PAG concentration, P = 0.13 and P = 0.65, respectively. The second part of the model was a generalized linear mixed model for the PAG concentration detected (but only for the observations where a non-zero amount was detected). The data here were approximately normally distributed, so no transformation was performed. In this model, it seemed that PAG concentration may have been lowered in the presence of α-amanitin treatment, but the difference only trended towards significant (P = 0.09). Again, the random effects in the second part of the model were essentially zero. Therefore, the random effects were dropped resulting in a significant effect of α-amanitin treatment on PAG concentration (P = 0.0247). Together, it appears that there may be some evidence that the presence of the treatment results in a significant decrease in the detected PAG concentration, with an estimated magnitude difference of 0.299 ng/ml.

Finally, a Gaussian model using PROC GLIMMIX in SAS with an ANCOVA model to account for SR-FLICA score was used to determine if SR-FLICA score was predictive of PAG concentration. Again, a two-part model was needed due to the PAG concentration having a zero-inflated mixture distribution. In the first part of the model, to predict the probability of any non-zero protein detection, there was no significant effect found due to the α-amanitin treatment or SR-FLICA score. Because the random effects were found to have zero effect, they were again dropped from the model. A simple ANCOVA model was fit and resulted in a negative but not significant effect of SR-FLICA score on the probability of PAG detection (effect estimate -0.01647, P = 0.1344).

In the second part of the model, for the amount of protein detected among observations with non-zero protein level detection, the data were roughly normally distributed so no transformation was necessary. The random effects again were all essentially zero and the effects of α-amanitin and SR-FLICA staining on PAG concentrations were non-significant, ($P = 0.17$ and $P = 0.75$, respectively). Using a simple ANCOVA model for the amount of non-zero PAG detected, there was no SR-FLICA score effect ($P = 0.8285$).

Correlation between SR-FLICA score and PAG concentration was analyzed (3 replicates, total $n = 42$), disregarding other factors (Fig. 4-11). No significant correlation ($P = 0.27$) was present and a linear regression line showed poor fit ($r^2 = 0.03$). High and low apoptosis embryos showed no difference in average PAG concentration (Fig. 4-12, $P = 0.96$).

A survival plot (Fig. 4-13) indicates the pregnancy survival rate of high and low apoptosis blastocysts throughout gestation. While there was a numerical increase in pregnancies established in the low apoptosis group (3 pregnancies established) compared to the high apoptosis group (1 pregnancy established), by the end of gestation, only 1 pregnancy remained in each group.

Pregnancy rate by cloning session and cell line are shown in Supplemental Figs. 4-2 and 4-3, respectively. However, no statistical analysis was performed on these factors. Rather they served as random effects in the statistical models to analyze effect of SR-FLICA staining, apoptosis score, and PAG concentration.

Discussion

Scientists recognize the need for a way to identify the most competent cloned embryos early in development in order to increase the efficiency of SCNT. We proposed the use of SR-FLICA, a non-toxic and non-invasive caspase activity reporter, to isolate those blastocysts that would be most successful following embryo transfer. While our analyses did not produce a method to statistically increase the probability of a cloned pregnancy on day 30 of gestation, incidence of apoptosis did serve as an indicator of cell number and gene expression of *KLF4*. Follow up studies could provide a significant increase in overall SCNT efficiency following embryo transfer.

While the initial aim of the study was to assess apoptosis as a predictor of pregnancy establishment using porcine blastocysts, a change was made to use bovine blastocysts instead. Due to challenges with estrus synchronization in pigs, embryo transfers were not successful in our relatively small research herd. Additionally, the time requirements to analyze hundreds of blastocysts to transfer multiple embryos per recipient was not practical when there is no consequence to transferring large number of embryos into a pig. From there, the most competent embryos will develop while those that are not will die off. Conversely, there is increased risk to a cloned bovine pregnancy with more than one developing clone. Therefore, there is a greater importance in being able to select the best embryos when only one embryo will be transferred to each recipient. Therefore, it was decided to perform transfer experiments using the bovine rather than porcine model.

From previous work assessing apoptosis in porcine SCNT blastocysts, clear differences in active caspase activity were apparent compared to the bovine SCNT blastocysts. Porcine blastocysts had overall increased levels of active caspases in both the high and low incidence of apoptosis blastocysts compared to their bovine counterparts. This increase in caspase activity could be the result of different culture systems as the oocytes are matured and embryos are developed in different species-specific media. Previous work analyzing apoptosis in *in vivo* and *in vitro* produced porcine and bovine blastocysts found an increased level of damaged cells (measured as the percent of cells with membrane damage, DNA strand breaks, and fragmented nuclei), and found increased damage in bovine blastocysts compared to porcine blastocysts (Pomar *et al.* 2005). However, different culture systems were used in this study compared to our study, which could have resulted in culture systems having differing effects on the embryos. Our bovine system could be a better match to the *in vivo* environment compared to the porcine embryo system, so the bovine blastocysts had lower caspase activity compared to the porcine blastocysts.

Previous unpublished work in our lab has found no significant difference in cell number per blastocyst based on caspase activity in porcine parthenogenetic blastocysts. Therefore, it was unexpected that a significant correlation was found in bovine SCNT blastocysts between incidence of apoptosis and average cell number per blastocysts. It was even more surprising that there was a statistical difference in high and low apoptosis bovine SCNT blastocysts average cell number per blastocysts, especially considering that far fewer blastocysts were analyzed in the bovine system compared to the porcine system. However, these findings do match our original hypothesis that blastocysts with higher

caspase activity would be lower quality than those with lower caspase activity. A possibility is that these different findings in the porcine and bovine embryos are a result of comparing parthenogenetic porcine blastocysts and bovine SCNT blastocysts, or the difference could be the result of different culture systems. Additionally, other studies have reported a significant but marginal negative correlation between cell number and apoptotic index (Knijn *et al.* 2003). The cell count data points to incidence of apoptosis being a novel, noninvasive indicator of embryo quality, as lower apoptosis embryos had significantly higher number of cells, a known indication of embryo quality (Matsuura *et al.* 2010).

Unfortunately, the differences in high and low apoptosis bovine SCNT blastocysts are essentially limited to cell number. Gene expression data found no correlation between incidence of apoptosis and relative gene expression. Additionally, only one of twenty genes had significantly different gene expression in high apoptosis compared to low apoptosis blastocysts. While it is interesting that the one differentially expressed gene, *KLF4,* is a gene associated with pluripotency and has increased expression level in the low apoptosis embryos compared to the high apoptosis embryos, it is the only one of three pluripotency genes that was found to be differentially expressed. *KLF4* is one of the four reprogramming factors used in induced pluripotent stem cells (Takahashi and Yamanaka 2006). SCNT blastocysts have lower expression of *KLF4* compared to IVF blastocysts (Zhou *et al.* 2013). While we found increased *KLF4* expression in low caspase activity blastocysts, previous reports have found that normally developing bovine SCNT conceptuses had decreased *KLF4* expression compared to abnormal conceptuses (Degrelle *et al.* 2012). However, other studies have reported increased porcine SCNT

embryo development with treatment of vitamin C was associated with increased *KLF4* expression (Huang *et al.* 2011).

Overall gene expression profiles across all genes analyzed was not different between the high apoptosis and low apoptosis blastocysts, as evident in the PCA and hierarchical clustering analysis. In both the PCA and hierarchical clustering analysis, there was no clear division of the high and low apoptosis blastocysts. This data contradicts our initial hypothesis that blastocysts with low apoptosis would have undergone proper genome reprogramming and have different gene expression compared to the high apoptosis blastocysts, as incidence of apoptosis does not appear to have a connection to gene expression patterns.

The most anticipated portion of these experiments was the results of the embryo transfers to validate the use of SR-FLICA as a non-toxic, non-invasive caspase activity reporter to select the blastocysts most likely to be successful following SCNT and embryo transfer. While other methods have been commonly used to detect apoptosis in embryos (Hardy 1999; Hao *et al.* 2003), they all require the termination of embryo development. Therefore, the first and perhaps most critical question to answer was if SR-FLICA staining would hinder the development of blastocysts following transfer. To our best knowledge, this is the first report of using SR-FLICA on viable embryos that were not terminated in development at the blastocyst stage. Fortunately, no significant difference in pregnancy rate was obtained from blastocysts that were stained with SR-FLICA compared to those that were not. With no evidence that SR-FLICA hinders early

embryonic development of pregnancy establishment, active caspase activity could serve as a useful biomarker on embryos in future studies.

There was also no evidence that SR-FLICA score calculated from the whole embryo served as a useful biomarker of pregnancy establishment. Increased power through more SR-FLICA stained embryo transfers could possibly lead to a significant finding down the road. Because of the necessity to also validate the non-toxic nature of SR-FLICA, only a portion of the embryos were stained and provided an apoptosis score. And of course because these are cloned embryos, very few of these embryos then resulted in pregnancy establishment. So increasing the number of transfers could provide data that could find a statistically significant predictive nature of apoptosis score. Additional studies utilizing *in vitro* produced embryos for transfer could also provide insight through more pregnancies established to better understand if apoptosis score has a significant effect on pregnancy establishment.

However, assuming that increasing observations leads to the same conclusions, more questions are raised. Perhaps the most intriguing question is how blastocysts with high levels of active caspase activity are able to continue to develop and establish pregnancies just as efficiently as those with low caspase activity? Previous unpublished work in our lab verified the ability of staining with SR-FLICA to identify apoptotic cells by also staining the cells with the more commonly used TUNEL stain, which identified DNA strand breaks. Additionally, studies that have used both FLICA and TUNEL to detect apoptosis have shown similar detection of percent of cells that are apoptotic (Bedner *et al.* 2000; Wang *et al.* 2017). Therefore, the detection of active caspase

activity by SR-FLICA does not appear to be in question. Because apoptosis had traditionally been evaluated through methods which involve destroying or killing the embryos through fixation, little is known about downstream development. However, SR-FLICA provides the opportunity to evaluate live blastocysts and track future development in the same embryo without the need to destroy or halt its development. Therefore, future studies are needed to evaluate how these embryos are coping with high levels of caspase activity without being destroyed through programmed cell death.

Another possibility is that SR-FLICA treatment results in a downstream reduction in apoptosis. SR-FLICA covalently binds to the cleavage site of active caspases, making the proteins ineffective at carrying out the apoptosis cascade in the cells. Our staining protocol was to expose embryos to 12 µM SR-FLICA (SR-VAD-FMK) for 2 hours. Studies using similar fluorescent stains at 10 µM of FAM-VAD-FMK for 3 hours reported only a 24% reduction in apoptotic cells (Amstad *et al.* 2001). Another study indicated that a 24 hour treatment of 10 µM FAM-VAD-FMK showed approximately 50% of the cells still died from apoptosis induction (Smolewski *et al.* 2001). Because our treatment was a low concentration and only 2 hours, we do not believe that the SR-FLICA treatment would have had a lasting effect. Any stimulus which was causing the increase in apoptosis would have still been present so more caspases would have continued to be activated, even if some caspases were inhibited by our treatment. The final aim of this study was to determine if there was a relationship between incidence of apoptosis on day 7 and PAG concentration between day 29 and 33 of gestation. Because PAGs are produced by the placenta and SCNT bovine pregnancies are riddled with placental abnormalities (Chavatte-Palmer *et al.* 2012), we hypothesized that increased

incidence of apoptosis would result in more abnormalities in the SCNT pregnancy, including the placenta, and therefore increased PAG concentrations. However, no relationship was found between apoptosis score and PAG concentration. In conclusion, apoptosis score was not useful in determining pregnancy establishment or PAG concentration, which is indicative in bovine pregnancies of late embryonic loss (Pohler *et al.* 2016).

All of these data were produced by analyzing active caspase activity through SR-FLICA staining and subsequent analysis at a whole embryo level. The apoptosis score represents the mean red pixel intensity of the whole embryo by analyzing the area inside the zone pellucida. Certain areas could possibly be more critical measures of embryo competency. For instance, a blastocyst with increased incidence of apoptosis in the inner cell mass but not the trophoblast could result in a lower mean red pixel intensity, or SR-FLICA score, compared to a blastocyst with a moderate incidence of apoptosis throughout the inner cell mass and the trophoblast. But if the incidence of apoptosis in the inner cell mass is the most critical region for embryo development, perhaps the first blastocyst should have a higher incidence of apoptosis compared to the second blastocyst. In studies using mouse blastocysts, the ICM is less resistant compared to the trophoblast and therefore incurs increased levels of apoptosis which can deplete the ICM of the required stem cells for future development resulting in compromised development (Pampfer 2000). A similar increased incidence of apoptosis in the ICM compared to the trophoblast has been reported in bovine blastocysts (Fabian *et al.* 2005). Therefore, future studies should evaluate embryos by morphological section to tease apart some of the more complex possibilities.

In conclusion, while there was a significant difference in cell number between day 7 bovine SCNT blastocysts with high and low incidence of apoptosis, no major differences were found in gene expression patterns, pregnancy establishment, or subsequent PAG concentrations. Embryo competency was not hindered as a result of SR-FLICA staining, so SR-FLICA could still serve as a useful tool for embryo quality assessment prior to embryo transfer. Future work should focus on apoptosis in distinct morphological regions including the inner cell mass and trophoblast to determine if more incidence of apoptosis in each region could be indicative of success following transfer while whole embryo apoptosis was not.

References

Amstad, P.A., Yu, G., Johnson, G.L., Lee, B.W., Dhawan, S., and Phelps, D.J. (2001) Detection of caspase activation in situ by fluorochrome-labeled caspase inhibitors. *Biotechniques* **31**(3), 608-10, 612, 614, passim

Aston, K.I., Li, G.P., Hicks, B.A., Sessions, B.R., Davis, A.P., Winger, Q.A., Rickords, L.F., Stevens, J.R., and White, K.L. (2009) Global gene expression analysis of bovine somatic cell nuclear transfer blastocysts and cotyledons. *Mol Reprod Dev* **76**(5), 471-82

Bedner, E., Smolewski, P., Amstad, P., and Darzynkiewicz, Z. (2000) Activation of caspases measured in situ by binding of fluorochrome-labeled inhibitors of caspases (FLICA): correlation with DNA fragmentation. *Exp Cell Res* **259**(1), 308-13

Benjamini, Y., and Hochberg, Y. (1995) Controlling the False Discovery Rate: A Practical and Powerful Approach to Multiple Testing. *Journal of the Royal Statistical Society. Series B (Methodological)* **57**(1), 289-300

Chavatte-Palmer, P., Camous, S., Jammes, H., Le Cleac'h, N., Guillomot, M., and Lee, R.S. (2012) Review: Placental perturbations induce the developmental abnormalities often observed in bovine somatic cell nuclear transfer. *Placenta* **33 Suppl**, S99-s104

Constant, F., Camous, S., Chavatte-Palmer, P., Heyman, Y., de Sousa, N., Richard, C., Beckers, J.F., and Guillomot, M. (2011) Altered secretion of pregnancy-associated glycoproteins during gestation in bovine somatic clones. *Theriogenology* **76**(6), 1006-21

Cox, L., Vanderwall, D.K., Parkinson, K.C., Sweat, A., and Isom, S.C. (2015) Expression profiles of select genes in cumulus-oocyte complexes from young and aged mares. *Reprod Fertil Dev* **27**(6), 914-24

Degrelle, S.A., Jaffrezic, F., Campion, E., Le Cao, K.A., Le Bourhis, D., Richard, C., Rodde, N., Fleurot, R., Everts, R.E., Lecardonnel, J., Heyman, Y., Vignon, X., Yang, X., Tian, X.C., Lewin, H.A., Renard, J.P., and Hue, I. (2012) Uncoupled embryonic and extra-embryonic tissues compromise blastocyst development after somatic cell nuclear transfer. *PLoS One* **7**(6), e38309

El-Shershaby, A.M., and Hinchliffe, J.R. (1974) Cell redundancy in the zona-intact preimplantation mouse blastocyst: a light and electron microscope study of dead cells and their fate. *J Embryol Exp Morphol* **31**(3), 643-54

Enright, B.P., Lonergan, P., Dinnyes, A., Fair, T., Ward, F.A., Yang, X., and Boland, M.P. (2000) Culture of in vitro produced bovine zygotes in vitro vs in vivo: Implications for early embryo development and quality. *Theriogenology* **54**(5), 659-673

Fabian, D., Koppel, J., and Maddox-Hyttel, P. (2005) Apoptotic processes during mammalian preimplantation development. *Theriogenology* **64**(2), 221-231

Fahrudin, M., Otoi, T., Karja, N.W., Mori, M., Murakami, M., and Suzuki, T. (2002) Analysis of DNA fragmentation in bovine somatic nuclear transfer embryos using TUNEL. *Reproduction* **124**(6), 813-9

Giraldo, A.M., Lynn, J.W., Purpera, M.N., Vaught, T.D., Ayares, D.L., Godke, R.A., and Bondioli, K.R. (2009) Inhibition of DNA methyltransferase 1 expression in bovine fibroblast cells used for nuclear transfer. *Reprod Fertil Dev* **21**(6), 785-95

Hao, Y., Lai, L., Mao, J., Im, G.S., Bonk, A., and Prather, R.S. (2003) Apoptosis and in vitro development of preimplantation porcine embryos derived in vitro or by nuclear transfer. *Biol Reprod* **69**(2), 501-7

Hardy, K. (1999) Apoptosis in the human embryo. *Rev Reprod* **4**(3), 125-34

Hardy, K., Handyside, A.H., and Winston, R.M. (1989) The human blastocyst: cell number, death and allocation during late preimplantation development in vitro. *Development* **107**(3), 597-604

Holm, P., Booth, P.J., Schmidt, M.H., Greve, T., and Callesen, H. (1999) High bovine blastocyst development in a static in vitro production system using SOFaa medium supplemented with sodium citrate and myo-inositol with or without serum-proteins. *Theriogenology* **52**(4), 683-700

Hosoe, M., Inaba, Y., Hashiyada, Y., Imai, K., Kajitani, K., Hasegawa, Y., Irie, M., Teramoto, H., Takahashi, T., and Niimura, S. (2017) Effect of supplemented sericin on the development, cell number, cryosurvival and number of lipid droplets in cultured bovine embryos. *Anim Sci J* **88**(2), 241-247

Huang, Y., Tang, X., Xie, W., Zhou, Y., Li, D., Zhou, Y., Zhu, J., Yuan, T., Lai, L., Pang, D., and Ouyang, H. (2011) Vitamin C enhances in vitro and in vivo development of

porcine somatic cell nuclear transfer embryos. *Biochemical and Biophysical Research Communications* **411**(2), 397-401

Isom, S.C., Li, R.F., Whitworth, K.M., and Prather, R.S. (2012) Timing of first embryonic cleavage is a positive indicator of the in vitro developmental potential of porcine embryos derived from in vitro fertilization, somatic cell nuclear transfer and parthenogenesis. *Mol Reprod Dev* **79**(3), 197-207

Knijn, H.M., Gjørret, J.O., Vos, P.L.A.M., Hendriksen, P.J.M., van der Weijden, B.C., Maddox-Hyttel, P., and Dieleman, S.J. (2003) Consequences of In Vivo Development and Subsequent Culture on Apoptosis, Cell Number, and Blastocyst Formation in Bovine Embryos1. *Biology of Reproduction* **69**(4), 1371-1378

Matsuura, K., Hayashi, N., Takiue, C., Hirata, R., Habara, T., and Naruse, K. (2010) Blastocyst quality scoring based on morphologic grading correlates with cell number. *Fertil Steril* **94**(3), 1135-7

Metsalu, T., and Vilo, J. (2015) ClustVis: a web tool for visualizing clustering of multivariate data using Principal Component Analysis and heatmap. *Nucleic Acids Res* **43**(W1), W566-70

Oback, B. (2008) Climbing Mount Efficiency--small steps, not giant leaps towards higher cloning success in farm animals. *Reprod Domest Anim* **43 Suppl 2**, 407-16

Pampfer, S. (2000) Apoptosis in Rodent Peri-implantation Embryos: Differential Susceptibility of Inner Cell Mass and Trophectoderm Cell Lineages— A Review. *Placenta* **21**, S3-S10

Park, E.S., Hwang, W.S., Jang, G., Cho, J.K., Kang, S.K., Lee, B.C., Han, J.Y., and Lim, J.M. (2004) Incidence of apoptosis in clone embryos and improved development by the treatment of donor somatic cells with putative apoptosis inhibitors. *Mol Reprod Dev* **68**(1), 65-71

Pohler, K.G., Pereira, M.H.C., Lopes, F.R., Lawrence, J.C., Keisler, D.H., Smith, M.F., Vasconcelos, J.L.M., and Green, J.A. (2016) Circulating concentrations of bovine pregnancy-associated glycoproteins and late embryonic mortality in lactating dairy herds. *J Dairy Sci* **99**(2), 1584-1594

Pomar, F.J.R., Teerds, K.J., Kidson, A., Colenbrander, B., Tharasanit, T., Aguilar, B., and Roelen, B.A.J. (2005) Differences in the incidence of apoptosis between in vivo and in vitro produced blastocysts of farm animal species: a comparative study. *Theriogenology* **63**(8), 2254-2268

Rocha, J.C., Passalia, F., Matos, F.D., Maserati, M.P., Jr., Alves, M.F., Almeida, T.G., Cardoso, B.L., Basso, A.C., and Nogueira, M.F. (2016) Methods for assessing the quality of mammalian embryos: How far we are from the gold standard? *JBRA Assist Reprod* **20**(3), 150-8

Smith, C., Berg, D., Beaumont, S., Standley, N.T., Wells, D.N., and Pfeffer, P.L. (2007) Simultaneous gene quantitation of multiple genes in individual bovine nuclear transfer blastocysts. *Reproduction* **133**(1), 231-42

Smolewski, P., Grabarek, J., Phelps, D.J., and Darzynkiewicz, Z. (2001) Stathmo-apoptosis: arresting apoptosis by fluorochrome-labeled inhibitor of caspases. *Int J Oncol* **19**(4), 657-63

Somers, J., Smith, C., Donnison, M., Wells, D.N., Henderson, H., McLeay, L., and Pfeffer, P.L. (2006) Gene expression profiling of individual bovine nuclear transfer blastocysts. *Reproduction* **131**(6), 1073-84

Takahashi, K., and Yamanaka, S. (2006) Induction of pluripotent stem cells from mouse embryonic and adult fibroblast cultures by defined factors. *Cell* **126**(4), 663-76

Vandaele, L., Goossens, K., Peelman, L., and Van Soom, A. (2008) mRNA expression of Bcl-2, Bax, caspase-3 and -7 cannot be used as a marker for apoptosis in bovine blastocysts. *Animal Reproduction Science* **106**(1), 168-173

Wang, L., Mehta, S., Brock, M., and Gill, S.E. (2017) Inhibition of Murine Pulmonary Microvascular Endothelial Cell Apoptosis Promotes Recovery of Barrier Function under Septic Conditions. *Mediators of Inflammation* **2017**, 15

Wang, Y., Su, J., Wang, L., Xu, W., Quan, F., Liu, J., and Zhang, Y. (2011) The effects of 5-aza-2'- deoxycytidine and trichostatin A on gene expression and DNA methylation status in cloned bovine blastocysts. *Cell Reprogram* **13**(4), 297-306

Wells, D.N., Misica, P.M., and Tervit, H.R. (1999) Production of cloned calves following nuclear transfer with cultured adult mural granulosa cells. *Biol Reprod* **60**(4), 996-1005

Wilmut, I., Schnieke, A.E., McWhir, J., Kind, A.J., and Campbell, K.H. (1997) Viable offspring derived from fetal and adult mammalian cells. *Nature* **385**(6619), 810-3

Zhou, Y., Huang, Y., Xie, W., Song, Q., Ji, Y., Zhang, Y., Ouyang, H., Lai, L., Pang, D., and Tang, X. (2013) Scriptaid affects histone acetylation and the expression of development-related genes at different stages of porcine somatic cell nuclear transfer embryo during early development. *Chinese Science Bulletin* **58**(17), 2044-2052

Figures

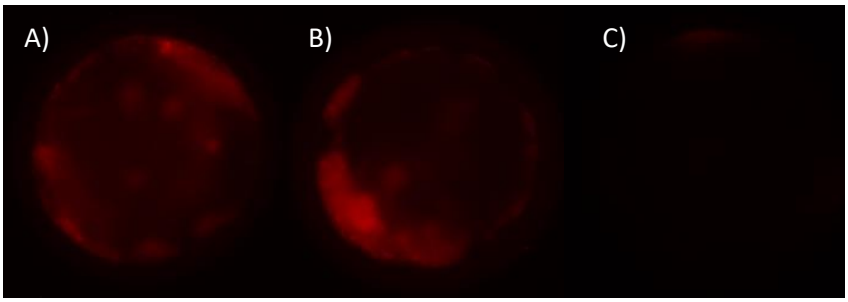

Fig.4-1. Bovine SCNT blastocysts with SR-FLICA staining. Bovine SCNT blastocysts which were classified as high incidence of apoptosis by SR-FLICA staining are shown in panel A and B. Low incidence of apoptosis have such low levels of floresence that the image appears empty, shown in panel C. Red indicates active caspase activity.

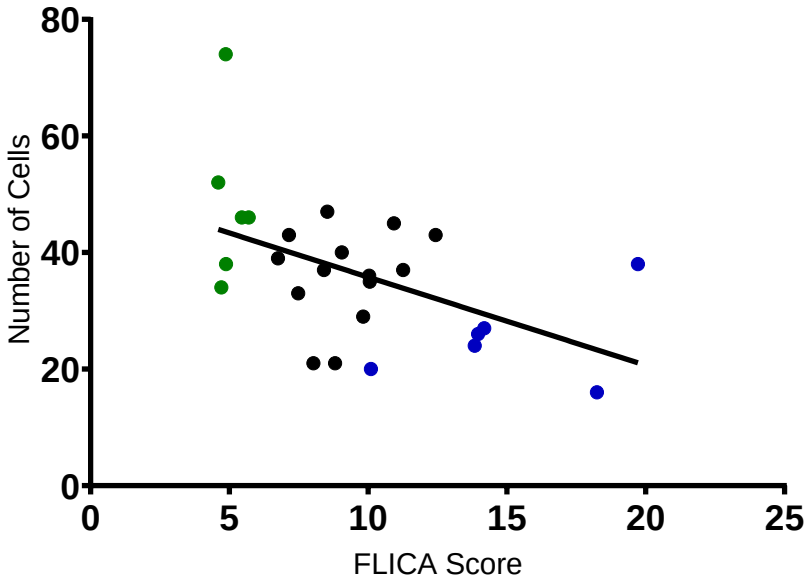

Fig. 4-2. Correlation between SR-FLICA score and cell number in day 7 bovine SCNT blastocysts. The relationship between cell number and the incidence of apoptosis in day 7 SCNT blastocysts (3 replicates, total n = 26) with a linear regression line. Significant correlation was found between the number of cells and relative level of apoptosis (r^2 = 0.25, P = 0.01). Blue and green indicate the top and bottom 20% of incidence of apoptosis, respectively.

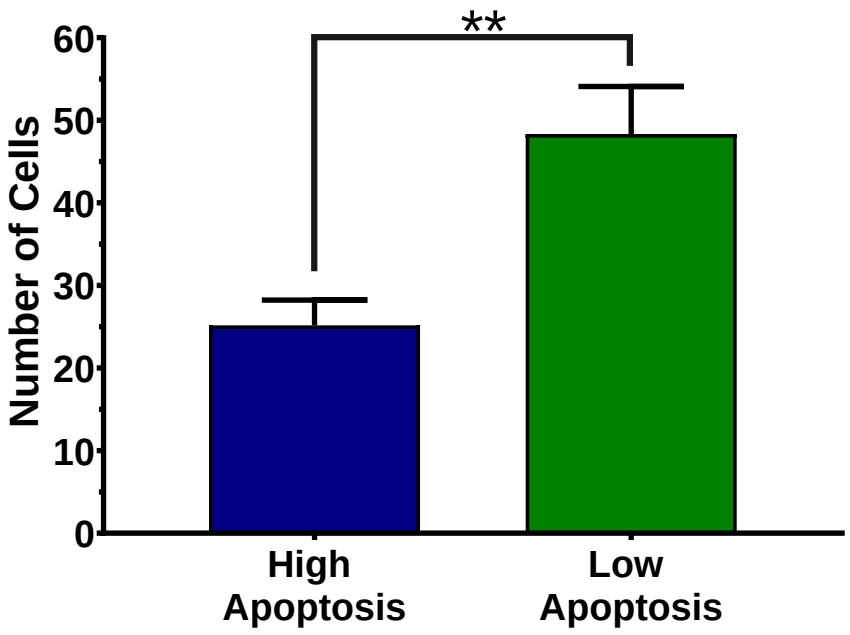

Fig. 4-3. Cell counts in day 7 blastocysts. Average number of cells of high (3 replicates, total n = 7) and low (3 replicates, total n = 6) apoptosis day 7 SCNT embryos with standard error bars. There was a significant difference between high and low apoptosis embryos (P = 0.005).

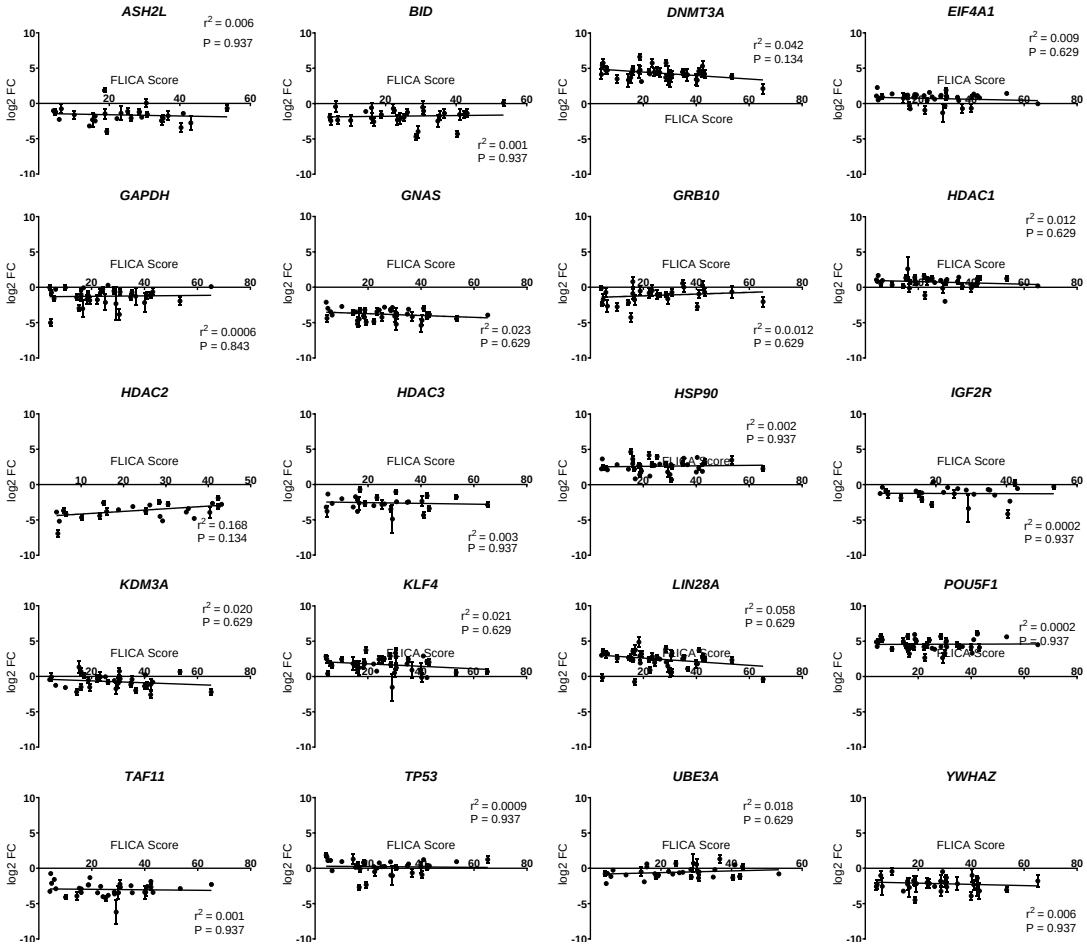

Fig. 4-4. Correlation between incidence of apoptosis measured by SR-FLICA score and log2 fold change value. Correlation for 20 genes expressed in day 7 bovine SCNT blastocysts. Error bars represent the standard error. Linear regression line is shown along with the fit of the line indicated by the r^2 value. Data represents 4 replicate cloning session with a total of 40 embryos analyzed. However, not every qPCR reaction worked, so number of samples analyzed per group for each gene can be found in Supplemental Table 4-3. Statistical significance of the correlation is designated by the FDR corrected P value for each gene. No significant correlation was found between FLICA score and gene expression in any gene analyzed.

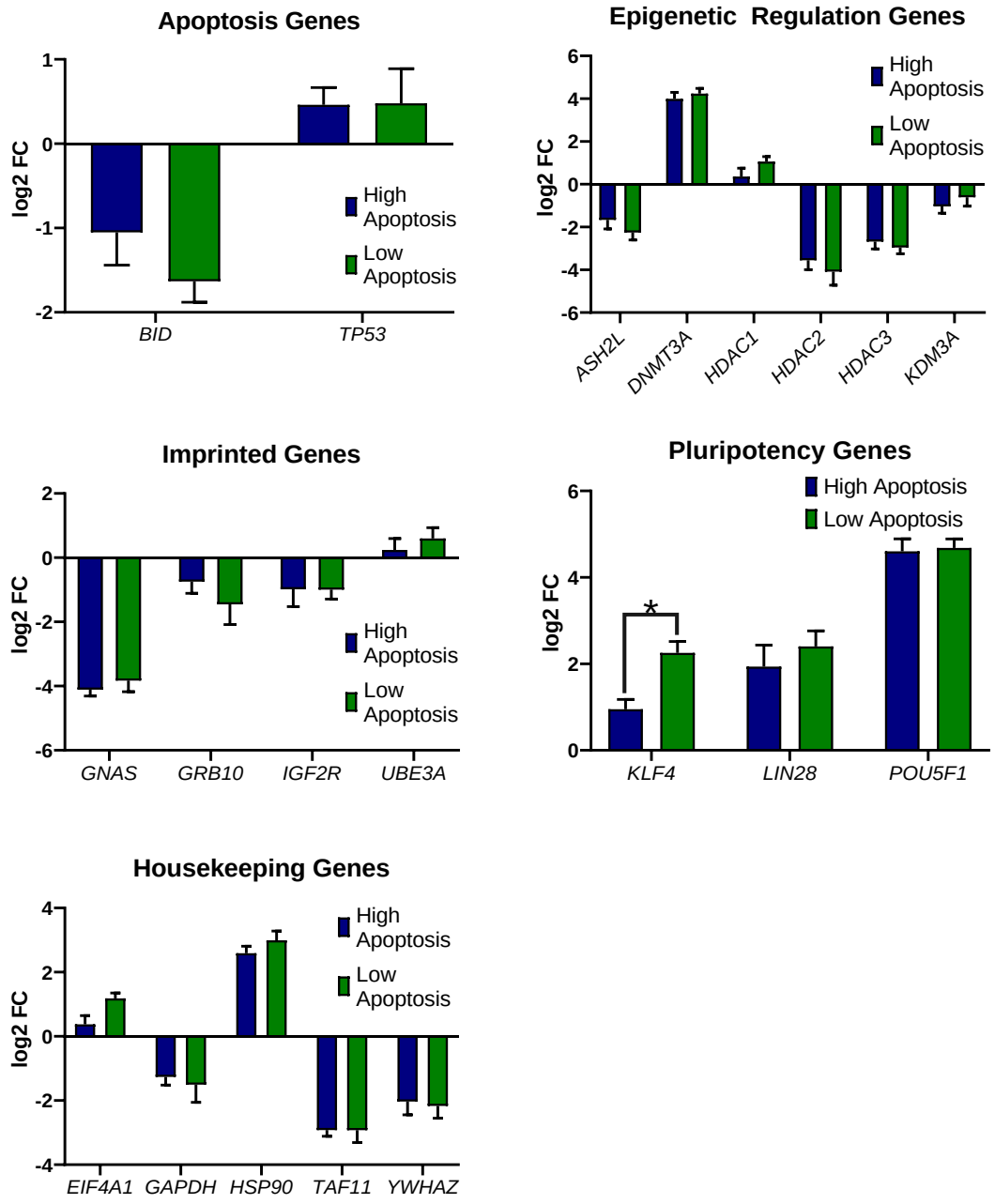

Fig. 4-5. Gene expression in high and low apoptosis blastocysts. Log2 fold change comparing gene expression of genes between SCNT blastocysts with high and low levels of apoptosis with standard error bars. Data represents 4 replicate cloning session (high n=9; low n=9). However, not every qPCR reaction worked, so number of samples analyzed per group for each gene can be found in Supplemental Table 4-4. A student's t-test was used to determine significantly different expression. P-values were adjusted for false discovery rate. Statistically different expression was found in *KLF4* (FDR P = 0.03).

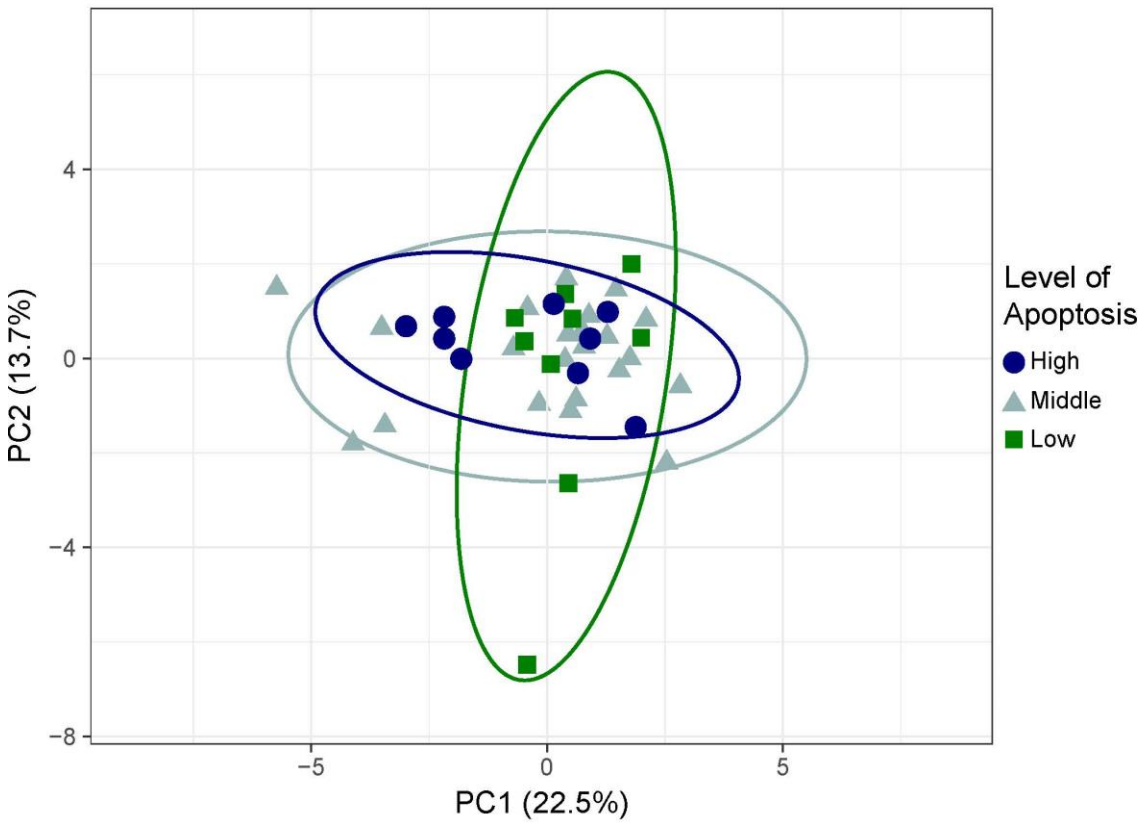

Fig. 4-6. Principal component analysis of ΔΔCT gene expression. Analyzed in blastocysts with the top 20% of apoptosis [high apoptosis (n = 9), blue circles], the bottom 20% of apoptosis [low apoptosis (n = 9), green squares], and the central 60% of apoptosis [middle embryos (n = 22), grey triangles] from 4 cloning sessions. No unit variance scaling was applied to each gene and singular value decomposition (SVD) with imputation was used to calculate principal components. X shows principal component 1 while Y shows principal component 2. PC1 and PC2 explain 22.5% and 13.7% of the total variance, respectively. Ellipses indicate the probability a new observation from the same group will fall within the ellipse with a probability of 0.95.

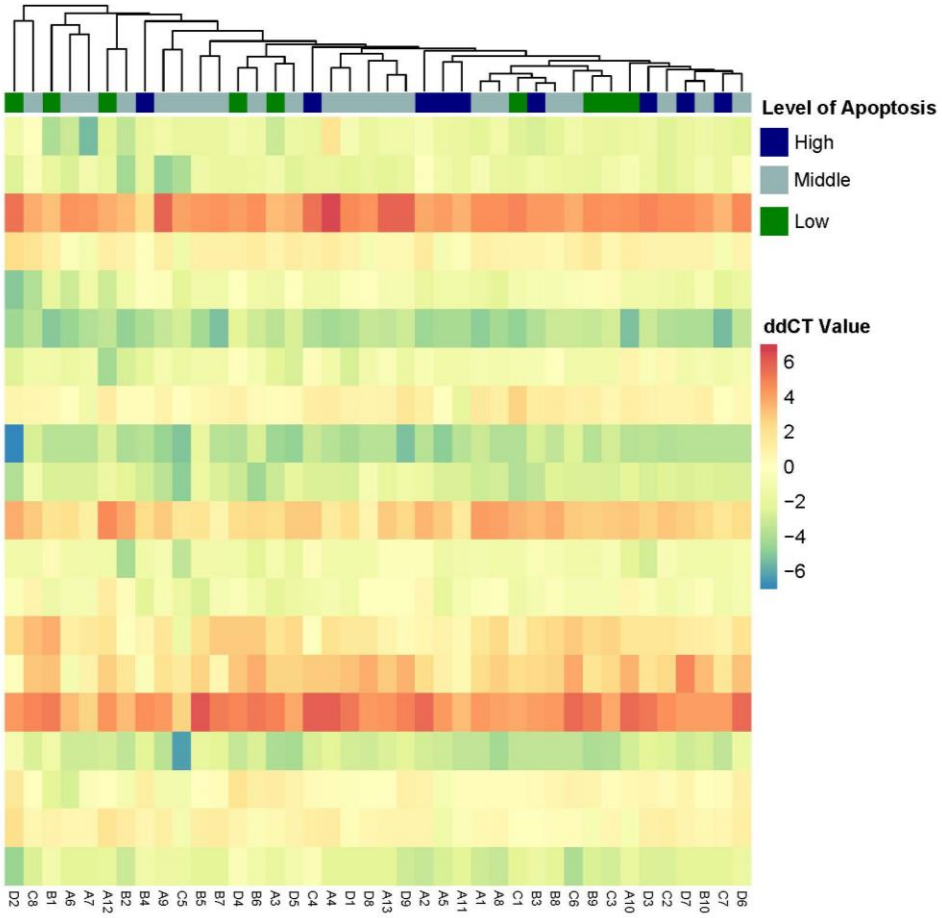

Fig. 4-7. Unsupervised clustering and heatmap analysis of ΔΔCT values of gene expression. Analyzed in blastocysts with the top 20% of apoptosis [high apoptosis (n = 9), blue], the bottom 20% of apoptosis [low apoptosis (n = 9), green], and the central 60% of apoptosis [middle embryos (n = 22), grey] from 4 cloning sessions. Red, yellow, and blue of the heatmap indicates ΔΔCT values. Unit variance scaling was applied. Imputation was used for missing value estimation. Samples were clustered using correlation distance and average linkage.

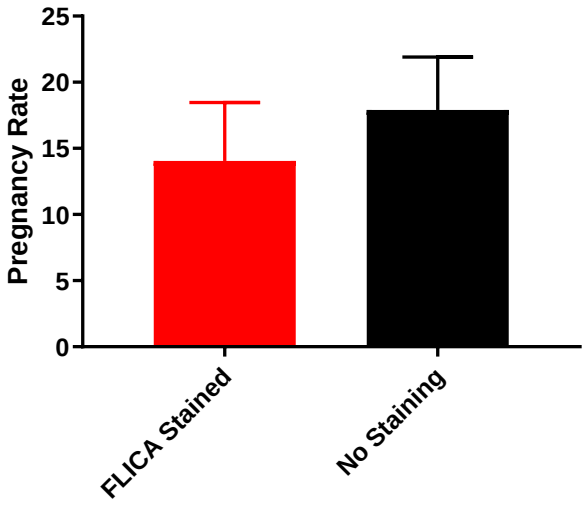

Fig. 4-8. Pregnancy rates from SR-FLICA stained and control blastocysts. Pregnancy rate between day 29 and 33 of gestation resulting from blastocysts that had be stained with SR-FLICA (total n = 64) and controls which had not be stained (total n = 34) from 4 embryo transfer sessions. Error bars represent the standard error. No significant difference in pregnancy rate resulted from embryos being exposed to SR-FLICA staining or not (P = 0.544).

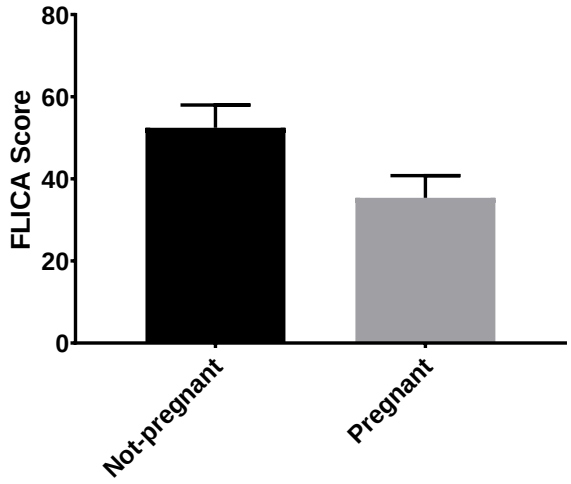

Fig. 4-9. Average SR-FLICA scores from embryos that failed to establish pregnancy and embryos that established pregnancy. Average FLICA score of embryos that resulted in a cow being not pregnant (total n = 27) and pregnant (total n = 9) between day 29 and 33 of gestation from 4 transfer sessions. Error bars represent the standard error. No significant difference was found in FLICA score between the embryos that produced a pregnancy and those that did not (P = 0.23).

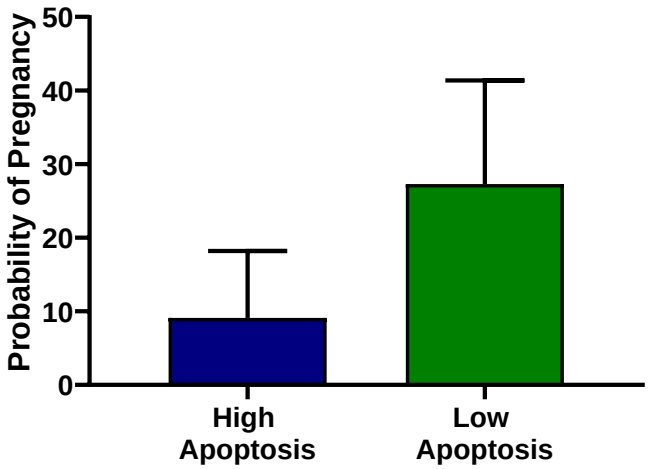

Fig. 4-10. Probability of pregnancy from high and low apoptosis blastocysts. Probability of pregnancy on day 29 to 33 of gestation resulting from day 7 blastocysts over 4 embryo transfer sessions with the top and bottom 20% of FLICA scores, high (total n = 11) and low apoptosis (total n = 11), respectively. Error bars represent the standard error. No significant difference was present using a binary response model (P = 0.2143).

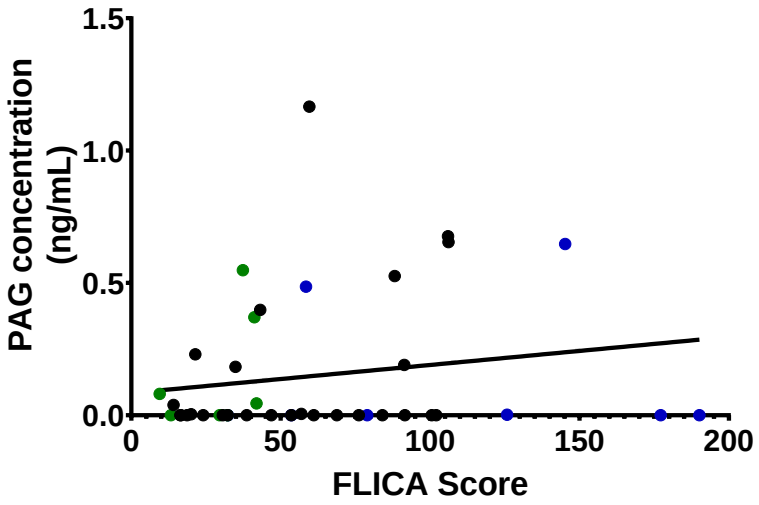

Fig. 4-11. Correlation between SR-FLICA score and PAG concentration. Correlation between FLICA score of day 7 blastocysts and PAG concentration between day 29 and 33 of gestation (total n = 42) from 3 embryo transfer sessions. Linear regression line is shown ($r^2 = 0.03$). No significant correlation was found between FLICA score and PAG correlation (P = 0.27). Green points indicate low apoptosis embryos from each transfer while blue points indicate high apoptosis embryos from each transfer.

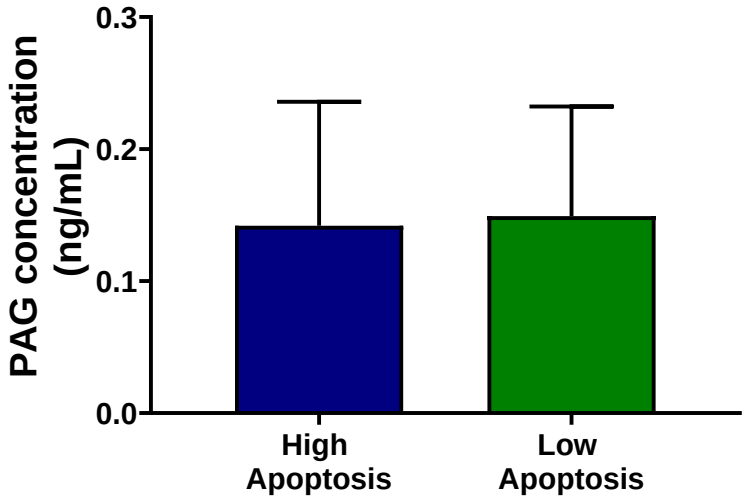

Fig. 4-12. Average PAG concentration from high and low apoptosis blastocysts. Average PAG concentration on day 29 to 33 of gestation from day 7 blastocysts with high (total n = 8) and low (total n = 7) levels of apoptosis from 3 embryo transfer sessions with standard error bars. There was no significant difference in PAG concentration based on incidence of apoptosis (P = 0.96).

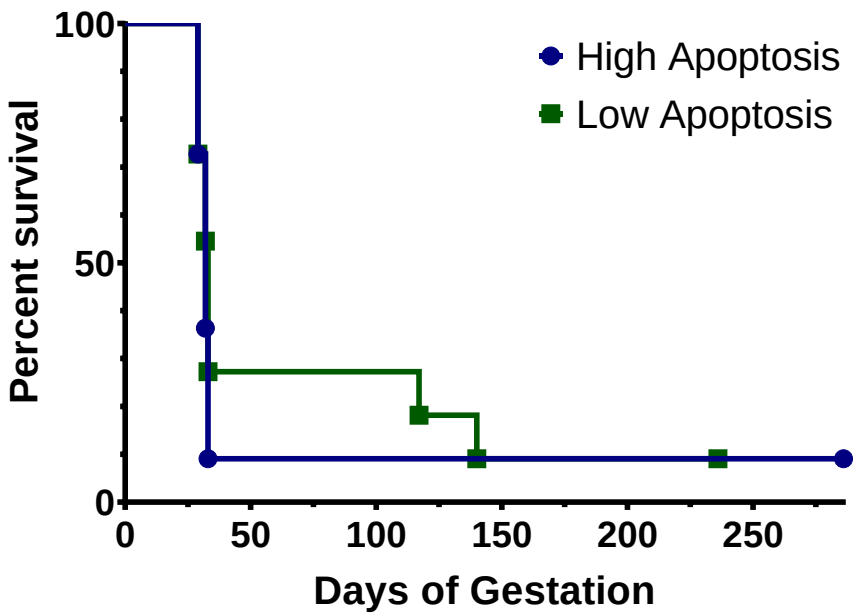

Fig. 4-13. Survival plot of high and low apoptosis blastocysts. Survival of pregnancies from high apoptosis (n = 11) and low apoptosis (n = 11) blastocysts. High apoptosis blastocysts are indicated in blue circles and low apoptosis blastocysts are indicated in green squares. One low apoptosis pregnancy remains on day 236 of gestation and is expected to calve shortly.

Supplemental Tables and Figures

Table S4-1. Developmental rates of SCNT embryos used in cell counts

Cloning Session	No. of embryos after injection	Fused embryos (%)	No. for IVC	Cleavage (%)	Blastocysts (%)
1	170	103/130 (79%)	40	36/40 (90%)	5/36 (14%)
2	175	127/153 (83%)	60	52/60 (87%)	14/52 (27%)
3	158	90/109 (83%)	45	40/45 (89%)	9/40 (23%)

Table S4-2. Developmental rates of SCNT embryos used in gene expression analysis

Cloning Session	No. of embryos after injection	Fused embryos (%)	No. for IVC	Cleavage (%)	Blastocysts (%)
1	192	104/162 (64%)	98	86/98 (88%)	13/86 (15%)
2	191	96/143 (66%)	64	60/64 (94%)	10/60 (17%)
3	176	120/155 (77%)	60	55/60 (92%)	7/55 (13%)
4	172	102/130 (78%)	92	81/92 (88%)	9/81 (11%)

Table S4-3. Summary statistics of apoptosis and gene expression correlation data

	No. of Samples	R squared	P-value	FDR
ASH2L	29	0.0070	0.6655	0.937
BID	28	0.0020	0.8226	0.937
DNMT3A	37	0.1625	0.0134	0.134
EIF4A1	40	0.0266	0.3147	0.629
GAPDH	36	0.0159	0.4637	0.843
GNAS	39	0.0470	0.1848	0.629
GRB10	27	0.0432	0.2980	0.629
HDAC1	38	0.0286	0.3099	0.629
HDAC2	25	0.2553	0.0100	0.134
HDAC3	28	0.0013	0.8570	0.937
HSP90AA1	40	0.0017	0.8007	0.937
IGF2R	26	0.0003	0.9366	0.937
KDM3A	32	0.0479	0.2290	0.629
KLF4	38	0.0646	0.1237	0.629
LIN28A	40	0.0560	0.1417	0.629
POU5F1	40	0.0003	0.9142	0.937
TAF11	35	0.0083	0.6034	0.937
TP53	37	0.0038	0.7154	0.937
UBE3A	35	0.0488	0.2020	0.629
YWHAZ	31	0.0074	0.6465	0.937

Table S4-4. Summary statistics of gene expression analysis

	High Samples	Low Samples	P-value	FDR
ASH2L	4	8	0.332	0.818
BID	4	7	0.219	0.818
DNMT3A	9	9	0.543	0.818
EIF4A1	9	9	0.022	0.223
GAPDH	8	9	0.708	0.944
GNAS	9	9	0.485	0.818
GRB10	5	7	0.404	0.818
HDAC1	8	9	0.135	0.818
HDAC2	4	6	0.555	0.818
HDAC3	4	7	0.573	0.818
HSP90AA1	9	9	0.280	0.818
IGF2R	5	7	0.985	0.997
KDM3A	8	8	0.425	0.818
KLF4	9	9	0.002	0.034
LIN28A	9	9	0.457	0.818
POU5F1	9	9	0.828	0.974
TAF11	7	9	0.997	0.997
TP53	8	9	0.971	0.997
UBE3A	7	9	0.479	0.818
YWHAZ	6	9	0.820	0.974

Table S4-5. Gene symbols of genes analyzed in qPCR with functional classification and gene name

Category and Gene	Gene Name
Apoptosis	
BAX	BCL2 Associated X. Apoptosis Regulator
BID	BH3 Interacting Domain Death Agonist
TP53	Tumor Protein P53
Epigenetic Regulation	
ASH2L	ASH2 Like, Histone Lysine Methyltransferase Complex Subunit
DNMT3A	DNA Methyltransferase 3A
DNMT3B	DNA Methyltransferase 3B
HDAC1	Histone Deacetylase 1
HDAC2	Histone Deacetylase 2
HDAC3	Histone Deacetylase 3
KDM3A	Lysine Demethylase 3A
Imprinted Genes	
GNAS	GNAS Complex Locus
GRB10	Growth Factor Receptor Bound Protein 10
IGF2R	Insulin Like Growth Factor 2 Receptor
UBE3A	Ubiquitin Protein Ligase E3A
Pluripotency	
KLF4	Kruppel Like Factor 4
LIN28	Lin-28 Homolog A
POU5F1	POU Class 5 Homeobox 1
SOX2	SRY-Box 2
Trophoblast Differentiation and Function	
ETS2	ETS Proto-Oncogene 2, Transcription Factor
Housekeeping	
EIF4A1	Eukaryotic translation Initiation Factor 4A1
GAPDH	Glyceraldehyde-3-Phospahete Dehydrogenase
HSP90	Heat Shock Protein 90
TAF11	TATA-Box Protein Associated Factor 11
YWHAZ	Tyrosine 3-Monooxygenase/Tryptophan 5-Monooxygenase Activation Protein Zeta

Table S4-6. Gene symbol of genes analyzed with qPCR with accession number used to design forward and reverse primers and respective primer sequences

Gene Symbol	Accession Number	Primers
ASH2L	NM_001205473.1	For:TGCCATCATAGCGGGAACAC Rev:ACGTTAGGTTGGCCAAAGCA
BAX	NM_173894.1	For:CGGGTTGTCGCCCTTTTCTA Rev:GCCCATGATGGTCCTGATCAA
BID	NM_001075446.N	For:ACGGTGACCTTCATCAACCA Rev:CCGAGTGGTCACTCAGTCC
DNMT3A	NM_001206502.1	For:CCATGTACCGCAAGGCTATCTA Rev:GCTGTCATGGCACATTGGAA
DNMT3B	NM_181813.2	For:GCCAAAGCTCTTCCGAGAAA Rev:GGGTGGAGGTACTGCTGTTA
EIF4A1	NM_001034228.1	For:CAGAAGCTCAACAGCAACAC Rev:CTTCTTGGTCACCTCAAGCA
ETS2	NM_001080214.1	For:GCAGGGCAAACCAGTTATACC Rev:AGAAACTGCCACAGCTGGATA
GAPDH	NM_001034034.2	For:GGGTCTTCACTACCATGGAGAA Rev:GTTCACGCCCATCACAAACA
GNAS	NM_181021.3	For:CCCGGGCCAAGTACTTCA Rev:GGTGAAGTGAGGGTAGCAGTA
GRB10	NM_001192586.1	For:TTGCTGGCAGGAAGCAGTA Rev:GCCTCGTTCCTGACTCTGTTA
HDAC1	NM_001037444.2	For:ATGTCCGAGTACAGCAAGCA Rev:CAGAACTCAAACAGGCCATCAAA
HDAC2	NM_001075146.1	For:AAGGAGGCGGCAAGAAGAAA Rev:TGGGATGACCCTGTCCGTAATA
HDAC3	NM_001206243.1	For:AGACATCGCTGCTGGTAGAA Rev:TGAAGTCCGGGGCAAAGTA
HSP90	NM_001012670.2	For:CATGGATAACTGCGAGGAGCTA Rev:AGATCCTCAGAATCCACCACAC
IGF2R	NM_174352.2	For:GGCAGATTCCACTCAAGTCA Rev:AGATCAAGGTGAGGTCTCCA
KDM3A	NM_001192872.1	For:GCTGCTGTACAAGAAGCAACA Rev:AGTTTGGCTGGGTCTGTCAA
KLF4	NM_001105385.1	For:GCGGCAAAACCTACACGAA Rev:CCATCCCAGTCACAGTGGTAA
LIN28A	NM_001193057.1	For:GCGGCCCAAAGGGAAGAATA Rev:CACTCCTTGGCATGATGGTCTA
POU5F1	NM_174580.2	For:AGAAGCTGGAGCCGAACC Rev:CTGCTTTAGGAGCTTGGCAAA

Gene Symbol	Accession Number	Primers
SOX2	NM_001105463.2	For:CCCAAGAGAACCCTAAGATGCA Rev:CCGTCTCGGACAAAAGTTTCC
TAF11	NM_001034276.1	For:AGAGAAGAAGCAGAAAGTGGATGAA Rev:GGTTCAGCTGCTCCTCAGAA
TP53	NM_174201.2	For:CCCATCCTCACCATCATCACA Rev:GCACAAACACGCACCTCAA
UBE3A	NM_001098462.1	For:TGACGACATTGAAGCTAGCC Rev:ACTGGTGGTAGTAGCGTTCTA
YWHAZ	NM_174814.2	For:AACAGCAGATGGCTCGAGAA Rev:GAAGCGTTGGGGATCAAGAAC

Table S4-7. Developmental rates of SCNT embryos used in embryo transfers

Cloning Session	Cell Line	No. of embryos after injection	Fused embryos (%)	No. for IVC	Cleavage (%)	Blastocysts (%)
1	A	101	84/97 (87%)	80	76/80 (95%)	12/76 (16%)
	B	97	83/86 (97%)	73	68/73 (93%)	10/68 (15%)
2	B	94	70/82 (85%)	50	47/50 (94%)	16/47 (34%)
	C	99	73/88 (83%)	59	54/59 (92%)	7/54 (13%)
3	D	262	205/244 (84%)	131	122/131 (93%)	28/122 (23%)
4	C	135	63/85 (74%)	49	44/49 (90%)	14/44 (32%)
	E	135	67/91 (74%)	47	30/47 (64%)	9/30 (30%)

Table S4-8. Embryo transfer records

Embryo ID	Session	Cell Line	α-amanatin Treatment[1]	SR-FLICA Staining[2]	Technician[3]	SR-FLICA Score	α-amanatin Well[4]	SR-FLICA Well[4]	Pregnant at first check[5]	PAG Concentration[6]
1	1	A	Yes	No	1.5	n/a	1	1	Yes	n/a
2	1	A	Yes	No	1.5	n/a	1	1	Yes	n/a
3	1	A	Yes	No	1	n/a	1	1	No	n/a
4	1	A	Yes	No	1	n/a	1	1	No	n/a
5	1	A	Yes	No	2	n/a	1	1	No	n/a
6	1	A	Yes	No	2	n/a	1	1	No	n/a
7	1	A	Yes	Yes	1	36.85	1	2	No	n/a
8	1	A	Yes	Yes	1	18.24	1	2	No	n/a
9	1	A	Yes	Yes	1	44.77	1	2	No	n/a
10	1	A	Yes	Yes	1	33.51	1	2	No	n/a
11	1	A	Yes	Yes	1	10.01	1	2	Yes	n/a
12	1	A	Yes	Yes	2	18.05	1	2	No	n/a
13	1	B	Yes	No	1.5	n/a	2	3	No	n/a
14	1	B	Yes	No	1	n/a	2	3	No	n/a
15	1	B	Yes	Yes	1.5	17.03	2	4	No	n/a
16	1	B	Yes	Yes	1	31.98	2	4	No	n/a
17	1	B	Yes	Yes	1	12.51	2	4	No	n/a
18	1	B	Yes	Yes	1	30.16	2	4	No	n/a
19	1	B	Yes	Yes	1	21.37	2	4	No	n/a
20	1	B	Yes	Yes	2	15.21	2	4	No	n/a
21	1	B	Yes	Yes	2	27.46	2	4	No	n/a
22	1	B	Yes	Yes	2	22.12	2	4	No	n/a
23	2	C	Yes	No	1	n/a	3	5	Yes	0.183
24	2	C	Yes	No	1	n/a	3	5	No	<0.000
25	2	C	Yes	No	1	n/a	3	5	No	<0.000
26	2	C	Yes	Yes	1	32.71	3	6	Yes	0.486
27	2	C	Yes	Yes	1	34.30	3	6	No	<0.000
28	2	C	Yes	Yes	1	21.64	3	6	No	<0.000
29	2	C	Yes	Yes	1	29.98	3	6	No	<0.000
30	2	C	Yes	Yes	1	49.05	3	6	No	0.081
31	2	B	Yes	No	1	n/a	4	7	No	<0.000
32	2	B	Yes	No	1	n/a	4	7	No	0.230
33	2	B	Yes	No	1	n/a	4	7	No	<0.000
34	2	B	Yes	No	1	n/a	4	7	No	<0.000
35	2	B	Yes	No	1	n/a	4	7	No	0.004

Embryo ID	Session	Cell Line	α-amanatin Treatment[1]	SR-FLICA Staining[2]	Technician[3]	SR-FLICA Score	α-amanatin Well[4]	SR-FLICA Well[4]	Pregnant at first check[5]	PAG Concentration[6]
36	2	B	Yes	No	1	n/a	4	7	No	0.039
37	2	B	Yes	Yes	1	41.10	4	8	No	<0.000
38	2	B	Yes	Yes	1	34.80	4	8	No	<0.000
39	2	B	Yes	Yes	1	48.44	4	8	No	<0.000
40	2	B	Yes	Yes	1	34.88	4	8	No	<0.000
41	2	B	Yes	Yes	1	32.28	4	8	No	<0.000
42	2	B	Yes	Yes	1	46.88	4	8	No	<0.000
43	2	B	Yes	Yes	1	58.48	4	8	No	0.526
44	2	B	Yes	Yes	1	38.64	4	8	No	0.190
45	2	B	Yes	Yes	1	53.56	4	8	No	<0.000
46	2	B	Yes	Yes	1	32.18	4	8	No	0.045
47	3	D	No	No	1	n/a	5	9	Yes	1.166
48	3	D	No	No	1	n/a	5	9	No	<0.000
49	3	D	No	No	1	n/a	5	9	Yes	0.676
50	3	D	No	No	1	n/a	5	9	No	0.398
51	3	D	No	No	1	n/a	5	9	No	<0.000
52	3	D	No	No	1	n/a	5	9	No	0.005
53	3	D	No	No	1	n/a	5	9	No	<0.000
54	3	D	No	No	2	n/a	5	9	No	<0.000
55	3	D	No	No	2	n/a	5	9	Yes	0.654
56	3	D	No	Yes	1	9.51	5	10	No	0.370
57	3	D	No	Yes	1	16.42	5	10	No	<0.000
58	3	D	No	Yes	1	21.44	5	10	Yes	0.548
59	3	D	No	Yes	1	24.07	5	10	No	<0.000
60	3	D	No	Yes	2	13.25	5	10	No	<0.000
61	3	D	No	Yes	2	20.03	5	10	No	<0.000
62	3	D	Yes	No	1	n/a	6	11	No	<0.000
63	3	D	Yes	No	1	n/a	6	11	No	0.647
64	3	D	Yes	No	1	n/a	6	11	No	0.002
65	3	D	Yes	No	1	n/a	6	11	No	<0.000
66	3	D	Yes	No	1	n/a	6	11	No	<0.000
67	3	D	Yes	No	2	n/a	6	11	No	<0.000
68	3	D	Yes	No	2	n/a	6	11	No	<0.000
69	3	D	Yes	No	2	n/a	6	11	No	<0.000
70	3	D	Yes	Yes	1	14.15	6	12	No	<0.000
71	3	D	Yes	Yes	1	18.66	6	12	No	<0.000

Embryo ID	Session	Cell Line	α-amanatin Treatment[1]	SR-FLICA Staining[2]	Technician[3]	SR-FLICA Score	α-amanatin Well[4]	SR-FLICA Well[4]	Pregnant at first check[5]	PAG Concentration[6]
72	3	D	Yes	Yes	1	32.30	6	12	Yes	0.683
73	3	D	Yes	Yes	2	16.57	6	12	No	<0.000
74	3	D	Yes	Yes	2	30.61	6	12	Yes	0.539
75	3	D	Yes	Yes	1.5	78.97	6	12	No	<0.000
76	4	E	No	Yes	1	91.56	7	13	No	<0.000
77	4	E	No	Yes	1	88.16	7	13	No	<0.000
78	4	E	No	Yes	1	91.34	7	13	No	<0.000
79	4	E	No	Yes	1	84.03	7	13	No	<0.000
80	4	E	No	Yes	2	41.92	8	14	Yes	0.803
81	4	E	Yes	Yes	1	53.57	8	14	No	<0.000
82	4	E	Yes	Yes	1	68.81	8	14	Yes	0.585
83	4	E	Yes	Yes	1	106.18	8	14	No	<0.000
84	4	E	Yes	Yes	2	41.2	8	14	No	<0.000
85	4	C	No	Yes	1	59.61	9	15	No	<0.000
86	4	C	No	Yes	1	102.04	9	15	No	<0.000
87	4	C	No	Yes	1	106	9	15	No	<0.000
88	4	C	No	Yes	1	43.15	9	15	Yes	0.723
89	4	C	No	Yes	1	61.08	9	15	No	<0.000
90	4	C	No	Yes	2	56.93	9	15	No	<0.000
91	4	C	Yes	Yes	1	190.12	10	16	No	<0.000
92	4	C	Yes	Yes	1	37.35	10	16	Yes	0.803
93	4	C	Yes	Yes	1	177.19	10	16	No	<0.000
94	4	C	Yes	Yes	1	29.60	10	16	No	<0.000
95	4	C	Yes	Yes	1	100.57	10	16	No	0.144
96	4	C	Yes	Yes	1	76.14	10	16	No	<0.000
97	4	C	Yes	Yes	2	145.19	10	16	No	<0.000
98	4	C	Yes	Yes	1	125.77	10	16	No	<0.000

[1] Some donor cells were treated with α-amanatin while others were not, marked in the column labeled "α-amanatin treatment."

[2] Some embryos were stained with SR-FLICA, while others were not to serve as controls, listed in the "FLICA stained" column.

[3] Two technicians were used for embryo transfer, listed as technician 1 and 2. A technician of 1.5 indicates a transfer where one technician could not pass the pipette and a second technician stepped in for assistance.

[4] The well used for α-amanatin treatment and SR-FLICA staining are indicated.

[5] pregnancy outcome based on ultra-sound pregnancy diagnosis between days 29-33 of gestation.

[6] PAG concentration on day 29-33 of gestation.

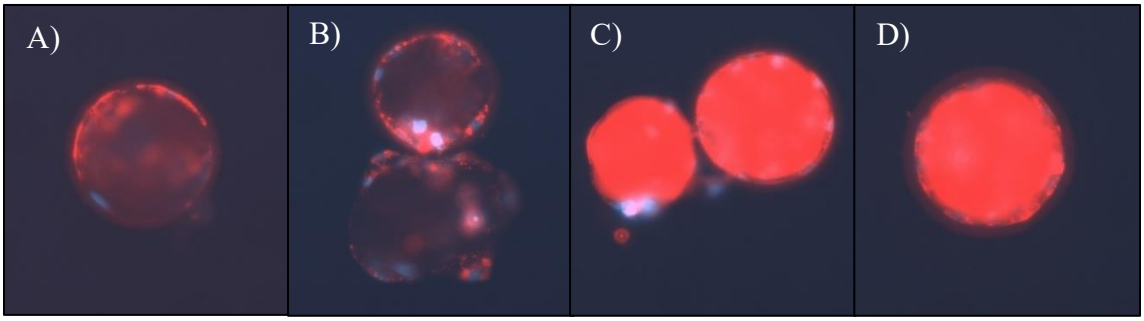

Fig S4-1. SR-FLICA stained porcine blastocysts. Porcine day 6 SCNT blastocysts with low incidence of apoptosis (Panel A and B) and high incidence of apoptosis (Panel C and D) based on SR-FLICA staining, shown in red fluoresence. Blastocysts have also been stained with Hoechst 33342 to indicate nuclei, shown in blue fluoresence. Red indicates active caspase activty while blue indicates the presence of DNA.

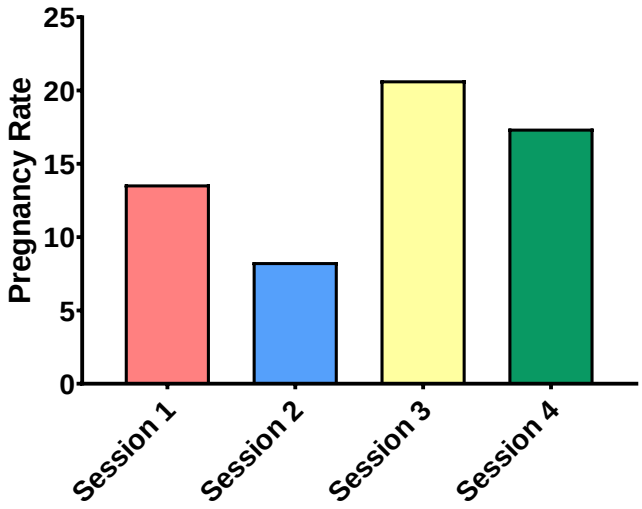

Fig. S4-2. Pregnancy rate from each cloning session (session A n = 22, session 2 n = 24, session 3 n = 29, and session 4 n = 23).

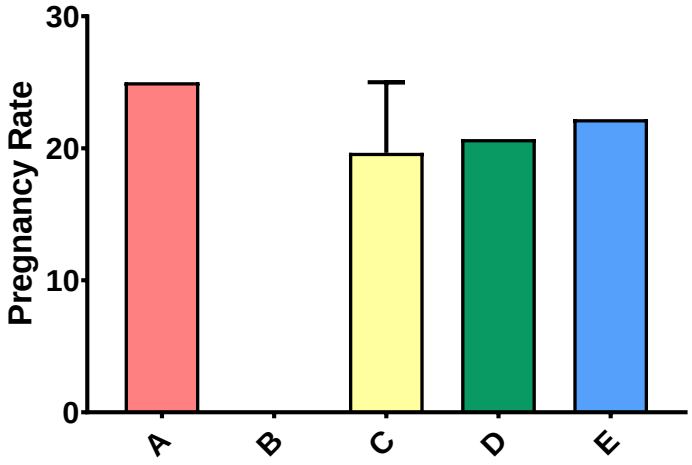

Fig. 4-3. Pregnancy rate from each cell line used in cloning (A [A cloning session] n = A2, B [2 cloning sessions] total n = 26, C [2 cloning sessions] total n = 22, D [A cloning session] n = 29, and E A cloning session n = 9).

CHAPTER V

SUMMARY

Abnormalities in cloned embryos and resulting pregnancies are believed to be the result of abnormal epigenetic reprogramming following somatic cell nuclear transfer (SCNT) and lead to failed establishment or maintenance of pregnancy. However, some cloned embryos and resulting pregnancies result in relatively normal pregnancies and cloned offspring. This led us to our hypothesis that in some cases, SCNT embryos undergo proper genome reprogramming, resulting in normal gene expression profiles, low levels of apoptosis, and normal development through gestation. We proposed the use of active caspase activity to isolate the embryos with high levels of apoptosis, a result of aberrant epigenetic reprogramming and gene expression, to identify the embryos most likely to fail following embryo transfer.

We concluded that SR-FLICA (Immunohistochemistry Technologies, Bloomington, MN, USA) was an accurate, non-invasive, and non-toxic method to assess apoptosis through caspase activity in embryos. By sorting day three porcine SCNT embryos by relative caspase activity, we were not able to isolate the most competent embryos based on blastocyst development rates and number of cells. Day six porcine SCNT blastocysts with high and low levels of apoptosis did not show differences in gene expression in 65 genes analyzed through qPCR. Taking a more global approach, day six porcine SCNT blastocysts with high and low incidence of apoptosis were evaluated for gene expression and DNA methylation patterns of the same individual blastocyst using RNA-seq and RRBS, respectively. While there were differences in gene expression and differential methylation between blastocysts with high and low incidence of apoptosis, no

gene ontology pathways were identified. Taken together with the relatively few differences between high and low apoptosis blastocysts, our data supported the hypothesis for a stochastic nature of reprogramming following SCNT where each individual blastocyst undergoes a unique epigenetic reprogramming and therefore has a unique gene expression profile. Finally, embryo transfers showed that the analysis of the whole blastocyst for active caspase activity in bovine SCNT blastocysts was not useful to predicting the embryos that would be successful at achieving a pregnancy following transfer.

As with any study, the project had several limitations that should be acknowledged. While DNA methylation and gene expression profiles provide answers to basic biology to understand how cloned embryos undergo reprogramming, the most applicable part of the project was determining if the approach of staining embryos with SR-FLICA would allow the identification of the most competent embryos. However, we were not able to significantly increase pregnancy rate based by sorting high and low apoptosis blastocyst, even when performing 98 embryo transfers. Because we used cloned embryos, there is an inherent flaw that the pregnancy rate is extremely low, a direct result of the inefficiency we are working to correct. Additionally, from these 98 transferred blastocysts, toxicity of SR-FLICA was also evaluated meaning not all of the embryos were stained and evaluated for level of apoptosis. From 98 total transferred blastocysts, only 15 had an established pregnancy at the first pregnancy check approximately one month into gestation. With the low number of established pregnancies, it would require many more transfers to show a significant difference in pregnancy rate, assuming that the trend for a higher pregnancy rate in the low apoptosis

blastocysts continues. Another approach that could have been more definitive is to analyze SR-FLICA scores in *in vitro* fertilized (IVF) blastocysts which would have increased pregnancy rates following transfer compared to cloned blastocysts [1, 2].

A second limitation to the overall study design was the necessity to switch from molecular analysis in porcine blastocysts to embryo transfer evaluation in bovine blastocysts. Due to technical challenges with synchronizing recipient gilts, estrus was never synchronized correctly to expect an embryo transfer to be successful in the porcine system. In addition to the technical challenge of estrus synchronization in pigs, there is also the challenge of the sheer number of blastocysts that are required in porcine SCNT embryo transfers. Previously reported porcine SCNT blastocyst transfers into a surrogate female transfer over 50 blastocysts per recipient [3, 4]. Because our goal was to compare the high to low apoptosis blastocyst, representing the top and bottom 20% or SR-FLICA scores, respectively, our study design ended up throwing out the middle 60% of blastocysts. Even with minimizing the number of transferred blastocysts per gilt to approximately 25 per group, the number of embryos that had to be created was vast. And as a result, the time required to analyze the embryos was quite excessive. From a production standpoint, it would make more sense to transfer all produced blastocysts into a recipient gilt as there is no detriment in a pig to having multiple successful embryos as pigs are litter bearing in nature. Therefore, the decision was made to perform the embryo transfer analysis in cattle where only one cloned blastocyst is transferred to avoid the risk of twin cloned pregnancies. However, it is unclear how much can be inferred from the porcine molecular findings to the bovine system. A review of DNA methylation in preimplantation embryos did point to species specific differences in epigenetic

reprogramming including timing and demethylation patterns [5], so a more thorough exploration into the epigenetic reprogramming of high and low apoptosis blastocysts in cattle could be necessary in the future.

The final and perhaps most significant limitation of the study is the inability to know if the observed apoptosis was truly a result of inadequate epigenetic reprogramming, as we assumed it was, or the result of another insult, such as *in vitro* culture conditions. Previous studies have documented that *in vitro* produced embryos undergo increased levels of apoptosis compared to their *in vivo* produced counterparts [6, 7]. The effects of *in vitro* culture could have been addressed by including IVF blastocysts, but rather we opted to include increased number of biological replicates of cloned and IVV embryos rather than including an IVF group. However, from a practical view point of trying to increase the efficiency of SCNT as the end goal, I believe that the best approach would have been to produce SCNT embryos and transfer them immediately to a surrogate female. Embryos cultured *in vivo* are known to be higher quality in terms of developmental potential and cell number [8]. There would have then been no question that the embryos were in their ideal culture conditions and any resulting apoptosis would have been the direct result of abnormalities in the embryo rather than response to the environmental conditions. Embryos could be flushed at the blastocyst stage and the same experimental design could have been utilized.

While even the best studies will have their limitations, our study provided many novel techniques and findings which enhanced the field of epigenetic reprogramming and developmental competence of cloned embryos. Our findings provided better

understanding of both the basic biology of epigenetic reprogramming in cloned embryos as well as the applicable evaluation of cloned blastocysts in attempt to increase the efficiency of the technology. While numerous studies have compared SCNT embryos to IVF or *in vivo* produced embryos [9-12], very few studies have compared SCNT embryos to one another. Those studies that have compared clones typically focus on differences past the preimplantation stage evaluating characteristics of the placenta [13, 14]. To the best of our knowledge, this is one of, if not the first, study to not only describe differences between "normal" and "abnormal" clones, but to compare individual cloned blastocysts in an attempt to isolate the most competent.

Additionally, the study had many technical novelties which provided unique data which has not previously been reported. Again to the best of our knowledge, this is the first time that both genomic DNA and total RNA have been isolated from individual blastocysts and analyzed on a large scale. Typically, pooled embryos have been used to overcome the challenge of such low abundance of DNA and RNA from individual blastocysts [15, 16]. Another more common approach has been to analyze individual embryos but evaluate specific regions or genes of interest, such as imprinted genes, rather than taking on a more global approach, which evaluates a much larger proportion of the genome [17, 18]. However, by isolating both DNA and RNA from individual cloned blastocysts and analyzing on a large scale, we were able to produce data that can better explain the nuances of epigenetic reprogramming in each individual embryo.

This is also the first reported use of reduced representation bisulfite sequencing (RRBS) for analysis between two phenotypically different groups rather than an

observational study in a livestock species. Previous reports have utilized RRBS to report on differences in sperm, eggs, and early developing embryos in cattle [19]. Other studies have focused on the differences in methylation patterns between various tissues [20]. However, this appears to be the first report of the use of RRBS to analyze DNA methylation patterns of porcine blastocysts. Additionally, we believe that this is also the first report of comparing the methylome of individual blastocysts to each other, rather than to other embryonic stages of development. We were also able to analyze a large number of individual blastocysts, providing a wealth of data on the DNA reprogramming that occurred in individual embryos.

While this study provided vast amounts of data that provided deeper understanding of both the basic biology and application of cloned blastocysts, there is of course always research that could be performed to follow up on the reported findings. Analysis for the incidence of apoptosis was performed on the whole blastocysts, where the average red pixel intensity for the entire area under the zona pellucida quantified the relative level of apoptosis. By repeating the analysis, only focusing on the inner cell mass, the blastocysts which were classified as high and low incidence of apoptosis could have been completely different. This change in up front analysis could have then affected the downstream outcomes, such as apoptosis level being predictive of pregnancy outcome. Until a more thorough analysis was performed taking into account the different morphological areas of the embryo, it would not be possible to write off SR-FLICA staining as a potential indicator of embryo quality. As technology continues to advance, it may also be possible to analyze DNA methylation and gene expression patterns on individual cells rather than on a whole blastocyst level. It could be possible in the

epigenetic reprogramming of the early embryo, in which cells have started to divide and the reprogramming occurs vastly differently in each cell. This could lead to a blastocyst with a mosaic pattern of DNA methylation and gene expression, which is obscured when analyzing the entire blastocyst. A single cell approach could provide an even more complex story of epigenetic reprogramming.

Future studies should also incorporate larger numbers of individual blastocysts into the analyses. While we believe that we exceeded the typical expectation of a handful of individual blastocysts per group, with more than 10 individual blastocysts included in each of our groups, there could always be more embryos included in the analysis. From our data, it appeared that including more biological replicates in each group made it more difficult to determine differential gene expression and DNA methylation patterns. Typically, it would be assumed that more biological replicates would increase statistical power and lead to more statistical differences between groups. However, because of the random nature of reprogramming in cloned blastocysts, increasing the number of biological replicates increases the amount of background noise and actually made it more challenging to identify genes and regions that were differentially expressed and methylated, respectively. Therefore, by including a high number of biological replicates, those genes and regions that were found to be statistically differentially expressed or methylated between the groups could be extremely biologically relevant and so be established as the true driving cause for the phenotypic difference.

Finally, future studies are needed to better understand why such a difference in apoptotic activity was identified in porcine compared to bovine blastocysts. Visually,

there was a staggering difference in the amount of caspase activity in cloned blastocysts where the porcine blastocysts had much higher levels of caspase activity compared to the bovine blastocysts. It would be fascinating to understand if these differences are the direct result of the embryo itself, perhaps differences in channels or pores result in the SR-FLICA being trapped in porcine blastocysts, whereas cow blastocysts are more efficient at clearing the SR-FLICA from the embryo. Or it is possible that the apoptosis response is different as a result of different culture systems. If this is the case, it would be interesting to understand if this pattern carries to other culture systems outside of the two used in our study. Finally, it is possible that the difference in level of apoptosis was a direct result of the ability or inability for the embryos to undergo proper epigenetic reprogramming following somatic cell nuclear transfer. Perhaps the cattle embryos are more efficient at epigenetic reprogramming after SCNT compared to the porcine embryos and as a result have a lower incidence of apoptosis.

In conclusion, this research provided a deeper understanding of the epigenetic reprogramming and gene expression of cloned porcine blastocysts with high and low incidence of apoptosis. While statistically there was no increase in pregnancy rate between high and low apoptosis blastocysts, increased replication could provide the statistical power necessary to support the numeric increase in pregnancy rate in the low apoptosis blastocysts. This research provided novel techniques and data to the field, including gene expression and methylation analysis of individual cloned blastocysts and comparison of cloned individual blastocysts to each other. Limitations in study design included using a limited number of embryo transfers, utilizing two species throughout the study, and the inability to know the cause of increased apoptosis in the cloned embryos.

Future studies should focus on apoptosis in the different morphological regions of the blastocysts, species-specific differences in apoptosis levels, and include large number of biological replicates when using cloned embryos.

References

1. Bauersachs S, Ulbrich SE, Zakhartchenko V, Minten M, Reichenbach M, Reichenbach H-D, Blum H, Spencer TE, Wolf E. The endometrium responds differently to cloned versus fertilized embryos. Proceedings of the National Academy of Sciences of the United States of America 2009; 106:5681-5686.
2. Suzuki J, Therrien J, Filion F, Lefebvre R, Goff AK, Smith LC. In vitro culture and somatic cell nuclear transfer affect imprinting of SNRPN gene in pre-and post-implantation stages of development in cattle. BMC developmental biology 2009; 9:9.
3. Li J, Svarcova O, Villemoes K, Kragh PM, Schmidt M, Bøgh IB, Zhang Y, Du Y, Lin L, Purup S, Xue Q, Bolund L, et al. High in vitro development after somatic cell nuclear transfer and trichostatin A treatment of reconstructed porcine embryos. Theriogenology 2008; 70:800-808.
4. Boquest AC, Grupen CG, Harrison SJ, McIlfatrick SM, Ashman RJ, d'Apice AJF, Nottle MB. Production of Cloned Pigs from Cultured Fetal Fibroblast Cells. Biology of Reproduction 2002; 66:1283-1287.

5. Young LE, Beaujean N. DNA methylation in the preimplantation embryo: the differing stories of the mouse and sheep. Animal Reproduction Science 2004; 82-83:61-78.

6. Gjørret JO, Knijn HM, Dieleman SJ, Avery B, Larsson L-I, Maddox-Hyttel P. Chronology of Apoptosis in Bovine Embryos Produced In Vivo and In Vitro. Biology of Reproduction 2003; 69:1193-1200.

7. Hardy K. Cell death in the mammalian blastocyst. Mol Hum Reprod 1997; 3:919-925.

8. Macháty Z, Day BN, Prather RS. Development of early porcine embryos in vitro and in vivo. Biology of reproduction 1998; 59:451-455.

9. Smith C, Berg D, Beaumont S, Standley NT, Wells DN, Pfeffer PL. Simultaneous gene quantitation of multiple genes in individual bovine nuclear transfer blastocysts. Reproduction 2007; 133:231-242.

10. Boiani M, Gentile L, Gambles VV, Cavaleri F, Redi CA, Scholer HR. Variable reprogramming of the pluripotent stem cell marker Oct4 in mouse clones: distinct developmental potentials in different culture environments. Stem Cells 2005; 23:1089-1104.

11. Hao Y, Lai L, Mao J, Im GS, Bonk A, Prather RS. Apoptosis and in vitro development of preimplantation porcine embryos derived in vitro or by nuclear transfer. Biol Reprod 2003; 69:501-507.

12. Isom SC, Stevens JR, Li R, Spollen WG, Cox L, Spate LD, Murphy CN, Prather RS. Transcriptional profiling by RNA-Seq of peri-attachment porcine embryos

generated by a variety of assisted reproductive technologies. Physiological Genomics 2013; 45:577-589.

13. Sim B-W, Park C-W, Kang M-H, Min K-S. Abnormal gene expression in regular and aggregated somatic cell nuclear transfer placentas. BMC Biotechnology 2017; 17:34.

14. Palmieri C, Loi P, Ptak G, Della Salda L. Review paper: a review of the pathology of abnormal placentae of somatic cell nuclear transfer clone pregnancies in cattle, sheep, and mice. Vet Pathol 2008; 45:865-880.

15. Smallwood SA, Tomizawa S-i, Krueger F, Ruf N, Carli N, Segonds-Pichon A, Sato S, Hata K, Andrews SR, Kelsey G. Dynamic CpG island methylation landscape in oocytes and preimplantation embryos. Nature Genetics 2011; 43:811.

16. Okae H, Chiba H, Hiura H, Hamada H, Sato A, Utsunomiya T, Kikuchi H, Yoshida H, Tanaka A, Suyama M. Genome-wide analysis of DNA methylation dynamics during early human development. PLoS genetics 2014; 10:e1004868.

17. Kang Y-K, Koo D-B, Park J-S, Choi Y-H, Chung A-S, Lee K-K, Han Y-M. Aberrant methylation of donor genome in cloned bovine embryos. Nature genetics 2001; 28:173.

18. Fauque P, Jouannet P, Lesaffre C, Ripoche MA, Dandolo L, Vaiman D, Jammes H. Assisted Reproductive Technology affects developmental kinetics, H19 Imprinting Control Region methylation and H19 gene expression in individual mouse embryos. BMC Dev Biol 2007; 7:116.

19. Jiang Z, Lin J, Ouyang Z, Dong H, Zheng X, Chen J, Marjani SL, Duan J, Tian X. DNA methylomes of bovine gametes and in vivo produced preimplantation embryos. Biology of Reproduction 2018; 99:949-959.

20. Zhou Y, Xu L, Bickhart DM, Abdel Hay EH, Schroeder SG, Connor EE, Alexander LJ, Sonstegard TS, Van Tassell CP, Chen H, Liu GE. Reduced representation bisulphite sequencing of ten bovine somatic tissues reveals DNA methylation patterns and their impacts on gene expression. BMC Genomics 2016; 17:779.

CHAPTER VI

CURRICULUM VITAE

Laura Moley

Education

- Utah State University- Logan, UT
  - PhD Student in Animal, Dairy and Veterinary Sciences with a Specialization in Reproduction and Development
  - ADVS Doctoral Research Fellow
  - Dissertation Topic: Effects of apoptosis on genetic and epigenetic determinants of successful pre- and peri-implantaiton embryo development
  - GPA: 4.0
- University of Missouri- Columbia- Columbia, MO
  - Bachelor of Science in Animal Sciences, May 2014
  - Captive Wild Animal Management Minor
  - Undergraduate Thesis: Efficacy of detecting serum concentrations of pregnancy associated glycoproteins for pregnancy diagnosis in deer.
  - GPA: 3.93

Work Experience

- Summer Fellow, San Diego Zoo Global, Reproductive Physiology-Endocrinology, Escondido, CA, Summer 2013
  - Research topic: Are estrogenic diets contributing to the reproductive decline of captive Southern White Rhinos?
  - Extracted phytoestrogens from feeds and conducted activation assays to determine estrogenicity of diet
  - Performed High Pressure Liquid Chromatography on feed extracts
  - Presented the data at the University of Missouri Undergraduate Research Forum and Summer Seminar Series at San Diego Zoo Institute for Conservation Research
- Zoo Keeper Intern, Dickerson Park Zoo, Springfield, MO, December 2012-January 2013
  - Fed diets and prepared enrichment (form of entertainment for animals such as adding toys to exhibit)
  - Cleaned and disinfected indoor housing and exhibits
  - Observed medical treatments, veterinary procedures, and training
- Undergraduate Research Assistant in Reproductive Physiology, Division of Animal Science, February 2012- May 2014
  - Data collection from Red Deer and cattle
  - Performed radioimmunoassays and ELISA assays

  - Extracted DNA from tissue samples
  - Organized samples and transferred into proper equipment to run assays
  - Enter data into excel spreadsheets
- Instructor, Kansas City Zoo, Education Department, May - August 2011, May - August 2012, and May - August 2014
  - Supervised weekly summer camp for children age 10-12 years
  - Taught curriculum for four camp themes and presented information about animals and animal artifacts

Service Involvement

- Utah's Hogle Zoo, Zoo Aide- April 2017- June 2019
  - Prepared diets, cleaned stalls, created enrichment for zebras, ostrich, and giraffe
- Missouri Horse Farm Volunteer- January 2011 – May 2014
  - Cleaned stalls and fed horses to provide optimal breeding conditions
- Cedar Creek Therapeutic Riding Center- February 2011- April 2011
  - Assisted riders by walking along side or leading the horse
- Spay and Neuter Kansas City, September 2009- June 2010
  - Cleaned incision regions, trimmed nails, injected some vaccines

Honors and Awards

- Third Place Oral Presentation, Graduate Student Symposium- Utah State University, August 2016
- Outstanding Senior, Division of Animal Science, University of Missouri- May 2014
  - Awarded to the top graduating senior in the animal science program each year
- Outstanding Junior / Senior Volunteer, University of Missouri Horse Farm- 2012-2013 and 2013-2014
- College of Agriculture, Food, and Natural Resources Honors Program
  - Awarded after application to students with a GPA over 3.3. Designed for high-ability students to achieve an individualized learning experience.
- American Society of Animal Science Undergraduate Scholar- 2011, 2012, 2013, and 2014
  - Awarded to the top 10% of each Animal Science class based on GPA

Teaching Experience

- Physiology of Reproduction and Lactation- Graduate Teaching Assistant, Utah State University, Fall 2016
- Physiology of Reproduction and Lactation- Graduate Teaching Assistant, Utah State University, Fall 2015
- Equine Assisted Activities and Therapies- Graduate Teaching Assistant, Utah State University, Fall 2014

- Reproductive Physiology- Undergraduate Teaching Assistant, University of Missouri, Spring 2014

Publications

- Pohler, K.G., J.A. Green, L.A. Moley, S. Gunewardena, W.T. Hung, R.R. Payton, X. Hong, L.K. Christenson, T.W. Geary, and M.F. Smith. 2017. *Circulating microRNA as candidates for early embryonic viability in cattle.* Mol. Repord. Dev.
- Tubbs, C.W., L.A. Moley, J.A. Ivy, L.C. Metrione, S. LaClaire, R.G. Felton, B.S. Durrant, and M.R. Milnes. 2016. *Estrogenicity of captive southern white rhinoceros diets and their association with fertility.* Gen Comp Endocrinol. 238:32-38.

Research Presentations

- Society for the Study of Reproduction Annual Conference 2017, Poster Presentation
- Society for the Study of Reproduction Annual Conference 2017, Flash Talk
- ASAS-SSR Joint Symposium SSR Annual Conference 2017, Poster Presentation
- Graduate Student Symposium Utah State University ADVS 2016, Oral Presentation (Placed 3rd)
- Graduate Student Symposium Utah State University ADVS 2015, Poster Presentation
- Society for the Study of Reproduction Annual Conference 2014, Poster Presentation

Assisted Reproductive Techniques

- Follicular aspiration from abattoir collected ovaries
- Porcine oocyte *in vitro* maturation
- Porcine parthenogenetic activation
- Porcine somatic cell nuclear transfer- fusion and activation
- Porcine embryo culture
- Assisted in ovum pick up in cattle
- Artificial insemination in cattle and horses
- Semen collection from stallions

Laboratory Techniques

- Reduced Representation Bisulfite Sequencing
- Fluidigm Biomark RT PCR
- Radioimmunassay
- ELISA assay
- Tissue RNA/DNA extraction
- Activation assay

- Phytoestrogen extraction from feed samples
- PCR
- High Pressure Liquid Chromatography
- Data collection and analysis using excel

Relevant Course Work

- Genetics of Agricultural Plants and Animals
- Applied Livestock Genetics
- Physiology of Domestic Animals
- Introduction to Statistical Reasoning
- Biotechnology in Animal Agriculture
- Issues in Animal Agriculture
- Introduction to Cell Biology
- Herpetology
- Problems in Animal Science- Graduate Experience Program
- Physiology of Reproduction
- Undergraduate Research
- Biochemistry
- Introduction to Organic Chemistry with Lab
- Reproductive Management
- Immunology
- Science Communication
- Design of Experiments
- Veterinary Physiology
- Endocrinology
- Epigenetics